WorldBus Final Report

Designing a sustainable ultra-long range aircraft

AE3200: Design Synthesis Exercise

Group 8

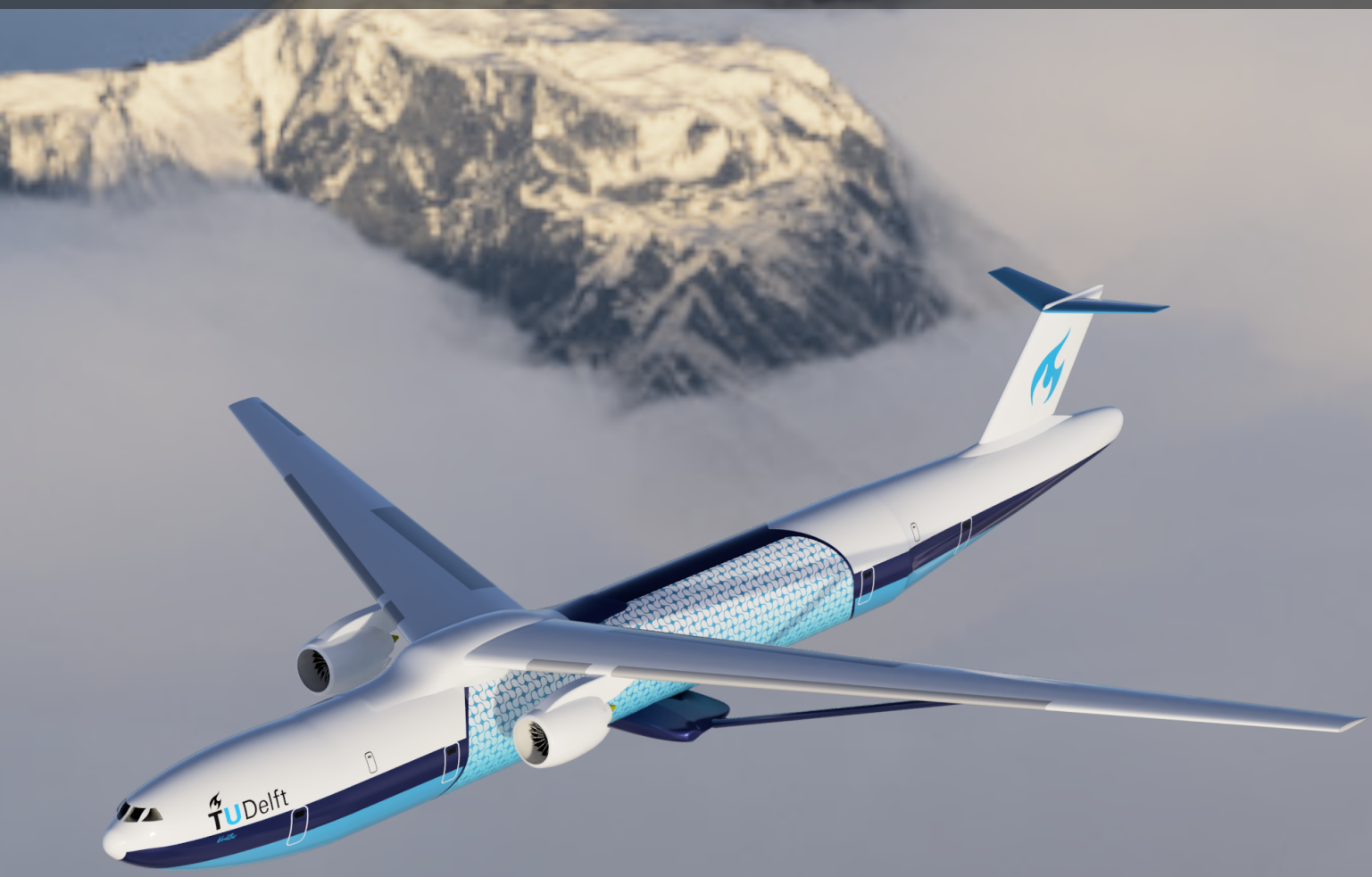

TU Delft

Page intentionally left blank.

WorldBus Final Report

Designing a sustainable ultra-long range aircraft

by

Group 8

Student Name	Student Number
Bouvy, Jelle (JB)	5107423
Bruin, Timo (TB)	5314356
Dubois, Theophile (TD)	5223210
Duursma, Matthijs (MD)	4886658
Hees, Sean van (SH)	4862473
Holtz, Bart (BH)	5078989
Jagt, Django (DJ)	5052327
Meijer, Sjoerd (SM)	5106761
Tromp, Silvano (ST)	5049237
Vousten, Luca (LV)	5110033

AE3200 - Design Synthesis Exercise

Version	Date	Affected chapters	Description of change
1	21/06/2023	All	New document

Project Tutor: Dr. C.D. Rans & Dr. S. Texeira de Freitas
Coaches: Dr. R.M. Groves, A. Stefanidi & I. Parmaksizoglou
TA: K. Smit
Project Duration: April, 2023 - June, 2023
Faculty: Faculty of Aerospace Engineering, Delft

Instructor: ir. J.A. Melkert

TU Delft

Executive overview

Around the globe, more and more people are becoming aware of the urgency to reduce humanity's environmental footprint. Aviation is subject to much attention in the discussion around climate change due to its environmental impact. This is especially the case for long-haul flights. These long-haul flights only account for 5.5% of all flights flown but produce about 50% of all aviation emissions.[1] WorldBus aims to change this by providing a sustainable alternative and reducing the carbon footprint of the aviation industry.

For a successful design, a number of requirements were given by the user that WorldBus needs to meet. These requirements are listed below:[2]

- WorldBus shall be able to provide a non-stop flight between any two major international airports (defined as more than 10 million passenger journeys per year).
- WorldBus shall perform this within the maximum travel time of 24 hours (from arrival at the departure airport to leaving the destination airport).
- WorldBus shall transport a minimum of 200 passengers, including provision for sleeping on board.
- WorldBus shall meet the minimum requirements of EASA CS-25 certification specification for large aeroplanes.
- WorldBus shall have an environmental impact of less than 10% of current long-haul aircraft (e.g. B787, A380) after considering, materials, manufacture, fuel, maintenance and recycling at end-of-life.
- WorldBus shall fly at least 4000 flight hours per year.
- WorldBus shall have an operational lifetime of at least 40000 flight hours.
- WorldBus shall have a maximum purchase price (before discount) of EUR 250 million.
- WorldBus shall have an average unit cost according to the expected production of 500 units over 20 years.
- WorldBus shall enter service in 2040.

Final design

The cumulation of the design project is a wide body, twin-engine, truss-braced aircraft. It can carry 200 passengers over a distance of 19 000 km within 24 hours. It uses two Rolls-Royce Trent 1000R engines that are modified to run on hydrogen. Furthermore, the cabin has a unique layout with two passenger cabins, one in the front of the aircraft and one in the back, being separated by a large hydrogen fuel tank. These cabins consist of two floors, giving WorldBus four separate passenger areas. WorldBus provides extra comfort to passengers by only offering economy+ and business class seats. This report provides an overview on how the team arrived at this design.

(a) **(b)**

Figure 1: Renders of WorldBus while in the air and on the ground.

[1] https://www.eurocontrol.int/publication/eurocontrol-data-snapshot-co2-emissions-flight-distance

[2] taken from the WorldBus project description 2023
https://brightspace.tudelft.nl/d2l/le/content/498709/viewContent/3130687/View

Financial analysis

Before analysing the finances related to the WorldBus project it is important to ensure a market exists for this aircraft. To analyse this the current market size for long-haul aircraft is analysed, together with growth expectations and the size of the new market reached by reducing the need for layovers on ultra-long-haul flights. Adding these up results in an achievable market share of 80% for all flights over 13 500 km, or 0.0352% of the complete aviation market.

Next, the higher comfort, short travel time, and substantially higher sustainability of WorldBus mean that passengers are willing to pay more for a ticket. For the ultra-long-range flights that WorldBus is targeting, an average ticket price of EUR 1944 for economy+ and, EUR 3240 for business class are predicted.

A flight has operational costs which consist of variable costs per hour and fixed costs per flight. The variable expenses consist of fuel cost, maintenance, and crew salaries adding up to a total of EUR 7463 EUR/hr. Fixed expenses consist of landing fees, turn-around charges, cargo loading, and consumption adding up to a total cost of 16194 EUR/flight.

The capital expenses of WorldBus consist of costs related to research & development (R&D) and manufacturing costs. The (R&D) costs are non-recurring costs and are analysed per subsystem. This resulted in a total cost of EUR 8.9 billion for 300 aircraft which is equivalent to EUR 29.7 million per aircraft. Manufacturing costs are recurring costs and are analysed per component as well. Here, the purchase price of two Rolls-Royce Trent 1000Rs, the extra costs for a liquid hydrogen tank, and the extra costs for manufacturing a T-tail are taken into account. Resulting in a total manufacturing cost of EUR 410 million. Adding these to gives a total capital cost of EUR 440 million per aircraft.

A final list price for WorldBus was established to be EUR 484 million which includes a safety/profit margin of 10 percent. This is almost double the user requirement of EUR 250 million. However, reference aircraft have a list price of EUR 300-450 million and therefore a list price of 500 million is not deemed unrealistic for WorldBus. Analysing the return on investment (ROI) for the customer leads to a value of 96 % under the condition that WorldBus has an achievable market share of 80% and flights are filled for a 100%. When looking at a combination of setbacks an ROI of 20%, which is comparable to current aircraft, is found when the actual market share is 60%, flights are filled to 80% capacity, ticket prices are 5% lower and the total costs per flight are 15% higher. This proves that the concept will be profitable from a customer's perspective, even taking into account the increased list price and possible setbacks.

Sustainable development strategy

It is no surprise that sustainability plays a major role in new aircraft designs. For WorldBus as well, a sustainable development strategy has been established. The framework used for this project is created by the International Organization for Standardization and is called ISO 26000.

First, social responsibility was taken into account by identifying and minimizing the negative impacts on society. Next, economic performance was investigated. For this, a market analysis was performed to ensure a need for this aircraft. Furthermore, proper budgets were established aligning the design with the cost requirements. Lastly, environmental management was looked into. As this makes up the majority of the sustainable development strategy it was elaborated on in more detail. Sustainability requirements were set up and from this certain aircraft characteristics, which should be checked continuously throughout the design, are determined. If these requirements were not met, solutions have been proposed to adopt a more sustainable design.

Design options

For the design selection, two separate trade-offs were performed. A selection of the best design was made based on their performance in four categories. Environmental impact, performance, costs, and passenger comfort.
The first trade-off focused on selecting the right wing and fuselage configuration. This resulted in three configurations namely a blended wing, a truss-braced wing and a multi-fuselage aircraft. The second trade-off focused on the propulsion system, from which it became clear that a liquid hydrogen-powered turbofan would be the best option. After looking into more detail for these three configurations a final trade-off was performed based on new criteria which exemplify where the designs differed. This trade-off showed that the truss-braced liquid hydrogen aircraft is the best contender to perform the WorldBus mission.

Fuselage Layout

In order to design the internal layout of the aircraft, some regulations had to be taken into account for emergency exits, lavatories, galleys, and for crew resting compartments. In total WorldBus houses six rest compartments for the crew, as we have a total of 12 crew members, six active at a time. The aircraft will include two emergency doors of type A, and one emergency door of type I. This allows for an evacuation of 139 passengers per cabin, (39 more than what is the WorldBus is currently designed for. As for the lavatories, one was included for every 25 passenger, thus 8 are included on the plane.

After designing, the internal layout of the two, two floor cabins, the exterior dimensions of the cabin could be determined, the fuel tank lengths were then added to that. Combined with the tail cone and the cockpit length, the final fuselage dimensions are shown in Table 1.

Table 1: Fuselage dimensions

Parameter	Unit	Value
Outer diameter	[m]	6.25
Number of business seats	[m]	82
Number of economy+ seats	[m]	118
Cockpit length	[m]	4.00
Nose cone length	[m]	12.50
Tail cone length	[m]	21.87
Primary tank length	[m]	23.86
Secondary tank length	[m]	5.07
Fuselage length	[m]	75.31

Aerodynamics

To ensure the design is made for optimal aerodynamic efficiency, various design choices are made, and updated, throughout the project. To start the wing and thrust loading diagram is created to find the optimal design point for performance requirements. Next, with the first estimations for the aspect ratio (AR) and the taper ratio (λ), the wing planform parameters are determined. This yielded the aerodynamic coefficients that should be achieved by the wing design, taking these into account provides a basis to determine the optimal airfoil.

As WorldBus flies at a cruise Mach of 0.87, multiple airfoils known for performance in transonic regimes were analysed. The airfoils are compared based on their stall behaviour, design lift coefficient, drag at design lift coefficient and critical Mach number. After a thorough evaluation, it became evident that the SC(2)-0712 is the most optimal airfoil for this mission as it scored equal or better on these criteria.

After the airfoil was chosen the aircraft could be analysed in more depth regarding lift and drag. No unexpected values arose here, strengthening the belief in this aerodynamic design. Now, in order to finish the complete design, the high-lift devices and control surfaces were designed based on the to-be-achieved maximum lift coefficient values and CS-25 requirements.

Lastly, verification of the used numerical model was performed by performing an analysis on the designed wing in XFLR5. Most values correspond with one another, only the Oswald efficiency factor is significantly lower using the team's numerical model. Therefore, one of the recommendations made is to investigate the Oswald efficiency factor in further detail to ensure its correctness.

Propulsion

In a conventional aircraft, the vast majority of the emissions are generated by the propulsion system. As one of the main goals for this project is to lower the climate impact by 90%, a climate-friendly propulsion system was required. A propulsion system based on green hydrogen was chosen for this reason, as hydrogen combustion does not produce any CO_2. For the engines, a hydrogen-fueled turbofan was selected. This combustion engine offers the best efficiency at the transonic speeds that the aircraft is targeting. A fuel cell-electric option would offer a higher efficiency, but this option was foregone because of the higher weight, and great cooling requirements.

The development of a new engine requires a lot of research and development when using conventional kerosene. To develop an entirely new engine specifically for hydrogen would likely be too complex to produce a final product by 2040. Hence, a highly efficient kerosene engine was selected to be converted to a hydrogen engine. Conversion will be much simpler than designing a new engine from scratch. The favourable properties of hydrogen over kerosene mean that the amount of produced NO_x gasses is projected to go down by 75%, and the amount of thrust produced will be 5% higher after the conversion. The engine selected to be converted is the Trent 1000R as it offers a very high efficiency at the thrust level required for cruise.

To eliminate interaction between the engine exhaust flows and the truss structure, the engines could be placed out no further than seven meters from the centre line of the fuselage. To improve safety in case of failure of the engine mounting system, the engines were placed below and out in front of the leading edge of the wing. This will allow the engines to fly in front of, above and then around the wing safely.

For storage of the fuel, liquid hydrogen was the only realistic option. High-pressure hydrogen of between 300 and 700 bar would be preferred because of its significantly higher simplicity. However, the relatively low density and high forces on the tank mean that the tanks would become far too large and hefty to allow for any sustainable flight. Therefore, liquid hydrogen has to be used for its greater volumetric density. The hydrogen tanks are insulated with a vacuum layer, as this offers the best insulation for a small thickness, further limiting the tank size, and therefore weight. A smaller secondary tank is fitted to allow for one hour of flight in case the main tank's insulation were to fail. Because its size is already limited it can be insulated with a polyurethane foam, which offers higher reliability than vacuum insulation.

Stability and control

To ensure that WorldBus was stable and controllable, first the wing was placed resulting in a longitudinal position of the leading edge of the mean aerodynamic chord of 30 m. A trade-off for the empennage configuration resulted in a T-tail since WorldBus has a high-wing configuration, which greatly benefits performance. To establish the most aft and forward center of gravity (c.g) a loading diagram was created from which it became apparent that the hydrogen tank could not be located in the back of the aircraft, since this would create too large of a shift in c.g. Placing the fuel tank in the middle resulted in a most aft and forward c.g of 33.15 m and 31.50 m respectively. To size the horizontal tail a scissor plot was created which resulted in a value for the horizontal surface area over the wing surface area Sh/S of 0.08, which is low compared to reference aircraft which have a value of around 0.2. This can be explained by the fact that WorldBus has a large horizontal tail moment arm due to the lengthy fuel tank and also has a T-tail, both decreasing the surface area of the horizontal tail. This ratio results in a surface area of 28.4 m for the horizontal stabiliser. The vertical tail is sized based on three stability criteria, crosswinds, directional stability, and torque due to one engine failure resulting in a value of 0.096 for Sv/S and a vertical tail area of 35.6 m^2.

Lastly, the undercarriage is sized and placed, where the main landing gear is placed at a longitudinal position of 34.8 m and the nose gear at 14.4 m. Since jetbridges typically reach up to 5 meters, the scrape back angle was set to 9° to ensure easy boarding of passengers. To store the undercarriage it was decided to attach the main landing gear to the truss structure and store it in the cowling with the truss structure since storage in the wing is not possible.

Performance

The take-off distance was found to be 1299 m which is lower compared to reference aircraft this is due to a high $C_{L_{max}}$ at take-off and excess thrust. Furthermore, the landing distance was found to be 2830 m which is high but could be significantly reduced by using reverse thrust or spoilers. It was found that WorldBus can't fly at the optimal speed for range at an altitude of 9 km. However, to reach the 19 000 km in 20.5 hours, the extra fuel needed can be taken out of the secondary fuel tank. With the payload range diagram, it was verified that WorldBus has a harmonic range of 19 000 km and a limiting load factor of $n = 2.6$ was found through the load diagram.

Structures

For the fuselage, it was decided that no windows will be fitted to the outer skin. This will eliminate most of the stress concentrations in the skin, allowing for a much lighter fuselage. Instead, screens will be fitted to the inside of the cabins. These will provide a real-time artificial view of the outside to comfort passengers.
The material selected for the fuselage is a carbon-fibre-reinforced polymer (CFRP). This material was chosen as it offers a much lower weight to a more traditional aluminium structure. As every kilo that can be saved on this extremely high-range aircraft is very valuable, CFRP was seen as the best option. CFRP does come with one drawback compared to aluminium, which is its low electrical conductivity. This means that a metal mesh has to be fitted to the skin to minimise the damage caused by potential lightning strikes.
The fuselage skin will be reinforced with 180 stringers going longitudinally along the fuselage. Furthermore, formers will be fitted to keep the stringers and skin together in sheer loads. These formers have a pitch of 50 cm. Altogether this fuselage structure is estimated to weigh 197 kN which is 12.7% of the operating empty weight (OEW).

For the liquid hydrogen tanks, two different design philosophies were applied.
The main tank carries all the fuel required to reach the maximum range. Because this tank carries a large amount of hydrogen, a large effort has to be made to make the tank walls as thin and light as possible to limit the weight of the tank. For this reason, the hydrogen will be held in an inner tank, which is surrounded by a second tank separated by a vacuum. Vacuum insulation was chosen as it is an order of magnitude thinner than passive foam insulation. This lower thickness means that the inner radius of the tank can be a lot bigger allowing for a significantly shorter tank, and therefore fuselage. This means that the aircraft will be much lighter and more efficient. For the inner tank, high alloy steel was selected as it is one of the few materials that can withstand the freezing temperatures of liquid hydrogen, and offered the lightest inner tank design. For the outer tank, a CFRP tank was designed as it was over 50% lighter than a comparable steel tank.
The secondary tank is designed with a much smaller capacity than the main tank. As the secondary tank has a much smaller

capacity, more space is available for insulation. For these reasons, a polyurethane foam insulated tank was preferred as the foam is much more lightweight than a heavy vacuum chamber. The inner tank is again made of high alloy steel for the same reasons outlined before. The insulating foam that was selected is a polyurethane foam that was specially designed to withstand the temperatures of liquid hydrogen.
Inside the tanks, a heating system will be placed to control the amount of hydrogen that is boiled each second. The vaporised hydrogen can then be extracted from the tank and transported to the engines through a compressor. The heating system is required to provide 325 kW of power to the hydrogen to facilitate the amount of vaporisation required during cruise.
In total the hydrogen tanks are estimated to weight up to 340 kN which is 21.9% of the OEW.

Lastly, for the wing and truss design, a program was made that analysed the loads and stresses along the span of the wing. In order to find the optimal (lightest) truss and the wing configuration, the truss position was altered multiple times, and for each truss position the truss force was computed. Using the truss force and the wing loading, internal load distributions were found. This distribution then allowed a stress analysis to be performed. To ensure that not a point along the wingbox failed, the thickness of the wingbox was increased until no failure occurred anywhere under the given load of 2.6 times the maximum take-off weight. After having found the final wingbox thickness for a given truss position, the total wing and truss weight was computed. This process was done for each truss position and the lightest configuration was taken to be optimal. Below in Table 2, the final values for the wing configuration are displayed.
In total the wing structure including the truss is estimated to weight up to 418 kN which is 26.8% of the OEW.

Table 2: Description of the wing results

Truss Length [m]	Weight [kg]	Wingbox thickness [mm]	Truss position from nose [m]
17	42561	26	36

The weights shown in Table 2, can be further optimised considering the inclusion of stiffeners along the wingbox, performing a fibre orientation analysis and including more accurate truss loading scenarios.

Materials and manufacturing

For the structures of the fuselage, wings, and the majority of the hydrogen tank CFRP was selected as the best material. The material offers better performance by such a large margin that it is almost inescapable. The main drawback of CFRP is first and foremost the much higher cost. Furthermore, the production of the material is highly energy intensive, with a large amount of associated CO_2 emissions. Lastly, CFRP is more difficult to inspect for wear. The microcracks that are usually relied on when inspecting aluminium are less likely to form for example. However, these drawbacks are largely outweighed by the high associated performance. The concern with regard to recycling is currently still very relevant. But recent developments are very promising, somewhat alleviating this concern.

The assembly of CFRP is generally simpler than metal structures. Larger parts are used with fewer fasteners and connection points. This significantly reduces the labour costs associated with production. Labour costs are further reduced by utilizing a lot more automated production methods like resin transfer moulding and automated tape laying. The methods will increase the required investment upfront, but lead to a much lower operating cost.

The production plan for the whole aircraft can be split into three main phases. In phase one, eight parallel stations are put up. These stations make sub-assemblies for things like the wing, fuselage, engine, or avionics. A parallel working structure is preferred here for two main reasons. First, it means that if one station is slightly delayed, the other stations can continue working as the other catches back up. Secondly, a parallel structure means that more stations working on identical products can be set up, to synchronise the delivery interval of all sub-assemblies.
The second phase of the production plan involves the transportation of all sub-assemblies to the main assembly plant. The phase will first move the subassemblies to their temporary storage location at the assembly plant.
In the final stage, the sub-assemblies are moved out of their temporary storage and assembled to the aircraft in order. The time between the finishing of a subassembly and it being assembled onto the aircraft should be minimised as much as possible to reduce the required storage space and cost.

At the final assembly plant, 300 aircraft have to be produced in 20 years. With a projected assembly time of one month per aircraft, this means that at least two aircraft will be undergoing assembly at the same time at the plant at any given time. The other stations will be scaled to fit this monthly delivery interval of two aircraft.

Sustainability analysis

The driving factor behind the development of the WorldBus is sustainable long-distance travel. Hence, it was essential to check whether these goals have been met. As Carbon Fibre Reinforced Polymer (CFRP) has been chosen as the primary

material, research was conducted into its manufacturing, production, repair and recyclability characteristics. Greenhouse gas (GHG) emissions per kg of material from producing CFRP are 9 times greater than that of steel and 3 times greater than that for aluminium. However, using reusing parts and recycled materials from decommissioned aircraft reduces this number significantly. As CFRP has just been gaining major traction in the aviation market, much research must still be conducted on its recyclability. As of today, from a complete aircraft, only 38% of composite structures will be recyclable. However, CFRP recycling is a rapidly developing field of technology, and with the first WorldBus only being decommissioned in 2060 this number is sure to increase.

Next, operations were evaluated. When looking into different types of hydrogen it becomes clear that the most used hydrogen of today, grey hydrogen, will not be acceptable for WorldBus. This is due to the fact that during the production of grey hydrogen a lot of CO_2 is emitted. Taking into account the amount of hydrogen required for a flight, this would lead to WorldBus emitting twice the amount of greenhouse gases compared to a Boeing 787-9 per passenger per km. The only difference is that the emissions are displaced to production, rather than operation. Then, the production of green hydrogen was investigated. Green hydrogen is made using electrolyis and uses green energy. Currently, only 0.5 mt of green hydrogen are produced per year, but since it is expected that green hydrogen production will increase a hundredfold by 2040, it is reasonable to expect WorldBus to fly on green hydrogen. The global warming potential (GWP) for the 787 is compared to the WorldBus, showing this design provides a reduction of 97% in GWP per passenger per km during flight.

Lastly, noise emissions are investigated. This does not consist of a completely accurate analysis, but rather an indication and methodology to analyse the noise produced by the airframe and engines. It was determined that the team aims for a similar or lower noise level as produced by the Boeing 787-9. Then, a methodology was discussed to determine the noise emissions of different aircraft components. Research regarding noise emission by truss-braced aircraft has also already been conducted, and the results are promising. The truss seems to act as a shield reflecting some noise produced by the engines and thus reducing total noise emissions. However, it must be noted that further research should be conducted in order to better understand this phenomenon.

Operations

A key requirement for WorldBus is ensuring passengers can travel from entry in the departure airport until exit from the arrival airport in less than, or equal to, 24 hours. All operations to be performed by the passengers before departure and after arrival take a part out , of 3.5 hours, of these 24 hours. Thus, in order to determine the maximum flight time, the operations for a passenger has been linked to a passing time to determine the time left for the flight. Next to this, WorldBus aims to reduce its environmental impact, and therefore it was investigated how this can be reduced during aircraft ground operations.

Starting with the latter two main innovations are expected to improve the aircraft's sustainability. An electrical green taxiing system and a ground power unit. After evaluation, the best option for an electrical green taxiing system would be an external system in order to reduce aircraft weight.

Innovations regarding passenger operations showed great potential in waiting time reduction and are therefore expected to widely be used at major airports in 2040. These innovations include biometric identification, self-service check-in and 4-door boarding. After taking all times into account it should be recommended that passengers arrive 2 hours prior to departure, and reserve up to 1 hour after disembarking for airport operations. Taking taxiing times into account as well, this results in an available flight time of 20 hours and 30 minutes.

Lastly, time was spent evaluating operations related to hydrogen production and storage. Agreements to develop hydrogen infrastructure around airports exist and plausible storage tanks are available. This should therefore not pose a threat to the choice of using liquid hydrogen as a fuel for WorldBus.

Design sensitivity analysis

For the complete design a sensitivity analysis has been performed. The parameters varied are range, velocity, altitude, passenger number, aspect ratio, tank placement and wing placement. All parameters are varied in positive and negative directions and their impact on the maximum take-off weight (MTOW) is quantified. From these analyses, it can be seen that no large fluctuations exist in the MTOW when small changes in input variables are made. Table 3 shows an example of a sensitivity analysis when changing range. Similar results are seen for the other input values and can be found in Chapter 17. Also, when looking at the results after the variation in input variables, it should be noted that WorldBus uses the most optimal value for the MTOW in each case. This is either due to having the lowest weight, or due to the fact that certain requirements are not met when these input variables are changed. It was found only for the aspect ratio that the currently used value does not result in an optimised MTOW based on the models used. This might be a product of the assumption that wing thickness is constant. It is recommended that 'decision parameters' (parameters which are

determined by a design choice) are investigated in more detail during further design stages.

Table 3: Results of the passenger number sensitivity analysis. The WorldBus design parameter is indicated in grey. An increase in weight and size is indicated in orange, a decrease in weight and size in green.

Range [km]	Change	MTOW [mt]	Change	Span [m]	Change
18 000	- 5.3%	215.2	- 3.8%	70.5	- 2%
19 000	-	223.8	-	71.9	-
20 000	+ 5.3%	238.4	+ 6.5%	74.2	+ 3.2%

RAMS

It is crucial to ensure the reliability, availability, maintainability and safety of the aircraft (RAMS) and its operations. Characteristics of WorldBus that differ from conventional aircraft might pose questions about whether the design is attainable while being reliable, available, maintainable and safe. For this reason, the RAMS characteristics were established and refined, reflecting the actual design.

All aspects of the design were analysed and considered for either reliability, availability, maintainability or safety reasons, or for multiple of these characteristics. Aspects considering the ways WorldBus differs from conventional aircraft are considered that might pose a threat to the RAMS of the aircraft. The CS-25 regulations were studied and a careful analysis of the design is done to obtain the elements of the design that might pose a threat. The aspects that differ from other conventional aircraft were investigated and were either disproved to be a threat to the design or a solution was found that was included in the design to mitigate the threat. The element that was found to be the most problematic is the fuel system which is only sensible as it bring many problems and much considerations with it as this is an innovative design concept.

Risk management

As the design progressed additional risks were identified. In the final design stage of WorldBus, risks regarding costs, scheduling, and technical performance have been found. The following new risks have been identified:

- R-C-06: Incorrect market assessment (3 & 5)
- R-C-07: Increasing fares (4 & 2)
- R-S-01-4: Increased engine modification time (3 & 2)
- R-S-06: Maintenance delays (3 & 2)
- R-P-08-1-e: Unsuitable fuel conditions (1 & 4)
- R-P-09-8: Pylon failure (1 & 4)
- R-P-10.1-7: Fuel sensor failure (2 & 3)
- R-P-11-3: Defect lavatories (1 & 3)
- R-P-11-4: Malfunctioning cabin screens (2 & 4)

The identified risks have been mitigated. These have to do with, for instance, installing fail-safe backup systems, and verification and validation practices during maintenance.

Future design phases

Concluding the report the future design phases of the WorldBus are discussed. The team provides a project design and development logic showing the to-be-completed activities after completion of the Design Synthesis Exercise (DSE). This is also shown in more detail using a Gantt chart to emphasize the time constraints related to various activities.

Finally, the support needed during the mission of the WorldBus is investigated and displayed using a block diagram. The main aircraft operations and possible maintenance operations are visualised.

Contents

Nomenclature

Symbols

Symbol	Definition	Unit
α	Angle of attack	[deg]
a_0	Speed of sound at sea-level (ISA)	[m/s]
A	Aspect ratio of main wing	-
$A_{element}$	Area of a wing element	[m^2]
A_m	Mean area	[m^2]
A_{tot}	Total Wing Area	[m^2]
A_w	Wing area	[m^2]
AMS	Achievable market share	-
AR	Aspect ratio	-
AR_h	Aspect ratio horizontal tail	-
b	Wingspan	[m]
b_h	Span horizontal stabiliser	[m]
B_r	Boom Area	[m^2]
b_v	Span vertical tail	[m]
$\frac{b_E}{b_h}$	Elevator span-to-tail span ratio	-
c	Speed of sound	[m/s]
C	Clamping factor	-
C_D	Drag coefficient (wing)	-
C_{D_0}	Zero-lift drag	-
$C_{D_{lift}}$	Lift induced drag coefficient	-
$C_{D_{misc}}$	Miscellaneous drag coefficient	-
C_d	Drag coefficient (airfoil)	-
$C_{L_{A-h}}$	Lift coefficient of aircraft without tail	-
C_{L_α}	Lift curve slope	-
$C_{L_{\alpha_h}}$	Lift curve slope of horizontal tail	-
$C_{L_{\alpha_{A-h}}}$	Lift curve slope of main wing	-
C_{L_h}	Lift coefficient of horizontal tail	-
$C_{L_{des}}$	Design lift coefficient	-
$C_{L_{des,M=0}}$	Zero Mach design lift coefficient	-
$C_{l_{\delta_\alpha}}$	Aileron control derivative	-
C_{l_p}	Roll damping coefficient	-
$C_{L_{max}}$	Maximum lift coefficient (wing)	-
$C_{l_{max}}$	Maximum lift coefficient (airfoil)	-
$C_{p,0}$	Lowest absolute value of pressure	-
C_p	Airfoil Element Pressure Coefficient	-
$C_{p,cr}$	Critical pressure coefficient	-
$C_{p,min}$	Minimum pressure coefficient of an airfoil	-
$C_{m_{ac}}$	Pitching moment coefficient around aerodynamic centre	-
$\frac{C_E}{C_h}$	Elevator chord-to-tail chord ratio	-
C_f	Skin friction coefficient	-
$\tilde{c}$	Mean aerodynamic chord length	[m]
$c(y)$	Local chord length along span	[m]
c_{d_0}	Zero-lift drag coefficient (airfoil)	-
c_{l_α}	Lift curve slope (airfoil)	-
c_r	Root chord	[m]
c_t	Tip chord	[m]
$\frac{c_f}{c}$	Chord and flaps ratio	-
D	Outer Tube Diameter	[m]

Symbol	Definition	Unit
d	Inner Tube Diameter	[m]
d_i	Inner tank diameter	[m]
d_f	Fuselage outer diameter	[m]
DOC	Direct operational costs	[EUR]
DPC	Development and production costs	[EUR]
e	Oswald efficiency factor	-
E	Young's modulus	[Pa]
F_{flaps}	Flap geometry factor coefficient	-
F_t	Force on trust	[N]
FF_c	Component form factor	-
g	Gravitational constant	[m/s^2]
h_{sc}	Screen height	[m]
IF_c	Component interference factor	-
I_{xx}	Area Moment of Inertia about x-axis	[m^4]
I_{zz}	Area Moment of Inertia about z-axis	[m^4]
I_{xz}	Product Moment of Inertia	[m^4]
k	Thermal Conductivity	[W/mK]
K	Limiting stress of material	[Pa]
I	Moment of inertia	[kg m^2]
l_f	Fuselage length	[m]
l_h	Moment arm of horizontal tail	[m]
L_s	Length along y-axis truss	[m]
L_t	Length truss	[m]
l_v	Longitudinal distance between vertical tail and wing aerodynamic chords	[m]
M^*	Critical Mach number	-
M	Mach number	-
M	Bending moment	[Nm]
MAC	Mean aerodynamic chord	[m]
MP	Market price	[EUR]
MV	Market volume	-
M_{cr}	Critical Mach number	-
M_{dd}	Drag divergence Mach number	-
M_F	Mass fuselage group	[kg]
MV	Market volume	-
M_W	Mass wing group	[kg]
M_x	Moment about x-axis	[Nm]
M_z	Moment about z-axis	[Nm]
n	Load factor	-
n_e	Number of engines	-
n_{ult}	Ultimate load factors	-
p	Internal pressure	[Pa]
P_{cr}	Critical buckling stress	[N]
p_e	Effective pressure	[Pa]
p_{e_0}	Effective pressure reference	[Pa]
p_p	Proof pressure	[Pa]
P	Roll rate	[deg/s]
P_{mw}	Static load per main gear wheel	[N]
P_{nw}	Static load per nose gear wheel	[N]
q	Dynamic pressure	[Pa]
q	Shear flow	[N/m]
q	Heat flow	[W]
qs_0	Shear flow constant	-
$2r_1$	Depth of fuselage near vertical tail	[m]
R	Radius	[m]
Re	Reynolds number	-
ROI	Return on investment	%

Symbol	Definition	Unit
S	Wing area	[m^2]
σ_z	Normal Stress	[Pa]
σ_{cr}	Buckling Stress	[Pa]
S_h	Horizontal stabiliser area	[m^2]
S_{wet_c}	Wetted area of analysed component	[m^2]
S_{Wf}	Wetted area fowler flaps	[m^2]
SF	Safety factor	-
$\frac{S_{flap}}{S_{ref}}$	Ratio of wing flapped area and wing area	-
θ	Element Angle	-
τ	Shear Stress	-
t	Skin thickness	[m]
t_{10}	Duration of flyover	[s]
t_i	Tank shell thickness	[m]
t_{ins}	Insulation thickness	[m]
T	Thrust	[N]
T	Temperature	[K]
T	Torsional moment	[Nm]
T_{rev}	Reverse thrust	[N]
T_{dis}	Disembarking time	[min]
T/W	Thrust-over-weight ratio	-
t/c	Thickness over chord ratio	-
v	Poisson's ratio	-
v	Welding efficiency	-
V	Velocity	[m/s]
V_{ap}	Approach speed	[m/s]
V_{cruise}	Cruise velocity	[m/s]
V_{LOF}	Lift-off speed	[m/s]
V_h	Velocity at horizontal surface	[m/s]
V_x	Internal shear force	[N]
V_z	Internal shear force	[N]
W	Weight	[N]
W_{tot}	Total Wing Weight	[N]
W_{TO}	Take-off weight	[N]
x_{brake}	Braking distance	[m]
X_{FCG}	Longitudinal position of fuselage group center of gravity	[m]
x_{LEMAC}	Longitudinal distance between AC nose and LEMAC	[m]
$\tilde{y}$	Vertical location	[m]
y_e	Lateral distance between AC centerline and engine	[m]
α	Angle of attack	[deg]
$\alpha_{L=0}$	Zero-lift angle of attack	[deg]
α_s	Stall angle	[deg]
α_{des}	Design angle of attack	[deg]
β	Prandtl-Glauert compressibility factor	-
β	Sideslip angle	[deg]
Γ	Dihedral angle	[deg]
γ	Specific heat ratio	-
γ_{ap}	Approach angle	[deg]
γ_{climb}	Flight path angle during climb	[deg]
δ_{flap}	Flap deflection angle	[deg]
ϵ	Downwash	[deg]
θ	Polar directivity	[deg]
θ	Angle with y-axis of truss	[deg]
κ	Airfoil efficiency factor	-
Λ	Sweep	[deg]
$\Lambda_{0.25c}$	Quarter-chord sweep	[deg]
Λ_h	Horizontal stabiliser sweep	[deg]
$\Lambda_{hingeline}$	HLD hingeline sweep	[deg]

Symbol	Definition	Unit
Λ_{LE}	Leading edge sweep	[deg]
λ	Taper ratio	-
λ_h	Taper ratio horizontal stabiliser	-
μ_r	Friction coefficient	-
ρ	Density	[kg/m^3]
σ	Sidewash	[deg]
σ	Stress	[Pa]
σ_{boom}	Stress of boom	[Pa]
σ_{circ}	Circular stress	[Pa]
σ_{long}	Longitudinal stress	[Pa]
τ	Aileron effectiveness	-
τ	Shear stress	[Pa]
ϕ	Azimuthal directivity angle	[deg]
ϕ_h	Dihedral angle horizontal stabiliser	[deg]

Abbreviations

Symbol	Definition
AC	Aircraft
ANOPP	Aircraft Noise Prediction Program
APU	Auxiliary power unit
BAT	Battery
CAD	Computer-Aided Design
CAMP	Continuous airworthiness maintenance program
CAPEX	Capital expenses
CFRP	Carbon-fibre reinforced polymer
CC	Conventional Configuration
CO_2	Carbon dioxide
COVID	Coronavirus Disease
CoG	Center of gravity
CS-25	Certification Specification for Large Aircraft
DAPCA	Development and Procurement Costs of Aircraft
DISE	Design Integration and Systems Engineering
DOT	Design option tree
EASA	European Union Aviation Safety Agency
EGTS	Electric green taxiing system
EMER	Emergency
EPNdB	Effective Perceived Noise levels
ESS	Essential
FAA	Federal Aviation Authority
FBS	Functional breakdown structure
FEM	Finite Element Method
FFD	Functional flow diagram
GEN	Generator
GGE	Greenhouse gas emissions
GHG	Greenhouse gas
GLARE	Glass reinforced laminate
GPU	Ground power unit
GWP	Global warming potential
H_2	Hydrogen
H_2O	Water
HLD	High lift device
HUD	Heads Up Display
INV	Inverter
JFK	John F. Kennedy airport

Symbol	Definition
L	Left
LCN	Load classification number
LE	Leading Edge
LEMAC	Leading edge mean aerodynamic chord
LH_2	Liquid hydrogen
LLT	lifting line theory
MAC	Mean aerodynamic chord
MIT	Massachusetts Institute of Technology
MLI	Multi layer insulation
MTOW	Maximum take-off weight
NO_x	Nitrous oxides
OEW	Operating empty weight
OEWCG	Operating empty weight centre of gravity
OPEX	Operating Expenses
OSHA	Occupational Safety and Health Administration
PAA	Propulsion airframe aeroacoustic
pax	Passenger
PNL_{max}	Maximum perceived noise level
PRV	Pressure relief valve
R	Right
RAMS	Reliability, availability, maintainability, and sustainability
R&D	Research and development
ROI	Return on investment
SPL	Sound pressure level
SSCI	Self-service check-in
TCI	Traditional check-in
TRU	Transformer Rectifying Unit
TTBW	Transonic truss-braced wing
USA	United states of america
VLM	Vortex lattice method
WB	Wingbox

1 Introduction

Greenhouse gas emissions pose an ever-growing problem to the climate. In the European Union alone, aviation contributes 3.8% of the total CO_2 emissions.[3] Eurocontrol has released a long-term forecast predicting a 40% increase in flight numbers compared to 2019 levels.[4] This shows aviation is one of the fastest growing contributors to worldwide greenhouse gas emissions (GGE). Thus, action is needed to reduce the impact of aviation on Earth's climate.

Contrary to the aviation sector, sustainable alternatives for ground transportation are plentiful, ranging from ride-sharing initiatives to public transportation, and from battery-electric vehicles to trains. However, the aviation sector has yet to find a sustainable alternative for long-distance travel. WorldBus aims to be the first aircraft capable of flying between any major airport worldwide whilst reducing its environmental impact by 90% compared to current long-haul aircraft. As of today, research into long-distance flights is limited. WorldBus will identify the feasibility of performing sustainable long-distance flights and identify which areas require additional research for the realisation of sustainable long-haul concepts.

WorldBus will allow passengers to travel the required distance within 24 hours from the departure airport door to the arrival airport door. The aircraft shall carry 200 passengers comfortably and fly 4000 hours per year, for at least 20 years. The WorldBus will cost EUR 484 million for a production size of 300 units, of which the first shall enter service in 2040. The mission will be performed using sustainable propulsion methods. However, the sustainability of an aircraft also entails the production process, service life, and end-of-life. To prolong the service life, WorldBus will be made of durable materials, such as carbon fibre-reinforced polymer and high alloy steel.

To provide a clear overview of the final design, Chapter 2 showcases WorldBus in its final shape. Then, the mission is explained in Chapter 3. After that, a review of the financial feasibility of the mission is performed in Chapter 4, followed by the sustainable development strategy in Chapter 5. With the frame and context of the design project established, Chapter 6 details out all design options and describes the process behind the decision for the final configuration. The various design processes and design inter-dependencies involved in the design of WorldBus are treated in Chapter 7. From there on, the detailed designs of the various relevant disciplines are treated. Firstly, the aerodynamics analysis of the design is explained in Chapter 9, focusing on the determination of the aerodynamic properties of the aircraft. The selected engine type and necessary modifications, and its location on the wing are discussed in Chapter 10. After that, the analysis of the WorldBus stability and control can be found in Chapter 11. Here, the wing is positioned, and the stabilisers and undercarriage are designed. The process behind the design regarding performance is explained in Chapter 12, where the airfield, flight, and climb performances are discussed. Furthermore, the payload-range and load diagrams are included. With the general subsystem designs known, the focus is shifted. Firstly, the structural designs of the fuselage, the fuel tanks, and the truss-braced wing are detailed and elaborated upon in Chapter 13. Expanding upon the structural designs, the materials and the manufacturing methods are selected in Chapter 14. Furthermore, the production plan and productional analysis are included.

Moving away from the detailed design, Chapter 20 contains the compliance matrix, which communicates the current compliance of the design with the established user requirements. To determine the sustainability of the WorldBus design and verify whether it meets requirements REQ-USER-SUS-01, the design sustainability analysis is included in Chapter 15. Furthermore, the operations related to travel by aircraft are discussed in Chapter 16. To verify the stability of the WorldBus design for varying input parameters, a sensitivity analysis is performed in Chapter 17. Reliability, availability, maintainability and safety characteristics (RAMS) are critically explored in Chapter 18 to ensure that the design has the most optimal and safe performance. In Chapter 19, possible risks are identified for which a contingency plan is devised. In Chapter 21, the development strategy after this design phase is discussed for which the future processes of the development and manufacturing phases are identified. Lastly, the conclusion and recommendations are given in Chapter 22.

[3] https://climate.ec.europa.eu/eu-action/transport-emissions/reducing-emissions-aviation_en
[4] https://www.eurocontrol.int/article/understanding-impact-climate-change-aviation

2

Final design

Over a period of 10 weeks, the team has worked on designing a fast, long range, sustainable aircraft. The accumulation of all of this work is a novel solution named WorldBus. A truss-braced aircraft that offers a drastic reduction in emissions, with a higher range than the all advanced aircraft on the market. WorldBus is truly one-of-a-kind, the final design can be seen in Figure 2.1. This chapter showcases the most important aspects of the aircraft and provides a concise overview. Moreover, the system characteristics are given, which include systems like the electrical layout and the fuel layout, among other systems. The remaining chapters in the technical report provide calculations and analyses to support the engineering decisions that were made and give a more detailed overview of all the technical aspects of the design. At the end of the report a technical drawing of WorldBus is included in Appendix E, which summarises the important dimensions of the aircraft.

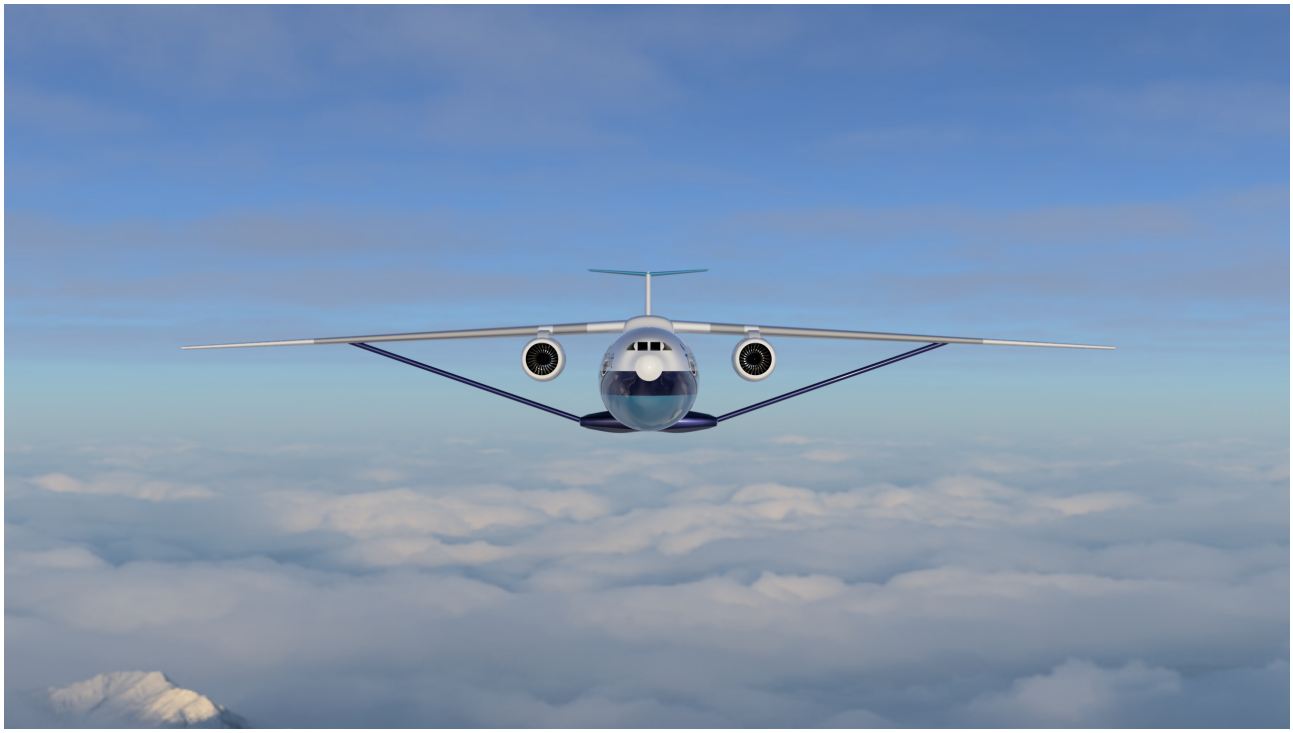

Figure 2.1: Render of WorldBus.

2.1. Design parameters

In this section, the performance characteristics of WorldBus are shown and some design parameters are given for the weight breakdown, finances, fuselage shape, internal layout, wing dimensions, empennage design and propulsion characteristics.

Mass breakdown

The WorldBus will carry 200 people minimum, each person accounting for 100 kg, luggage and bodyweight included. Furthermore, the fuel mass will provide the aircraft with a range of 19 000 km. Overall, the aircraft will be 4000 kg lighter than the current top-of-the-line, Boeing 787-9 Dreamliner. Table 2.2, gives an overview of the weight distribution of the WorldBus design.

Finances

Compared to today's aircraft prices of 300-350 million, the WorldBus will be on the expensive side, with a listing price of EUR 484 million. However, this is justified by the many innovative properties the aircraft comes with; extreme comfort, revolutionary sustainability and non-stop worldwide range. Despite the high price, this project would be very profitable for any airline willing to invest in the future of aviation, WorldBus.

Table 2.1: Finance parameters

Parameter	Value	Unit
Return on investment (ROI)	90%	-
Listing price	484	[million EUR]
Fixed operational cost / flight	16194	[EUR]
Variable operational cost / hr	7463	[EUR]
Manufacturing cost	410.5	[million EUR]
Research & development cost	29.7	[million EUR]
Number of aircraft in fleet	300	-

Table 2.2: Mass parameters

Parameter	Value	Unit
MTOW	223780	[kg]
OEW	158585	[kg]
Fuel	45186	[kg]
Payload	20007	[kg]

Fuselage design

WorldBus' fuselage contains passengers, crew, cargo and fuel. One thing that stands out is the length of 75.3 m, making WorldBus one of the longest transport aircraft. The fuselage of WorldBus is comparable in size to an Airbus A380 with a smaller diameter. Table 2.3 shows a number of fuselage parameters.

Internal layout

WorldBus makes use of a unique and innovative cabin layout. Not only does the fuselage have two floors, but there are two separate cabins. One cabin is right behind the cockpit, and another is at the end of the plane. In between the two cabins, the main fuel tank is located. Then, as WorldBus is designed to fly up to 19 000 km, distances that can take up to 21 hours, WorldBus is fitted exclusively with Economy+ and Business class seats that provide enough room for a comfortable flight for passengers. Even though WorldBus carries only 200 passengers, it still has two aisles since a large part of the fuselage is occupied by the hydrogen fuel tank.

Table 2.3: Fuselage parameters.

Parameter	Value	Unit
Tail cone length	21.9	[m]
Nose cone length	12.5	[m]
Fuselage length	75.3	[m]
Fuselage diameter (outer)	6.25	[m]

Table 2.4: Layout parameters

Parameter	Value	Unit
# of business seats	80	-
Business seat pitch	1.51	[m]
Business seat width	0.538	[m]
# of economy+ seats	120	-
Economy+ seat pitch	0.97	[m]
Economy+ seat width	0.478	[m]
# of emergency exits	12	-
# of aisles	2	-
# of toilets	8	-

Wing Design

The wing design of the WorldBus is also pushing engineering boundaries. WorldBus has wide, slender, highly swept, truss-braced wings. Moreover, a high-wing configuration is used to house the truss. The high sweep of the wing delays the occurrence of shockwaves on the wings. Shockwaves are prominent in the transonic regime and increase drag significantly, and thus are crucial to mitigate. Table 2.5 contains values for various wing planform parameters.

Truss

The truss is one of the most important components of the WorldBus design. As the truss carries a large part of the load, the wing is alleviated from some of the structural loads. Because of this, the wingspan can be increased, weight is decreased and a more efficient overall design is achieved for WorldBus.

Table 2.5: Wing planform parameters.

Parameter	Value	Unit
LE wing sweep	32.7	[deg]
Wing taper ratio	0.3	-
Wing span	71.9	[m]
Wing area	369.4	[m]
Wing dihedral	-2.11	[deg]
Wing aspect ratio	14	-

Table 2.6: Truss parameters.

Parameter	Value	Unit
Truss length	16.9	[m]
Position from nose	36.1	[m]
Spanwise connection	20.8	[m]
Load carried	2452329	[N]

Control surfaces

Various control surfaces and high lift devices (HLD) are used on the WorldBus. A combination of flaps and slats were used to reach the necessary C_{Lmax}. In Table 2.7, some geometrical properties of the control and HLDs used on the WorldBus are displayed.

Empennage Design

The WorldBus has a T-tail due to its high wing position. This allows for a more efficient pitch control, and higher stall angle of attack, as the downwash from the wing does not affect the flow over the horizontal tail, due to its higher position.

Table 2.7: Control surfaces parameters

Parameter	Value	Unit
Flaps length	10.6	[m]
Flaps chord	1.9	[m]
Slats length	15.8	[m]
Slats chord	0.6	[m]
Elevator length	5.3	[m]
Elevator chord	0.8	[m]
Rudder span	5.9	[m]
Rudder chord	1.8	[m]
Aileron span	6	[m]

Table 2.8: Empennage data

Parameter	Value	Unit
Horizontal tail area	27.8	[m^2]
Vertical tail area	35.6	[m^2]
Position from nose	70.5	[m]

Performance

In Table 2.9 some of the main performance characteristics of this aircraft are shown. The WorldBus will be the commercial aircraft with the longest range ever to be produced. Furthermore, the emission reduction value, is a percentage reduction in emissions compared to today's long range aircraft, like the B787-9, or A350-1000.

Table 2.9: Performance data

Parameter	Value	Unit
Stall speed	72.3	[m/s]
Cruise speed	265	[m/s]
Cruise altitude	9	[km]
Max speed	338	[m/s]
Max altitude	15.3	[km]
Emission reduction	97	[%]
Range	19000	[km]
Flight duration	20.5	[hrs]

Propulsion design

The WorldBus will be the first hydrogen-powered long-haul aircraft to exist. It is powered by a modified Trent-1000 engine, that now takes gaseous hydrogen as its fuel. The cryogenic liquid hydrogen tanks necessary to store the fuel, are placed in the centre of the fuselage, in the middle of the two passenger cabins.

Table 2.10: Tank data

Parameter	Value	Unit
Main tank length	23.9	[m]
Main tank diameter	5.7	[m]
Second tank length	5.06	[m]
Second tank diameter	5.06	[m]

Table 2.11: Engine data

Parameter	Value	Unit
Nacelle diameter	3.8	[m]
Nacelle length	6.2	[m]
Spanwise position	7	[m]
Max thrust	380	[kN]

2.2. System interfaces

This section provides an overview of the different system interfaces that are part of the WorldBus design. First, the electrical architecture is given, showcasing the different electrical components in the aircraft. This is followed by a hydraulic system layout. Then, the interactions between hardware & software within the aircraft are shown. Following this, an overview of the environmental control is given. Finally, a fuel system layout is shown that displays how the liquid fuel is moved from the fuel tank to the engines.

2.2.1. Electrical system

In Figure 2.2, the electrical block diagram is showcased. This shows all the aircraft systems that rely on electrical power from the aircraft. This gives both a high and low-level overview of the electrical systems in the aircraft. In the low-level diagram, various electrical buses (black rectangles) can be seen, these act as junction points, where input electricity can be transferred to other electrical systems. In the case of an aircraft, systems like the cabin lighting, the cockpit screens and more, would each be connected to a bus to receive the power they need.

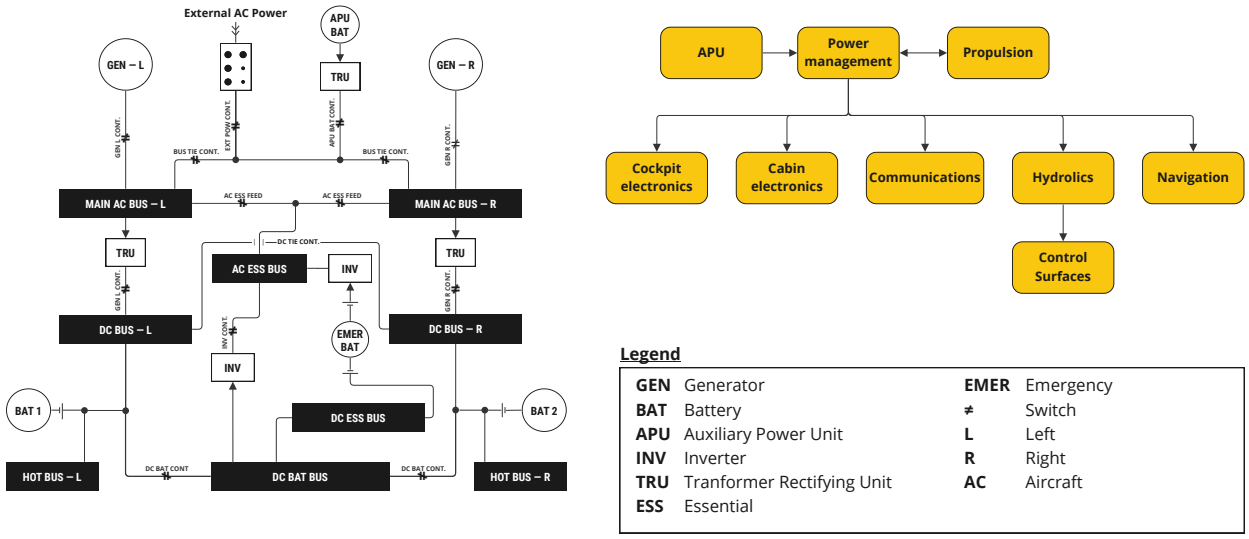

Figure 2.2: Electrical block diagram of aircraft.

2.2.2. Hydraulic system layout

In Figure 2.3, the hydraulic system layout diagram is shown. This diagram shows the preliminary makeup of the hydraulic systems, emphasizing the redundancies designed in the system, the fluid flow, and the components it attends.

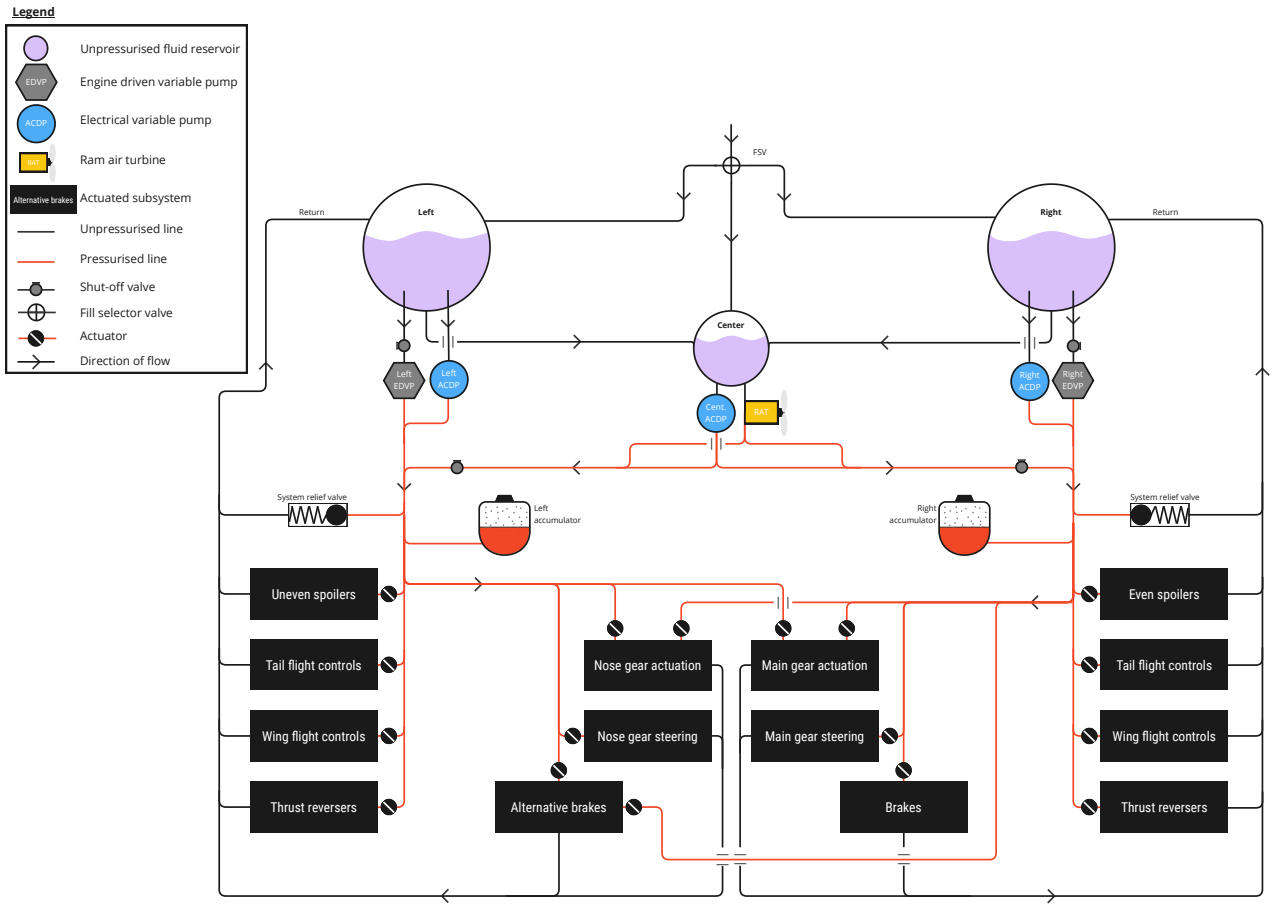

Figure 2.3: Hydraulic system layout of aircraft.

2.2.3. Hardware & software

In Figure 2.4, the relations between the hardware components and the various software systems on board of the aircraft are shown. The arrows show the flow of information or signals from sensors to software, to actuators etc. This allows for a greater understanding of the aircraft system as a whole and facilitates the integration of each system into the general structure of the aircraft.

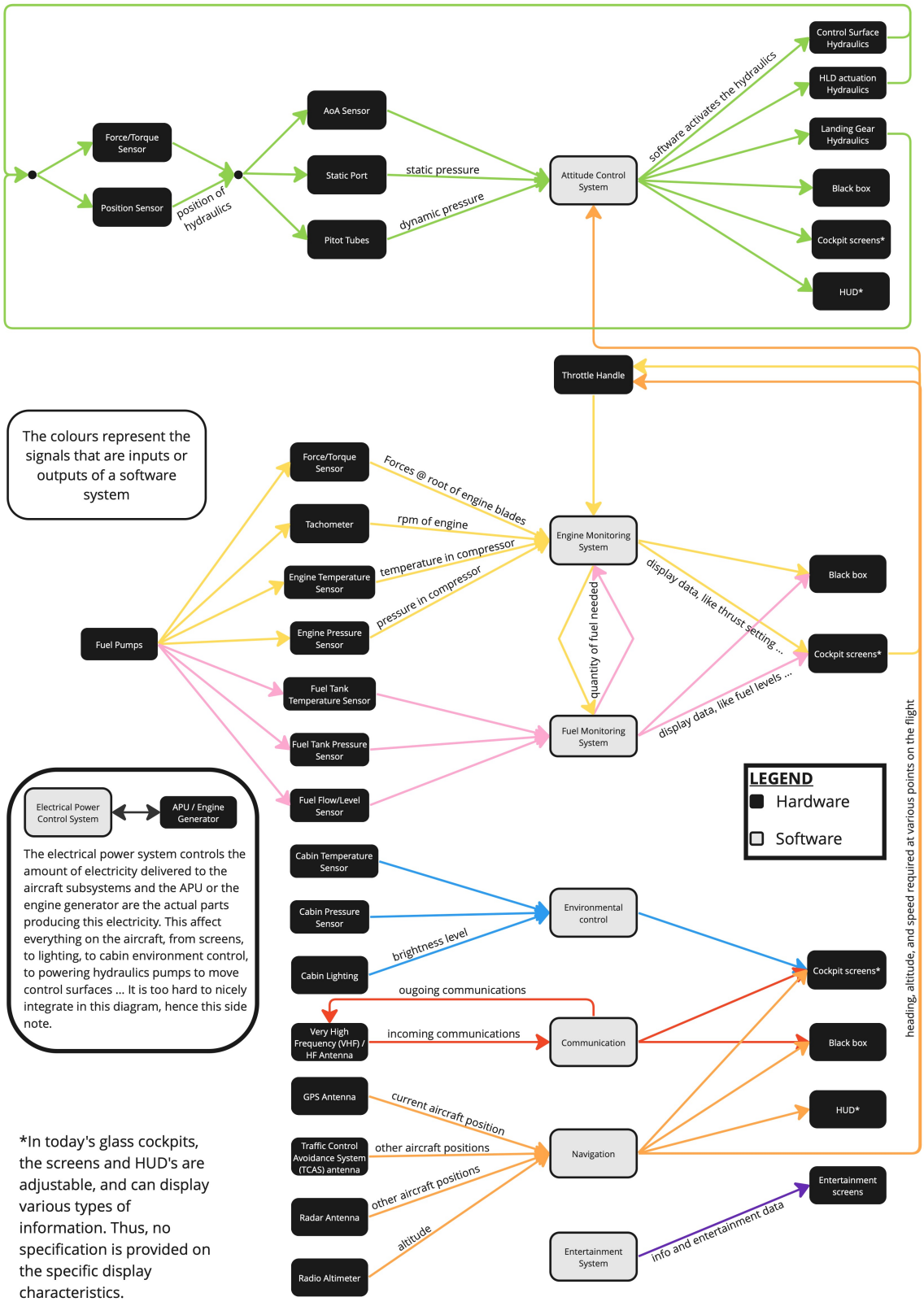

Figure 2.4: Hardware and software block diagram

2.2.4. Data Handling

In Figure 2.5, the flow of data from inside the aircraft, from the aircraft to the ground, and from ground to aircraft, is displayed. Additionally, it is shown through which hardware the data is passed before transmitted to the respective destination.

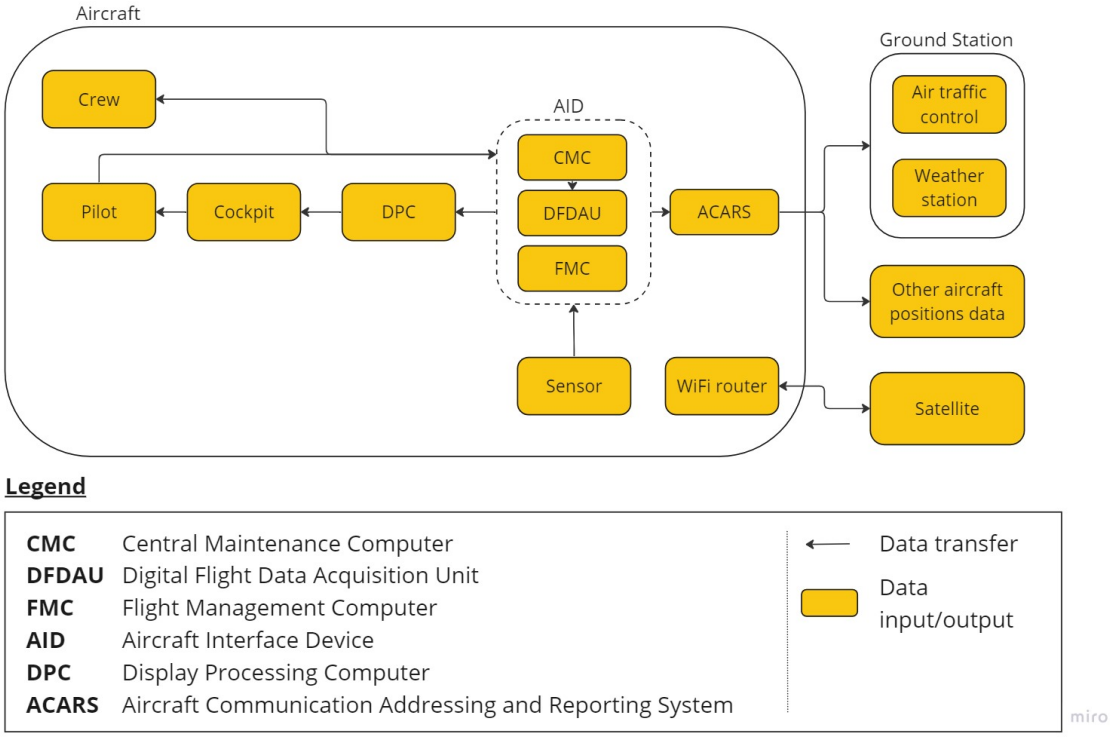

Figure 2.5: Data handling block diagram

2.2.5. Environmental control

In Figure 2.6, the functioning of the cabin environmental control system is displayed. This system controls the temperature and pressure of the cabin, by providing the perfect mix of outside air and current cabin air. The air is passed through multiple heat exchangers to reach the necessary air temperature. In this case, the arrows represent the airflow.

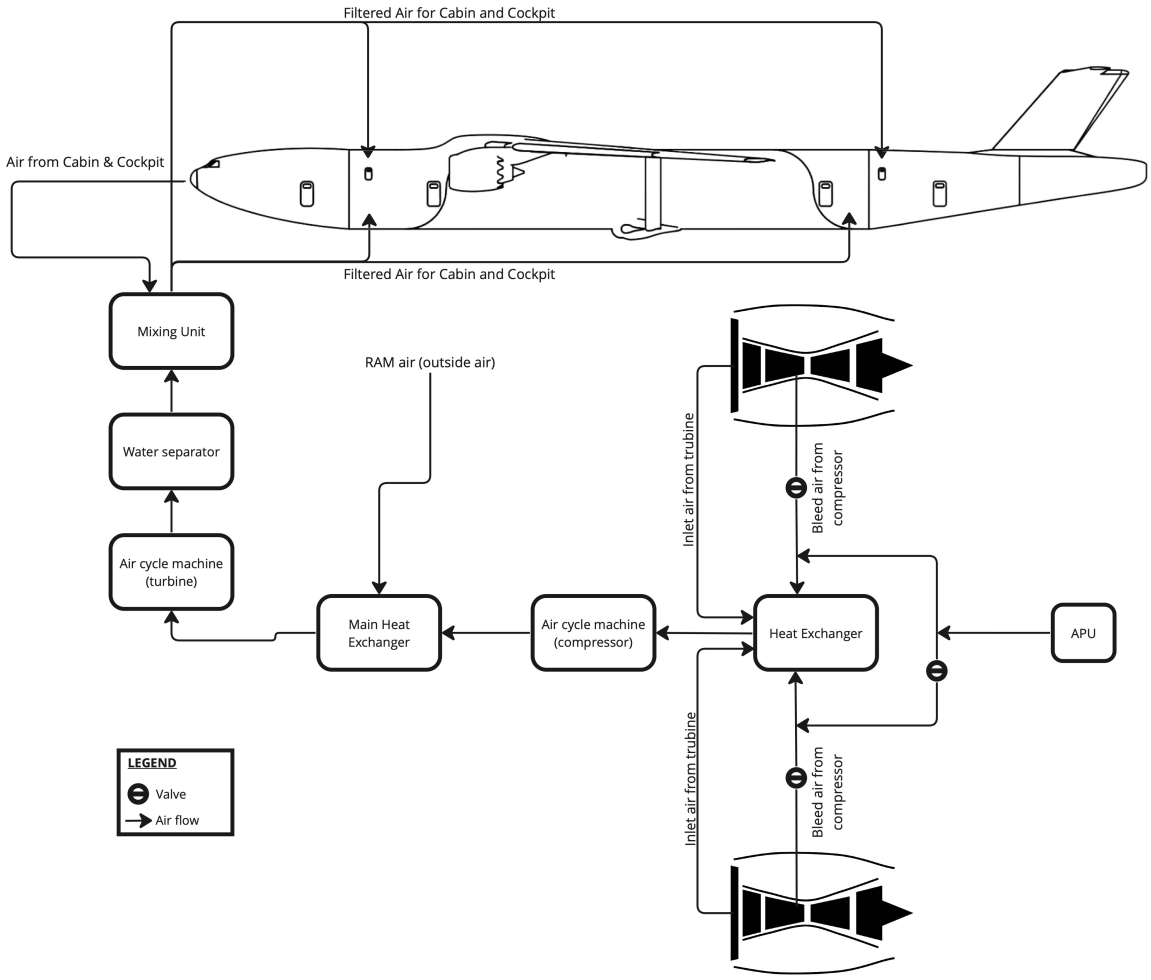

Figure 2.6: Environmental control diagram

2.2.6. Fuel system layout

In Figure 2.7, the fuel system layout diagram is shown. This diagram shows the preliminary makeup of the fuel systems, emphasizing flows to and from the fuel tanks and their integration with the engines.

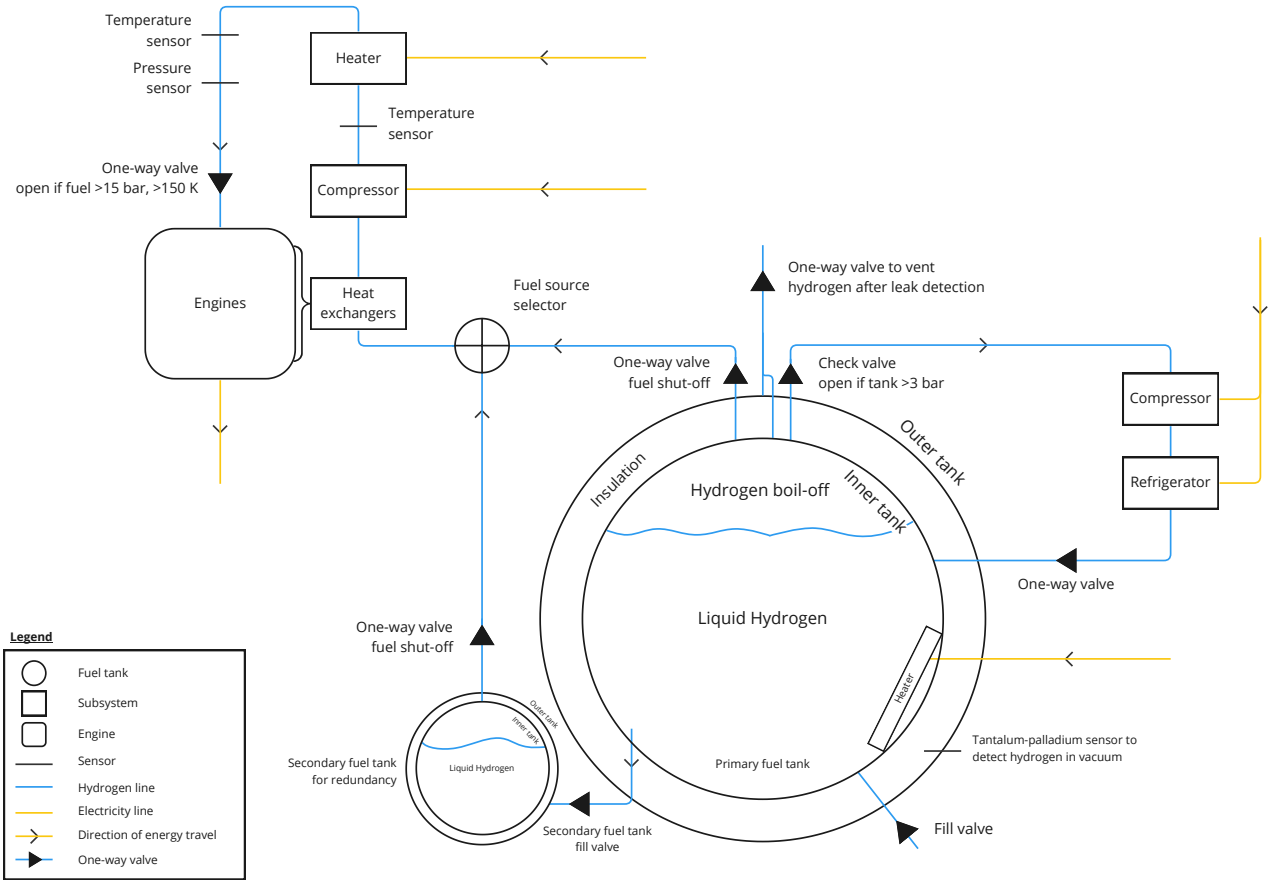

Figure 2.7: Fuel system layout of aircraft.

3

Mission analysis

Throughout this chapter, the mission of WorldBus will be analysed. First, the project objective will be elaborated upon. Next, the functional flow diagram and functional breakdown structure will be briefly addressed. Concluding this chapter, the subsystem requirements shall be discussed.

3.1. Project objective

This section will elaborate upon the objective, the need and the user requirements of this project.

3.1.1. Objective statement

”Design, with 10 students and within 10 weeks, an aircraft that is climate-friendly and can non-stop fly 200 passengers to and from any major airport in the world.” [1]

3.1.2. Need statement

In 2022, aviation is responsible for 2-3% of all greenhouse gas emissions. More specifically, approximately 6% of all flights are responsible for 51% of all emissions. [5] These are the long-haul flights, which are, unfortunately, also the hardest flights to replace with sustainable alternatives such as an electric car or train. Therefore, it is of utmost importance to develop a long-distance climate-friendly aircraft in order to minimise climate impact caused by aviation.

3.1.3. User requirements

At the foundation of each project, ordered by a client, lay the user requirements. This client defines the mission and minimum demands to be met by the final product. For WorldBus, these requirements are described in Table 3.1 [1]:

[5] https://www.flightglobal.com/networks/at-6-of-flights-long-haul-services-emit-51-of-co2-eurocontrol/142445.article

Table 3.1: User requirements

Category	ID	Requirement
Performance	REQ-USER-PERF-01	WorldBus shall be able to provide a non-stop flight between any two major international airports (defined as more than 10 million passenger journeys per year).
	REQ-USER-PERF-02	WorldBus shall perform this within the maximum travel time of 24 hours (from arrival at the departure airport to leaving the destination airport).
	REQ-USER-PERF-03	WorldBus shall transport a minimum of 200 passengers, including provision for sleeping on board.
Safety and Reliability	REQ-USER-SAF-01	WorldBus shall meet the minimum requirements of EASA CS-25 Certification Specification for Large Aircraft
Sustainability	REQ-USER-SUS-01	WorldBus shall have an environmental impact of less than 10% of current long-haul aircraft (e.g. B787, A380) after considering, materials, manufacture, fuel, maintenance and recycling at end-of-life.
Engineering Budget	REQ-USER-BUD-01	WorldBus shall fly at least 4000 flight hours per year
	REQ-USER-BUD-02	WorldBus shall have an operational lifetime of at least 40000 flight hours.
Costs	REQ-USER-COS-01	WorldBus shall have a maximum purchase price (before discount) of EUR 250 million.
	REQ-USER-COS-02	WorldBus shall have an average unit cost according to the expected production of 500 units over 20 years.
Other	REQ-USER-OTH-01	WorldBus shall enter service in 2040.

3.2. Functional flow diagram

In the functional flow diagram (FFD), an analysis is done of the mission to find the functions that the aircraft needs to perform. Not only is a FFD useful to get an overview of the mission, but it also aids in generating requirements. Crucially, requirements are set up so that the mission can be performed. If a FFD is set up correctly, the aircraft will perform all the functions of the FFD when all requirements are met. The first step in creating a FFD is finding the highest functions. This is shown in Figure 3.1.

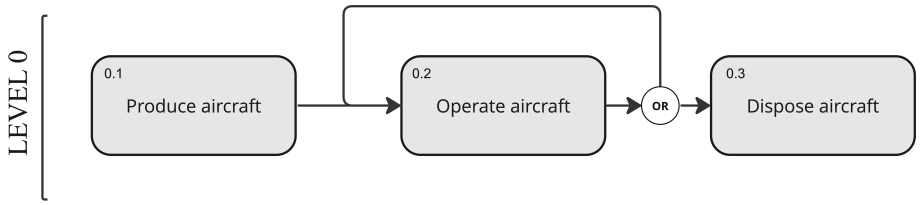

Figure 3.1: Highest level of FFD

Each of these functions can then be worked out to a lower level to find out what subfunctions need to be performed to complete the main function. It is important to note that fundamentally only function 0.2 is relevant for the operation of the aircraft and its interaction with the environment. However, in order to have a complete overview of the entire life-cycle of WorldBus, functions 0.1, 0.2, and 0.3 are all worked out in more detail.

Produce aircraft

In Figure 3.2, the function to produce the aircraft is shown.

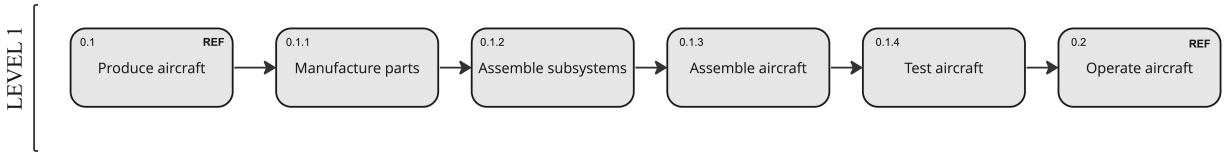

Figure 3.2: Flow diagram of the 'produce aircraft' function.

Operate aircraft

The largest part of WorldBus' lifetime is spent during operation. As such, this part is worked out in most detail. In Figure 3.3, the main components of the 'operate aircraft' function are shown. However, a more detailed and elaborate overview is provided in Appendix A.

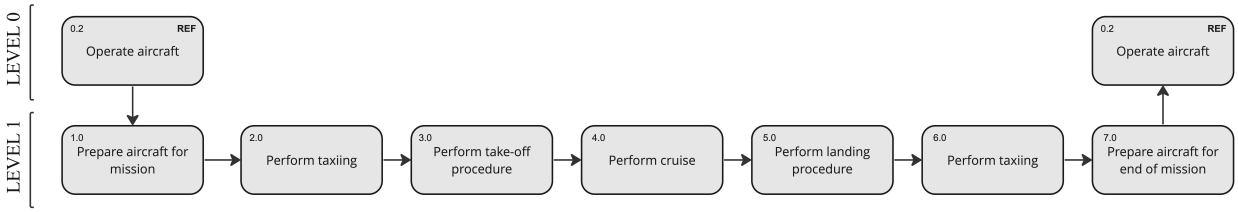

Figure 3.3: Flow diagram of the 'operate aircraft' function.

Dispose aircraft

Finally, when WorldBus has been in operation for approximately 20 years, it will reach its end-of-life. Here, it is important to consider what will happen to the aircraft when it cannot fly anymore. After all, if not properly taken into account, the structure could still have a negative impact on the environment. A flow diagram for the disposal of the aircraft is given in Figure 3.4.

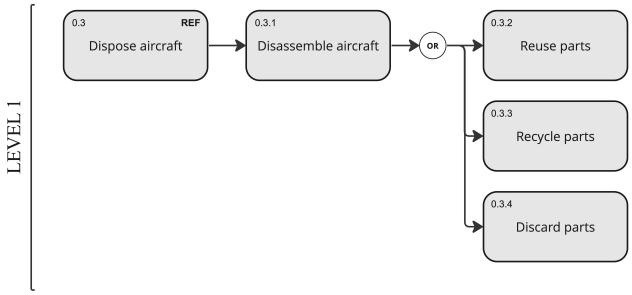

Figure 3.4: Flow diagram of the 'dispose aircraft' function.

3.3. Functional breakdown structure

The functional breakdown structure (FBS) provides an alternative overview for the functions that need to be performed by WorldBus. Instead of a flow diagram, the functions are listed in a hierarchical structure. While this eliminates the possibility to show how different functions flow into each other, it does give a better way to represent functions that are not suitable for a flow diagram. For example, functions that are time-independent. An overview of the FBS is given in Appendix B.

3.4. Subsystem requirements

In order to clearly lay out all key, user and subsystem requirements, a requirement discovery tree has been made and it is shown in Appendix C. The format of the tree is an 'AND' tree so that the corresponding top-level requirement will not be met whenever a sub-level requirement is not met. The first branches of the tree divide the requirements into 'system requirements' and 'mission requirements' sections. System requirements dictate how the system and its subsystems should function, whereas the mission requirements concern what the system does [2].

4

Financial analysis

When designing a new aircraft, the financial feasibility of this enterprise must be carefully investigated. In this chapter, a revised financial analysis will be elaborated upon. First, a market analysis will be performed in Section 4.1. Then a cost breakdown, portraying both the capital expenses and the variables expenses, will follow in Section 4.2. Furthermore, the first two sections will be combined in a return on investment (ROI) analysis in Section 4.3. This return on investment calculation method will be used in constructing the final financial picture, portraying the list price and return on investment of the enterprise, in Section 4.4. After this, where necessary, the models used are validated in Section 4.5. Lastly, conclusions and recommendations to the financial analysis will be discussed in Section 4.6.

4.1. Market analysis

It is of great interest to analyse the market before designing a product. This analysis consists of three primary aspects, namely the market size, the projected pricing of the service delivered by the aircraft and, which is more interesting from a manufacturer's perspective, the list prices of comparable aircraft. These aspects are evaluated by carefully looking into the current state of affairs. Lastly, a SWOT analysis will be presented.

4.1.1. Market size

When analysing a product's financial feasibility, it is important to establish the size of the demand for this product. The project specifically aims to deliver ultra-long-haul flights with a range of 19 000 km, producing 90% fewer emissions compared to current aircraft. To estimate the size of the market for such flights, the market for long-haul flights was analysed. Although relevant data for ultra-long-haul flight is unavailable, long-haul flights (greater or equal to 4000 km) could be found to make up 6% of total flights in 2020 and 5.5% in 2021 [3]. These flights contributed to approximately 51.9% and 43.9% of total aviation emissions in each respective year. This fact confirms the necessity of the mission of WorldBus. However, it must be noted that WorldBus will fly from any two major airports in the world, thus focusing mostly on the flight with a very high range. This means the WorldBus will operate in the niche market of ultra-long-haul flights. This market will be defined as the market for flights above 13500 km.

The initial market sizing was based only on the 10 longest existing flights as shown in Table 4.1. This number was then evaluated against the total number of flights and it was stated that approximately 0.022 % of flights worldwide fall within the mission's objective.

Table 4.1: Top 10 longest existing flight routes

Routes considered			
From	**To**	**Distance [km]**	**# of flights/week**
San Francisco	Singapore	13593	42
Dallas	Sydney	13804	11
Houston	Sydney	13834	1
Singapore	Los Angeles	14111	16
Dubai	Auckland	14198	14
New York	Auckland	14291	6
Dallas	Melbourne	14552	2
Perth	London	14584	11
Newark	Singapore	15417	12
New York	Singapore	15422	14
Sydney	Amsterdam	16643	0
London	Auckland	18336	0
Beijing	Buenos Aires	19267	0

It should be noted that this market share of 0.022% only takes into account the flights from approximately 13 500 km to 15 500 km into account, and not the flights covering the extra 4000 km and that, thus, still fall within the design range of the WorldBus. As no data exists yet on these added routes, assumptions to determine this market size will be made and explained in detail.

First, for the top 10 longest existing flight routes as shown in Table 4.1, it is seen that the range increase from number 10 to number 1 is 2000 km. This means that, for these ultra-long-haul flights, the routes that are performed for a 2000 km range increase, represent 0.022% of the market size. However, it is not expected from the market size consistently increase with 0.022% for each 2000 km added to the range. When analysing the market share per flight distance it can be seen that with increasing flight distance the market share decreases [4]. In Table 4.2 the total assumed market share is shown with a decrease in market size of just over 41% per added 2000 km range.

Table 4.2: Market share per flight distance

Range	Market share
$13500 - 15500$	0.022%
$15500 - 17500$	0.0135%
$17500 - 19500$	0.085%
$13500 - 19500$	0.044%

Completing the calculation, it followed that, assuming the total annual number of flights is 33 million, there is a demand of about 14520 ultra-log-haul flights (flights with a range of more than 13 500 km) per year. By inspecting data on the total number of flights per year and disregarding the temporary dip in demand during the COVID pandemic, it could be concluded that the demand for flights has been growing linearly [6]. If the demand is assumed to keep increasing at the identified rate, it follows that, by the time the mission's aircraft are aimed to be delivered in 2040, the total demand will equal approximately 21000 flights per year. This number will even increase to 35600 flights towards the end of the lifetime of the fleet in 2080. Unfortunately, it is unrealistic to assume that the designed product will capture a 100% market share of this market. What will, however, give this mission's product a superior position compared to the competition is the fact that it is projected to achieve a 90% reduction in emissions. As was discussed in the baseline report, sustainability in aviation is becoming of increasing importance to customers, noting that customers are even willing to spend more money for increased sustainability [2]. For this reason, it was assumed that the to-be-designed WorldBus will be able to achieve an 80% market share over the ranges ranging from 13 500 km up to 19 500 km. This results in 0.0352% of the total market to be served by WorldBus. This established market seems to be too small for the desired number of 500 delivered aircraft, something that will be discussed in further detail in Section 4.4.

4.1.2. Ticket pricing

Another important aspect of the financial analysis is the ticket pricing. In order to establish a ticket price for the mission's ultra-long-haul flights, the current ticket prices of comparable routes were evaluated. It followed that the prices for economy class tickets for comparable return flights were, on average, close to EUR 1800 [2]. This average, however, also takes into account flights with layovers. Furthermore, these prices are related to economy-class comfort. The designed product will not provide standard economy comfort classes but rather focuses on delivering seats of economy+ and business class standards. For economy+ class, it was assumed that ticket prices can be increased by 80% and ticket prices for business class seats are 3 times more expensive than regular economy class tickets [5].

Continuing the ticket price analysis, it was discovered during research that customers are willing to spend 15% more on

[6] https://www.statista.com/statistics/564769/airline-industry-number-of-flights/

their ticket price if promised that the flight will be 30% more sustainable [6]. It is expected that the mission's product will be able to respond to this opportunity adequately and that, since the reduction in emission will be 90% instead of 30%, ticket prices can be made 20% more expensive. The current price for a regular single flight economy ticket for flights of the determined range was approximately 900 EUR. Thus, combining the stated factors for WorldBus, the ticket price for an economy+ class ticket for a single flight will be EUR 1944 and for business class this price will be EUR 3240.

4.1.3. Aircraft price

Another aspect of the market analysis is the aircraft price. This time, the manufacturer's perspective is taken into account. As will follow later, some challenges will be faced when establishing the list price of the WorldBus. In Table 4.3, the list prices of some reference aircraft are listed.

Table 4.3: List prices of comparable aircraft

Aircraft	**Range**	**List Price (million EUR)**	**Corrected for inflation to 2023 (million EUR)**
Airbus A340-500	16668	239 (2011)	317 [7]
Boeing 747-8	15000	383 (2023)	383 [8]
Airbus A350-1000	16000	336 (2018)	400 [9]
Airbus A380	15200	406 (2018)	484 [10]
Boeing 777-200LR	15800	316 (2019)	371 [11]
Boeing 787-9	14100	256 (2006)	367 [12]

As can be read from Table 4.3, it can be noted that all list prices adjusted for inflation of aircraft with comparable ranges lie above EUR 300 million. The prices adjusted for inflation aim to show what one would pay today for new aircraft boosting new improvements. As McKinsey has researched, the latest-generation aircraft is about 15-20% more fuel efficient than previous generations, thus providing a significant increase in sustainability over generations. [13] However, this is still not quick enough and a decline in fuel efficiency gains of 3.4% is expected each year as their limits are being approached. WorldBus aims to revolutionise the design and propulsion system of an aircraft, this will improve the sustainability of the aircraft by 90%. The whole reason to push for better fuel efficiencies is to reduce environmental impact and WorldBus provides a solution that greatly surpasses all designs on the market as of today. This reduction in emissions will be obtained, whilst also enabling flight between any two major airports in the world.

These facts will, most probably, increase the aircraft list price and therefore it must be investigated whether this is the case, and if so, whether it is still profitable to keep in operation

4.1.4. SWOT analysis

A SWOT analysis is an analysis in which the strengths, weaknesses, opportunities and threats of a product are portrayed. Such an analysis was also performed for WorldBus and the result is depicted in Figure 4.1.

[7] https://aerocorner.com/aircraft/airbus-a340-500/

[8] https://simpleflying.com/boeing-747-8-value/#:~:text=How%20much%20is%20the%20Queen,longer%20sells%20the%20Jumbo%20Jet.&text=According%20to%20ch%2Daviation.com's,position%20of%20most%20valuable%20jet.

[9] https://simpleflying.com/airbus-a350-1000-worth-2021/

[10] https://simpleflying.com/airbus-a380-worth-2021/

[11] https://aerocorner.com/aircraft/boeing-777-200lr/

[12] https://www.flightglobal.com/boeing-adds-747-8-777f-and-787-9-to-price-list/67339.article#:~:text=Boeing%20yesterday%20released%20its%20latest,%24178.5%20million%20to%20%24188%20million.

[13] https://www.mckinsey.com/industries/aerospace-and-defense/our-insights/future-air-mobility-blog/fuel-efficiency-why-airlines-need-to-switch-to-more-ambitious-measures

Figure 4.1: SWOT analysis WorldBus

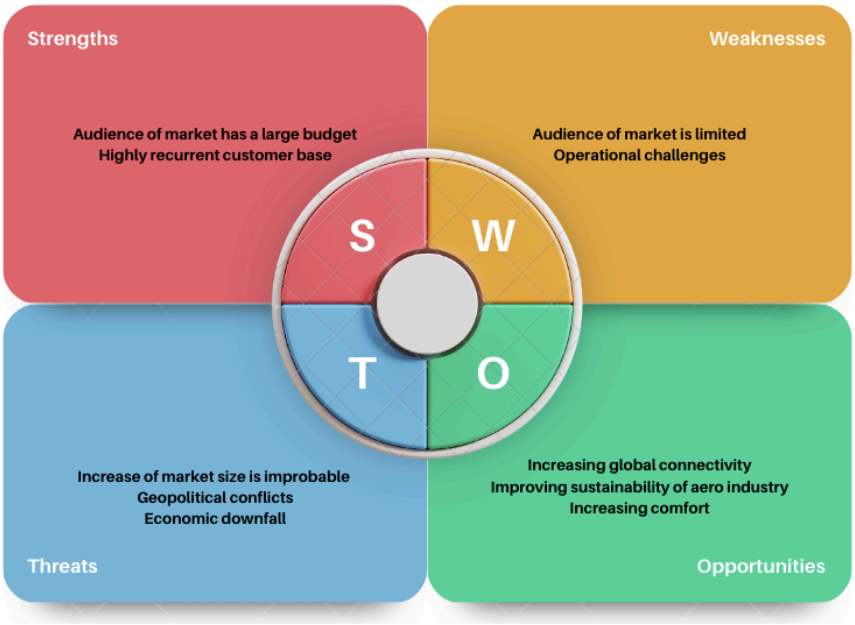

4.2. Costs breakdown

In order to be able to see if an investment is going to be profitable, it is essential to determine the costs related to the design. These costs can be broken down into two main parts, the first being the operational expenses and the second being the capital expenses. The operational expenses are approximated to see if operations with WorldBus will be profitable. The capital expenses are estimated to see if the requirement of a maximum aircraft selling price of EUR 250 million is reasonable. A visual representation of the costs breakdown is portrayed in Figure 4.2.

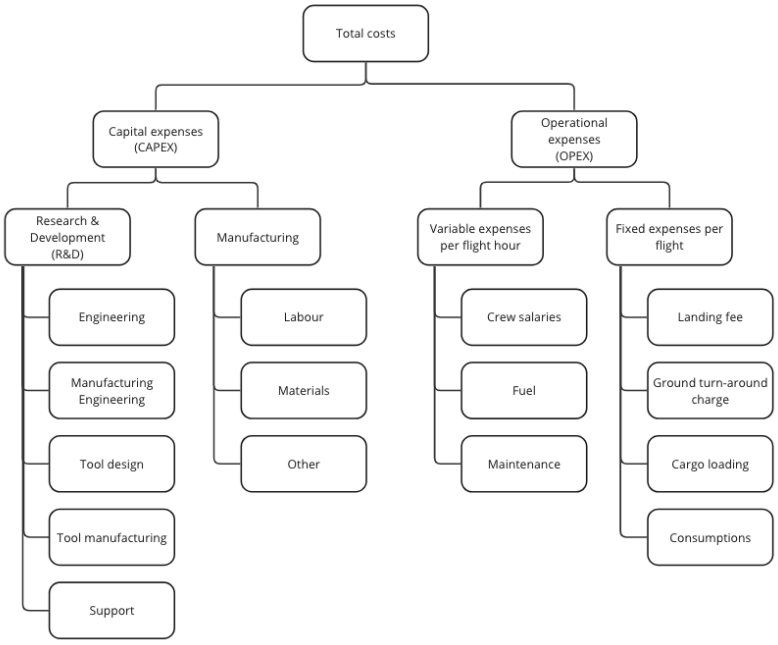

Figure 4.2: Costs breakdown diagram

4.2.1. Operational expenses (OPEX)

To be able to determine if operations are going to be profitable, the operational expenses must be identified. These costs can be divided into two parts, the variable expenses per flown hour and the fixed costs per flight.

Variable expenses per hour of flight

The variable expenses can be identified to consist of 3 main components, namely the crew salaries, the fuel and the maintenance of the aircraft. A substantial part of the operating costs of a flight is dedicated to the aircraft crew. The amount consists of a lot of facets such as pilots' and copilots' salaries, salaries of other flight personnel, trainees and instructors for the personnel, personnel expenses, employee benefits and pensions, and taxes on the payroll. Extensive research was executed by the FAA to make an estimation of these crew costs. The hourly cost of the crew of a wide-body aircraft with less than 300 passengers, flying according to a P-5.2 schedule, was identified to be approximately 1850 EUR/hr [7] [2].

Another interesting aspect of the variable costs is the cost related to the fuel of the aircraft. Instead of fuelling the aircraft with regular kerosene, the aircraft has been designed to have green hydrogen as a propellant. The cost of this propellant is currently 4.59 EUR/kg, however, due to an expected decrease in electricity price and production costs due to advancements in technology, the price of green liquid hydrogen is expected to decrease to 1.56 EUR/kg by 2040.[14] From calculations it was concluded that approximately 3000 kg of hydrogen is required per hour of flight, meaning that the hourly cost of the fuel will be around 4900 EUR/hr. This means that flying with hydrogen will actually be cheaper than flying with kerosene.

The last component of the hourly costs is related to maintenance. Since the type of aircraft is not yet existent, an estimate of the maintenance costs is based on a wide-body aircraft with 300 seats or less, since the design is required to house a minimum of 200 passengers and a wide-body has the most costs. These maintenance costs are based on the labour, the repair, the maintenance of materials, airworthiness allowance provision and overhauls deferred of airframes and aircraft engines, aircraft interchange, applied maintenance burden-flight equipment and net obsolescence & deterioration of expendable parts. The maintenance costs for a wide-body 300 seats and below aircraft are estimated by the FAA to be 1300 EUR per block hour [7]. However, since the designed aircraft is completely new, maintenance costs are expected to be significantly higher. For example, the maintenance costs of the Boeing 787 Dreamliner were in the range of 2300 EUR/hr.[15] An increase in maintenance costs of 50% is accounted for, constituting a total of 1950 EUR/hr.

Fixed expenses per flight

The fixed expenses per flight can be identified to consist of 4 main components, namely the landing fee, the ground turn-around charge, the cargo loading and the provision of consumptions. To land at an airport a landing fee has to be paid by the airline. These costs vary greatly between airports. The landing fee at JFK is known and will therefore be used as a reference point, also recognising the fact that this airport meets the assignment airport requirement in being a major international airport. The landing fee was around 15.5 EUR per 1000 kg in 2020. [16] The final MTOW is approximately equal to 220 000 kg, which results in a total landing fee of approximately EUR 3400 [2]. When arriving at an airport, external parties are sometimes present for turning around and serving the aircraft. As a reference point, these costs for a Boeing 737 aircraft are about EUR 1500. Therefore, it is estimated that for heavier aircraft and the ground turnaround charge with inflation is around EUR 3000. [17] Another element of the costs related to ground operations is cargo loading. The fee that a cargo loading organisation will charge depends on the MTOW of the aircraft. Looking at a brochure from Maastricht-Aachen airport, it can be stated that the cargo loading will amount to a maximum of EUR 2500 per flight. To be able to accommodate a comfortable flight for 200 passengers, it is important to reserve enough consumption. On average, an economy meal costs an airline EUR 4 and a business class meal costs an airline EUR 25.[18] Furthermore, we know that we will have 83 business class passengers and 117 economy class passengers. If it is then assumed that passengers are served 3 meals per flight, the total required budget will come down to EUR 1404 for economy class and EUR 6225 for business class. This means a total budget for consumption of EUR 7629 is required per flight. An overview of the operational costs is shown in Table 4.4

Variable expenses	EUR/hr	Fixed expenses	EUR/flight
Fuel cost	3663	Landing fee	3065
Maintenance	1950	Turn-around charge	3000
Crew salaries	1850	Cargo loading	2500
		Consumption	7629

Table 4.4: Operational costs overview

[14] https://www.structuresinsider.com/post/green-hydrogen-current-and-projected-production-costs
[15] https://myaircraftcost.com/boeing-787-8/
[16] https://simpleflying.com/the-cost-of-flying/
[17] See footnote 16
[18] https://www.vox.com/the-goods/2020/2/10/21117507/airplane-food-explained

4.2.2. Capital expenses (CAPEX)

Starting off, the design will require some capital expenses. As there is a requirement for a maximum aircraft selling price of EUR 250 million, it is essential that these costs will be lower than this amount. Else, the selling price must be increased in collaboration with the customer. The capital expenses can be split into two parts, the costs of research & development and costs related to manufacturing.

Costs of research & development

Every new design will require some research & development (R&D) costs. Especially for innovative designs, these costs are generally very significant and must be considered in the pricing of an aircraft. R&D can be divided into five categories: engineering, manufacturing engineering (materials and equipment), tool design, tool fabrication and support (quality inspection and testing [8]. Note that these costs are non-recurring. The costs related to these R&D activities per subsystem have been analysed by a team at Massachusetts Institute of Technology for multiple aircraft and the results are portrayed in Table 4.5 [9]. Note that the costs have been adapted for inflation as the research stems from 2002. Besides the correction for inflation, also the costs related to the development of hydrogen propulsion have been altered. From extensive research it was found that the development of hydrogen propulsion is approximately 20% more expensive than regular kerosene systems [10], this was integrated into the price of R&D for the installed engines as depicted in Table 4.5.

Table 4.5: Research and development costs per kg of each component.

Component	Total
Wing (EUR/kg)	54,729
Empennage (EUR/kg)	160,976
Fuselage (EUR/kg)	99,056
Landing gear (EUR/kg)	7,707
Installed engines (EUR/kg)	32,192
Systems (EUR/kg)	105,888
Payload (EUR/kg)	33,225

Costs of manufacturing

The costs related to the manufacturing process can be divided into 3 subgroups, labour, materials and some remaining costs summarized as 'Other'. Again, most subsystem costs are based on research at Massachusetts Institute of Technology [8]. However, the manufacturing costs for the wing, fuselage, and propulsion system have been analysed separately.

Since it is decided to use CFRP for the manufacturing of the fuselage and wing, their material costs will be slightly higher. It is expected that the difference in costs will decrease over time, but there will still be a 25% difference by 2030. Since approximately 25% of the manufacturing costs of wings and fuselage is made up of material costs [8], it is fair to say that the total increase in manufacturing costs will be 6.25%.

As the team has decided to use existing Rolls-Royce Trend 1000R engines, the costs can be estimated more precisely than through statistical information. The purchase price of the engine is approximately EUR 20 million, but since we need 2 engines, the total costs will be EUR 40 M million. [19] This purchase price will be used as the manufacturing cost. Furthermore, since hydrogen is used, hydrogen fuel tanks must also be budgeted for. From research by the French ministry of Innovation, it was found that for liquid hydrogen the tank price would be approximately 245 EUR/kg H2 [11]. This means we will end up with a total tank cost of EUR 10.8 million, compared to only EUR 50000 for kerosene tanks. [20] Therefore EUR 10.75 million will be added to the manufacturing costs of 'Systems'. Furthermore, the manufacturing of the empennage is expected to be more expensive due to the selection of a T-tail. Thus, an extra 20% is added. An overview of the manufacturing costs is presented in Table 4.6.

[19] https://www.reuters.com/article/us-ana-rolls-royce-hldg-engines-idUSKCN1162OD
[20] https://www.made-in-china.com/products-search/hot-china-products/Kerosene_Tank_Price.html

Table 4.6: Recurring cost for each component

Component	Total
Wing (EUR/kg)	2,956
Empennage (EUR/kg)	7,644
Fuselage (EUR/kg)	3,171
Landing Gear (EUR/kg)	682
Installed Engines (EUR)	40000
Systems (EUR/kg)	1,395
Payload (EUR/kg)	1,740
Final Assembly (EUR/kg)	202

Total capital expenses

Using the final weights of the subsystems from the Class II weight estimations and other more precise calculations and inspecting Table 4.5 and Table 4.6, Table 4.7, in which the total costs are portrayed, could be generated. The R&D costs are portrayed as the cost per aircraft, this number is generated by dividing the total costs by 300, which is the number of aircraft that will be delivered.

Table 4.7: Final values for capital expenses per subsystem

Subsystem	RnD (million EUR)	Manufacturing costs (million EUR)	Total costs (million EUR)
Wing	7.3	125.6	132.9
Empennage	1.4	20.7	22.1
Fuselage	11.1	113.4	124.5
Landing gear	0.2	4.9	5.1
Installed engines	1.3	40	41.3
Systems	6.3	37.6	43.9
Payload	2.1	35.0	37.1
Final assembly	-	33.3	33.3
Total	410.6	29.7	**440.3**

Thus, the expected capital costs of the designed aircraft are going to be around EUR 440 million, which is more than the initially established selling price. It is expected that the costs related to the engine will decrease by 2040, but that will not lead to the aspired costs decrease to be able to sell the aircraft for a list price of 250 M EUR. Summarising, the increased capital expenses of the WorldBus compared to regular aircraft can be attributed to:

- 20% increase in R&D costs related to hydrogen propulsion
- 25% increase in material costs of wing, fuselage and empennage due to the use of CFRP
- An additional 10.5 M EUR for the inclusion of a hydrogen tank instead of a kerosene tank
- 20% increase in manufacturing costs of empennage due to use of T-tail
- 20 M EUR increase in engine costs due to utilization of existing engines instead of developing own engines

This, as well as a high wing weight, causes the list price of the WorldBus to be approximately 25% above the mean capital expense per aircraft that is calculated based on the reference aircraft list prices discussed in Table 4.3. It is assumed that the list prices of the reference aircraft are approximately 10% higher than the capital expenses per aircraft, meaning that the mean capital expense per aircraft is 352 M EUR.

4.3. Return on investment

To evaluate if purchasing the designed aircraft will be a profitable enterprise from an airline's perspective and, thus, to evaluate if the designed aircraft will actually be bought, it is essential to perform a return on investment (ROI) calculation. The ROI is calculated using Equation 4.1.

$$ROI = \frac{(MP - DOC) \cdot MV \cdot AMS \cdot Lifetime - DPC}{Investment} \cdot 100 \tag{4.1}$$

In Equation 4.1 MP stands for market price, which is the revenue per flown flight and can be established by using the ticket prices stated in Subsection 4.1.2 and multiplying these by the numbers of economy+ and business class passengers

respectively. The DOC stands for the direct operational costs, which are the costs related to a single flight and are explained for in Subsection 4.2.1. The MV stands for the market volume or market size and is discussed in Subsection 4.1.1. The AMS stands for the achievable market share which is also discussed in Subsection 4.1.1 and the DPC stands for the development and production costs which is simply equal to the purchase price. Different scenarios were thought of and their respective ROIs were calculated. These results were used in the final determination of the list price and the return on investment at this list price shall be stated in Section 4.6.

4.4. Final financial picture

When all aspects of the financial situation have been analysed, the final financial strategy can be established. In defining this strategy, the goal is to make sure that the project in its entirety will be profitable for both the parties involved: the manufacturer and the customer (airline). Whereas the manufacturer will impose a minimum constraint for the list price, the maximum constraint will be posed by the customer. The manufacturer must make sure to have a list price higher than the capital expenses in order to make a profit and the customer must have a list price low enough to have a comfortable profit margin (ROI).

Before one can establish the magnitude of these constraints, first a decision must be made as to how many aircraft shall be manufactured. As was established in Subsection 4.1.1, the expected market size is way too large for the initial desire of 500 aircraft. If 500 aircraft are produced, there will be an excess of more than 300 aircraft in 2060, causing a huge cost inefficiency and decreasing the return on investment. Therefore, in terms of ROI, it would be more desirable to produce as few aircraft as possible, as in this case, all aircraft produced will be constantly flying. On the other hand, a smaller amount of produced aircraft will increase the list price, as the capital expenses related to R&D per aircraft will increase. It was found that the ideal combination of ROI and list price was found when the amount of aircraft produced is equal to 300.

Now that the amount of aircraft produced is established, one can continue with investigating the financial constraints. Starting with the minimum constraint posed by the manufacturer, one is quickly directed to Subsection 4.2.2 to find the magnitude of the capital expenses. In this section the capital expense per aircraft, assuming 300 aircraft are produced over a span of 20 years, was determined to be approximately EUR 440 million. Keeping in mind the initial user requirement of a list price of a maximum of EUR 250 million, this is a rather high number. However, looking at the list prices of reference aircraft with a comparable range in Table 4.3, it can be stated that the initial requirement was very ambitious in the first place. Still, whereas the reference aircraft have list prices of EUR 300-450 million, WorldBus would be sold for a list price in the range of EUR 500 million. This seems unrealistic. Then the question remains what the reason of this high value is. This question can be answered by looking at the valuation performed in Subsection 4.2.2. From this section, it can be concluded that several subsystem costs turned out higher due to the innovative character of the design, justifying the increased capital expenses and list price. Also, the wing weight of the WorldBus seemed on the high side compared to those of reference aircraft. As all costs are directly proportional to the subsystem weight, this also increased the capital expenses.

Assuming this wing weight is valid, after all the wing weight of the Boeing 747 is $43\,000$ kg compared to 42.500 kg for the WorldBus, the minimum constraint for the list price from a manufacturer's perspective can be stated to be EUR 484 million. This includes a safety/profit margin of 10% to be able to deal with possible financial setbacks from a manufacturing and development perspective.

Now that the minimum constraint has been established, it is relevant to look at the maximum list price requirement imposed by the customer. This requirement will be primarily based on the return on investment that is achievable at the stated list price. Also, a customer will not be willing to pay too much above the market price for aircraft when no good reasoning is provided. It is assumed that: 15 aircraft will be produced per year over a span of 20 years, the aircraft lifetime is 20 years, the market size is equal to the market size as discussed in Subsection 4.1.1, the achievable market share is 80%, the DPC are equal to the ones discussed in Subsection 4.2.1, ticket pricing is as determined in Subsection 4.1.2 and flights are expected to be fully booked. In this scenario, the return on investment at a list price of EUR 484 million is expected to be 96%, meaning a profit of EUR 140 billion in absolute terms will be achieved. This is more than enough return on investment to keep the project interesting from a customer's perspective. Still, this return on investment is calculated based on more or less ideal circumstances. Normal return on investments for aircraft are in the range of 5 to 12 % [21]. It is assumed that, in order for the enterprise to stay attractive to customers, a return on investment of 20% is required. This point can be approximated by making certain circumstances less ideal. The following worst-case scenarios can be overcome to still keep this profit margin:

- The achievable market share is allowed to drop from 80% to 37%
- The flights may be only filled for 46 % instead of 100%
- The ticket prices may decrease by 26%

[21] https://www.im.natixis.com/en-institutional/insights/there-s-value-in-planes

- The total costs per flight may increase by 80%

It is necessary to note that these worst-case scenarios may not be combined and are only calculated as stand-alone setbacks. One realistic scenario combining these set-backs has been sketched as an example and is as follows:

- The achievable market share is 60%
- The flights are only filled for 80%
- Ticket prices are 5% lower than expected
- Total costs per flight are 15% higher than expected

In such a doom scenario, the return on investment will still be 20%. These comfortable margins were presented to the customer and a list price of EUR 484 million was accepted. Since now both the list price constraint from the manufacturer and the customer have been adhered to, project WorldBus is granted a green light from a financial perspective.

4.5. Verification and validation

Most items discussed in this chapter are already based on research and investigation into reference aircraft and aircraft activities and, thus, do not need any validation. One aspect of the financial analysis, however, must be validated. the calculation of the capital expenses, for manufacturing as well as R&D, is performed based on a model proposed by MIT [8]. The results of this model were validated by reperforming the calculations through a second model, namely the DAPCA IV model described by Raymer [12]. Whereas the model proposed by the team from MIT determined the costs of R&D and manufacturing separately, the DAPCA IV model only gives the total costs. Still, the final values should be approximately the same. As discussed earlier, the total capital expenses calculated by means of the MIT model amounted to a total of EUR 440 million when the favourable wing weight was assumed. When the same weights and input variables are used for the model from Raymer, a total capital expense per aircraft of Eur 422 million was found. This means that there is a difference of 4%, which is deemed to be within an acceptable margin. Therefore, the MIT model for capital expenses is accepted.

4.6. Conclusions and recommendations

In this chapter, finally, the list price of the WorldBus and its expected return on investment has been established. Fortunately, it could be concluded that the enterprise will be profitable from a manufacturer's perspective as well as a customer's perspective and that the project, thus, does not have to be shut down. The final list price was established to be EUR 484 million. At this list price, there will be a 10% profit margin for the manufacturer and the customer will face a 90 % return on investment.

Further research into the financial picture of the WorldBus project is encouraged, with recommended focus points listed below:

- Further investigate the market for ultra-long-haul flights. Investigate how many people would be willing to choose a direct flight over a lay-over and what price they would be willing to pay for this luxury
- Further investigate the development of hydrogen fuel costs
- Further investigate the capital expenses related to the research and development of ground-breaking new designs
- Investigate the financial feasibility of using excess aircraft for shorter-range flights. Find out if flights under these circumstances are profitable

5

Sustainable development strategy

For the last decades, global surface temperatures have been rising continuously, with the last years being some of the hottest years on record. Currently, there is a two-thirds likelihood that annual average surface temperatures will increase by $1.5\,°$ in the coming five years. This will lead to increased frequency and increased intensity of extreme heatwaves, droughts, storms, and heavy rainfall, which will greatly impact ecosystems, agriculture and water resources. Despite these prospects, global emissions still have to drop, with 2022 being the year with the highest emissions recorded in human industry. [22] Therefore, environmental sustainability has become an increasingly more important aspect in the design of any new aircraft.

Furthermore, the aviation industry became more aware of the negative impact it could have on society. Therefore, social sustainability gained more significance in the design process as well, over the last year. It encompasses the well-being of individuals and society, and efforts to reduce negative impacts on society such as noise emissions or potential human rights abuses.

Lastly, due to the increased competition in the industry, there has been a rising emphasis on economic sustainability. Economical sustainability refers to the ability of an organization to maintain long-term economic viability.

For the design process of WorldBus, a sustainable development strategy was already developed in the Baseline Report [2] to adopt environmental, social and economic sustainability. This strategy was then reviewed in the Midterm Report [13]. In this report, the strategy will be briefly reviewed again. In Chapter 15, a sustainability analysis for the design will be performed following this strategy.

5.1. Strategy

The International Organization for Standardization has created a standard for sustainable development (ISO 26000) in any design process which integrates the concepts of environmental management, social responsibility and economic performance [14]. This definition and framework for what is considered to be part of sustainable development are used in the sustainable development strategy for WorldBus.

Concerning social responsibility, several negative impacts on society have been identified. These include factors such as aircraft noise emissions and the deterioration of climate and air quality due to greenhouse gas emissions. Furthermore, potential human rights abuses could be present during the sourcing of materials and production process, which should also be taken into consideration. Also, high ticket prices could result in a societal division with the high ticket prices only being accessible to the affluent. Various solutions have been proposed to mitigate the aforementioned negative impacts. One of those solutions would be advocating for governmental subsidies to promote sustainable flying. With these subsidies, the high ticket prices could be reduced, making sustainable flying accessible to most of society. Furthermore, particular attention should be given to the use of materials and parts with traceable origins. This way, forced or child labour can be excluded from the design process. Lastly, a specific focus should be put on environmental aspects like greenhouse gas emissions and noise emissions throughout the design process. This will mostly be addressed with environmental management.

For economic performance, it is crucial to conduct a thorough market analysis to investigate the market need and to ensure that there is a demand for the aircraft that's being designed. Furthermore, it is important to establish proper budget figures per design phase and per aircraft component. By doing this, the design can be aligned with the cost requirements. The economic performance will also benefit from efficient resource utilization and minimizing waste.

In terms of environmental management, the main focus is on resource utilization and prevention of waste, greenhouse gas

[22] https://www.theguardian.com/environment/2023/jun/02/el-nino-may-push-heating-past-15c-urgent-action-avert-catastrophe

emissions and noise emissions. A strategic approach is provided to address these environmental considerations. Firstly, specific requirements for these aspects have been set up and aircraft characteristics are identified for assessment. Secondly, a verification process is described to ensure compliance of the characteristics with the requirements. Thirdly, in case of non-compliance, a course of action has been established to aim for compliance. Each of these steps will be further elaborated in Section 5.2, Section 5.3, Section 5.4 and Section 5.5; respectively.

5.2. Requirements

In the Baseline Report, six requirements on sustainability were set up [2]. In the Midterm Report, these requirements were reviewed [13]. A requirement on the amount of emissions was changed to a requirement on the Global Warming Potential (GWP) value of the emissions. Further, one of the requirements was to limit emissions during fuel production. However, several numbers in the requirements still needed to be determined. To determine these values, further investigation was necessary which is performed in this report. Following this investigation, the other requirements were updated as well.

Firstly, the percentages limiting the emissions during operation, during production and manufacturing and during the production of liquid hydrogen still had to be determined. These percentages depend on the top-level requirement stating 90% reduction compared to current long-haul aircraft [15]. Thus, the aforementioned percentages combined shall result in a 90% reduction. In Subsection 15.3.2, it was found that WorldBus had a reduction of 97% of emissions during operations. Subsequently, this value was used in the corresponding requirement. Furthermore, in Subsection 15.3.1 it was assumed that when WorldBus enters service, it can make use of solely green hydrogen. Therefore, the requirement limiting emissions of fuel production was set to requiring zero emissions. In literature, it was found that approximately 3% of the emissions in the entire life cycle of an aircraft originate from production and manufacturing [16]. Considering both aforementioned percentages, in order to achieve a 90% reduction in total emissions, the production and manufacturing must not exceed an additional 43% of emissions compared to the Boeing 787-9. For the requirement regarding recyclability at the end-of-life, the percentage was set at a minimum of 60% which is similar to the recyclability rates of current long-haul aircraft that are recycled [17]. With regards to the noise emissions, it was decided to require the aircraft to produce less noise than a similar long-haul aircraft. The requirement limiting the amount of waste was not considered anymore, which will be further highlighted in Chapter 15. Finally, the required service life of the aircraft was extended to 20 years for financial reasons. This exceeds the initial service life requirement from the sustainability requirements in the Midterm Report [13]. Therefore, the service life requirement for sustainability was removed. All updated requirements are listed below.

1. REQ-SUS-ENRG-1 The aircraft shall reduce total GWP emissions by 97% compared to a Boeing 787-9 during operation.
2. REQ-SUS-ENRG-2 The production of 1 kg of liquid hydrogen will produce emissions with at most a GWP of 0.00 kg.
3. REQ-SUS-BEF-2 The entire production and manufacturing process of the aircraft shall reduce total GWP emissions by 43% when compared to the production of a Boeing 787-9.
4. REQ-SUS-NOIS-2 The aircraft shall reduce the cumulative noise by 5 dB compared to a Boeing 787-9.
5. REQ-SUS-END-1 A minimum of 60% of the aircraft shall be reusable or recyclable.

Furthermore, two additional factors were incorporated alongside the requirements. Firstly, it should be determined whether components or parts have a traceable and document origin, possess certification for environmentally responsible sourcing and are free from child or forced labour. Secondly, the accessibility of components and parts was taken into consideration in the trade-off process. This way, it was ensured that maintenance can be conducted when required or that parts have a sufficiently long lifetime without needing maintenance.

5.3. Aircraft characteristics

Following the requirements and considerations from Section 5.2, some aircraft characteristics should be checked during every design phase. All characteristics are listed below.

1. GWP of emissions per passenger-kilometre.
2. GWP of emissions for producing 1 MJ of LH_2.
3. GWP of emissions during production.
4. GWP of emissions during manufacturing.
5. Emitted noise by the aircraft.
6. Service life.
7. Fractions of materials that are recyclable at the end of life.

5.4. Requirement verification

Having set up the requirements and identified the aircraft characteristics to be checked, the characteristics from Section 5.3 should meet the requirements from Section 5.2. In Chapter 15, the aircraft characteristics will be calculated if possible and estimated otherwise. When the aircraft characteristics meet the requirements, they will be documented. If this is not the case, further action is needed which will be discussed in Section 5.5. Next to this, it would be important for future design phases to perform real-world aircraft testing. This process will be highlighted in Section 5.5 as well.

5.5. Non-compliance with sustainability requirements

Several solutions have been proposed in the Baseline Report [2] and Midterm Report [13] in case the aircraft characteristics do not match the requirements. The solutions to adopt a more sustainable design are listed below. Further solutions when requirements are not met will be discussed in Chapter 15

- Over-designing parts to improve long-term structural integrity to be able to reuse them at the end of life.
- Expanding the functionality of parts to make reuse easier.
- Performing a design review to lower noise emissions. This could include lowering the fan tip steep, lowering the fan pressure ratio, lowering jet exhaust velocity, using special noise-absorbing material, and making the aircraft more aerodynamic to prevent turbulent flow.
- Performing a design review to lower greenhouse emissions by making the aircraft more efficient. This could be done by optimizing structures to reduce weight or optimizing aircraft shapes to reduce drag.
- Flying at different altitudes to lower the GWP value of emissions.
- Using renewable energy resources in the production process and for the production of hydrogen.

6

Design Options

In this chapter, the main design options that were considered in the midterm report are summarised. This showcases how the team arrived at a truss-braced configuration with hydrogen propulsion, rather than a different configuration and propulsion system.

6.1. Design options

One of the first challenges to address with the design of WorldBus was the large design space. The goal is to create an aircraft that can fly at least 19 000 km and can bring passengers from the departure airport's entrance to the destination airport's exit within 24 hours. Within these constraints, there are almost too many designs that could potentially solve the issue at hand. In order to limit the design space, and to maximise the probability of finding a feasible design, two different design option trees (DOTs) were made: one for the propulsion system and one for the aircraft configuration. A DOT was made to find all possible design solutions. However, many options could be eliminated a priori for a variety of reasons. For instance, a catapult was considered, but that will not provide the range required. This left the team with five different configuration options: a traditional swept wing design, a blended wing body, a box wing, a truss-braced wing or a multi-fuselage. For the propulsion system, six different options were considered: a liquid hydrogen turbojet, a liquid hydrogen turboprop, a liquid hydrogen turbofan, a turbofan running on synthetic kerosene, a ducted fan using liquid hydrogen and fuel cells, and finally, a ducted fan using lithium-ion batteries.

6.2. Preliminary trade-off

For both the configuration trade-off and the propulsion trade-off, a number of criteria were chosen that would aid in finding the best option for the configuration and the propulsion system. To select criteria that were appropriate, four needs were identified that are important to meeting the user requirements. They are the following:

- The aircraft needs to have the lowest impact on the environment possible.
- The aircraft needs to have the highest performance possible.
- The aircraft needs to be as cheap as possible.
- The aircraft needs to be as comfortable as possible.

Every criterion is chosen to be relevant to these needs, and the weight of the criterion is chosen based on how much it will impact the need. The criteria and weights are listed in Table 6.1 and Table 6.2 for the configuration trade-off and the propulsion system trade-off, respectively.

Table 6.1: The relative importance of configuration criteria in percentages weighted by score.

	Environmental impact	High performance	Cheap design	Passenger comfort	Total criterion weight
Need importance	**4**	**3**	**2**	**1**	**-**
Aerodynamic efficiency	40	50	0	30	34
Mass	30	50	10	0	29
Manufacturing	30	0	40	20	22
Compatibility airport	0	0	20	40	8
TRL	0	0	30	10	7
Total percent	100	100	100	100	100

Table 6.2: Determining the relative importance of propulsion criteria in percentages weighted by score.

	Environmental impact	High performance	Cheap design	Passenger comfort	Total criterion weights
Need importance	**4**	**3**	**2**	**1**	**-**
Propulsion system weight	20	40	20	0	24
Emissions	40	0	0	60	22
Delivered energy per stored energy mass unit	20	30	0	0	17
Delivered energy per stored energy volume unit	20	30	0	0	17
Cost	0	0	40	40	12
TRL	0	0	40	0	8
Total percent	100	100	100	100	100

With the criteria established, a trade-off was performed for both the configuration selection and the propulsion type. The result of this trade-off is shown in Figure 6.1. Every option was awarded a total score based on how well that option performed in the trade-off, and a sensitivity analysis was performed to verify that the winner(s) of the trade-off was not the result of an imbalanced trade-off. If this were the case, small changes in the relative importance of different criteria could result in a different design performing best in the trade-off. With the sensitivity analysis, a specific weight was decreased by 5 percentage points and one by one all other weights would be increased by 5 percentage points. The 'max' and 'min' columns indicate the best and worst scores achieved in the trade-off during the sensitivity analysis. As can be seen in Subfigure 6.1a, for the configuration trade-off, the blended wing, truss-braced wing, and the multi-fuselage perform best. Then, for the propulsion trade-off, the liquid hydrogen turbofan is clearly the best option as shown in Subfigure 6.1b. Moreover, the sensitivity analysis showed that the relative performance of every option was not incidental.

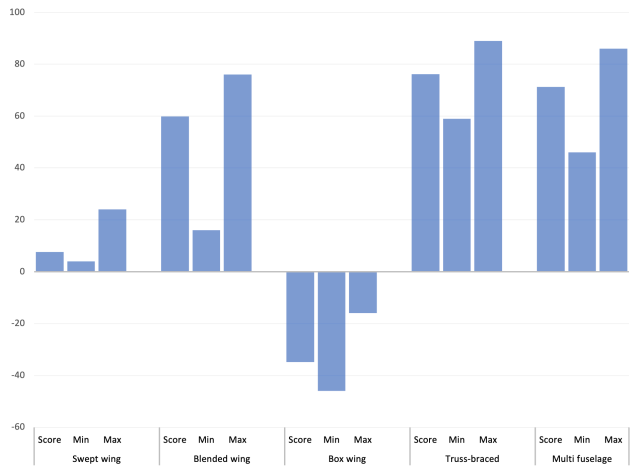

(a) Configuration trade-off.

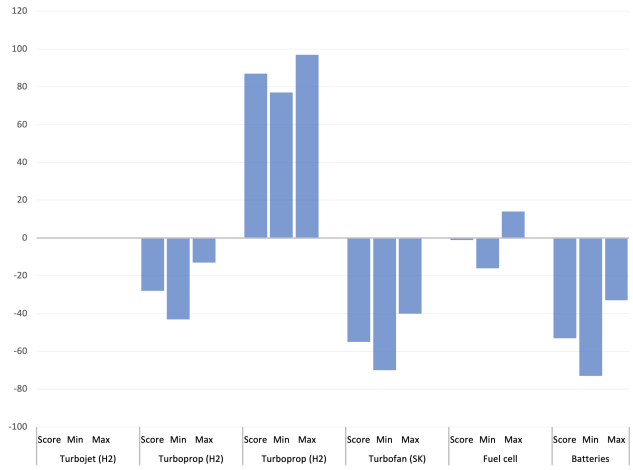

(b) Propulsion system trade-off.

Figure 6.1: Results of preliminary trade-offs. The 'min' and 'max' columns indicate, respectively, the lowest and highest scores achieved by the design in the sensitivity analysis.

From the trade-off, three combinations of configurations and propulsion types were chosen for further analysis. From the propulsion trade-off, it was clear that a liquid hydrogen turbofan would be the best option. During the sensitivity analysis, it scored best 100% of the time, regardless of which weights were changed. Then, for the configuration, three options

were considered after the trade-off: the blended wing, the truss-braced wing, and the multi-fuselage aircraft. As stated, every aircraft will use the liquid hydrogen turbofan propulsion system.

6.3. Final trade-off

For the three design options as listed in Section 6.2, new criteria were established that would best exemplify where the designs differed so that the best option could be chosen. After all, every design uses the same propulsion type, so having a criteria 'engine efficiency' would not be useful as all designs perform identically in that criterion. Similar to before, the criteria were given relative weights based on how they influenced the needs. This leads to the criteria as given in Table 6.3.

Table 6.3: Determining the relative importance of the final design criteria in percentages weighted by score.

	Environmental impact	**High performance**	**Cheap design**	**Passenger comfort**	**Total weight**
Need importance	**4**	**3**	**2**	**1**	**-**
Aerodynamic efficiency	60	60	30	0	48
Manufacturing & maintenance	40	0	40	0	24
Airport compatibility	0	40	30	0	18
Passenger comfort	0	0	0	100	10
Total percent	100	100	100	100	100

Performing the final trade-off with the corresponding criteria shows that the truss-braced liquid hydrogen aircraft is the best contender to perform the WorldBus mission. This can be seen in Figure 6.2. In the sensitivity analysis too, the truss-braced aircraft consistently came in first place.

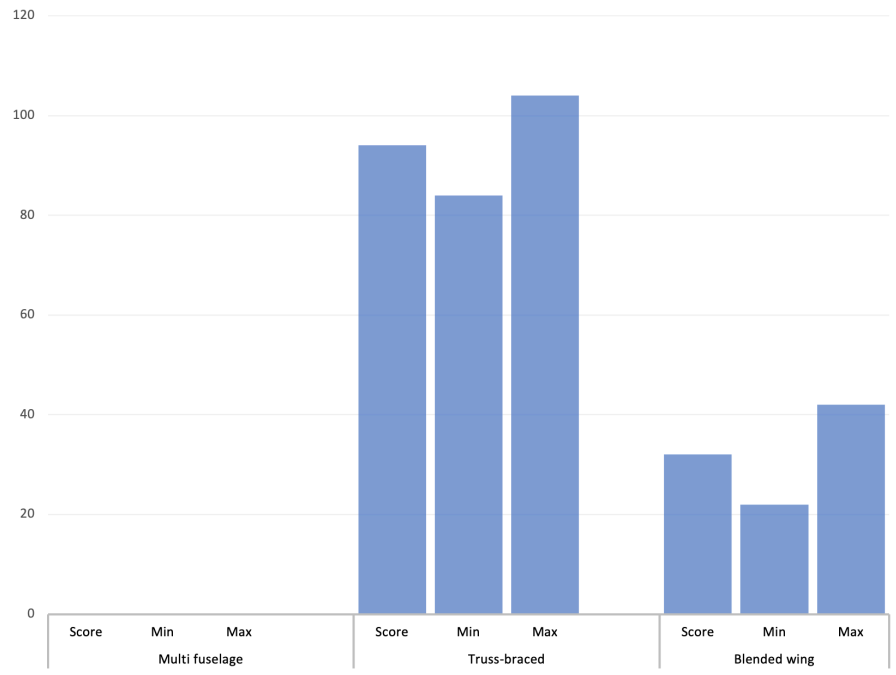

Figure 6.2: Results of final trade-off. The 'min' and 'max' columns indicate, respectively, the lowest and highest scores achieved by the design in the sensitivity analysis.

7

Design integration and systems engineering

Design integration and systems engineering (DISE) concerns the correct and effective integration of different system and subsystem designs within a project. If not done properly, different disciplines will produce various systems and designs that will not function together, leading to a below optimal design or even failure of the design. An efficient and productive DISE approach requires cooperative and pragmatic communication, in which the responsible engineers have a complete overview of the interrelations between the various systems and designs. Section 7.1 elaborates further on the DISE strategy used during the WorldBus design process, and Section 7.2 breaks down the mass allocation among the various aircraft systems.

7.1. Design Integration

When designing a product, it is crucial to keep in mind that each subsystem being designed and optimised, needs to be joined together during the final assembly. Without proper integration of systems and design procedures, the final product would not function as intended resulting in delays and increased R&D costs. Furthermore, the subsystems of an aircraft are heavily interrelated, and these relationships can be complex. This section intends to explain how information was centralised for this design process and how it was distributed to serve the individual subsystem design procedures. This, in turn, provided the group with high confidence that the aircraft as a whole will function as intended when all subsystems are put together.

To start the design process, a Class I weight estimation was used. In order to perform this estimation some external information is needed. Reference aircraft data is found, as well as mission and engine data, to compute a first estimate of the aircraft's maximum take-off weight (MTOW), operational empty weight (OEW), and fuel weight. These weights are then distributed to the various technical disciplines involved. These include aerodynamics and fuel tank design. From aerodynamics, the wing planform, the high lift devices (HLD), and the control surfaces were sized. In addition, the drag and lift performance of the aircraft was also analysed. The fuel tank design outputs the dimensions and weight estimate of both the primary and secondary liquid hydrogen tanks.

Further down the line, this information is fed into the fuselage sizing procedure, the internal layout section, and a Python program which computes the weight of the wing and the truss structure. This data is then fed into a program that designs the structure of the fuselage. In the end, all data is transferred into a Class II weight estimation. The Class II results are fed back into the Class I weight estimation and stability and control. Using the outputs from stability and control, the undercarriage can be positioned and sized for ground stability. This entire process is updated and performed multiple times until the weight variations between consecutive iterations become negligible. This iteration process increases the accuracy of the design as the Class II weight estimation is more precise than the Class I weight estimation, and more information about the aircraft is known as this process progresses.

As all the information is centralised in one Excel file, and all the values are automatically updated in every sheet when any new value was found, there is high confidence that the aircraft design will function as a whole without any issues. The last things that need to be done are analysing the aircraft performance, analysing the financial feasibility of the project, and analysing the sustainability of the project. These three analyses verify that the user requirements are still being complied with at the end of the design process.

The entire described process is visualised in Figure 7.1. The blocks represent the major design processes and the arrows show the flow of information between each process. The arrows are labelled, which displays the information or data transferred to and from a specific design section.

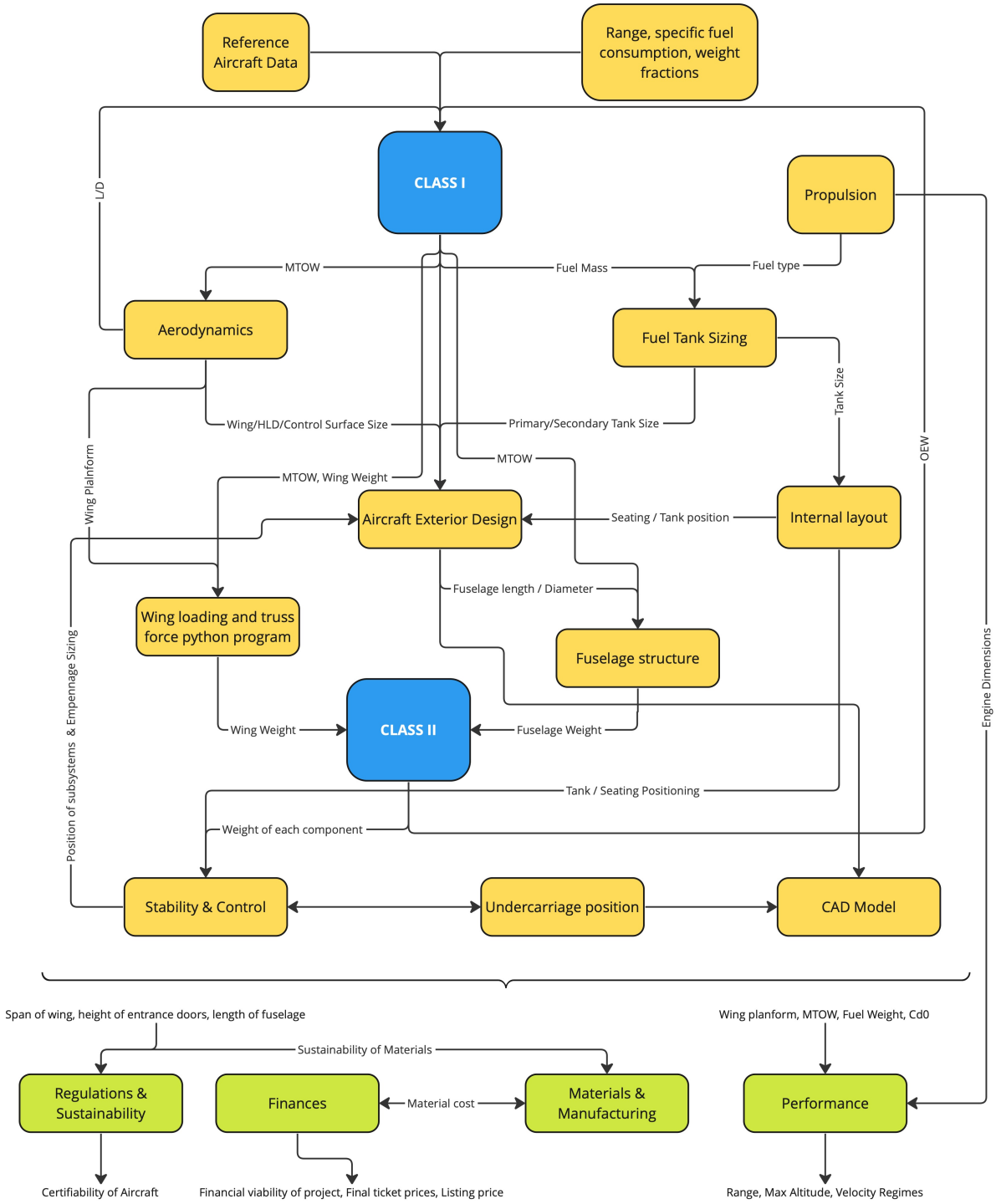

Figure 7.1: Design process interrelations diagram.

7.2. Mass budget

In order to have a successful design of WorldBus it is important to take into account that certain components of the aircraft might turn out heavier than initially estimated. The effect of a single change is large. For example, the fuel tank might be heavier than expected, which causes the wing to become larger, and as a result, larger engines are required, for which a larger fuel tank is needed. This is called the 'snowball effect'. To prevent this from happening, it is important to have accurate estimates for the weight fractions of the aircraft. To make sure the design of WorldBus will remain feasible when subsystems increase in weight, a contingency margin of 10% is applied to all aircraft components and 20% to the fuselage and wing components since these are calculated separately from the Class II weight estimations. It should also be noted

that the WorldBus design has a strict upper limit for the MTOW, as airports do not allow for a wingspan larger than 80 m.[23] With the wing loading achieved in Section 9.1 a strict upper limit for the MTOW of 276 966 kg is found. In Table 7.1 the mass breakdown of WorldBus is given. It gives an overview of the various aircraft weights, such as OEW and MTOW, for the final design. Moreover, it gives a breakdown of the mass of aircraft components. When reviewing the MTOW after the contingency margins are applied, it becomes apparent that it stays 20 000 kg below the upper MTOW limit of the WorldBus design.

Table 7.1: Mass budget breakdown.

Mass	**Calculated value (kg)**	**Max value (kg)**	**Contingency margin(kg)**
Wings	42 576.7	51 092.0	8515.3
Fuselage	20 091.8	24 110.2	4018.4
Empennage	2710.0	2981.0	271.0
Landing gear	7225.2	7947.7	722.5
Propulsion system	50 258.2	55 284.0	5025.8
Systems	17 973.9	19 771.2	1797.4
Operating items	2342.4	2576.7	234.2
Miscellaneous	15 579.9	17 137.9	1558.0
OEW	158 584.7	180 927.0	22 342.3
Payload	20 006.8	22 007.9	2000.7
Fuel	45 185.8	51 344.9	6159.1
MTOW	223 777.3	254 279.4	30 502.1

[23] https://www.nwcg.gov/sites/default/files/committee/docs/iabs-temp-atb-airport-ramp-consideration-update-2019.pdf

8

Fuselage layout

In this chapter, the design of the fuselage is discussed. First, all relevant parameters established in the previous design phase will be provided and updated if applicable. Thereafter, two drawings of the fuselage layout and fuselage cross-section will be presented. The emergency exits, lavatories, galleys, sleeping space for the crew, stairs, overhead storage, and cargo compartment will be discussed. It is worth noting that in the design of WorldBus the passenger compartment is divided into two separate cabins.

8.1. Fuselage sizing

In the previous design phase, a preliminary fuselage cross-section was designed. With these dimensions, the entire fuselage can be sized. In Table 8.1, all relevant parameters regarding the cross-section can be seen.

Table 8.1: Dimensions of the fuselage cross-section

Parameter	Unit	Business Class	Economy+ Class
Number of seats abreast	-	4	7
Seat width	[m]	0.538	0.478
Armrest width	[m]	0.080	0.060
Clearance distance	[m]	0.02	
Width of cabin	[m]	3.77	5.01
Width of headroom	[m]	3.03	4.37
Aisle height	[m]	1.94	
Aisle width	[m]	0.51	
Shoulder height	[m]	0.95	
Headroom height	[m]	1.68	
Floor height	[m]	0.20	

From the internal layout, the inner- and outer diameters of the fuselage were determined. Using those values, the nose cone, tail cone, and tail length were found. The cockpit length was estimated on a fixed value. From the number of passengers and configuration details, the number of rows and consequently the cabin length was estimated. Since the fuel tank is incorporated into the fuselage, the tank length is added to the fuselage. Moreover, differently from the previous design phase, the secondary tank is moved from the tail to behind the primary tank due to its increased size. Therefore, the length of the secondary tank must also be added to the fuselage. In addition, the lengths of the tanks differ from the previous design phase due to the design iterations performed. A change in weight means, among other things, a change in fuel needed, and therefore a change in tank length. Adding all lengths provides a total fuselage length. All sizes are given in Table 8.2.

The values from Table 8.1 and Table 8.2 have been verified in the midterm report [13]. This involved inputting data from the Boeing 757-200 into our calculation method and comparing the results with actual aircraft data. The deviations observed were found to be below 5%, indicating that our method provides reasonable and correct results.

8.2. Fuselage layout and cross-section

In Figure D.1 given in the appendix, the top view of the fuselage layout is presented. The placement of the emergency exits, lavatories, galleys, crew rest compartments, and the stairs are included in this layout. In Figure 8.1, the fuselage cross-section is presented. These drawings show that placing the fuselage parts and passengers inside the designed fuselage is feasible. In a further design phase, this design could be further optimised and adapted to the airline's wishes if necessary.

Table 8.2: Fuselage dimensions

Parameter	Unit	Value	Parameter	Unit	Value
Inner diameter	[m]	5.90	Outer diameter	[m]	6.25
Seat pitch business class	[m]	1.51	Seat pitch economy+ class	[m]	0.97
Front cabin length	[m]	15.82	Aft cabin length	[m]	15.82
Cockpit length	[m]	4.00	Nose cone length	[m]	12.50
Tail cone length	[m]	21.87	Tail length	[m]	10.00
Primary tank length	[m]	23.86	Secondary tank length	[m]	5.07
Tank margin	[m]	0.75	Fuselage length	[m]	75.31

Several characteristics of the top view are worth mentioning. In the current layout, there are a total of 118 economy seats, instead of the required 117. This will be beneficial for the revenue as one extra ticket can be sold. However, the user can also choose to use the space of this extra seat for other purposes, such as additional galley space or an additional lavatory. In the current layout, 102 passengers are seated in the front cabin of which 43 are in business class, and 99 passengers are seated in the aft cabin, of which 40 are in business class. Furthermore, the space under the cockpit in the lower deck is now used to give space to three business seats, and a crew rest compartment for two crew members. Lastly, in the current layout, a margin of 10 cm between different fuselage sections is taken. In practice, this margin could be further reduced providing even more space available in the fuselage as assembly accuracy is increased.

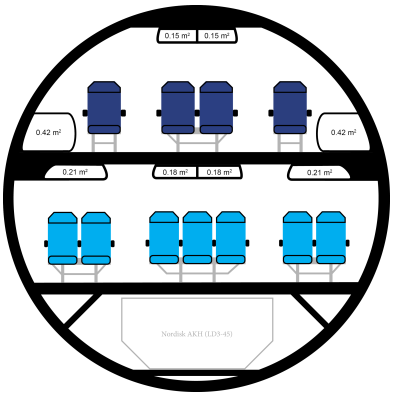

Figure 8.1: Fuselage cross-section

8.3. Emergency exits

The number of emergency exits follows from EASA certification specification 25.807 [18]. For 102 passengers, one type I and two type III emergency exits are required [19]. However, WorldBus is equipped with two type A and one type III emergency exits. The type I emergency exit features a 46 cm wider width and a 61 cm taller height compared to a type I emergency exit [19]. This leaves a margin which allows for an increased passenger number for possible future configuration options without design alterations. This allows for at least 139 passengers per cabin. The two type A exits will also function as entrance doors. The type III exits are located on the upper deck, such that passengers are able to evacuate the aircraft without needing to use the stairs. The dimensions of the emergency exits can be observed in Table 8.3.

8.4. Lavatories

Regulations do not prescribe a minimum number of lavatories. In the current layout, four lavatories, i.e. on average 1 per 25 passengers, are incorporated per cabin. The lavatory's layout dimensions can be observed in Table 8.3 [19].

8.5. Galleys

Typically, a minimum of $0.0283\,m^3$ of galley volume per passenger is present on the aircraft [19]. On the lower deck, the galley volume will be located under the stairs providing a galley volume of $2.61\,m^3$ which corresponds to $0.0318\,m^3$ per passenger. On the upper deck, the galley volume will be located behind the stairs providing a galley volume of $1.995\,m^3$ which corresponds to $0.0665\,m^3$ per passenger. This extra space could also be used to store additional equipment like first aid kits, blankets, pillows or waste disposal.

8.6. Crew rest compartment

On long-haul flights, the crew would be scheduled for long periods of time, surpassing the duty time limitations specified by regulations [18]. To improve the crew well-being and comply with these requirements, the WorldBus design incorporates crew rest compartments in the aircraft to allow the crew to rest during long flights. In total, the on-duty crew will consist of two pilots and four flight attendants, so six rest compartments are incorporated into the aircraft. The dimensions of the compartment's layout can be seen in Table 8.3. One crew rest compartment giving space for two crew members is located under the cockpit.

8.7. Stairs

The cabin designs span two decks, so staircases are needed to allow passengers to move between decks. In the staircase design, OSHA staircase requirements were used as guidelines.[24] The stairs are designed with a step depth of 26 cm, step width of 91.44 cm, and step height of 19.27 cm. The rise of the stairs is 2.12 m, so the staircases will consist of 11 steps, resulting in a total horizontal staircase length of 2.86 m.

8.8. Storage compartments

The aircraft design incorporates two storage compartments. In the cabin, four overhead storage compartments are present in economy+ class, and two overhead storage compartments together with two side storage compartments are present in business class. The areas of the storage compartments can be observed in the cross-section of Figure 8.1. Together they provide a total storage volume of 23.76 m^3 taking into account the seating configuration from Figure D.1. Next to the in-cabin storage compartment, the fuselage also has a storage compartment with an area of 4.95 m^2 underneath the cabin from the lower deck. Its total volume is 55.79 m^3. Both cargo compartments combined provide sufficient space for the passenger luggage, which is assumed to require a total volume of 28.24 m^3 [13].

For the design of the cross-section, the Nordisk AKH (LD3-45) standard cargo box is drawn into the compartment to demonstrate the compartment size. This cargo box could be used to optimise the cargo loading into the aircraft, or provide easy cargo handling at the airport.

Table 8.3: Cabin facilities dimensions.

Facility	Unit	Dimensions
Type A emergency exit, width × height	[cm × cm]	106.7 × 182.9
Type III emergency exit, width × height	[cm × cm]	50.8 × 91.4
Lavatory layout, width × length	[cm × cm]	91.4 × 91.4
Galley volume lower deck	[m^3]	2.61
Galley volume upper deck	[m^3]	1.995
Crew rest compartment layout, width × length	[cm × cm]	75.0 × 200.0
Stairs, step depth × step width × step height	[m × m × m]	26.0 × 91.44 × 19.27
Staircase, width × length × height	[m × m × m]	91.44 × 2.86 × 2.12
Overhead storage volume	[m^3]	23.76
Cargo compartment volume	[m^3]	55.79

8.9. Conclusion and recommendations

In conclusion, the layout presented in this chapter demonstrates the feasibility of incorporating all cabin amenities into the fuselage design of WorldBus. It successfully accommodates the required 200 passengers and corresponding amenities while providing enough comfort and complying with the CS25 regulations. A list of further recommendations can be found below.

- In practice, the layout should be further optimised and customised to align with the specific preferences and requirements of an airline. For instance, an airline may have specific needs such as additional lavatories or crew rest compartments.
- In the existing layout, an additional economy+ class seat is included. However, the space used for this seat could also be utilized for other purposes as well. The decision regarding its utilization should also be made based on the preferences and requirements of the specific airline.
- The stairs are designed according to OSHA staircase requirements. However, it is important to note that stairs in aircraft may need to meet different, potentially less stringent, requirements. In the further design phase, safety institutions should be consulted to address this aspect.

[24] https://www.osha.gov/laws-regs/regulations/standardnumber/1910/1910.25

9 Aerodynamics

WorldBus aims to be a sustainable aircraft capable of flying exceptionally long distances. To achieve this, the aerodynamic efficiency preferably is very high. A lower aerodynamic efficiency increases drag and, thus, increases weight. This chapter starts with analysing the wing loading and thrust-over weight diagram in Section 9.1, from here the wing planform could be designed in Section 9.2. With the most important coefficients now determined, an airfoil is chosen in Section 9.3 and with this chosen a complete wing and drag analysis could be performed in Section 9.4 and Section 9.5. After this, the high-lift devices and control surfaces have been sized in Section 9.6 and Section 9.7. Finally, verification was performed in Section 9.8 to ensure correctness after which a conclusion was written and recommendations were made in Section 9.9.

9.1. Wing loading and thrust-over-weight diagram

The wing and thrust loading diagram form an essential first step in determining the design parameters for the wing. In order to create an aircraft with optimal performance, a high wing loading W/S combined with a low thrust-over-weight ratio T/W is desired. This is due to the fact that a high wing loading results in a smaller wing surface area and thus less drag. A low thrust-over-weight is advantageous as it reduces the engine size and weight needed, thus reducing overall weight and fuel consumption.

While designing the wing loading and thrust-to-weight diagram, use has been made of eight different performance requirements as explained in the AE1222-II ADSEE course [19]. As the preliminary design was included in the midterm report, estimated values for $C_{L_{max}}$ could be updated [13]. This leaves only the stall speed to be estimated in order to determine the wing loading for stall during clean and landing configuration. The former will be a limiting factor in this wing loading diagram as can be seen in Figure 9.1. The intersection of this line with the minimum performance requirement for take-off yields the initial design point for this wing. This point has a value of $5941\,\mathrm{N/m^2}$ for the wing loading and a value of 0.27 for the thrust-over-weight ratio.

9.2. Wing planform design

Once the wing loading is established from the wing loading and thrust-to-weight diagram, the surface area can be calculated with the maximum take-off weight. The wing aspect ratio is set to 14 as mentioned in the midterm report, which is important for aerodynamic efficiency [13]. In addition, a taper ratio (λ) of 0.3 is chosen based on reference aircraft and to approximate an optimal elliptical lift distribution. Then, the wing planform parameters can be established which are shown in Table 9.1. Equation 9.1 until Equation 9.7 are used for the establishment of some of these values [19].[25]

$$b = \sqrt{SA} \tag{9.1}$$

$$\cos(\Lambda_{0.25c}) = 0.75\frac{M^*}{M_{dd}} \tag{9.2}$$

$$c_r = \frac{2S}{(1+\lambda)b} \tag{9.3}$$

$$c_t = \lambda_t c_r \tag{9.4}$$

$$MAC = \frac{2}{3}c_r\frac{1+\lambda+\lambda^2}{1+\lambda} \tag{9.5}$$

$$\Lambda_{LE} = \tan^{-1}\left[\tan(\Lambda_{0.25c}) + \frac{4}{AR}\left(0.25\frac{1-\lambda}{1+\lambda}\right)\right] \tag{9.6}$$

$$\Gamma = 3 - \frac{\Lambda_{0.25c}}{10} - 2 \tag{9.7}$$

In Equation 9.1 until Equation 9.7, b is the span of the wing, S is the surface area of the wing, and A is the aspect ratio. Equation 9.2 is used to make a first estimate of the sweep angle, where $\Lambda_{0.25c}$ is the quarter chord sweep angle, M^* is the technology factor for supercritical airfoils which equals 0.935, and M_{dd} is the drag-divergence Mach number which equals

[25] https://www.fzt.haw-hamburg.de/pers/Scholz/HOOU/AircraftDesign_7_WingDesign.pdf

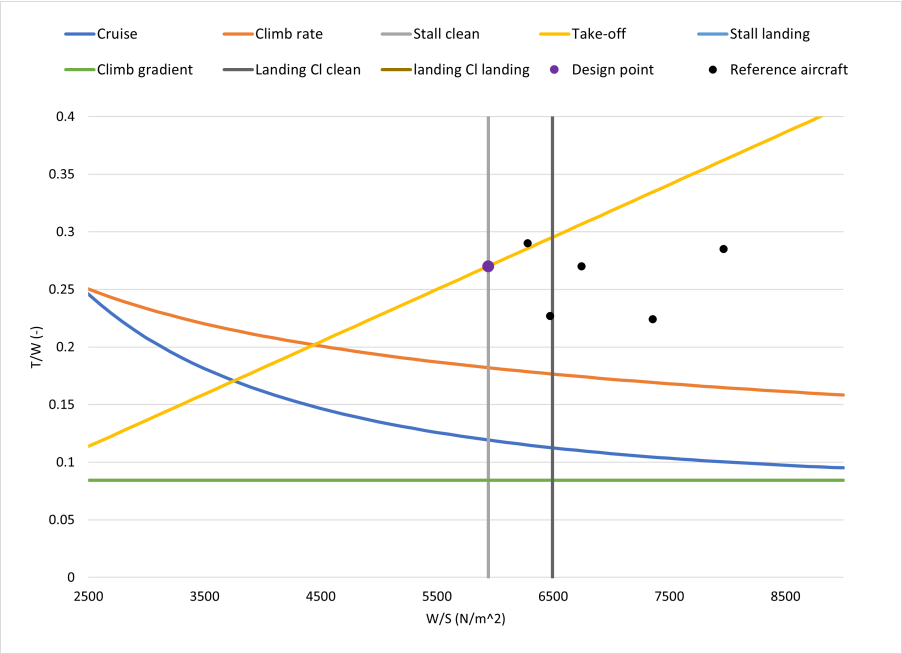

Figure 9.1: Wing loading and thrust-over-weight diagram.

$M_{dd} = M_{cruise} + 0.03$. Lastly, c_r and c_t are the root chord and tip chord respectively, MAC is the mean aerodynamic chord, and Γ is the dihedral angle.

Table 9.1: Wing planform parameters

Parameter	Unit	Value	Parameter	Unit	Value
Wing surface area	[m^2]	369.4	Tip chord	[m]	2.4
Aspect ratio	-	14	Mean aerodynamic chord	[m]	5.6
Span	[m]	71.9	Quarter chord sweep	[deg]	38.8
Taper ratio	-	0.3	Leading edge sweep	[deg]	40.1
Root chord	[m]	7.9	Dihedral	[deg]	-2.1

9.3. Airfoil selection

Now that the wing is designed and the to-be-achieved coefficients are clear, a matching airfoil must be chosen. In the midterm report, a short trade-off has been made between 4 airfoils [13]. The SC(2)-0714 excelled in all criteria. As this airfoil is one of multiple phase 2 supercritical airfoils designed by NASA, a number of these are analysed to determine if the SC(2)-0714 is the most appropriate airfoil from this set. The analysed airfoils are shown in Table 9.2 together with the coefficients on which they have been evaluated.

In order to select one of these airfoils, more coefficients and values should be calculated. Using a technique explained in ADSEE, the design lift coefficient, $C_{L_{des}}$, for the wing is determined with Equation 9.8 [20].

$$C_{L_{des}} = \frac{1.1}{q}\left\{\frac{1}{2}\left[\left(\frac{W}{S}\right)_{startofcruise} + \left(\frac{W}{S}\right)_{endofcruise}\right]\right\} \tag{9.8}$$

In Equation 9.8, q takes the dynamic pressure into account. Now, in order to choose an airfoil, the three-dimensional lift coefficient must be translated into a two-dimensional lift coefficient. This is done using Equation 9.9. This equation uses the estimated value of $40°$ for the wing sweep. However, during the design process, this value will most likely change and, thus, the design lift coefficient will be updated.

It should be noted that the lift coefficient calculated in Equation 9.9 is for a high Mach number. As analysing airfoils using XFLR5 (version 6.59) is done at low Mach numbers, compressibility effects should be taken into account.[26] This is done using the Prandtl-Glauert correction as shown in Equation 9.10.

[26] `https://sourceforge.net/projects/xflr5/files/6.59/`

$$C_{l_{des}} = \frac{C_{L_{des}}}{cos^2\Lambda} \tag{9.9}$$

$$C_{l_{des,M=0}} = C_{l_{des}}\sqrt{1-M_{cr}^2} \tag{9.10}$$

As can be seen in Equation 9.10, the critical Mach number must be known to determine the $C_{l_{des}}$ at which the airfoil will be analysed. Determining the critical Mach number, or M_{cr}, is done by looking at pressure coefficients. More specifically, the minimum pressure coefficient of an airfoil ($C_{p,min}$) and the critical pressure coefficient ($C_{p_{cr}}$). The value for M at which these pressure lines intersect is known as the critical Mach number.[27] Finally, the Reynolds number (adjusted for the leading edge sweep) is to be established using Equation 9.13.

$$C_{p,min} = \frac{C_{p,0}}{\sqrt{1-M^2}} \tag{9.11}$$

$$C_{p_{cr}} = \frac{2}{\gamma M^2}\left\{\left[\frac{1+\left(\frac{\gamma-1}{2}\right)M^2}{1+\left(\frac{\gamma-1}{2}\right)}\right]^{\frac{\gamma}{\gamma-1}} - 1\right\} \tag{9.12}$$

$$Re = \frac{\rho\cos(\Lambda_{LE})V_{cruise}MAC}{q} \tag{9.13}$$

It should further be noted that in Equation 9.11, for $C_{p,0}$, the lowest absolute value of the pressure is used. For the calculation of the critical pressure coefficient γ is used, which represents the ratio between the specific heats of air at constant pressure versus constant volume.

During analysis of the parameters in Table 9.2 and the graphs in Figure 9.3, it is observed that three airfoils demonstrate unwanted stall behaviour, meaning they have a sharp drop in C_l during stall. Therefore, these are no longer considered. Another important factor is the C_d at $C_{l_{des}}$ where it can be seen that the SC(2)-0712 has a lower C_d, lower $C_{l_{des}}$ and a higher M_{cr} compared to the SC(2)-0714 and SC(2)-0614. This means that the SC(2)-0712 is the most efficient airfoil for this use case and is therefore selected to be used in the WorldBus design. In Figure 9.2 the airfoil is shown with its parameters displayed in Table 9.3, gathered from XFLR5 at the cruise Reynolds number of 3.1×10^7.

Table 9.2: Airfoil characteristics

Airfoil	t/c	α_{des}	$C_{l_{des}}$	C_d at $C_{l_{des}}$	$C_{l_{max}}$	C_m at $C_{l_{des}}$	Unwanted stall behaviour	M_{cr}
SC(2)-0610	10	-1.02	0.313	0.006	2.43	-0.105	yes	0.754
SC(2)-0612	12	-1.14	0.323	0.006	2.49	-0.111	yes	0.735
SC(2)-0614	14	-1.29	0.329	0.007	2.54	-0.116	no	0.724
SC(2)-0710	10	-1.84	0.318	0.006	2.45	-0.123	yes	0.744
SC(2)-0712	12	-1.94	0.323	0.006	2.51	-0.126	no	0.734
SC(2)-0714	14	-2.15	0.328	0.007	2.58	-0.137	no	0.725

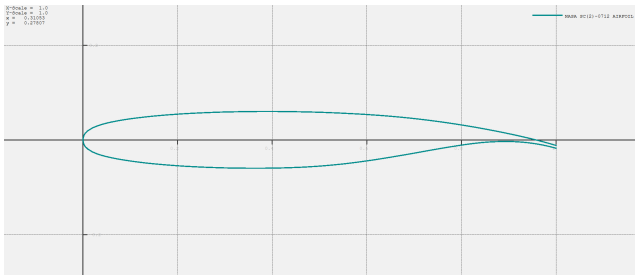

Figure 9.2: Nasa SC (2)-0712 airfoil

Table 9.3: Parameters for NASA SC (2)-0712 airfoil at RE=3.1×10^7.

Parameter	**Unit**	**Value**
$C_{l_{max}}$	-	2.5
α_{stall}	[deg]	22
α_0	[deg]	-4.61
t/c	-	0.12
Camber	-	2.2%

[27] http://www.akiti.ca/Mcrit.html

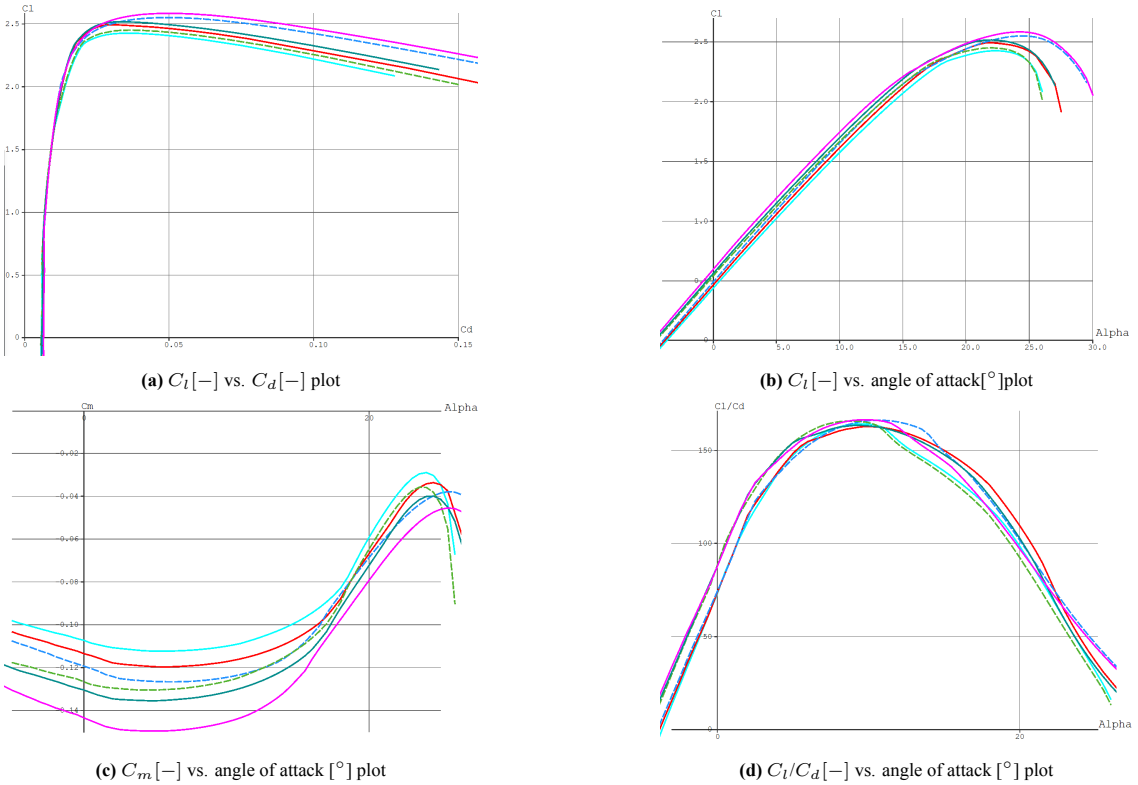

(a) $C_l[-]$ vs. $C_d[-]$ plot

(b) $C_l[-]$ vs. angle of attack[°]plot

(c) $C_m[-]$ vs. angle of attack [°] plot

(d) $C_l/C_d[-]$ vs. angle of attack [°] plot

Figure 9.3: Airfoil characteristics plots for a Reynolds number of $3.1 * 10^7$. SC(2)-0610 (**Cyan**), SC(2)-0612 (**Red**), SC(2)-0614 (**Blue**), SC(2)-0710 (**Green**), SC(2)-0712 (**turquoise**) SC(2)-0714 (**Purple**)

9.4. Wing analysis

Once the airfoil has been selected, the wing can be further analysed. In Section 9.2 the sweep of the airfoil was estimated with Equation 9.2. However, now the critical Mach number of the airfoil is known to be 0.734 and the critical Mach number of the wing, which is assumed to be the same as the cruise Mach, is 0.87, the sweep angle of the leading edge is reevaluated and is calculated using Equation 9.14. The new sweep angle was found to be 32.7 °. From here, the quarter chord sweep is calculated using Equation 9.15, resulting in a value of 31.1 °.

$$\lambda_{LE} = \arccos\left(\frac{M_{cr,airfoil}}{M_{cr,wing}}\right) \quad (9.14) \qquad \Lambda_{0.25c} = \tan^{-1}\left[\tan(\Lambda_{LE}) - \frac{4}{AR}\left(0.25\frac{1-\lambda}{1+\lambda}\right)\right] \quad (9.15)$$

The lift curve slope (C_{L_α}) is analysed at cruise conditions, at a Mach of 0.87, and at sea level conditions, at a Mach of 0.2 (landing speed). Since Equation 9.17 can only be used for a Mach smaller than 0.8, Equation 9.16 is used for cruise condition [21].

$$C_{L_\alpha} = \frac{2\pi A}{2 + \sqrt{AR^2 + 4}} \quad (9.16) \qquad C_{L_\alpha} = \frac{2\pi A}{2 + \sqrt{\left(\frac{A\beta^2}{\kappa}\right)^2\left(1 + \frac{tan^2(\Lambda_{0.5c})}{\beta^2}\right) + 4}} \quad (9.17)$$

$$\beta = \sqrt{1 - M^2} \quad (9.18) \qquad \kappa = \frac{C_{l_\alpha}}{2\pi} \quad (9.19)$$

Where β is the Prandtl-Glauert compressibility factor and κ is the airfoil efficiency factor calculated with Equation 9.18 and Equation 9.19 respectively. The cruise Mach number and the lift curve slope of the airfoil (C_{l_α}) are used for this calculation. This resulted in a value for C_{L_α} of 5.45 rad^{-1}, for cruise conditions, and 5.05 rad^{-1}, for sea level conditions.

Finally, multiple stall angles of the wing should be computed. In order to do so, the maximum lift coefficient at cruise and sea level flight should be determined. This is done using the DATCOM method with Equation 9.20 and Equation 9.21 [12].

$$C_{L_{max}} = \left[\frac{C_{L_{max}}}{C_{l_{max}}}\right] C_{l_{max}} + \Delta C_{L_{max}} \tag{9.20}$$

$$\alpha_s = \frac{C_{L_{max}}}{C_{L_\alpha}} + \alpha_{L=0} + \Delta\alpha_s \tag{9.21}$$

The values for $\frac{C_{L_{max}}}{C_{l_{max}}}$ and $\Delta C_{L_{max}}$, which accounts for the compressibility effects on $C_{L_{max}}$, were found to be 0.79 and -0.31 respectively in Raymer [12]. This leads to a value of $C_{L_{max}}$ of 1.96, at sea level, and 1.67, in cruise. Continuing with the stall angle of attack, a value of 3.2 is found for $\Delta\alpha_s$, accounting for the compressibility effects on α_s, using Raymer [12]. The zero-lift angle of attack is deduced from analysis in XFLR5 (version 6.59), yielding $-4.61\,°$.[28] The remaining variables have been calculated in Equation 9.16, for cruise, Equation 9.17, for landing, and Equation 9.20 for both situations. Now, starting with the stall angle of attack during cruise, a value of $16.1\,°$ is obtained. For sea level, at a flight speed of 0.2 Mach, a value of $20.8\,°$ is calculated.

9.5. Drag analysis

Performing an analysis regarding the drag consists of two main components as shown in Equation 9.22. Namely, zero-lift drag which is described in Subsection 9.5.1 and lift-induced drag which is described in Subsection 9.5.2. The zero-lift drag will be established for different components of the aircraft and the lift-induced drag will take the contribution due to generated lift into account.

$$C_D = C_{D_0} + \frac{{C_L}^2}{\pi A e} \tag{9.22}$$

9.5.1. Zero-lift drag

To calculate the zero-lift drag contribution the component build-up method from Raymer is used [12]. The general formula used is Equation 9.23, the different components will be discussed throughout this section.

$$C_{D_0} = \frac{1}{S_{ref}} \sum_c C_{f_c} F F_c I F_c S_{wet_c} + C_{D_{misc}} \tag{9.23}$$

Parasite drag

The first coefficient to be determined is the flat plate skin friction coefficient (C_{f_c}). This coefficient is contributed to by laminar as well as turbulent flow over the wing calculated with Equation 9.24 and Equation 9.25 respectively. To calculate the total value of the flat plate skin friction coefficient, the weighted average of both flows is taken over each component. An example is given for the wing during cruise flight Equation 9.26.

$$C_{f_{lam,c}} = \frac{1.328}{\sqrt{Re}} \tag{9.24}$$

$$C_{f_{tur,c}} = \frac{0.455}{(log_{10}Re)^{2.58}(1 + 0.144M^2)^{0.65}} \tag{9.25}$$

$$C_{f_{wing}} = 0.5 C_{f_{lam}} + 0.5 C_{f_{tur}} \tag{9.26}$$

The component that form factor (FF_c) is calculated for the fuselage, wing, horizontal tail, vertical tail, struts, pylons and nacelles. Formulas from Raymer have been used to establish these values [12]. Furthermore, the component interference factor (IF_c) takes into account the increase in drag, due to interference between components and is specifically important for the struts, pylons, and nacelles. Lastly, S_{wet_c} is the wetted area of the component analysed.

Miscellaneous Drag

Miscellaneous drag, $C_{D_{misc}}$ is caused by 5 main components. Fuselage upsweep, landing gear, flaps, excrescence & leakage and wave drag. All have been evaluated using Raymer's theory [12].

Conclusion

The zero-lift drag values generated per component are shown in Table 9.4, where it can be seen that the fuselage, the wing and the overall miscellaneous drag have the largest contribution. It is important to notice the drag the struts add, as this is only 3.9 percent of the total CD_0 of 0.0128.

[28] `https://sourceforge.net/projects/xflr5/files/6.59/`

Table 9.4: Final zero lift drag values per component

Component	Fuselage	Wing	Horizontal tail	Vertical tail	Struts	Pylons	Nacelle	Miscell-aneous	Total
C_{D_0}	0.00421	0.00368	0.00049	0.00053	0.00049	0.00009	0.00131	0.00197	0.01276
Percentage of total C_{D_0}	32.96	28.83	3.87	4.12	3.87	0.68	10.25	15.42	100.00

9.5.2. Lift induced drag

In addition to zero-lift drag, lift-induced drag is also a component of the total drag coefficient. To calculate the lift-induced drag Equation 9.27 is used [12], where the Oswald efficiency factor (e) is calculated with Equation 9.28 [20]. This resulted in a lift-induced drag of 0.0044.

$$C_{D_{lift}} = \frac{C_L^2}{\pi A e} \tag{9.27}$$

$$e = 1.78 * (1 - 0.045 * AR^{0.68}) - 0.46 \tag{9.28}$$

9.6. High lift devices

In order to determine the necessary high lift devices (HLD) that are to be used on the wing, the maximum lift increase from clean configuration should be determined. As explained in Section 9.4, the maximum lift coefficient during clean configuration, at sea level, is 1.97. Furthermore, during the drafting of the wing and thrust loading diagram, a maximum value for the lift coefficient has been determined, which equals 2.8 during landing configuration. From these two values, it can be deduced that the to-be-chosen high-lift devices should provide an increase in $C_{L_{max}}$ of 0.83. To ensure no stall happens during landing, a safety margin of 0.1 is added resulting in a final lift coefficient increase of 0.93.

As a way to achieve this $\Delta C_{L_{max}}$, use will be made of a combination of leading edge and trailing edge HLDs. Fowler flaps will be used for the trailing edge and the leading edge will make use of slats. Fowler flaps are mainly used to increase the maximum lift coefficient and slats mainly contribute towards a higher stall angle. Both are favourable during landing and take-off.

Sizing the HLDs is the next step. Using Equation 9.29, the necessary spanwise portion of these HLDs in relation to the total wing is determined. For this, the increase in the lift coefficient, ΔC_{lmax}, should also be determined. Using the equation for Fowler flaps, a value of 1.573 is determined [20].

$$\frac{S_{wf}}{S} = \frac{\Delta C_{L_{max}}}{0.9 \Delta C_{l_{max}} \cos(\Lambda_{hingeline})} \tag{9.29}$$

Now, the reference flapped and slatted surface can be determined using Equation 9.29 and their location along the wing can be established. The slats will start at one meter from the fuselage and continue for $16.9\,\text{m}$, and the flaps will start at five centimetres from the fuselage and continue for $23\,\text{m}$.

9.6.1. Lift curve

The use of high-lift devices increases the slope of the lift curve and shifts it to the left. To calculate the lift curve slope with the high lift devices deployed, Equation 9.30 is used. S' is the wing surface area when the high-lift devices are deployed and $C_{L_{alpha_{clean}}}$ is calculated in Section 9.4. To calculate the shift in the zero lift angle of attack, Equation 9.31 is used. Here, $\Delta_{\alpha_{L=0_{airfoil}}}$ is assumed to be $-15\,^\circ$ for landing and $-10\,^\circ$ for take-off [20].

$$C_{L_{\alpha_{flapped}}} = \frac{S'}{S} * C_{L_{\alpha_{clean}}} \tag{9.30}$$

$$\Delta\alpha_{L=0} = \Delta\alpha_{L=0_{airfoil}} \frac{S_{WF}}{S} \cos(\Lambda_{hingeline}) \tag{9.31}$$

The lift curve slopes for clean and flapped (extended flaps and slats) configurations are shown in Figure 9.4. Where the stall angles are calculated with Equation 9.21, at the corresponding $C_{L_{max}}$ and C_{L_α} values for the different configurations. With the equations mentioned before, the linear part of the lift curve slope is established, whereas for the curved part the same behaviour as the airfoil is used.

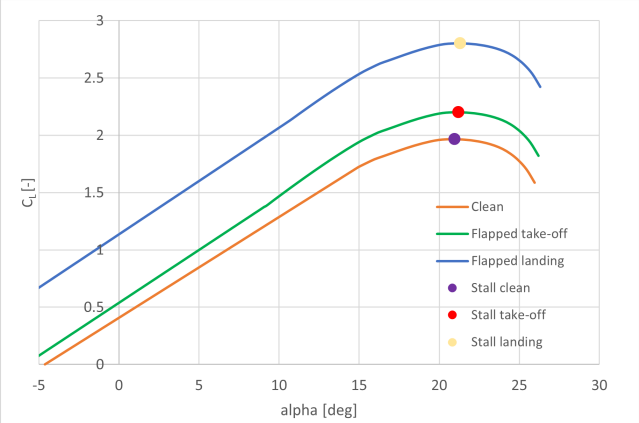

Figure 9.4: Lift curve graph for clean and flapped configurations

9.6.2. Miscellaneous drag due to high-lift devices

Now that the area for both the slats and the flaps has been determined, the additional drag of these devices when extended can be calculated. As different deflection angles are used for take-off and landing, multiple values are determined using Equation 9.32 in Table 9.5. The same equation is used to determine the miscellaneous drag for the slats.

$$\Delta C_{D_{flap}} = F_{flap}\left(\frac{c_f}{c}\right)\left(\frac{S_{flap}}{S_{ref}}\right)(\delta_{flap} - 10) \tag{9.32}$$

In Equation 9.32, F_{flaps} is a coefficient taking into account various flap geometry factors. $\frac{c_f}{c}$ shows the ratio of the chord length with flaps extended versus without extended flaps, $\frac{S_{flap}}{S_{ref}}$ shows the ratio of the reference wing flapped area to the total wing area and lastly, δ_{flap} is the angle that the flaps are deflected at.

Table 9.5: Drag increment due to high lift devices

$\Delta C_{D,0_{flaps,landing}}$	0.0437
$\Delta C_{D,0_{flaps,take-off}}$	0.0073
$\Delta C_{D,0_{slats,landing}}$	0.0051
$\Delta C_{D,0_{slats,take-off}}$	0.0026

9.7. Control surfaces

When designing an aircraft, it is important to size various aspects in order to achieve optimal aerodynamic performance. It is, however, also of great importance to incorporate control surfaces in this design to allow a pilot to manoeuvre the plane when necessary. The control surfaces enabling these manoeuvres are discussed in this section.

9.7.1. Aileron sizing

Ailerons are used to create a roll moment during flight. As stated in the CS-25 regulations [18], an aircraft, during a steady 30 ° banked turn, should be able to reverse the turn direction by rolling 60 ° in the opposite direction. This movement must not take more than 7 seconds. Analysing this requirement gives a minimum roll rate P of $8.57\,°\text{s}^{-1}$. This value will be kept in mind as a minimum when completing Equation 9.33.

$$P = -\frac{C_{l_{\delta_a}}}{C_{l_p}}\delta_a\left(\frac{2V}{b}\right) \tag{9.33}$$

The speed and wingspan are known and the deflection angle can be chosen, which leaves the aileron control derivative $C_{l_{\delta_a}}$ (see Equation 9.34) and the roll damping coefficient C_{l_p} (see Equation 9.35) to be determined.

$$C_{l_{\delta_a}} = \frac{dC_l}{d\delta_a} = \frac{2c_{l_\alpha}\tau}{S_{ref}b}\int_{b1}^{b2} c(y)y\,dy \tag{9.34}$$

$$C_{l_p} = -\frac{4(c_{l_\alpha} + c_{d_0})}{S_{ref}b^2}\int_0^{b/2} y^2 c(y)\,dy \tag{9.35}$$

These equations have been filled in using a maximum aileron deflection angle δ_a of $20\,°$, based on reference aircraft. Next to this, c_{l_α} takes the airfoil lift curve slope into account, τ is the aileron effectiveness, y is the spanwise location and $c(y)$ relates to the chord of the wing at a specific spanwise location. It is decided that the aileron starts at a wing span of $b1 = 29m$ and ends at $b2 = 35m$. Filling in these values yields a roll rate of $20.72\,°\text{s}^{-1}$. This is higher than the minimum roll rate determined at the beginning of Subsection 9.7.1, thus, confirming this as an effective aileron design.

9.7.2. Elevator Sizing

Elevators are used to create a pitching moment during flight. They are located at the horizontal tail. To size the elevators, two values are of importance, namely $\frac{C_E}{C_h}$ and $\frac{b_E}{b_h}$, which are the elevator chord-to-tail chord ratio and the elevator span-to-tail span ratio. The latter typically has a value between $0.8 - 1$ and is chosen to be 1 for simplicity of the design and manufacturing and a value of 0.24 was found for the chord ratio with the method from M. H. Sadreay [22]. This resulted in an elevator area of $4.34\,\text{m}^2$. In addition to these two values, the maximum deflection angle of the elevator is also of importance and is chosen to be $-25\,°$ for upward deflection and $20\,°$ for downward deflection.

9.7.3. Rudder

As seen in CS-25 regulations [23], the aircraft should be able to land whilst enduring $90\,°$ crosswinds with a maximum speed of $10.28\,\text{m/s}$. Using the method from M. H. Sadreay, a rudder area of $9.94\,\text{m}^2$ has been found [22].

9.8. Verification

During the aerodynamic design of the aircraft, much thought has been given to its efficiency and feasibility. Along the way, verification procedures have been performed, which will be discussed in detail throughout this section.

The aerodynamic analysis makes extensive use of numerical modelling, therefore, verification has continually been performed to ensure its correctness. Static verification was performed, ensuring the correct use of equations. Sensitivity analysis has been performed, ensuring small changes in input variables do not result in unexpected large fluctuations of output variables. Lastly, extensive verification is done by modelling the aircraft in XFLR5 (version 6.59).[29]. This provided the team with multiple aerodynamic characteristics to be compared with the numerical model and are shown in Table 9.6.

Table 9.6: Comparison of Aerodynamic characteristics calculated values and from XFLR5 (version 6.59)

Parameter	Computed value	XFLR5 Value	Δ
Cl_{design}	0.36	0.36	0.00%
α_{trim}	-0.523	-0.454	-13.19%
e	0.66	0.96	45.90%
$C_{D_{induced}}$	0.0044	0.0030	-32.05%
C_D	0.0172	0.0163	-1.01%

As can be seen in Table 9.6, the difference in drag coefficient is below 10%, confirming the accuracy of the numerical model. However, when looking at the induced drag, a difference of 32% is visible, which can be explained by the difference in the Oswald efficiency factor. It seems that XFLR5 (version 6.59) overestimates this factor. These values were found using the vortex lattice method (VLM), however when using the lifting line theory (LLT) in XFLR5 (version 6.59) value for $C_{D_{induced}}$ of 0.0043 was found which is very close to the computed value so it was found that the VLM method underestimates $C_{D_{induced}}$.[30] Lastly, the trim angle differs by 13%, an acceptable difference.

9.9. Conclusion and recommendations

In this chapter, the final wing design has been made and analysed to ensure its efficiency. First, the minimum performance requirement had been determined yielding the wing loading for which the aircraft should be designed. Next, the wing planform was designed providing important coefficients to be achieved by the wing. With these coefficients, a matching airfoil (SC(2)-0712) was found. This airfoil was chosen based on sublime aerodynamic performance when evaluating its drag, design lift coefficient and critical Mach number. Having chosen the airfoil, a more detailed analysis of the aerodynamic properties of the wing was performed ensuring a viable and efficient design. For example, the sweep angle was determined based on delaying drag divergence over the wing, thus improving its aerodynamic characteristics. The drag was analysed for different components of the aircraft and it was found that the truss only has a 3.9% contribution to the total zero-lift drag. Finally, in order to accommodate for take-off, landing and manoeuvrability, sizing was performed for HLDs and control surfaces.

[29] https://sourceforge.net/projects/xflr5/files/6.59/

[30] https://www.dlr.de/as/en/Desktopdefault.aspx/tabid-188/379_read-625/

Further research into the WorldBus is encouraged, with recommended focus points for aerodynamics listed below:

- Investigate the use of a combination of airfoils over the wingspan in order to improve aerodynamic properties.
- Perform an analysis evaluating the effect of winglets on wing drag.
- Perform an analysis evaluating the use of wing twist to ensure root stall happens before tip stall.
- Investigate in further detail the aerodynamic drag produced by the landing gear pods, the wing protrusion and the unique tail cone.
- Perform a detailed analysis regarding the lift and drag produced by the truss, and how to optimise this.
- Perform an analysis on the model using computational fluid dynamics (CFD) software.
- Perform wind tunnel tests.
- Further investigate the Oswald efficiency factor to ensure a correct value is used during calculations.

10 Propulsion

For the propulsion system, a hydrogen-powered turbofan will be used. To lower the complexity of engine development, a kerosene engine will be converted into a hydrogen engine rather than developing one from scratch. The process of selecting and designing the engines will be outlined in this chapter. For the hydrogen storage, liquid hydrogen will be stored in a tank inside the fuselage. The design of this fuel tank is further outlined in Chapter 13.

10.1. Engine conversion

In the midterm report, it had been decided to use an existing kerosene-powered turbofan that will be modified to run on the boil-off of the liquid hydrogen. For this, a short list of turbofans was made and some general parameters were researched as shown in Table 10.1.

Table 10.1: Engine option overview.

Engine type	**Take-off thrust (kerosene / H_2)** [kN]	**Mass** [kg]	**Length** [m]	**Fan diameter** [m]
Rolls Royce Trent 1000R	360.4 / 378.4	6114	4.738	2.85
Rolls Royce Trent XWB	431.0 / 452.6	7550	5.812	3.00
General Electric 90-115B	513.9 / 539.6	8762	7.281	4.2
Engine Alliance GP 7000	363.0 / 381.2	6712	4.92	3.16

While currently no hydrogen turbofans exist, more and more research is being done on the topic. Last year, Airbus announced that they are aiming to test a GE passport to run solely on liquid hydrogen by 2027 and have a fully hydrogen-powered aircraft by 2035.[31] But this begs the question on how a kerosene turbofan can be converted to hydrogen and what effect this will have on the performance of the engine.

Modifications

In theory, the only modifications that are required to use hydrogen as a fuel source are a new fuel injector and a system to take care of the liquid hydrogen boil-off in the tank. However, a number of properties differ between hydrogen and kerosene that encourage the modifications of other engine components. For instance, compared to kerosene, hydrogen requires lower ignition energy, is more diffusive and has wider flammability limits. This can be seen in the combustion chamber outlet temperature. In a study from 2021, the researchers found that after converting a TF33 turbofan from kerosene to hydrogen, the combustion outlet temperature was approximately 1.4% lower for hydrogen than for kerosene [24]. Because of this lower temperature, there is more design freedom in the material selection for the combustion chamber and it is recommended to take advantage of these properties.

Other differences resulting from converting a turbofan to hydrogen is that the mass flow rate of the fuel decreases by approximately 60% [24]. Then, it was observed that the air-fuel ratio for hydrogen was higher than that of kerosene, meaning that more effective cooling is possible with the bypass air.

These results are backed up by other analyses too. For example, in a study from 2021, researchers used Matlab to analyse the performance of a hydrogen General Electric GE90 turbofan and found similar results for the mass flow and thermal efficiency [25]. The thrust of the engines increased by 16.27% and the total emission of nitrogen oxide was reduced by 68.25% during cruise at an altitude of 10 668 m and a Mach number of 0.83. However, the researchers found that by optimising the engine in terms of bypass ratio and fan pressure ratio, the nitrous oxides emissions could be reduced by another 3.94% per 1 kg of burnt fuel.

[31] https://www.airbus.com/en/newsroom/stories/2022-02-the-zeroe-demonstrator-has-arrived

Concluding, it is very likely that it is possible to convert a kerosene turbofan to run on hydrogen without drastic modifications to the engine. Moreover, a conservative 5% increase in thrust is predicted in the amount of thrust generated by the engine for all engines listed in Table 10.1. In the column for take-off thrust, the thrust value is given both for the kerosene-powered engine and the hydrogen-powered variant.

10.2. Engine selection

In Chapter 7, the MTOW was stated to be equal to 223 780 kg, and the T/W is equal to 0.27. As a result, a total thrust of 592.5 kN is required. This means that in a two-engine configuration, every engine from Table 10.1 should be suitable for WorldBus. It is preferable to have the smallest, lightest, most reliable and most efficient engine that can still provide the required thrust. However, finding quantitative data on fuel consumption has been proven difficult. Manufacturers like Rolls Royce and General Electric do not list thrust-specific fuel consumptions while other sources only provide estimations.[32,33] For a proper analysis, this is not ideal as one engine might be heavier, but its improved efficiency could outweigh the extra mass of the engine itself and reduce the overall weight of the aircraft. But as this information is not available, it has to be assumed that all engines have similar efficiency, an assumption that does not seem unreasonable.[34] Then, in regards to reliability, all engines perform quite similarly as well, with all of the options boasting more than 99.9% dispatch reliability.[35,36,37,38]

Now that it is assumed that all engines have similar efficiencies and have similar reliability figures, a clear winner can already be seen from the possible engines in Table 10.1 without performing a formal trade-off. The Rolls Royce Trent 1000R is the lightest and smallest engine out of all the four options. While it has the lowest thrust, two Rolls Royce Trent 1000R still provide enough thrust for the MTOW of 223 780 kg, with room to spare. A summary of the engine parameters for the Rolls Royce Trent 1000R is given in Table 10.2.[39] The thrust has been increased by 5% to reflect the predicted thrust gain as a result of modifying the engine to run on hydrogen.

Table 10.2: Summary of engine parameters for Rolls Royce Trent 1000R running on liquid hydrogen.

Mass	6114 kg
Nacelle length	6.17 m
Maximum radius	1.9 m
Fan diameter	2.85 m
Take-off thrust	378.4 kN
Continuous thrust	339.5 kN
Bypass ratio	>10
Dispatch reliability	99.9%

10.3. Engine location

The next step in completing the engine configuration is placing the engines. In the midterm report [13], it was already established that the engines would be placed on the wing, instead of podded to the fuselage. However, now the exact location needs to be determined. A number of factors need to be taken into account. For instance, the location of the truss will limit the available space to place the engine as the truss cannot be in the wake of the engine. Then, to maximise the bending relief from having the engine mounted on the wing, it is preferable to have the engine placed further outward. However, this influences the required size for the vertical tail as the aircraft still needs to be controllable if one engine is inoperative. In other words, the placement of the engine influences the structure of the wing and the size of the vertical tail. For a preliminary design, Equation 10.1 from ADSEE I is commonly used [19]. This is a simple statistical relation between the engine location and the span derived from other two-engined aircraft.

[32] https://www.geaerospace.com/propulsion/commercial/ge90

[33] https://www.rolls-royce.com/products-and-services/civil-aerospace/widebody/trent-1000.aspx#/

[34] https://simpleflying.com/the-worlds-most-powerful-aircraft-engines/

[35] https://www.rolls-royce.com/products-and-services/civil-aerospace/widebody/trent-1000.aspx#/

[36] https://www.rolls-royce.com/media/our-stories/discover/2019/the-trent-xwb-let-me-count-the-ways.aspx

[37] https://blog.geaerospace.com/product/the-ge90-engine-a-technological-pioneer-surpasses-100-million-hours/#:~:text=It%20also%20has%20a%20world%20class%20dispatch%20reliability%20rate%20of%2099.97%20percent.

[38] https://www.prnewswire.com/news-releases/engine-alliance-completes-100th-gp7200-engine-specific-fuel-consumption-improvement-noted-98508904.html

[39] https://www.google.com/url?sa=t&rct=j&q=&esrc=s&source=web&cd=&ved=2ahUKEwiEpcXE77D_AhU7hPOHHXvKCDkQFnoECBEQAQ&url=https%3A%2F%2Fwww.easa.europa.eu%2Fen%2Fdownloads%2F7733%2Fen&usg=AOvVaw3_04OEPO9iXV4EMBJMFZyO

$$y_e = 0.35\frac{b}{2} \tag{10.1}$$

where y_e is the distance between the aircraft's centre line and the engine's centre line and b is the wing span. This formula was used in early design phases. However, after the supporting truss for the wing was designed, it became apparent that at this location the exhaust from the engine would intersect the truss at this location. Therefore, it was decided that the engine had to be moved more inboard, as moving the truss would adversely affect its effectiveness. Moving the engine means that the yaw created in an one-engine-out scenario is reduced, allowing for a smaller rudder. However, it also means that the relief that is caused lowered, but the moment on the wing from the thrust is reduced. Overall moving the engine inward by 40 per cent was not seen as a major compromise. It will increase the noise inside the cabin, But since the hydrogen tank is located in the middle of the aircraft, it means that this effect should be significantly reduced.

For the vertical and longitudinal positioning, a parametric program was developed. The design of this program and the engine pylon is discussed in more detail in Subsection 13.3.3 This program designs a truss structure as shown in Figure 10.1.

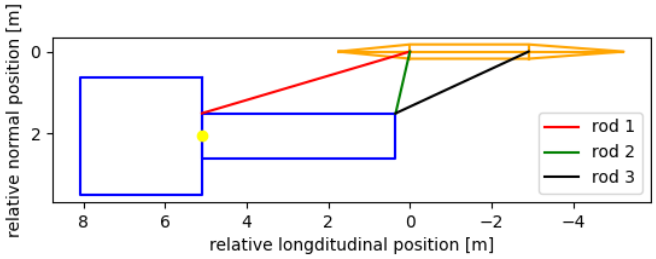

Figure 10.1: Positioning of engine with respect to the centroid of the quarter chord

To determine the boundary conditions for the engine placement, similar aircraft like the Antonov An-158, C17 Globemaster III, and Kawasaki C-2 were analysed.[40,41,42]. These aircraft were selected because of their similar size and high-wing configuration. From this analysis, it was decided that the engine should be below the wing. This will allow for easier installation and maintenance checks. The back of the engine should also be in front of the quarter chord. This is done to ensure safety in case the engine breaks loose. In such a scenario, the forward position will ensure that the engine can fly forward and over the wing. In addition the forward position allows the weight of the engine to create a negative moment around the y-axis. This moment helps alleviate the positive moment created by the wing sweep.

[40] https://en.wikipedia.org/wiki/Antonov_An-148
[41] https://www.af.mil/About-Us/Fact-Sheets/Display/Article/1529726/c-17-globemaster-iii/
[42] https://en.wikipedia.org/wiki/Kawasaki_C-2

11

Stability and control

Stability and controllability (S&C) is another important aspect of aircraft design and in this chapter, the stability and controllability characteristics will be discussed. The first parameter that must be considered in this S&C analysis is the placement of the wing, which will be discussed in Section 11.1. Secondly, the empennage must be designed in an appropriate manner as described in Section 11.2, Section 11.3 and Section 11.4. Lastly, the undercarriage must be designed to satisfy ground stability. This is discussed in Section 11.5

11.1. Wing placement

To analyze the stability and controllability of the aircraft and design the empennage accordingly, it is first important to determine the location of the leading edge of the wing x_{LEMAC}. This is done by identifying the mass and the location of the centre of gravity of several individual aircraft components, including the wing, fuselage, engines, fuel tanks, empennage and fixed equipment. The wing and engines will be categorized in the wing group with mass M_W and c.g. location $(\frac{x}{\bar{c}})_{WCG}$ and the rest will be categorized in the fuselage group with mass M_F and c.g. location X_{FCG}. To find the individual c.g. locations, empirical relations were used. The c.g. locations of the tank followed from the tank placement. Furthermore, the location of the centre of gravity for the operating empty weight ($(\frac{x}{\bar{c}})_{OEWCG}$) was assumed to be at $0.35\bar{c}$. Using Equation 11.1, an x_{LEMAC} of 30 m was found. This value will be used for the design of the horizontal tail and empennage. [19]

$$x_{\text{LEMAC}} = X_{\text{FCG}} + \bar{c}\left[\left(\frac{x}{\bar{c}}\right)_{\text{WCG}} \frac{M_{\text{W}}}{M_{\text{F}}} - \left(\frac{x}{\bar{c}}\right)_{\text{OEWCG}} \left(1 + \frac{M_{\text{W}}}{M_{\text{F}}}\right)\right] \tag{11.1}$$

11.2. Empennage configuration trade-off

In this section, different empennage configurations will be researched so that a trade-off can be performed. The selected empennage will provide the foundation for further sizing of the stabiliser surfaces to satisfy the S&C requirements. When looking into the configurations, it is important to note that the WorldBus makes use of a high-wing configuration with the engines mounted on the wings. This influences the feasibility of certain configurations as it is quite undesirable to have the horizontal stabiliser located in the wake of the engine and of the wing. This will likely happen when the horizontal stabiliser is located at approximately the same height as the main wing.[43] Furthermore, it is crucial that the aircraft does not suffer from deep stall characteristics. In Figure 11.1, different configurations are shown. In Table 11.1 a trade-off between the configurations is performed based on three criteria: mass, cost and aerodynamic performance. The columns indicate the different criteria. The rows indicate the empennage configuration. A score is given from - - (lowest), to + + (highest) with a matching colour. A numerical value shows the total score of the different options. One option is chosen as the baseline and hence scores ± in all criteria. Since the tail plays such a critical role in the stability of the aircraft, performance was awarded the highest weight. Ultimately, the T-tail configuration proved to be the most suitable design and was therefore selected as the empennage type for WorldBus.

[43] https://simpleflying.com/t-tail-aircraft/

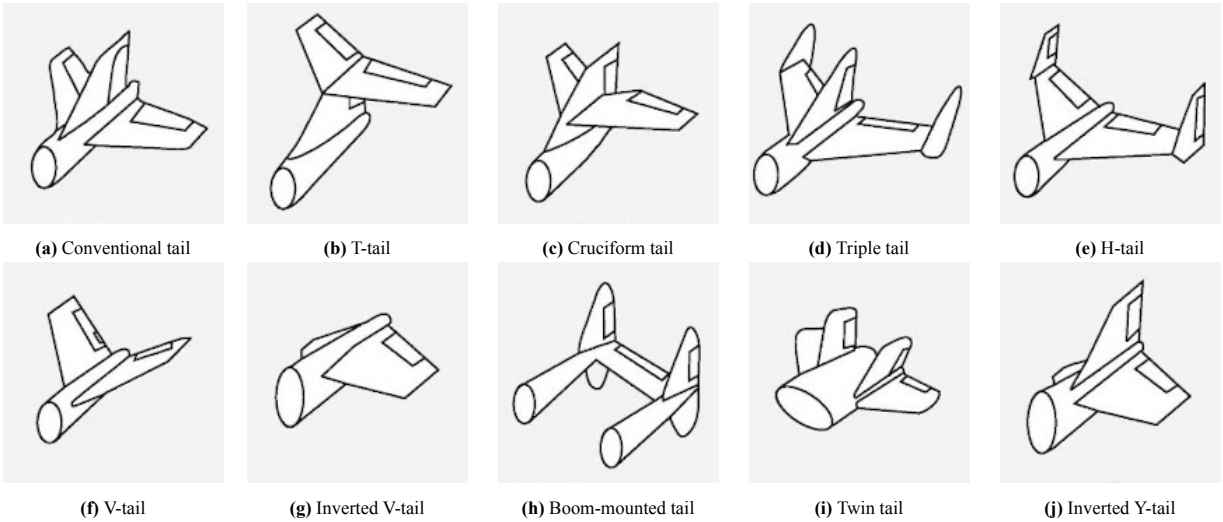

(a) Conventional tail **(b)** T-tail **(c)** Cruciform tail **(d)** Triple tail **(e)** H-tail

(f) V-tail **(g)** Inverted V-tail **(h)** Boom-mounted tail **(i)** Twin tail **(j)** Inverted Y-tail

Figure 11.1: Illustrations of tail configurations

Table 11.1: Empennage configuration trade-off for high-wing configuration aircraft.

Empennage configuration	**Mass**	**Cost**	**Aerodynamic Performance**	**Total score**
Criterion Weight	2	3	5	10
Conventional tail – Reference	(±)	(±)	(±)	(±) 0
T-tail	(-) Stronger tail required due to location of horizontal stabiliser.	(-) Increased manufacturing complexity due to increased loading.	(++) Located outside wake of engines and wing and better deep stall characteristics.[44]	(++) 5
Triple tail	(- -) Additional structural elements needed to support three tail surfaces.[45]	(- -) Added complexity to control three separate tails.	(+) Decreased roll moment and an improved efficiency of horizontal tail.[46]	(- -) -5
H-tail	(-) Additional structural elements required for two tail surfaces.	(- -) Increased control complexity.	(+) Decreased roll moment and an improved efficiency of horizontal tail.[47]	(-) -3
Cruciform tail	(-) Stronger tail required due to location of horizontal stabiliser.	(-) Added complexity increases the costs.	(+) Comparable with T-tail with better deep stall characteristics but reduced effective aspect ratio.[48]	(±) 0

[44] https://simpleflying.com/t-tail-advantages-disadvantages/
[45] https://infogalactic.com/info/Lockheed_Constellation
[46] https://www.kitplanes.com/h-tails-and-triple-tails/
[47] https://www.kitplanes.com/h-tails-and-triple-tails/
[48] https://eng.libretexts.org/Bookshelves/Aerospace_Engineering/Fundamentals_of_Aerospace_Engineering_(Arnedo)/02%3A_Generalities/2.02%3A_Parts_of_the_aircraft/2.2.03%3A_Empennage

V-tail	(+ +) Less surface area.	(-) Increased complexity of design and manufacturing.	(±) Good performance in crosswinds, improved roll stability and decreased drag.[49]	(-) -1
Inverted V-tail	(++) Less surface area.	(-) Increased complexity of design and manufacturing.	(±) Comparable to V-tail with better roll performance.[50]	(+) +1
Boom-mounted tail	(- -) Additional structural weight.	(- -) Additional structural components will increase costs.	(+) Increased controllability and pitch stability.[51]	(- -) -5
Twin-tail	(+) Splitting of aerodynamic loads results in lower required structural support.[52]	(-) Increased manufacturing complexity increases costs.	(+) Better performance in case of engine failure and better performance in high-wing configuration.[53]	(+ +) +4
Inverted Y-tail	(±) Tail is similar in shape as Y-tail, except for a dropped angle of the horizontal stabilisers.	(-) Due to increased manufacturing complexity, costs will be slightly higher.	(+) Better performance since configuration has slightly less trouble with handling wake of wing and engine in case of high-wing.[54]	(+) +2

11.3. Horizontal stabiliser design

To be able to guarantee longitudinal stability, a horizontal stabiliser is introduced to counter unwanted pitching moments. In this section, the design parameters of this horizontal stabiliser will be determined. To do that, first, a loading diagram will be made to establish the range of the location of the centre of gravity. Furthermore, the stability and controllability will allow the generation of a scissor plot. From this scissor plot, a horizontal stabiliser surface can be deducted together with the taper ratio, aspect ratio, sweep and maximum thickness-to-chord ratio with its location, the entire horizontal stabiliser can be designed.

11.3.1. Loading diagram

In the loading diagram, the c.g. range of the aircraft will be determined. This is done by loading the aircraft in four phases: first, all business class seats together with the window- and middle seats in the economy+ class will be filled. After that, all aisle seats of the economy+ will be filled. In order to find the most extreme c.g. locations, for both loadings, two scenarios will be considered: loading from the front of the aircraft to the back and vice versa. Then, the secondary tank will be filled after which, lastly, the primary tank will be filled.

As we will see later in Figure 11.3, it is beneficial to keep the centre of gravity range in the loading diagram as small as possible. This has everything to do with the different moments that will be caused in flight due to the change in the centre

[49] https://www.kitplanes.com/design-process-v-tails/
[50] https://www.sciencedirect.com/topics/engineering/aircraft-engineering#:~:text=The%20short%20version%20of%20the,is%20called%20a%20proverse%20roll.
[51] https://simpleflying.com/twin-boom-aircraft-pros-cons-guide/
[52] https://www.quora.com/What-is-the-advantage-of-a-twin-tail-on-an-aircraft-as-opposed-to-a-standard-single-vertical-stabiliser
[53] http://what-when-how.com/flight/tail-designs/
[54] http://what-when-how.com/flight/tail-designs/

of gravity. To compensate for this, we will end up with a very large horizontal tail. This would of course not be ideal from a weight perspective.

What differentiates the conceptual design from regular aircraft designs, is the fact that it contains a fuel tank that has a length of almost 24 m. When the tank is placed behind the cabin, as is common for regular aircraft, this would significantly push the most aft cg backwards and provide a rather inefficient and large c.g. range. Therefore, to account for this, the team has decided to put the primary fuel tank and the secondary fuel tank in the middle of the aircraft, splitting the cabin into two equal parts: one cabin in front of the fuel tank and one cabin aft the fuel tank. This can be clearly seen in Appendix D.

Due to the presence of two separate cabins, loading of the forward and aft cabins will take place simultaneously. This will decrease the c.g. range during these loading phases since the c.g. lies between the two cabins. It is decided to calculate the c.g. range without taking this into account since it is preferred to have the most extreme values. Therefore, in practice, the horizontal stabiliser results to be over-designed.

For the loading diagram, when weight is added to the aircraft, the new location of the c.g. is plotted against the total weight. The loading diagram can be seen in Figure 11.2. The most extreme c.g. locations are depicted in Table 11.2. [26].

Table 11.2: Center of gravity positions in most extreme scenarios

	x_{cg} [m]	$\frac{x_{cg}}{\bar{c}}$
Most aft c.g.	33.15	0.55
Most forward c.g.	31.50	0.26

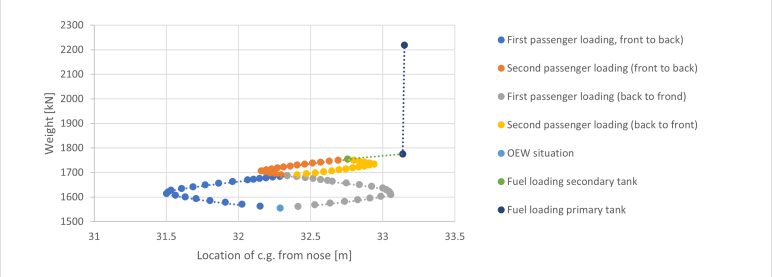

Figure 11.2: Loading diagram with primary fuel tank in middle of cabin

11.3.2. Scissor plot

Having established the most forward and most aft c.g. location, a scissor plot can be used to determine the ratio of the horizontal tail surface over the main wing surface S_h/S. In the scissor plot, shown in Figure 11.3, two lines are plotted as a function of $x_{c.g.}$. The line with the positive slope corresponds to the stability requirement displayed in Equation 11.2. Every point left from this curve is stable and right from this curve is unstable, due to the fact that in these scenarios the neutral point will be in front of the most aft c.g. The line with the negative slope corresponds to the control requirement displayed in Equation 11.3. Every point right to this curve is controllable and left to this curve is uncontrollable. In Equation 11.2 and Equation 11.3, S_h stands for the horizontal tail surface, $C_{L_{\alpha_h}}$ stands for the slope of the lift curve of the horizontal tail, the $C_{L_{\alpha_{A-h}}}$ stands for the slope of the lift curve of the main wing, $\frac{\delta\eta}{\delta\alpha}$ stands for the change in downwash with respect to angle of attack, l_h stands for the moment arm of the horizontal tail, $\bar{c}$ stands for the mean aerodynamic chord, $\frac{V_h}{V}$ stands for the velocity ratio of the horizontal tail compared to the wing, C_{L_h} stands for the lift coefficient of the horizontal tail, $C_{L_{A-h}}$ stands for the lift coefficient of the aircraft without the tail and $C_{m_{ac}}$ stands for the pitching moment coefficient around the aerodynamic centre.

$$\frac{S_h}{S} = \frac{1}{\frac{C_{L_{\alpha_h}}}{C_{L_{\alpha_{A-h}}}}\left(1-\frac{d\epsilon}{d\alpha}\right)\frac{l_h}{\bar{c}}\left(\frac{V_h}{V}\right)^2}\bar{x}_{c\cdot g.} - \frac{\bar{x}_{ac}-0.05}{\frac{C_{L_{\alpha_h}}}{C_{L_{\alpha_{A-h}}}}\left(1-\frac{d\epsilon}{d\alpha}\right)\frac{l_h}{\bar{c}}\left(\frac{V_h}{V}\right)^2} \tag{11.2}$$

$$\frac{S_h}{S} = \frac{1}{\frac{C_{L_h}}{C_{L_{A-h}}}\frac{l_h}{c}\left(\frac{V_h}{V}\right)^2}\bar{x}_{cg} + \frac{\frac{C_{m_{ac}}}{C_{L_{A-h}}}-\bar{x}_{ac}}{\frac{C_{L_h}}{C_{L_{A-h}}}\frac{l_h}{\bar{c}}\left(\frac{V_h}{V}\right)^2} \tag{11.3}$$

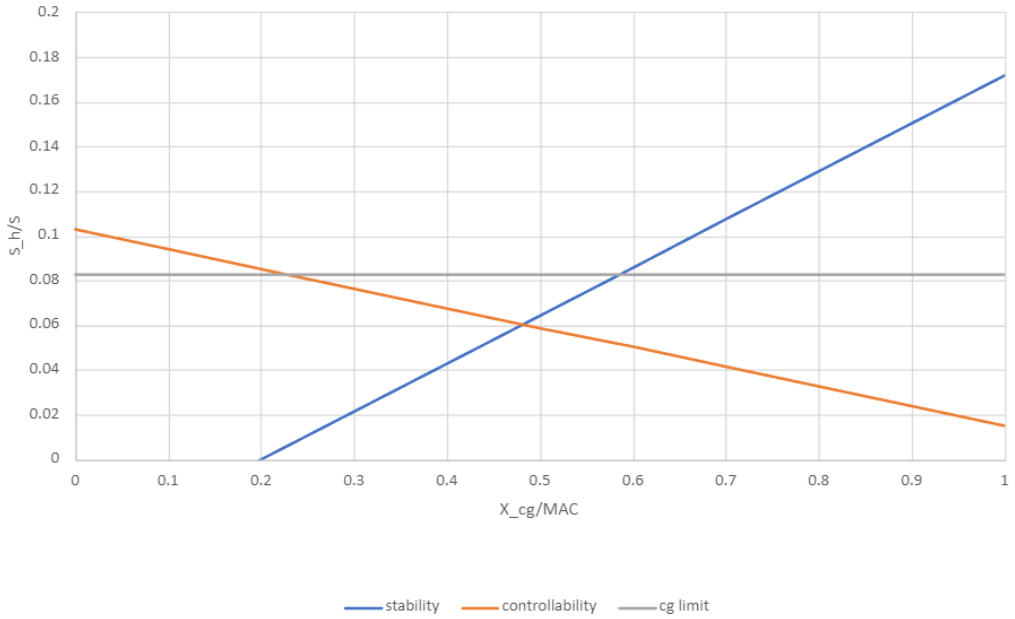

Figure 11.3: Scissor plot

When choosing a value for S_h/S, the c.g. range must fit within the stability and controllability curve for the smallest possible S_h/S. For WorldBus, a ratio of 0.08 was found, meaning WorldBus will have a horizontal tail of 28.39 m^2. This ratio can be considered to be extraordinarily low. When inspecting reference data, it was found that the ratio is often at least 0.2, making it double the size of the discovered horizontal tail. This strange phenomenon can also be dedicated to the immense fuel tank, which has increased the fuselage length and, indirectly, the horizontal tail moment arm. A longer arm means less surface is needed to provide the countering stability moments. In addition to the moment arm, the T-tail configuration also decreases the surface of the horizontal tail since this has an effect on the velocity ratio $\frac{V_h}{V}$.

11.3.3. $C_{m_{ac}}$

Most of the values in Equation 11.2 and Equation 11.3 were determined in other sections or are based on data from reference aircraft. However, one parameter, namely the $C_{m_{ac}}$ required some additional effort. This pitching moment coefficient can be analysed to consist of 4 main contributors, the wing, the fuselage, the flaps and the nacelles. The contribution of the nacelle is -0.05 [27]. The formula for the other contributions are shown in Equation 11.3.3, Equation 11.3.3 and Equation 11.3.3.

$$C_{m_{ac}} = C_{m_{ac_w}} + \Delta_f C_{m_{ac}} + \Delta_{fus} C_{m_{ac}} + \Delta_{nac} C_{m_{ac}} \tag{11.4}$$

$$C_{m_{\text{ac}}} \approx \text{Cm}_{0,\text{airfoil}} \cdot \frac{A\cos^2\Lambda}{A + 2\cos\Lambda} \tag{11.5}$$

$$\Delta_{fus} C_{m_{\text{ac}}} = -1.8\left(1 - \frac{2.5 b_f}{I_f}\right)\frac{\pi b_f h_f I_f}{4S\bar{c}}\frac{C_{L_0}}{C_{L_{\alpha_{A-h}}}} \tag{11.6}$$

$$\begin{aligned}\Delta C_{m_{\Downarrow}} = \mu_2 \left\{-\mu \Delta C_{L_{\text{max}}}\frac{c'}{c} - \left[(C_L + \Delta C_{L_{\text{ma}}})\left(1 - \frac{Swf}{S}\right)\right]\frac{1}{8}\frac{c'}{c}\left(\frac{c'}{c} - 1\right)\right\} \\ + 0.7\frac{A}{1 + 2/A}\mu_3 \Delta C_{I_{\text{max}}} \tan\Lambda_{1/4} - C_L \cdot (0.25 - \frac{x_{ac}}{\bar{c}})\end{aligned} \tag{11.7}$$

In order for the aircraft to be stable, it is required to have a negative pitching moment coefficient. To satisfy this requirement, it was found that the location of the aerodynamic centre should not be located further than 0.28 times the MAC from the

MAC leading edge location. This condition was therefore satisfied and ultimately, it followed that the $C_{m_{ac}}$ was equal to -0.30.

11.3.4. Final design

Having determined a value for S_h/S, one still needs to select a taper ratio λ_h, aspect ratio AR_h, sweep angle Λ_h and dihedral angle ϕ_h to fully design the horizontal stabiliser. These follow from conventional parameters used in the industry for jet transport aircraft and are shown in Table 11.3 [28]. The maximum thickness-to-chord ratio $(t/c)_{max_h}$ and its location $\frac{x_{(t/c_{max_h})}}{\bar{c_h}}$ follow from the airfoil used, which is the NACA 0012 airfoil. This airfoil was chosen because of its symmetrical shape, high lift curve slope, large range of usable angles of attack and thickness to chord ratio of 12%. [26].

Table 11.3: Design parameters horizontal tail

Parameter	Value	Unit
λ_h	0.5	-
AR_h	4	-
Λ_h	20	deg
ϕ_h	5	deg
$(t/c)_{max_h}$	0.12	-
$\frac{x_{(t/c_{max_h})}}{\bar{c_h}}$	0.30	-

11.4. Vertical stabiliser design

To guarantee stability and controllability in the yaw direction, a vertical stabiliser is introduced. For the design of the vertical tail, the ratio of the vertical tail surface over the main wing surface S_v/S is the most important consideration. This value is determined by adhering to the three different stability criteria listed below.

1. A cross wind of at least 20 knots must be sustained during take-off and landing.
2. The aircraft must be directionally stable, meaning positive weathercock stability ($C_{n_\beta} > 0$) and positive damping of Dutch roll.
3. The torque generated when one engine fails should be counteracted.

These requirements can be combined into one equation shown in Equation 11.8 with factors given in Equation 11.9 and Equation 11.10. [29].

$$\frac{S_v}{S} = \frac{1}{a_v \eta_v k \beta \left(1 + \frac{\partial \sigma}{\partial \beta}\right)} \left[\beta k_2 \left(A \frac{d_f}{b}\right)^2 + \frac{C_D}{(n_e - 1)} \frac{y_e}{c_{MAC}}\right] \left(\frac{c_{MAC}}{l_v}\right) \tag{11.8}$$

$$k = 0.167 \left(2.5 + \frac{b_v}{2r_1}\right) \tag{11.9}$$

$$k_2 = 0.14 \exp\left(\frac{x_{c/4}}{l_f}\right)^5 - 0.045 \tag{11.10}$$

In Equation 11.8, a_v is the lift curve slope of the vertical tail, η_v the vertical tail efficiency, β the sideslip angle, A the aspect ratio of the main wing, d_f the fuselage outer diameter, b the span of the main wing, C_D the drag coefficient, n_e the number of engines, y_e the spanwise distance from the centre line of the aircraft to the engine, c_{MAC} the mean aerodynamic chord, and l_v the longitudinal distance between aerodynamic centres of the wing and vertical tail. $\frac{\partial \sigma}{\partial \beta}$ represents the variation in sidewash angle with sideslip angle. Lastly, for the determination of the factors k and k_2, $x_{(c/4)}$ is the location of the quarter chord, l_f is the total fuselage length, b_v is the span of the vertical tail and $2r_1$ is the depth of the fuselage in the vicinity of the vertical tail.

Filling in the values for the parameters gave a value for S_v/S of 0.096, resulting in a vertical tail area of $35.6\,\text{m}^2$. This value is comparable to that of reference aircraft and was therefore accepted to be valid.
Having determined a value for S_v/S, one still needs to select a taper ratio λ_v, aspect ratio AR_v, sweep angle Λ_v, and dihedral angle ϕ_v to complete the design of the vertical tail. Again, these follow from conventional parameters used in the industry for jet transport aircraft and can be observed in Table 11.4 [28]. For the vertical tail, the airfoil NACA-0012 is chosen again, since the vertical tail airfoil should be symmetrical, have a thickness ratio of about 12% and should have a large range of angles of attack [26].

Table 11.4: Design parameters vertical tail

Parameter	Value	Unit
λ_v	0.85	-
AR_v	1	-
Λ_v	40	deg
ϕ_v	0	deg
$(t/c)_{max_v}$	0.12	-
$\frac{x_{(t/c_{max_v})}}{\bar{c_h}}$	0.30	-

11.5. Undercarriage design

Lastly, the undercarriage must be designed in order to be able to guarantee the stability and controllability of the aircraft when performing ground operations. First the undercarriage must be sized, after which its location must be determined. Finally, it must be checked if the undercarriage can be stored, while the aircraft is in flight.

11.5.1. Undercarriage sizing

For large transport jets, the number of main wheels follows from Equation 11.11, where f stands for the ratio between landing weight and maximum take-off weight. The number of nose wheels used is 2. Furthermore, following from the fact that total the number of main wheels is below 12, the main gear is assumed to have 2 struts. As the aircraft will be designed to land only on paved surfaces in good condition, it is assumed that a minimum load classification number (LCN) of 50 should be taken into account. The tire pressure was consecutively determined by means of Equation 11.12. In order to make sure that an aircraft is steerable, at least 8% of the aircraft's weight should furthermore be carried by the nose landing gear. Following from this requirement, Equation 11.13 and Equation 11.14 could be formulated to estimate the static load per main gear wheel (P_{mw}) and the static load per nose gear wheel (P_{nw}). Now that the static loads and the tire pressure had been established, the tire sizes could be estimated from statistical data from Torenbeek as shown in Figure 11.4.

$$N_{mw} = f \cdot W_{TO}/210,000 \tag{11.11}$$

$$p = 430 \cdot \ln LCN - 680 \tag{11.12}$$

$$P_{mw} = 0.92 \cdot W_{TO}/N_{mw} \tag{11.13}$$

$$P_{nw} = 0.08 \cdot W_{TO}/N_{nw} \tag{11.14}$$

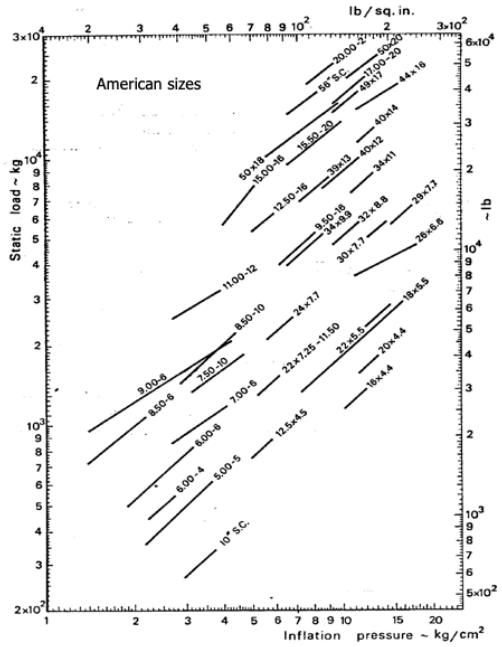

Figure 11.4: Diagram from Torenbeek, assisting in sizing of wheels undercarriage

11.5.2. Undercarriage positioning

The longitudinal position of the main landing gear depends on the scrape angle and the tip-back angle, where the scrape angle should always be smaller than the tip-back angle. For the tip-back angle, first, a value of 15° was chosen, whereas a scrape angle of 13° was selected. Figure 11.5 portrays the different angles. However, since the aircraft has a very large fuselage length, adhering to these requirements would mean that the height of the doors would exceed 5 meters, which will make it challenging to board passengers because jetbridges typically reach up to five meters.[55] To accommodate a lower floor height, it was decided to lower the scrape-back angle to 9°. This smaller scrape angle and therefore more shallow tail, means that the fuselage is a lot more aerodynamic. Although a smaller scrape angle will increase the take-off length required, because the angle of attack that can be achieved is lower on the ground. Lowering the landing gear length also comes with the added benefit that the track width can be lowered. Something that is especially valuable, as having a high-wing configuration means that the gear cannot simply go inside the wing.

Moving on to the longitudinal position of the nose gear, this value should be chosen in such a way that the nose gear will carry at least 8% of the load when the aircraft is on the ground. The lateral position of the main landing gear depends on 3 constraints, where the most outwards position will be the final one. The constraints are related to overturn, tip clearance and engine clearance. After careful investigation, the 'overturn' constraint was the limiting requirement. This makes sense as the high wing configuration means that a wing- or engine strike is very unlikely to happen.

[55] https://www.adelte.com/airports/passenger-boarding-bridges/#1649239264783-1d968bf9-81b3

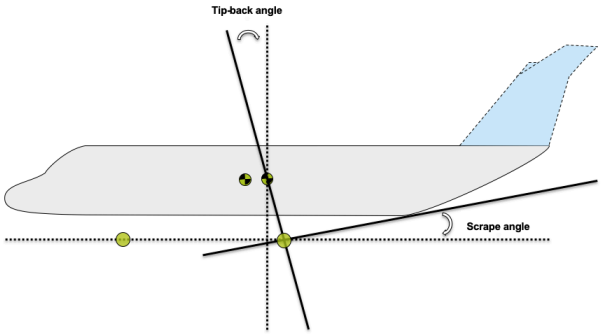

Figure 11.5: Figure portraying angles for longitudinal positioning of undercarriage

A different solution to making the gear shorter with the accompanying disadvantages was also considered. A partially retractable gear could be installed to lower the aircraft when it has reached the gate. This would allow for a better scrape angle. However, such a system requires a lot of power and therefore weight. It also does not have the benefits of being able to place the landing gear closer to the centreline of the aircraft. For these reasons, an increase in takeoff and landing distances is preferable with the accompanying aerodynamic improvements.

11.5.3. Storing the undercarriage

After the undercarriage has been sized and positioned, it is important to verify whether the designed undercarriage can actually be stored during flight. Whereas in normal aircraft configurations, the undercarriage is mounted on and stored in the wing, this is rather complicated in the case of a high-wing configuration. To accommodate the undercarriage for the high-wing truss-braced aircraft, it was chosen to attach the main landing gear to the truss structure and to also store it in a cowling within the truss structure. The feasibility of this design was tested with respect to the length of the landing gear and space in the fuselage and was deemed to be a legitimate option. An illustration of this system is shown in Figure 11.6.

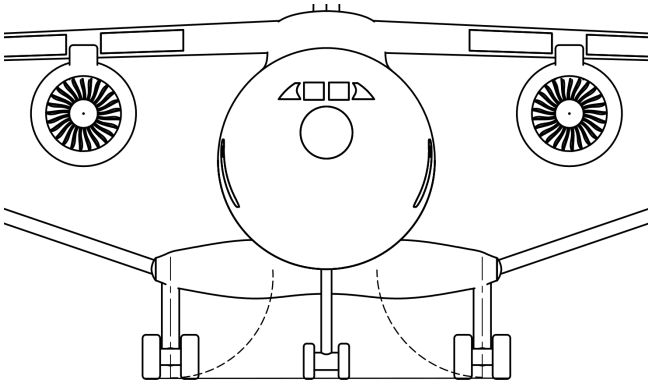

Figure 11.6: Illustration of landing gear deployment and storage system

11.5.4. Undercarriage design values

In Table 11.5, all undercarriage parameters are portrayed. The reference frame for the positions of the undercarriage is as follows: the longitudinal frame (x-coordinates) starts at the tip of the nose, the lateral frame (y-coordinates) starts at the middle of the fuselage and the height (z-coordinates) starts at ground level.

Table 11.5: Landing gear design parameters

Parameter	Value	Unit
Number of main wheels	8	-
Number of nose wheels	2	-
Number of main gear struts	2	-
Longitudinal position of main landing gear	34.78	m
Longitudinal position of nose landing gear	14.41	m
Height of landing gear (ground to lowest side of cabin)	3.16	m
Lateral position of main wheels	4.92	m
Static load per main wheel	252.37	kN
Static load per nose wheel	87.78	kN
Main wheel width	0.508	m
Main wheel diameter	1.27	m
Nose wheel width	0.3048	m
Nose wheel diameter	1.016	m

11.6. Verification and validation

To verify the calculations performed for stability and control, unit tests have been performed on all formulas used. In addition to verification, validation has been performed by comparing the values to reference aircraft.

To validate the positioning of the wing of WorldBus, reference data of the Boeing 787-9 was analysed. It was found that the leading edge of the root of the wing of the Boeing 787-9 was at 30% of the total aircraft length.[56] Inspecting the values that were found for WorldBus, it could be stated that in this design, the wing was positioned at 27% of the total aircraft. Thus, the position of the wing of WorldBus was deemed valid.

For the design of the horizontal tail of the WorldBus, a detailed program was developed. In order to check the validity of this program, it was rerun, this time using input values from our reference aircraft, the Boeing 787-9. The system can be easily checked, since for the Boeing 787-9 all input variables were available and the ratio S_h/S is known that has to be compared. When all input variables were put in the program, an S_h/S of 0.18 was found, whereas this value should have been 0.20.[57] This difference can be attributed to the fact that the c.g. range of the Boeing 787-9 was not known and, therefore, some assumptions had to be made. The second part of the validation process would consist of comparing the S_h/S of the WorldBus to the S_h/S of reference aircraft. Here, a problem seems to arise. Whereas the S_h/S of the WorldBus is found to be 0.08, the S_h/S of reference aircraft are normally around 0.2. However, this difference can be easily explained. Due to the increased moment arm, caused by the increased aircraft length due to the lengthy fuel tank, a smaller stabilizer surface is required to deliver the required countering moments. In addition to the moment arm, WorldBus has a T-tail configuration which also decreases the surface area of the stabilizer. Therefore, the established S_h/S of the WorldBus and the entire horizontal surface design are deemed valid.

The design of the vertical tail was validated in the same matter as the horizontal tail. For the vertical tail, a value for S_v/S of 0.103 was found with the program whereas this value is 0.106 according to the vertical tail area and wing area of the Boeing 787-9.[58] This difference is only 3% and, therefore, the program is validated. WorldBus has a value of 0.096, which is in an acceptable range, validating the vertical stabilizer design.

To validate the calculations with regards to the undercarriage, reference data from the Boeing 787-9 was analysed. It was found that the distance between the nose wheel and the landing gear was $25.8\,\mathrm{m}$.[59] When filling in the values in the used formulas, a distance of $21.6\,\mathrm{m}$ was found. The tip-back angle and scrape angle are estimated to be 15 and 12 degrees respectively, since they are unknown. This 19.4% difference can therefore be explained by these estimations made. For WorldBus, a scrape bank angle of $9\,\mathrm{deg}$ was used to make sure the doors of the aircraft stay below $5\,\mathrm{m}$. This is unconventional but when looking at aircraft with a comparably long fuselage like the AN-225, an angle of 9 degrees is found and therefore is deemed a realistic value as long as the HLD's are able to provide enough lift during take-off for a short take-off distance

[56] https://www.lissys.uk/samp1/index.html
[57] https://www.lissys.uk/samp1/index.html
[58] https://www.lissys.uk/samp1/index.html
[59] https://www.boeing.com/assets/pdf/commercial/airports/acaps/787.pdf

11.7. Conclusion and recommendations

The main conclusion that can be drawn from this chapter is the fact that WorldBus will be stable and controllable. To achieve this, appropriate horizontal and vertical stabilizers had to be designed. The horizontal stabilizer depends highly on the c.g. range of the aircraft, which is established by means of a loading diagram. It was found that, in contrast to regular aircraft designs, the fuel tank must be placed in the middle of the cabin to not have a too large aft-most c.g. location. Based on this design choice, the horizontal (S_h/S) and vertical tail (S_v/S) surface to wing surface ratios were calculated, a value of 0.07 for S_h/S and a value of 0.09 for S_v/S were found. Although these values seem on the low side, this characteristic can be contributed to the long moment arm caused by the long aircraft length and T-tail of WorldBus.

Further analysis into the stability and control of WorldBus is recommended, focussing on the points listed below:

- For the wing placement is it recommended to analyse it further when the actual centre of gravity positions are known.
- For the horizontal stabilizer some assumptions have been made based on literature it is recommended to further analyse it when these values are known
- For the vertical stabilizer some assumptions have been made based on literature it is recommended to further analyse it when these values are known.
- For the loading diagram analyse the effect of loading passengers in both cabins at the same time on the cg range and the size horizontail tail.
- For the undercarriage it is recommended to further analyse the effect of the small scrape angle and large tip back angle.
- Analyse the eigenmotions of WorldBus.

12 Performance

In this chapter, the performance of the aircraft is analysed. First, the airfield performance is analysed in Section 12.1 after which the flight and climb performance is discussed in Section 12.2. Lastly, the payload range and the load diagram are analysed in Section 12.3 and Section 12.4

12.1. Airfield performance

To be able to find out whether an aircraft will perform as required for operations at airports, the airfield performance must be analysed. First, the take-off performance is analysed in Subsection 12.1.1. Then, in Subsection 12.1.2, the landing performance is analysed.

12.1.1. Take-off performance

To analyse the take-off performance the field length is evaluated. This is the total length that the aircraft needs to be able to take off. The take-off field length was analysed at International Standard Atmosphere (ISA) sea level conditions. Furthermore, no slope or wind is taken into account.

The field length is split up into two parts, the ground run and the airborne phase. For the lift-off speed (V_{LOF}), $1.05V_{min}$ is used. Here V_{min} is the minimum velocity at a maximum lift coefficient of 2.2 for take-off as specified in Section 9.6. To calculate the ground run distance (s_{ground}) Equation 12.1 is used [30].

$$s_{ground} = \frac{V_{LOF}^2 W}{2g(T - D - \mu_r(W - L))_{avg}} \tag{12.1}$$

$$D = 0.5\rho V^2 S(C_{D_0} + \phi \frac{C_L^2}{\pi e A R} Cl \tag{12.2}$$

$$\phi = \frac{(16h/b)^2}{1 + (16h/b)^2} \tag{12.3}$$

In the calculation for the drag used in Equation 12.1 the ground effect is taken into account by introducing parameter ϕ. The calculation of this parameter depends only on the height of the wing compared to the ground (h) and on the span of the wing (b). To calculate the friction drag, a friction coefficient (μ_r) of 0.02 is assumed. The average values for lift and drag were calculated at a speed of $0.7V_{LOF}$ [30][31].

The airborne phase consists of two parts, transition and climb. The horizontal distance covered during the transition and climb phase is calculated using Equation 12.4 and Equation 12.5 respectively [30].

$$x_{trans} = \frac{V_{LOF}^2}{0.15g} \sin\gamma_{climb} \tag{12.4}$$

$$x_{climb} = \frac{h_{scr} - (1 - \cos\gamma)\frac{V_{LOF}^2}{0.15g}}{\tan\gamma} \tag{12.5}$$

Here, γ_{climb} is the flight path angle during climb and is assumed to be equal to 3 °. h_{scr} is the screen height which is equal to 11 m as specified by CS25 [23]. When adding these three distances a total take-off distance of 2276 m was found. A factor of 1.15 for safety is applied as specified by CS25 regulations [23] resulting in a total take-off distance of 1299 m. This is deemed to be an acceptable take-off field length, so no design alterations have to be made.

12.1.2. Landing performance

For the landing performance, the landing field length is analysed in a similar manner as the take-off field length. Again no slope or wind is taken into account for these calculations. To calculate the airborne distance, Equation 12.6 is used [30].

$$x_{total-airborne} = \frac{V_{ap}^2}{\Delta ng} \sin\gamma_{ap} \frac{h_{scr} - (1 - \cos\gamma_{ap}) \frac{V_{ap}^2}{\Delta ng}}{\tan\gamma_{ap}} \tag{12.6}$$

Here, V_{ap} is the approach speed equal to $1.3V_{min}$, where V_{min} is the minimum velocity at a maximum lift coefficient of 2.8 for landing as specified in Section 9.6[30]. Δn and γ_{ap} are the change in load factor and the approach angle, which were assumed to be 0.1 and 3 ° respectively [30]. Lastly the screen height h_{scr} is equal to 15 m as specified by CS25 regulations [23].

The ground run distance is split up into the transition phase and the ground brake distance. It was assumed that the transition phase takes 2 seconds resulting in a transition distance x_{tr} of $2.6V_{min}$ [30]. The breaking distance is calculated in an identical manner as the ground run distance with Equation 12.7 [30].

$$x_{brake} = \frac{V_{ap}^2 W}{2g(T_{rev} + D + \mu_r(W - L))_{avg}} \tag{12.7}$$

Here, T_{rev} is the reversed thrust applied by the engines for landing, and μ_r is the friction coefficient for landing, which is assumed to be 0.4 [31]. Again the average drag and lift are calculated at a speed of $0.7V_{ap}$. When adding these three distances and applying a safety factor of 1.43 determined by the 'Civil Aviation Authority', this results in a landing distance of 2830 m when no reverse thrust or spoilers are used.[60] This might seem like a relatively large value, however, this distance can be shortened by applying reverse thrust and spoilers so no problems are foreseen for regular operations. When reverse thrust is applied, a required landing distance of 1777 m is found.

12.2. Flight and climb performance

Essential information for the determination of cruise altitudes is portrayed in a so-called flight envelope. In the flight envelope shown in Subfigure 12.1a, you can see several lines, each representing various speeds for optimal climb rate, climb angle, endurance, range, and glide performance at different altitudes. Also, minimum velocity (orange line), maximum velocity (light blue line) and stall speed (dark blue line) are plotted. As we are an ultra-long-range aircraft, ideally, we would like to fly along the green line (best-range performance line). Overall, the flight envelope is a diagram which shows the possible velocity and altitude combinations at which an aircraft can fly. Some are optimal some are not, but it is a useful chart for pilots to know whether they are flying efficiently for a desired performance.

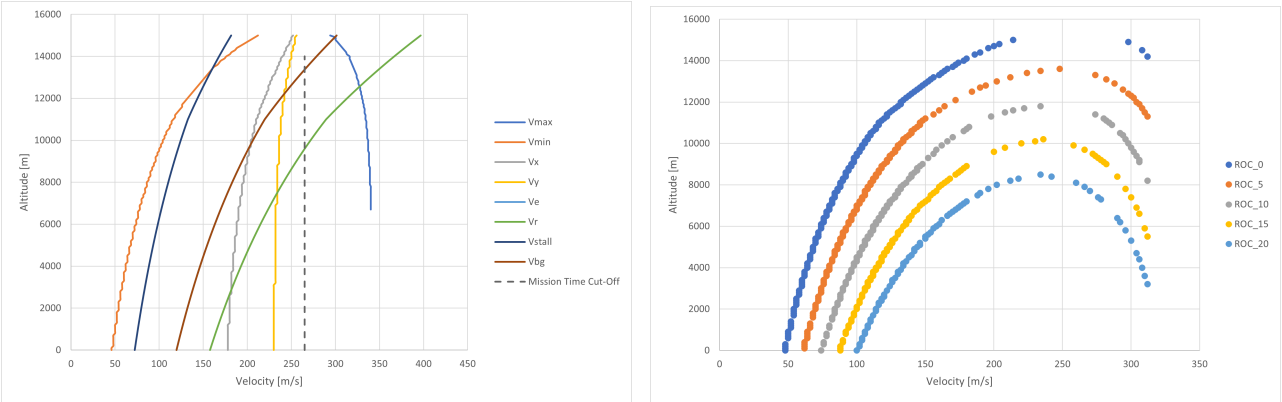

(a) Flight Envelope

(b) Rate of Climb Graph

Figure 12.1: Performance diagrams

Unfortunately, at the design cruise altitude of 9 km, the speed for optimal range performance is 255.6 m/s. This is slightly too low for the mission of this project; where the 19 000 km have to be flown in 20.5 hours, equivalent to a minimum speed of 265 m/s (dashed line). Flying at the speed for optimal range performance, the 19 000 km would be flown in 21.3 hours resulting in a total duration of 24.8 hours of travel time. Furthermore, to achieve optimal range performance at 265 m/s the aircraft would have to fly at an altitude of 9.6 km. Thus, it can be seen that the design point of 265 m/s at 9 km is not optimal for range performance. However, the flight envelope suggests that the engines can provide enough power to fly the aircraft at the required cruise speed of 265 m/s, at the cruise altitude of 9 km. This means that we will not be flying as efficiently as possible, but completing the mission is still possible as our engines are powerful. When flying at this altitude

[60] https://publicapps.caa.co.uk/docs/33/20130121SSL07.pdf

and speed the fuel needed would increase by 194 kg this could be taken out of the secondary tank in which 2205 kg is stored.

It is important to have an insight into the rate of climb performance of an aircraft, this information may assist a pilot in clearing obstacles and in evaluating the size of the take-off distance at different airports. This rate of climb differs per altitude, varying with the difference in available power and power required for propulsion and is plotted in Subfigure 12.1b.

12.3. Payload range diagrams

Payload range diagrams depict the relationship between the different payloads and ranges of the aircraft. It is constructed based on the MTOW, fuel weight, fuel weight used for cruise, the operational empty weight and the payload. The payload range diagram is presented in Figure 12.2.

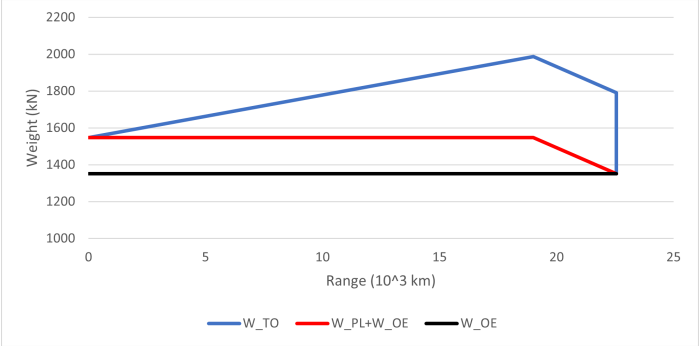

Figure 12.2: Payload range diagram

In Figure 12.2 the most left point where the red and blue line start is the zero fuel weight together with maximum payload. Then fuel is added until the maximum take-off weight is reached which is at the harmonic range of 19 000 km. Then payload is removed until no passengers are present resulting in a maximum range of 22 500 km.

12.4. Load diagram

A load diagram defines the velocity range an aircraft can operate in as well as the maximum load factors it may encounter during manoeuvres. Therefore this diagram helps pilots operate within safe boundaries and flight conditions. The diagram consists of two plots: the manoeuvre load diagram and the gust load diagram the final diagram is shown in Figure 12.3 from which it can be concluded that the gust load diagram is the limiting factor with a load factor of 2.588.

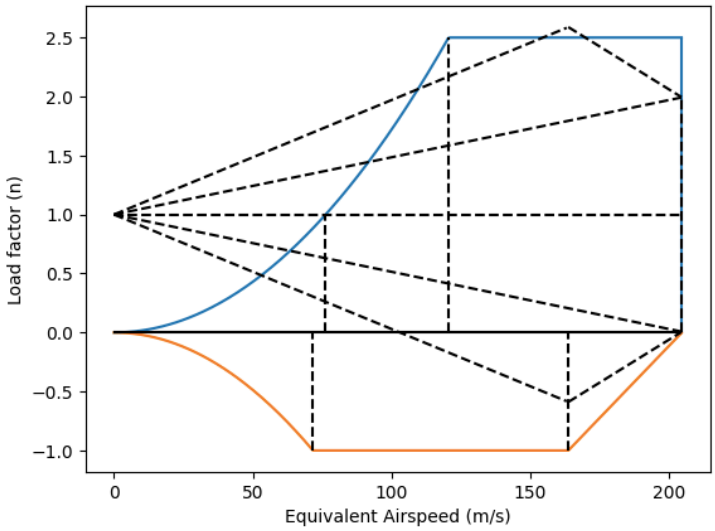

Figure 12.3: Load diagram

12.5. Verification and validation

To verify the model used for the performance of the aircraft unit tests have been used to check the correctness of the model. In addition to unit testing, the values can be validated by comparing them to reference aircraft. For the take-off distance, a value of 1299 m was found for WorldBus while the Boeing 787-9 has a take-off distance of 2800 m.[61] This difference can be explained by the fact that WorldBus has a higher $C_{L_{max}}$ at take-off, is lighter and has excess thrust since an existing engine has been chosen. When comparing the landing distance a value of 1777 m was found for WorldBus whereas the Boeing 787-9 has a landing distance of 1520 m. [62] Since the difference between these two values is within an acceptable margin, the landing distance calculation is deemed valid.

The payload range diagram that was constructed in Section 12.3 was validated by comparing it to the payload range diagram of a Boeing 787-9.[63] It was noticed that the diagrams were not the same, which can be attributed to the assumption that, in MTOW circumstances, the fuel tank is fully filled while also using the maximum payload. Normally, when the fuel tanks are full, the aircraft cannot take on as many passengers as it would exceed its MTOW, and vice versa when having full payload capacity, the fuel carried onboard is decreased. However, WorldBus has been designed for a range of 19 000 km when the aircraft is completely fueled, with 200 people on board, their baggage and crew. Thus, the only design point in the payload range diagram at MTOW is maximum fuel and maximum payload. This explains the difference between the Boeing payload-range diagrams. If the tanks and internal configuration had been designed differently, the diagrams would have looked similar.

12.6. Conclusion and recommendations

The take-off distance of WorldBus is shorter compared to the Boeing 787-9 which is due to a higher $C_{L_{max}}$ at take-off, a lower MTOW and excess thrust. Additionally, the landing distance is higher which is due to the fact no reverse thrust or spoilers are used. When flying at a speed of 265 m/s at an altitude of 9 km WorldBus is not flying at optimal speed and therefore can't fly as efficiently as possible. However, when a little extra fuel is used out of the secondary tank, the mission can be achieved. Lastly, with the payload range diagram, it was verified that Worldbus has a range of 1900 km.

Further analysis of the performance of WorldBus is recommended of which the focus points are listed below.

- For the airfield performance it is recommended to take more critical conditions into account such as crosswinds, rain, and runway slope.
- For the airfield performance some assumptions were made for thrust, drag, velocities, flight path angles, and friction coefficients. To get more accurate results a more detailed analysis based on known values needs to be performed.
- For flight and climb performance revise exhaust flow and bypass airflow velocities for the Trent 1000.
- For the payload range diagram a better analysis can be performed by not assuming that the fuel tank is fully filled while also using maximum payload.

[61] https://aerocorner.com/aircraft/boeing-787-9/
[62] https://aerocorner.com/aircraft/boeing-787-9/
[63] https://www.boeing.com/resources/boeingdotcom/commercial/airports/acaps/787.pdf

13

Structures

In this chapter, the sizing and mass for a number of structural components are established. Firstly in Section 13.1, the structure of the fuselage is discussed. In this section, the skin, stringers, and frames will be analysed as well as other structural system implementations that will be explored. In Section 13.2, detail is given to the tanks located in the fuselage as well as other subsystems necessary for the system are designed. Finally, in Section 13.3, detailed wing, strut and engine pylon designs are performed based on the loads acting on the wing. All computations performed in this chapter are based on the coordinate system shown in Figure 13.1

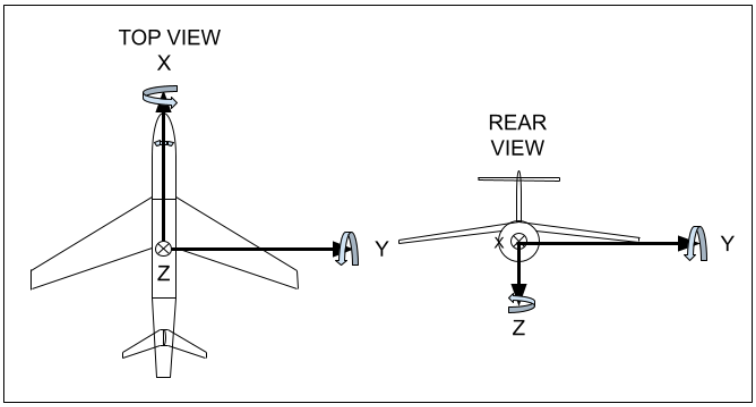

Figure 13.1: Coordinate system, positive axis and moment directions

13.1. Fuselage structural design

As the shape and diameter have been determined, more detail can be introduced by determining the number and location of the stringers, determining the number of frames based on the spacing, and determining skin thickness. These structural parts have an influence on the structural weight.

13.1.1. Skin thickness

For the fuselage design, the skin is designed to account for internal stresses caused by pressure differences. The circumferential and longitudinal stresses in a pressure vessel can be calculated with Equation 13.1 and Equation 13.2 [32]. CS-25 regulations, specifically CS 25.841(a), state: "Pressurised cabins and compartments to be occupied must be equipped to provide a cabin pressure of not more than 2438 m (8000 ft) at the maximum operating altitude of the aeroplane under normal operating conditions." [18]. The cabin is then pressurised at a pressure of an altitude of 2000 m for comfort. This creates a pressure difference (Δp) that acts on the skin.

$$\sigma_{circ} = \frac{\Delta p R}{t} \tag{13.1}$$

$$\sigma_{long} = \frac{\Delta p R}{2t} \tag{13.2}$$

Here, R is the radius of the fuselage, t is the thickness and the circumferential and hoop stresses are taken to be the yield stress of the applicable material. R equals 3.1 m , Δp equals 48.8 kPa , σ_{circ} and σ_{long} are set to be 0.4 MPa. The applied material would result to be CFRP. The thickness is then taken to be the largest thickness out of the two equations and results in a skin thickness of 0.38 mm. However, for the ease of manufacturing and for the reason that the skin does

not only have to protect against stresses but also possible debris flying against the fuselage, the skin thickness is taken to be 1 mm.

13.1.2. Stringer selection

The stringers are an important load-carrying member in the fuselage responsible for the bending moment in the fuselage. They are directed in the length of the fuselage. At cruise, the fuselage frame tends to 'droop' around the main wing due to the structural weight of the aircraft itself. This causes the upper part of the fuselage to experience tension, and the lower part to experience compression.

In order to have a structure that can handle these loads, it is important to determine the internal shear stress and bending moments that occur in the aircraft. These values will determine what kind of stiffening elements are needed for the fuselage. For this, the MTOW at take-off has been identified as the most critical load case. To get an accurate estimate of the internal shear and bending moments for WorldBus, the fuselage structure has been divided into a number of different sections. First, it is assumed that the weight of the fuselage itself, together with the fixed equipment, is spread uniformly over the entire length of the fuselage. Then, the main fuel tank weight, secondary fuel tank weight, empennage, and payload weight are also considered as distributed loads at their respective locations. For instance, the fuel tank is approximately 24 m long and starts at 20 m from the nose. Its load is then distributed over this area. Finally, the lift provided by the wing and the horizontal stabiliser, and the weight of the wing and the engines are assumed to act as point loads on the structure. The result of the internal shear and bending moment can be seen in Figure 13.2. The internal shear force has simply been calculated with Equation 13.3 for distributed loads, and with Equation 13.4 for point loads. At every point, the internal shear force of all the different components can be added together to find the total internal shear force.

$$V_x = -\int_0^x f(x)dx \tag{13.3}$$

$$V_x = -P \tag{13.4}$$

Then, to find the bending moment at a position relative to the nose, the total internal shear force diagram, as given in Subfigure 13.2a, is simply integrated from the nose up until that position.

The largest bending moment occurs where the wing is mounted to the fuselage. Here, a large torque is applied to the fuselage as the wings sweep means that the resulting lift vector is positioned behind the location where the wing is attached to the main fuselage. Since the stringers need to carry the bending moment, the size and amount of stringers are directly influenced by the magnitude of the bending moment.

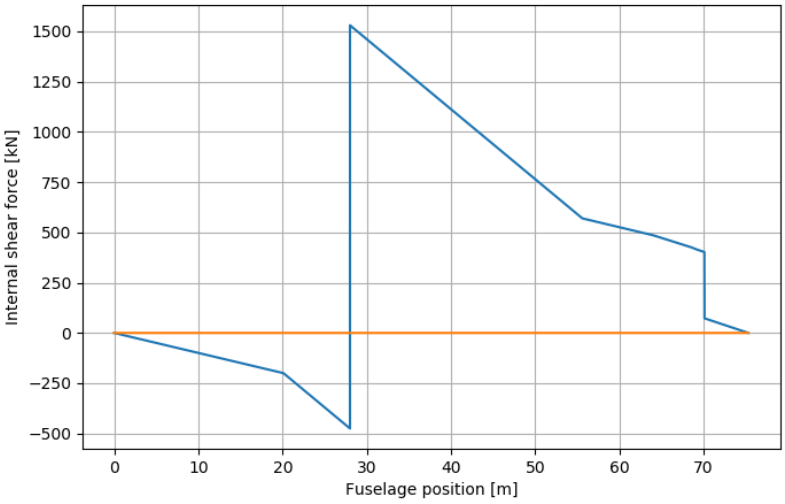

(a) Internal shear force in fuselage.

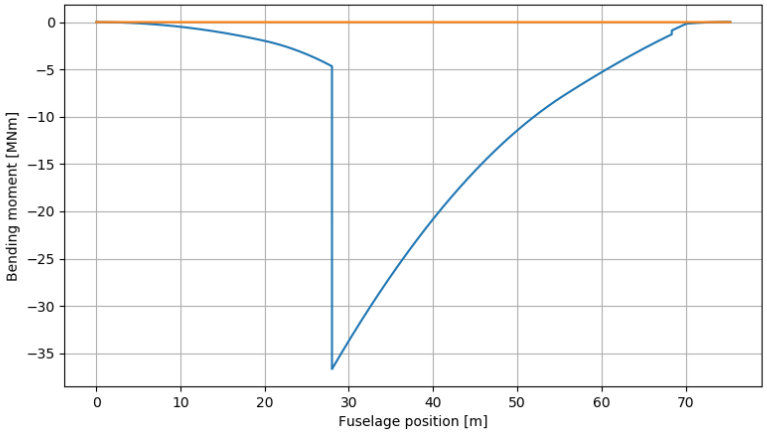

(b) Bending moment in fuselage.

Figure 13.2: Internal shear force and corresponding bending moment in fuselage due to lift and weight forces.

To obtain a structural fuselage approximation, it is assumed that the stringers will fully cope with bending loads, whereas the skin will deal with shear, torsion and pressure. In reality, this is not entirely true. Although the stringers do carry the majority of the bending loads, they are also subjected to the other loads. Therefore, a hat-shaped stringer is the best choice. Such a shape has good performance in all load cases and is especially able to deal with high compression loads, which is particularly experienced by the lower part of the fuselage. Also, if the fuselage will be composite, the stringers and fuselage can be produced in one go. In comparison, the process is less labour-intensive compared to a metal fuselage.

13.1.3. Stringer number and placement

To stiffen the aircraft, stiffeners and longerons are used. Longerons are stiffeners with a larger cross-sectional area. In this analysis, only stringers are considered. A conventional cross-section has between 50-100 stiffening elements. Using the absolute maximum bending moment with the material maximum yield stress, it was determined that a stiffening area of $1318\,\mathrm{cm}^2$ is required. This value is based on an idealised boom analysis method.

$$\sigma_{boom} = SF \cdot n_{2.5} \cdot \frac{M}{I}\tilde{z} \tag{13.5}$$

This means that about 180 stringers with a cross-sectional area of $7.3\,\mathrm{cm}^2$ is the most optimal solution. This is due to the size of the aircraft. The fuselage is larger than most conventional aircraft, and due to its size, this stringer configuration is reasonable. In case a composite material is used, such as CFRP, a safety factor (SF) of two is used.

For the stringer placement, the bending moment is in the direction of the y-axis, meaning that the fuselage lower half experiences a compressive force and the top side experiences tension. Around halfway, at the horizontal axis, the moment and forces are the lowest, hence the least stringers are located here. Only a few stringers are located around here for structural integrity.

Finally, the weight is optimised by reducing the stiffening area based on the reduction of the bending moment in sections. As can be seen in Subfigure 13.2b, there is a change in the bending moment. To reduce the structural weight, a step-wise approach is used, based on the fraction of the bending moment with respect to the maximum bending moment. Reducing the stiffening elements towards the ends is beneficial as the loads decrease, requiring fewer elements, and thus reducing the weight.

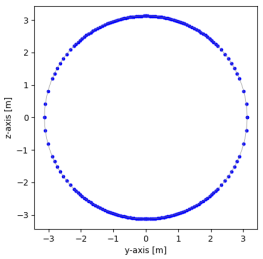

Figure 13.3: Schematic stringer placement in the center of the fuselage

13.1.4. Formers sizing

For a more complete structural representation, the structural formers were also sized. Formers are used to maintain the shape of the fuselage and to reduce the column length of the stringers to prevent general instability of the structure [33]. Formers are typically placed about 50 cm apart [64]. As formers carry small loads, they can be made of light structures. For the size of the formers, the frame area of the KC-135 fuselage panel was used [34], due to very little information being available about former sizes. This gives an approximation of the volume required in the fuselage, which was 1.29 m^3. This is however an overestimation as the size of the frames reduces in the conical parts of the fuselage. Yet, this does give a good representation of the required mass.

13.1.5. Screens replacing windows

The future in air travel could be that windows are replaced with screens, as shown in Figure 13.4 [65]. By removing cabin windows from aircraft, critical loads around the window cut-outs are removed, allowing for a more evenly distributed load.

Figure 13.4: Screens replacing windows artist impression

This removes the reinforcements around the windows, which lowers the structural weight. Data indicated that for each kilogram of weight saved in the design phase, the total plane weight will decrease by 1.25 kg [35]. For the WorldBus final design concept, about a 900 kg structural weight decrease can be observed. As an effect, sustainability would improve due to reduced fuel consumption. Also, the waste material produced from making cut-outs is significantly reduced, improving sustainability even more. Utilizing lightweight panels that can curve with the fuselage shape, the added weight of the screens can be kept to a minimum.[66]

Removing windows from the cabin also has its drawbacks. From research, it has been observed that about 80% would not fly a windowless aircraft due to feeling claustrophobic. Also, the option of not being able to take real pictures is a drawback according to passengers [35]. Furthermore, latency between visual and physical perception could cause more cases of motion sickness [36]. To minimise this, a live feed has to be used on the screens such that the difference in this perception is minimised. Finally, heat is generated, increasing the internal cabin temperature. Current aircraft are outfitted with a climate control system only capable of a few settings. However, it is expected that future aircraft have a more sophisticated climate control system implemented.

Another large drawback that has to be considered is the fact that much less natural light will be available inside the cabin. This means that in the event that power in the cabin is lost, it will be a lot darker than in a conventional aircraft, as light can only enter the cabin through the windows in the doors. To combat this the exit routes on the aisles will be painted with fluorescent paint, to ensure that they are visible in low-light conditions. To further mitigate this risk, the light inside the cabin will be dimmed during take-off and landing operations. These are typically regarded as the high-risk section of a flight. Thus to lower the time that the passengers' eyes need to adjust to the dark cabin in case of a power loss, the lights are dimmed preemptively. Lastly, the flight crew will be outfitted with more versatile flashlights than airlines conventionally do to aid them in emergency response work.

Although using screens to replace windows has quite some drawbacks, many systems could be improved ensuring that the

[64] https://aerotoolbox.com/fuselage-structure/
[65] https://www.dezeen.com/2014/11/07/cpi-technology-consultancy-transparent-aircraft-cabin-interior/
[66] https://www.nhk.or.jp/strl/english/publica/bt/81/4.html

effect of these drawbacks is minimised or even fully mitigated. This will be beneficial for the passenger experience. From a manufacturing point-of-view, this replacement has significant structural benefits, as well as sustainable improvements. Therefore, it has been decided to incorporate this design choice.

13.1.6. Lightning strike

With the use of CFRP for the skin, the weight of the aircraft is significantly reduced. CFRP is however a poorer electrical conductor than aluminium that is conventionally used as fuselage skin material. If an aircraft with aluminium skin is struck with lightning, lightning will attach to an extremity such as the wing tip or nose. The lightning then attaches to the fuselage and is conducted through the skin to exit at some other extremity. However, since the CFRP fuselage skin does not conduct very well, an alternative has to be thought of as the skin would otherwise result to get damaged. The lighting has to be guided safely across the fuselage such that no electrical equipment is affected or more importantly no sparks get to the fuel system that would ignite the hydrogen.[67] A metal mesh in the skin gives protection against lightning as it conducts electricity through the outside of the vessel. Areas that are more prone to lightning strikes are given additional protection such as wire bundle shields.[68]

13.1.7. Results

After weight optimisation, the fuselage results can be seen in Table 13.1. The numbers presented in Table 13.1 are based on current optimisation. These values will be used for further determination of the structural weight, which is influenced by the material selection in the upcoming chapter. It must be noted that this section is not perfect as some assumptions have been made which do not apply to reality. It must be noted that the volume of the stringers will double if a composite is going to be used.

Table 13.1: Description of the fuselage results

Structural part	Volume [m^3]
Skin	1.36
Stringers	4.63
Formers	2.10

13.2. Tank sizing

In the case of the storage of hydrogen, a revaluation was made for the tank design along with a design for a buffer tank. The buffer tank is present in case of a failure in the main tank system and contains enough fuel for one hour of flight.

13.2.1. Main tank system

When considering the storage of liquid hydrogen (LH_2), the incredibly low storage temperature of 20 K is the main design constraint. A good tank design needs to find a way to insulate the liquid hydrogen with as little mass as possible whilst fitting within the spacial constraints of the aircraft. First, the inner tank is designed. This tank serves to hold the LH_2 and withstand the pressure inside the tank. A material selection had to be made for the main tank for which high alloy steel, age-hardened aluminium and carbon fibre-reinforced polymer (CFRP) were considered as options for the skin of the inner shell. These materials were selected as they are commonly used for pressure vessel design. CFRP was eliminated because it cannot withstand the thermal environment, leaving only steel and aluminium. The inner tank design was based on methods used for designing cryogenic hydrogen tanks for future aircraft applications [37]. Knowing the outer tank diameter, the outer tank shell thickness and the insulation thickness, the inner tank diameter can be obtained. Using Equation 13.6, the inner tank shell thickness (t_i) can be calculated.

$$t_i = \frac{p_p d_i}{v(\frac{2K}{SF} - p_p)} \tag{13.6}$$

Where p_p is the proof pressure that is obtained by including a safety factor of 1.4 in the venting pressure, which is the maximum pressure inside the tank. SF is the safety factor which is assumed to be 1.4, d_i is the inner tank diameter, v is the weld efficiency that is taken to be 0.8 and K is the limiting stress of the material. The limiting stress was taken to be the yield stress of 1480 MPa. The internal tanks are designed for a proof pressure of three bar.

Around the inner tank, an insulation layer is required to limit the amount of hydrogen that boils during flight and to protect the structure of the aircraft. For an insulation material, multiple insulation foams were analysed that ended up not being able to withstand the temperature of liquid hydrogen. One insulation foam that was able to perform in such an environment, is a specially developed form of polyurethane (PUR) [38]. Cryogenic thermal insulation systems that incorporate a vacuum environment can provide the lowest possible heat transfer from the local environment to the stored cryogen. Vacuum in combination with multi-layer insulation (MLI) systems can provide the most optimal thermal insulating capability [39]. Soda lime borosilicate glass bubbles were also considered as an option for the insulation layer in the vacuum, which at

[67] https://www.scientificamerican.com/article/what-happens-when-lightni/
[68] https://mainblades.com/article/this-is-what-you-should-know-about-boeing-787-lightning-protection/

first was a promising option because they might alleviate buckling of the outer vacuum wall. However, too little is known about the mechanical effect of the application of glass bubbles in a vacuum. Hence MLI was preferred due to its higher thermal resistance. When designing the outer tank using a vacuum layer as insulation, the outer tank was designed based on methods for other vacuum chambers [40]. And as stated earlier, when designing polyurethane foam as an insulator, no outer tank had to be designed.

The diameter of the outer tank was taken to be the diameter of the fuselage with a clearance of 10 cm to allow space for tubing, stiffeners for the fuselage and some room for inspection and maintenance. The thickness of the tank is determined using an external pressure design procedure for cylindrical shells [40]. This procedure described a method in which a thickness is assumed and the required moment of inertia is compared to the estimated moment of inertia of the stiffeners. This is an iterative trial-and-error design procedure that results in a thickness for which the estimated moment of inertia is higher but closest to the required moment of inertia of the stiffeners. The tanks were designed for an external pressure equal to sea level pressure with a safety margin of 1.4. This method results in a good high alloy steel tank. However, it is prohibitively heavy. To improve this design the tank and stiffeners were changed to CFRP. This was done by scaling the thickness of the walls by the ratio of Young's moduli between CFRP and high alloy steel. This will lead to an over-designed tank as the greatly increased thickness will mean that the buckling pressure goes up, as this is mostly a function of geometry rather than material strength. Meanwhile, the strength of the walls remains the same through the scaling. Unfortunately, this means that the tank is heavier than it could be if the design was further optimised. Because no better method for designing CFRP tanks could be found this resulted to be the final design for this part of the design.

The required thickness of the insulation was based on a designed amount of allowable boil-off per day. A boil-off of 1% per 24hr was found to be a good design point for a low loss with acceptable insulation thickness. This dictates the amount of energy that is allowed to come through the insulation. For the first design, MLI was used in combination with a vacuum layer to limit the thickness of the insulation (t_{ins}). Which is calculated using Equation 13.7, resulting in a thickness of 1 cm. For polyurethane, this resulted in a thickness of 1.47 m.

$$q = \frac{k}{t_{ins}} A_m \Delta T \tag{13.7}$$

In Equation 13.7 q is the heat flow, k is the thermal conductivity of the insulation material, A_m is the mean area of inner and outer insulation surfaces and ΔT is the difference in the temperature between the liquid hydrogen and the surface area of the tank. The surface temperature will have to be kept at 5 °C by a small heating system to avoid ice forming on the surface. Following Equation 13.7 1.8 kW of power will be more than enough.
This concludes the final tank sizing, for which the parameters can be seen in Table 13.2. It is clear that for a vacuum-insulated tank, the outer vacuum jacket contributed the most to its weight. The PUR insulated tank offers a better specific weight, however, due to the low inner diameter the length has to be prohibitively large. Therefore, the cylindrical tank results to be designed from an inner high alloy steel tank, an insulation layer using MLR and a vacuum with a CFRP outer tank to keep the vacuum layer airtight.

Table 13.2: Parameters of the liquid hydrogen main tank for different configurations.

Parameter	Value
Inner tank length	26.71 [m]
Inner tank diameter	5.67 [m]
Inner tank mass	3041.53 [kg]
Insulation thickness	0.01 [m]
Amount of stiffeners	148 [-]
Stiffener spacing	0.17 [m]
Outer tank length	26.74 [m]
Outer tank diameter	5.7 [m]
Outer tank mass	68103.17 [kg]
Total tank mass	78816.13 [kg]

13.2.2. Buffer tank system

Because the main tank is utilising liquid hydrogen insulated with a thin vacuum, the risk of failure for this tank is deemed to be high. In this case, failure would include anything that stops the tank from delivering enough hydrogen to power the engines and could include anything like valve failure, failure of the heating system, or loss of the vacuum in the insulation layer. For this reason, a secondary buffer tank was designed. It holds reserve fuel to ensure one hour of nominal flight when the main tank fails.

Because this tank is designed for redundancy, alternatives to vacuum insulation were reconsidered. Polyurethane foam would be preferred over a vacuum layer for this reason. Because polyurethane offers much lower thermal resistance, a higher percentage boil-off rate has to be accepted for this option. However, since the buffer tank can be considerably smaller, a higher fractional boil-off still translates to a smaller boil-off w.r.t. the main tank. To eliminate boil-off, high-pressure hydrogen storage was also reconsidered. This would be the simplest solution for storage, as the high pressure inherently forces the hydrogen out of the tank, meaning that only a valve is needed for flow control. However, these tanks were found to be an order of magnitude heavier than the PUR-insulated tanks due to the high pressures involved.

All tanks were designed to hold one-twentieth of the volume of the main tank. Because this tank is designed to allow for a 20+ hr flight. This means that the buffer tank can facilitate one hour of flight time. The weights for the designed liquid

hydrogen tank are shown in Table 13.3.

Table 13.3: Liquid hydrogen buffer tanks.

Insulation type	**Outer diameter** [m]	**Mass** [kg]
Vacuum insulated	4.27	3098
PUR (50%/day B.O.)	5.16	886
PUR (100%/day B.O.)	4.51	886

Table 13.4: Compressed hydrogen buffer tanks.

Diameter [m]	**300 bar**	**700 bar**
CFRP	6.36	5.21
steel	6.19	4.93
titanium	625	5.09
aluminium	6.38	5.40

Mass [kg]	**300 bar**	**700 bar**
CFRP	64,100	121,900
steel	88,100	208,900
titanium	107,000	258,200
aluminium	130,600	326,200

13.2.3. Venting system

The liquid hydrogen tank uses its own boil-off to pressurise the tank. This means that in cases where the boil-off is higher than the amount of fuel being used, the pressure inside the tank will build up.

If leakage occurs in the inner or outer tank, as earlier explained, the tank would be compromised and the fuel would have to be jettisoned. The heating component inside the tank that would normally regulate the boil-off could then be heated further to speed up the vaporisation rate of the liquid hydrogen which would then have to be vented into the outside environment.

Since the gaseous hydrogen has a lesser density, the venting system would have to attach to the top of the fuel tank. The system would have to go from the inner fuel tank all the way to the outside of the fuselage. The optimal location for the venting system is in the same compartment where the fuel tank is located. This way, the venting system stays isolated from the passengers, including the crew members, keeping them safe in case of a leak in the fuel system. If both the inner and outer tank would be compromised and gaseous hydrogen would end up outside of the outer tank inside the isolated compartment the fuel tank sits in, the whole compartment would have to be vented. The compartments the fuel tanks sit in are isolated such that when leakage occurs, the hydrogen will not reach the passenger or any other person in the aircraft. Since the density of gaseous hydrogen is only 7% of the density of air, a venting system would not be complex as the hydrogen would leave the top of the fuselage when given an opening in the fuselage.[69]

13.2.4. Heating system

As mentioned in this section, the hydrogen that will be powering the engines is stored in a liquid form. However, the hydrogen that is extracted from the tank will be in a gaseous form. This makes transporting the fuel much simpler as the temperature constraints aren't nearly as strict. However, because the natural boil-off rate of the tank is limited by the insulation, a heating system is required to control the amount of fuel coming from the tank. The tank cannot simply be designed for a boil-off equal to the consumption as the thrust settings are variable. And when the aircraft is not flying, the hydrogen in the tank should not have to be vented. As hydrogen is not only expensive but also bad for the environment[41]. Inside the tank, a 10% margin is included for the boil-off gas to be extracted when the tank is full. At a nominal cruise, the heating system has to output over 325 kW to vaporise the required 0.7 kg of LH_2 every second. At full throttle, this increases to 962 kW. This heat is obtained from bleeding air from the engine. Through a heat exchanger, the air heats up the hydrogen, and after the bleed air is then cooled it will be used for pressurizing the cabin. This amount of power is less than 2% of the energy generated by the engines and should therefore be very feasible.

13.2.5. Maintenance

Designing the outer engine to be made of CFRP means that it is not possible to be taken apart without damaging the outer tank shell. Another way has to be found for the inspection and repair of the main tank. Since the fuel system has to include a venting system, the entry of the inside of the tank for tools could be done via the valves of the venting system. This can be done using tools for visual inspection and a small robot can be designed for the inspection and repair that can be controlled from the outside of the tank.

[69] https://h2tools.org/hyarc/hydrogen-data/basic-hydrogen-properties

13.2.6. Sloshing

Sloshing is the movement of a fluid inside a moving tank. The motion of the liquid can impose forces on the structure which can change the centre of gravity of the aircraft and can have a major impact on the control and safety of the aircraft. For liquid hydrogen, sloshing presents additional problems. As sloshing takes place, the surface area of the liquid hydrogen increases and accelerates the boil-off which poses potential hazards.[70] Especially since the fuel tank is designed to be quite long, it is important to account for this problem. Therefore, baffles are introduced into the fuel tank design. Baffles dampen the effect of sloshing inside the tank. Baffles are structural elements inside the tank that have an additional mass that makes the fuel tank heavier. For this reason, the sloshing elements have to be chosen to be as light as possible while limiting the destructive effects.

13.2.7. Fuel dumping

In case of an emergency kerosene-powered aircraft can dump part of their fuel to be able to quickly land after a heavy takeoff. The (CS 25.1001(b)) requirement states that an aircraft has to be capable of dumping the required amount of fuel for a safe landing within fifteen minutes [18]. For WorldBus to be able to evaporate for example twenty-five per cent of its fuel in the required fifteen minutes, a total heating power over $5.6\,\mathrm{MW}$ is required. This is over an order of magnitude more power than would be required from an engine during nominal operation. It is not realistic to be able to extract this amount of power in case of an engine-out scenario. Therefore, WorldBus had to be designed to be capable of landing with a full fuel tank.

Of course, a scenario in which dumping of fuel is absolutely required is still imaginable. Extraction from the tank in gaseous form would be preferable. However as outlined before, it is not feasible to boil all the fuel in the tank in a rapid fashion through the heating system. An alternative where the vacuum insulation layer is compromised by letting air flow in the vacuum chamber, allowing a lot more energy to flow into the tank passively was imagined. The introduction of air would however also mean that a lot of ice would form inside the vacuum chamber, ruining the MLI structure. Because this would essentially mean a loss of the tank this was not deemed as a viable option. This only leaves the option of dumping the hydrogen in liquid form. The main concern with this is the very sudden change in temperature in the structure. To avoid contact between the aircraft skin and the liquid hydrogen it would have to be dumped at the rear of the aircraft. A tubing system would have to be designed that can withstand the sudden change in temperature when dumping is initiated. This is something where a lot more research has to be done, and testing has to be done to investigate the effects of dumping liquid hydrogen into the atmosphere behind the aircraft.
This has to be a high priority in the strategy for developing WorldBus further as the inability to find a solution for dumping fuel could mean that the WorldBus concept cannot be turned into a product with satisfactory safety levels.

13.3. Wing loading, wingbox and truss design

In this section, the truss, the wingbox and the engine pylons design processes will be explained. Furthermore, the optimisation approach used to find the best truss location is also going to be explained.

[70] https://www.element.com/nucleus/2022/simulating-gust-induced-sloshing-in-the-fuel-tank-of-a-liquid-hydrogen-powered-aircraft

13.3.1. Assumptions

Table 13.5: The assumptions that regard Section 13.3

ID	Assumption	Effect	Justification
AS.WB.GEOM.1	Thin-walled wingbox	This reduces the moments of inertia, and simplifies the computations for stresses and deflections	This is acceptable as reducing the moment of inertia, increases internal stresses of the structure, and thus it leads to a slightly over designed wingbox
AS.WB.GEOM.2	Constant wingbox thickness, for all span positions	This simplifies computations, but it increases wingbox weight	Most of the loads are carried by the starting portion of the wing, and thus that section needs a higher thickness than the tip section. Assuming the entire wing has the same thickness as the initial section leads to more over designing of the wingbox
AS.TR.LOAD.1	Truss only carries tensile and compressive forces	Computations are simplified. Omission of shear forces and moments that may be introduced into the truss by the attachment points can lead to an under designed truss	The tensile and compressive loads carried by the truss will be multiple orders of magnitude higher. The wing root can carry the gross of the longitudinal shear and torsion. The truss being over designed for the tensile and compressive forces, and the safety factor provide load contingency.
AS.TR.LOAD.2	The weight, drag, and lift of the truss are negligible	simplified calculations, but an under designed I_y for standstill compression due to the truss weight, and under designed for bending performance due to weight, lift, and drag effects and perturbations.	The load carried by the truss is multiple orders of magnitude greater than the weight of the truss. In addition, the current safety factor and eventual design for buckling performance provide sufficient margin to safely transfer the smaller bending moments.
AS.TR.LOAD.3	Lift over the span is constant	The truss analysis can be performed in a realistic time span. The total lift stays the same, but the root is exposed to a smaller lift force and the tip to a larger lift force than in reality. This affects only the load the truss takes. If the actual distributed load were to be analysed for the truss, the load on the truss would be smaller	The assumption results in a somewhat over designed truss. This, in turn, overestimates the wingbox load alleviation. This is compensated for with generous safety margins and assumption **AS.WB.GEOM.2**.

13.3.2. Optimisation approach

A truss-braced wing configuration allows for a higher wingspan and a higher aspect ratio for a wingbox design similar to that of a non-braced wing. The truss is loaded in tension during flight and, thus, transfers lift loads to the fuselage. This alleviates the wing from both shear and moment loads. Furthermore, the introduced compression in the wing by the angle of the truss alleviates the bending tension of the lower wingbox skin and increases the criticality of upper wingbox skin buckling.

The truss-braced wing design can vary in the placement of the truss and the stiffness of the wingbox. The sizing of the truss depends only on its experienced load, which, in turn, depends only on its placement. It is expected that one combination of these should result in the lightest possible truss-braced wing configuration. To find this value, a strategy was devised to examine every combination, to a reasonable resolution, of truss placement and wingbox thickness. It is expected that part of these combinations will not hold up to the loads and fail instead, low thickness and short truss combinations, for example. However, there will be a border at which a range of combinations will function. Of these combinations, some trusses lay within the possible envelope as dictated by the undercarriage. Of those combinations, the lightest will be selected. A visual representation of this can be seen in Figure 13.5.

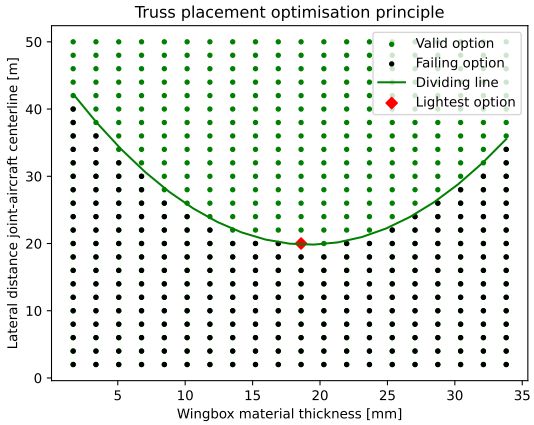

Figure 13.5: Visual representation of the truss placement optimisation principle.

13.3.3. Engine loads

To get a complete design of the wing it is important to know what forces the engine will put on the wing and where they will be located. To get an answer to this question the structure that connects the engine to the wingbox has to be designed. For this project, a simple truss structure was designed that connects the engine to the wing using three rods. On the engine two mounting points were identified on the engine core. The first point is located aft of the fan, and the second is located at the trailing edge of the engine core. These two points are connected to the front and aft spar of the wingbox with the truss structure mentioned earlier. To make the truss structure a statically determinate system the rods are pin supported at the spars and the engine. A drawing of the final design is shown in Figure 10.1

With the concept of the engine pylon set it is now a question of finding the optimal engine position to minimise the mass of the structure. The lateral position has already been fixed in Section 10.3. Hence only the longitudinal and normal positions need to be optimised. This is done by varying the position of the engine until the weight of the structure converges to a minimum following the BFGS algorithm.

The forces that the engine puts on the wing were analysed for both full forward thrust and reverse thrust in 2.5 and -1 g conditions. With such a wide range of load combinations manual computation is not efficient. Hence a Python program was developed to optimise the engine position. It sizes the rods to withstand either yield when in tension or Euler buckling when in compression.

For materials, high alloy steel, aluminium, titanium and CFRP were analysed. From the metal structures titanium was the most lightweight structure. Offering an improvement of 19% over high alloy steel. CFRP is two-thirds lighter still. However, the high-temperature environment that the engines create means that CFRP cannot be applied. This in combination with the better fatigue characteristics is why titanium was identified as the preferred material for the rods. The final results from the pylon design are included in Table 13.6

Table 13.6: Final dimensions of engine pylons

Rod type	**Diameter** [mm]	**Estimated cost** [EUR]
rod 1	326	45800
rod 2	193	4700
rod 3	350	35600

13.3.4. Wingbox sizing

In order to perform the aforementioned optimisation approach, it was necessary to estimate loads on the wing. Furthermore, an internal stress analysis was performed to determine the minimum wing structure size and weight to support design loads of the aircraft.

The design loads were obtained from the manoeuvre and gust loading diagrams provided in Section 12.4. From these diagrams, it can be seen that the most extreme load factor that aircraft will experience is 2.588, $n_{ult} = 2.588$. This means that the wing have to generate 2.588 times the MTOW in lift and not fail under such loads. A truss-braced aircraft's wing supports four main loads; the aerodynamic loads, the wing weight, the engine thrust and weight loads, and finally the truss loads.

The aerodynamics are composed of two forces, the drag and the lift. To estimate the loads along the length of the wing, the wing planform was divided into a grid of small areas. The lift and drag were then computed over each of the elemental areas. The lift was computed from the pressure distribution data, obtained from XFLR5. Only the component of the pressure distribution perpendicular to the airstream was considered to be the lift. Thus, after finding the pressure difference between the upper and lower surface, each pressure coefficient was adjusted using the elemental area angle with respect to the chordwise centre line of the airfoil and the angle of attack. This can be seen in Figure 13.6.

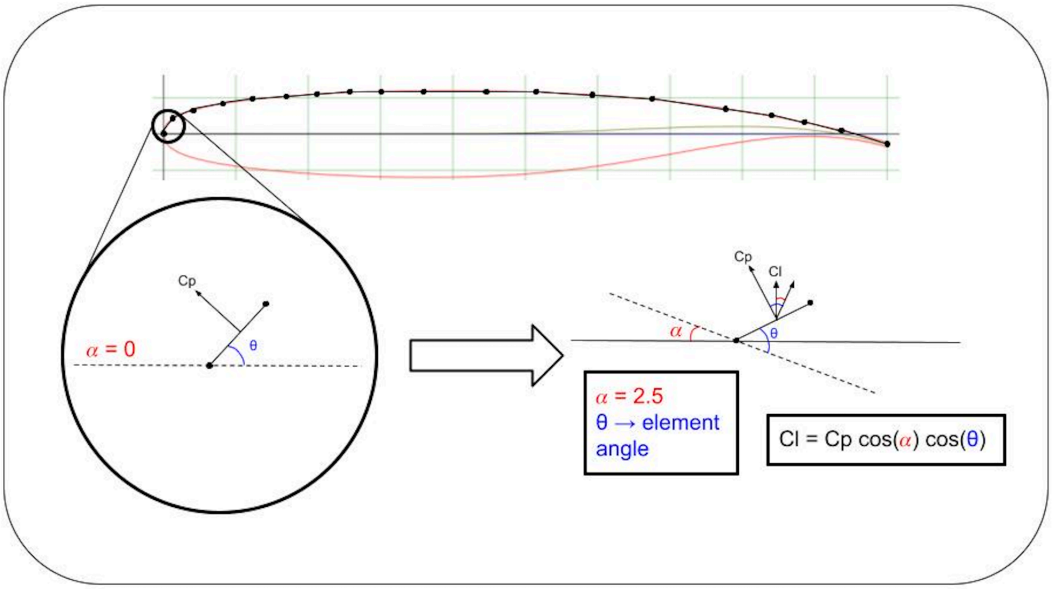

Figure 13.6: From pressure coefficient to lift, angle adjustment.

$$C_l = C_p \cdot \cos(\theta) \cdot \cos(\alpha) \tag{13.8}$$

where C_p is the pressure coefficient, C_l is the lift coefficient, θ is the element angle and α is the angle of attack.

$$\text{lift} = C_l \frac{1}{2} \rho V^2 \cdot A_{element} \tag{13.9}$$

where ρ is the air density at cruise altitude (9 [km]), V is the cruise velocity and $A_{element}$ is the surface area of the wing element.

The drag was also computed for each elemental area; however, the pressure distribution was not used as the drag on a wing is not just due to the pressure pushing back opposite to the travel direction, but also the friction of the air over the entire fuselage wetted area. The friction component is a too difficult to compute for an elemental area at this stage of the design, thus a constant total aircraft drag coefficient value of 0.02516 was obtained from the aerodynamics computations by adding the zero lift drag coefficient from Subsection 9.5.1, and the induced drag coefficient from Subsection 9.5.2.

$$\text{drag} = C_d \frac{1}{2} \rho V^2 \cdot A_{element} \tag{13.10}$$

where C_d is the drag coefficient.

The weight of the wing is also a major player when computing the wing loads. Each elemental area was assigned a portion of the total wing weight value computed by the class II iteration.

$$\text{weight} = \frac{A_{element}}{A_{tot}} \cdot W_{tot} \tag{13.11}$$

where A_{tot} is the total surface area of the wing, and W_{tot} is the total wing weight value.

The engine loads were determined using the procedure explained in Subsection 13.3.3. As for the obtention of the truss loads, the procedure is explained in Subsection 13.3.5.

Once the loads were found for each elemental area on the wing, the data was compiled as a force distribution over equidistant points along the span of the wing. This data was then arranged into the loading diagrams in Figure 13.7, Figure 13.8 and Figure 13.9; following the sign convention shown in Figure 13.1 where each axis and moment direction shown, are considered to be the positive directions.

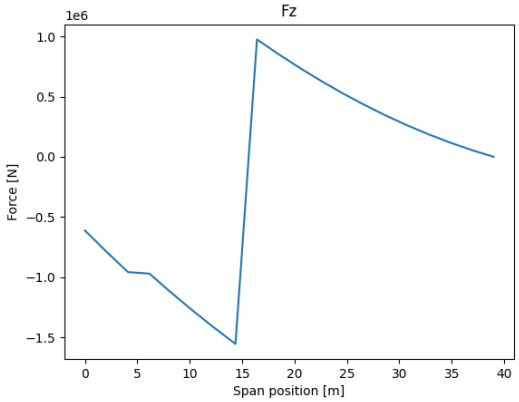

Figure 13.7: Force in the z-direction

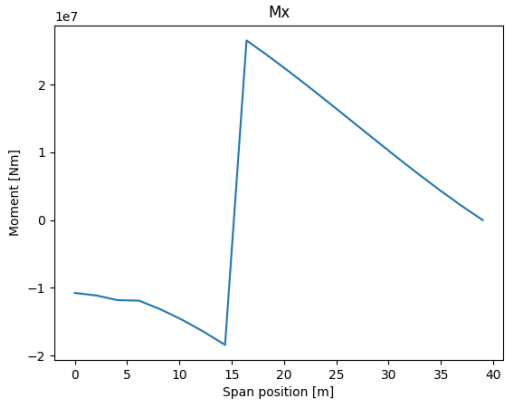

Figure 13.8: Moment in the x-direction (wing bending)

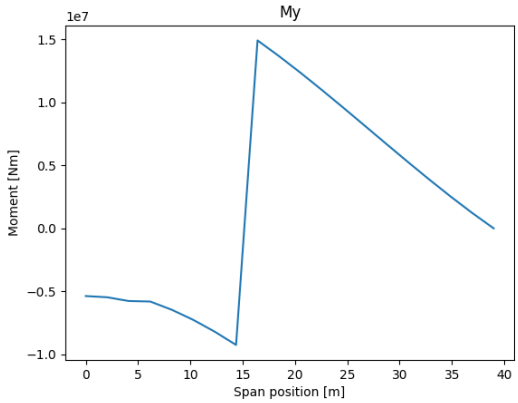

Figure 13.9: Moment in the y-direction (wing torsion)

Figure 13.10: Relevant wing loading diagrams

Using the internal loads from the loading diagrams, buckling, tensile and shear stress computations were done for 128 points along the skin of the wing-box at various positions along the span using Equation 13.12, Equation 13.13 and Equation 13.14; respectively. The crippling failure mode was not investigated as no stringers are used for the wingbox design at this stage. The stresses were computed for both an aluminium and CFRP wing-box. CFRP was chosen as the final material as explained in Section 14.1. The thickness of the wingbox was increased until all points along the wing box satisfied the material's shear, buckling and tensile strength properties. The weight of the wing-box could then be calculated, to compare each truss position and wing-box thickness combination as explained in Subsection 13.3.2.

$$\sigma_{cr} = C\frac{\pi^2 E}{12\left(1-v^2\right)}\left(\frac{t}{b}\right)^2 \tag{13.12}$$

where v is the Poisson's ratio, b is the length of the element chordwise and C is a factor that depends on the clamping conditions of the panel being analysed for buckling. In this case it is 4, assuming SSSS clamping, S meaning simply supported. Furthermore, the "E" is the elastic modulus, and t is the thickness of the wingbox.

$$\sigma_y = \frac{(M_x I_{zz} - M_z I_{xz})\, z + (M_z I_{xx} - M_x I_{xz})\, x}{I_{xx} I_{zz} - I_{xz}^2} \tag{13.13}$$

where M_i are moments about the x or z axes, I_{ii} are moments of inertia and I_{xz} is the product moment of inertia. x and z are the distances, along the x and z axes, of the element from the centroid of the wingbox.

$$\Delta q = -\frac{V_z I_{zz} - V_x I_{xz}}{I_{xx} I_{zz} - I_{xz}^2} \left[\sum_{r=1}^{n} B_r y\right] - \frac{V_x I_{xx} - V_z I_{xz}}{I_{xx} I_{zz} - I_{xz}^2} \left[\sum_{r=1}^{n} B_r x\right] + \frac{T}{2A_m} \tag{13.14}$$

Where q is the shear flow, V_i are the shear forces along the various axes, B_r are the approximated boom areas dispersed across the wingbox circumference, T is the torsional moment and A_m is the enclosed area of the wingbox cross-section.

$$\tau = \frac{q s_0 + \Delta q}{t} \tag{13.15}$$

Where τ is the shear stress, "t" being the wingbox thickness and $q s_0$ is an extra shear flow constant that has to be added to Δq, to essentially close the wingbox cross-section.

13.3.5. Truss sizing

Before the truss is evaluated structurally, its integration needs to be defined. As its main purpose is to alleviate lift loads during flight and wing weight loads during standstill, longitudinal force components should be minimised. Therefore, the truss will only be positioned orthogonally to the fuselage centre line, as can be seen in Subfigure 13.11a. This also ensures that angle θ, which is the angle of the truss as seen in Subfigure 13.11b, is as upright as possible, to transfer vertical loads with a high efficiency. Furthermore, the preferred location to integrate the truss and the fuselage is at the main landing gear fairing. This reduces overall drag as it shortens the total fairings needed and limits the length of the truss being exposed to airflow. Moreover, its further outboard attachment point keeps the truss more upright, which benefits its load-bearing efficiency. Nonetheless, all truss placement options will be evaluated to see if the main landing gear limitation affects overall wing weight.

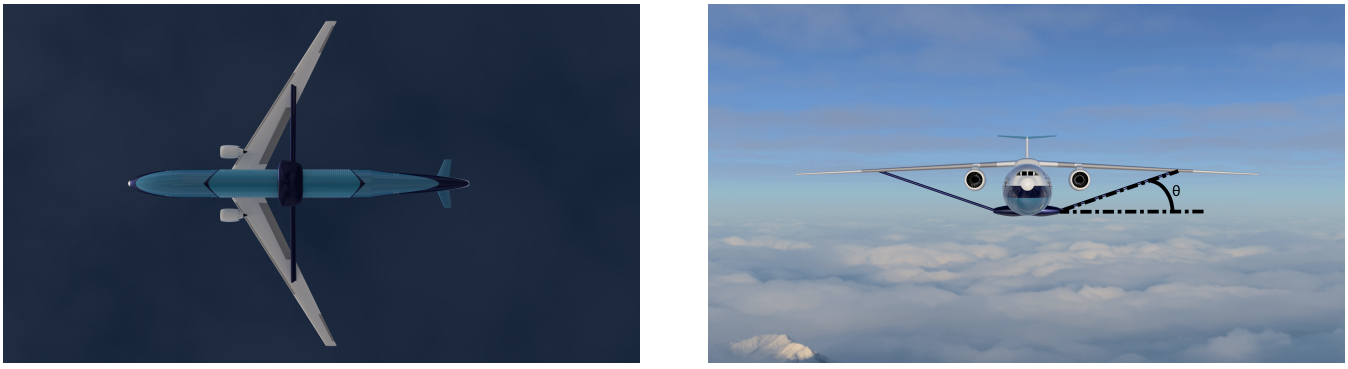

(a) WorldBus as viewed from the top.

(b) WorldBus as viewed from the front.

Figure 13.11: Two angles of the WorldBus design. Together, the orientation of the truss can clearly be made out.

The truss-braced wing structure has reaction forces in six degrees of freedom at the root of the cantilever-like wing, in addition to a reaction force through the truss. This means that the structure has seven unknown reaction forces in three-dimensional space. Therefore, the truss-braced wing is statically indeterminate to the first degree. The load on the truss only depends on the location of its joint with the wing, and the wingbox and truss stiffness. When the truss load is found, the other reaction forces can be found through three-dimensional static analysis.

With the use of theoretical knowledge from the book *Mechanics of Materials* by R.C. Hibbeler, it was determined that the *method of superposition* would be the most appropriate approach for the statically indeterminate truss-braced wing

structure [42]. This method of superposition was applied to find the reaction forces acting on the structure. Initially, a program performing a finite element method (FEM) analysis was initially constructed to calculate the reaction forces to a high accuracy. However, the limited time frame of this design stage hindered the fine-tuning and verification of the model. Instead, a simplified and existing analytical model was used from a feasibility study on the simplified structural analysis of truss-braced wings C.L. Dym and H.E. Williams [43]. The conclusion of their research was that truss buckling, truss drag, and truss weight should be taken into account in the truss sizing for a more realistic result, but that their simplified model gives a reasonable insight into what actual performance of a truss-braced wing will be.

To adapt the simplified model to the WorldBus concept, the assumption that lift and drag are a constant-distributed load over the entire wingspan had to be made. This is the assumption with the most significant impact. The actual lift and drag loads are highest at the wing root and decrease linearly towards a minimum at the tip. The assumption of constant wing loading overestimates the (truss-less) deflection of the wing at the joint. As a result, the stiffness of the truss is designed to compensate more deformation than will realistically occur. In this sense, the truss is over designed and will be adjusted accordingly in a later design stage. This will result in a slightly lower wing alleviation, causing the current wingbox to be under designed. However, because of assumption AS.WB.GEOM.2 made in the wingbox design and the included safety factor, the wing weight is not expected to exceed its current budget in a later design stage. Conversations with structures expert Calvin Rans confirmed the applicability of the approach and the reasonability of the constant load assumption [71].

The simplified analytical equations to find the load in the truss by C. Dym and H. Williams span Equation 13.16, until Equation 13.21 [43]. A visual representation of the studied load case from the case-study is shown in Figure 13.12.

$$F_t \sin\theta = \frac{-k_t w(L_s)\sin 2\theta}{1 + (k_t/k_{be})\cos 2\theta} \tag{13.16}$$

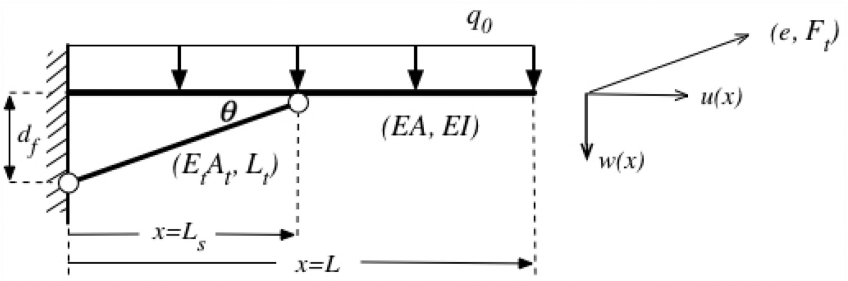

Figure 13.12: A schematic representation of the truss-braced wing being modelled as a supported cantilever beam. Material and section properties are indicated. The schematic includes a constant distributed load, q_0 [43].

In Equation 13.16, F_t is the force exerted on the truss, θ is defined as the angle between the truss and the horizontal. Furthermore, k_t is defined as Equation 13.17, where E_t, A_t, and L_t are the Young's modulus of the truss material, the cross-sectional area of the truss, and the length of the truss, respectively. In similar fashion, k_{be} is defined as Equation 13.18, where E, A, and L_s are the Young's modulus of the wingbox material, the cross-sectional area of the wingbox, and the lateral distance of the truss-wing joint along the span, respectively. Lastly, $w(L)$ is defined as Equation 13.19, with q_0 is the constant-distributed load.

$$k_t = \frac{E_t A_t}{L_t} \tag{13.17}$$

$$k_{be} = \frac{EA}{L_s} \tag{13.18}$$

$$w(L_s) = \frac{q_0 L^4}{24EI}\frac{\alpha^2(\alpha^2 - 4\alpha + 6)}{[1 + k_{\text{eff}} L_s^3/3EI]} \tag{13.19}$$

In Equation 13.19, α is defined as Equation 13.20 and k_{eff} is defined as Equation 13.21.

$$\alpha = \frac{L_s}{L} \tag{13.20}$$

$$k_{\text{eff}} = \frac{k_t \sin 2\theta}{1 + (k_t/k_{be})\cos 2\theta} \tag{13.21}$$

[71] Communication with C. Rans, dd. June 7, 9, 2023

As can be seen from Equation 13.16 up to Equation 13.21, the force in the truss is varied by altering its placement (angle θ and distance L_s), the stiffness of the truss and wingbox ($E_t A_t$, EI and EA, respectively). This confirms that the optimisation approach as explained in Subsection 13.3.2 is appropriate.

The calculation contains A as an input value that should be a product of the load exerted on the truss. Therefore, the entire calculation is iterated until it converges to a stable A.

In the final step, the truss itself is designed according to its expected load. Its weight can be calculated using the selected material and its calculated sizes. The ultimate load cases are examined for the truss performance (n=2.5 in flight and stand-still). These lead to a tensile stress and a compressive stress. To ensure a sufficient buckling performance, an estimation is done to spread the cross-sectional area over a hollow cylinder shape for an increased moment of inertia. To find this, the necessary moment of inertia (I_y) is determined using the equation for critical buckling stress (P_{cr}) Equation 13.22. To find the outer diameter (D), Equation 13.23 is used, which is derived from the equation for the cross-sectional area (A) Equation 13.24 and the equation for the moment of inertia (I_y) Equation 13.25 [44].[72] It is found that the diameter of this cylinder would approach 75 cm. However, this simplified design does not yet contain stiffeners. It is estimated that the use of stiffeners can decrease the needed cylinder diameter significantly, although this requires further research. The resulting effect in weight and drag have no impact on the current estimation, as they are assumed to be negligible at this stage.

$$P_{cr} = \frac{\pi^2 E I_y}{L^2} \tag{13.22}$$

In Equation 13.22, E and L are the Young's modulus and truss length, respectively.

$$D = \sqrt{\left(\sqrt[4]{\frac{64 I_y}{\pi}} + 16\frac{A}{\pi}\right)\frac{1}{8\sqrt{A/\pi}}} \tag{13.23}$$

In Equation 13.24 and Equation 13.25, d is the inner diameter of the hollow cylinder.

$$A = \pi(\frac{D^2}{4} - \frac{d^2}{4}) \tag{13.24}$$

$$I_y = (\frac{D^4 - d^4)\pi}{64} \tag{13.25}$$

13.3.6. Results

After weight optimising the truss and wingbox weight and truss position, the results can be seen in Table 13.7.

Table 13.7: Description of the wing results

Wing Support Type	Truss Length [m]	Weight of system [kg]	Wingbox thickness [mm]	Truss position from nose [m]
Truss-braced	17	42561	26	36
None	-	43886	27	-

The numbers presented above are the optimal numbers for a range of truss positions, ranging from the outside of the engine, to the tip of the wing. The final longitudinal position of the truss is 36.5 m from the nose. This means the truss can connect to the fuselage using the main landing gear's cowling; positioned at 34.8 m from the nose. This will increase a bit the length of the landing gear cowling but, it ensures additional unnecessary drag is not added by attaching the truss to the fuselage with its own cowling. This would add drag, reduce efficiency and increase weight of the design, which is never desirable.

Furthermore, similar computations were performed but without the truss (assuming the truss forces are zero). The weight of the wing was then calculated, and it turned out to be only 3% heavier than when the truss is included. This is not what was expected, as the entire purpose of the truss, is to alleviate loads and allow for the wing to be a lot of lighter, without adding too much drag. In this case, the weights are so similar, that including the truss in the design could be a net negative to the overall aircrafts performance.

This similarity between the truss-less wing weight and the truss-braced wing weight, can be explained with two theories. Firstly, the support loads applied on the wing by the truss are very high in magnitude. This leads to higher maximal internal loads (than if the truss was omitted) along the wing. As the wing is designed with constant thickness, the required

[72] https://www.structuralbasics.com/moment-of-inertia-formulas/#4-moment-of-inertiahollow-circular-tube-section-formula

thickness to support these high maximal loads, is relatively big. Following the assumption of constant thickness along the wingbox (done for simplicity), the wingbox is now extremely over designed.

Optimising the thickness of the wingbox to precisely support the loads of each section (and not max loads of the entire wing), would reduce this weight significantly. Ideally, the wing and truss weight would then be lower than the wing weight without the truss. This shall be analysed further, when the wingbox and truss structures have been designed in more detail. The pros and cons of using a truss-braced wing will then be much clearer.

To better this analysis, and increase the accuracy of the weight calculations, stringers and different carbon fibre orientation configurations should be considered. Currently, the wingbox assumes a 60% tape laying with fibres at $45\,°$ and 40% tape laying with fibres at $0\,°$ (from the chord to tip direction). This however, is not optimised to support shear and tension simultaneously. Thus, the orientation of the fibres could be revisited to optimally transfer the wing loads, through the wingbox. Furthermore, the weight of the wingbox could be optimised, by including stringers and variable thickness along the span, to reduce weight and tailor more accurately for loads at various span positions. It is expected that the wing weight should decrease to a value in the ballpark of $25\,000$ kg after being fully optimised.

Lastly, it is recommended to perform further analysis of the complex loading of the truss. Aside from the main compressive and tensile components, a physical truss will experience minor shear forces and bending moments through its joints. In addition, the truss weight and its aerodynamic forces will exert additional load on the truss. In addition, the truss needs to be analysed with various stiffener designs for its crippling stress. These contributions can increase the weight of the truss, but the essential stiffeners will likely decrease the size of the truss, which decreases aerodynamic forces. Furthermore, examining the statically indeterminate structure with the true varying distributed load instead of a simplified constant distributed load will concentrate the lift forces closer to the clamped root of the wing. This takes away part of the load carried by the truss, which will decrease its required size and weight.

13.4. Verification and validation

In order to verify the numerical models used to perform the preliminary design of the WorldBus structures, a number of unit tests and system tests are performed. These tests are explained in Subsection 13.4.1. An overview of these tests can be found in Table 13.8. Furthermore, plans and strategies are devised for the validation of the WorldBus structural designs. These plans and strategies are included in Subsection 13.4.2

13.4.1. Verification of numerical analysis

As the analysis of the structures has been performed numerically through programming, the viability needs to be investigated. This is done through unit tests (UT) and system tests (ST). The verification and validation of the code is explained in this section.

Fuselage program

The fuselage program was verified by manually calculating the required stiffening area and comparing these values to the output by the python program (ST.FUS.1). Manually, a stiffening area value of $2652\,\text{cm}^2$ was obtained, yielding an error of approximately 0.56%, a rounding error.

The program was verified through a unit test (UT.FUS.1). Initially, results were obtained that returned a stiffening far too large due to the fact that the units between the parameters were inconsistent. After adjustments, a more realistic value was obtained which met the expectations.

Finally, the program was optimised by changing the number of stringers such that a representative stringer area was obtained (ST.FUS.2). For the chosen material, a stiffening area was obtained. Using a conventional number of stringers, a far too large stringer cross-sectional area was obtained. To obtain a more realistic result, the number of stringers was increased which yielded a stringer cross-sectional area closer to reality.

Validation for the fuselage program is performed by comparing the results found in literature (ST.FUS.3). According to a MIT study, the fuselage weight is approximately 23% of OEW [45]. For WorldBus, the weight fraction is approximately 15%. This difference can be explained based on the detail. The study is based on reference aircraft, which have been fully designed. The WorldBus fuselage weight is currently based on skin, stringers, and frames only. Other structural elements such as the bulkheads and longerons have not been analysed. These elements would increase the structural weight of the fuselage, for which it would approach a 23% weight fraction.

Tank program

It is essential to make sure the tank design is correctly verified and validated as it makes up a significant part of the mass of the aircraft. The tank design for the main tank is split up in the calculation of the inner tank, the insulation layer and the outer tank. The tank design for the secondary tank is split up into the calculation of the inner tank and the insulation layer. A unit test is applied for each of these elements in the fuel tank design.

For each step in the verification, the results are compared to other fuel tanks (ST.TANK.1). The concept of the design is based on existing liquid hydrogen tanks. The calculated thickness of the inner tank can be compared to other pressure vessels, the outer tank can be compared to other external pressure vessels and the insulation layer can also be compared to the insulation of existing liquid hydrogen tanks.

For the main tank, the calculated thickness of the inner tank of 1.36 mm can be compared to the 1.3 mm thickness for existing liquid hydrogen tanks. [73]
For the secondary tank, the calculated thickness of 0.53 mm is considerably lower, this can be explained since the amount of fuel is also significantly lower and a spherical tank is less sensitive to buckling than a cylindrical tank. The thickness of the outer tank of 6.35 mm can not be compared, since no reference material is available for carbon fibre vacuum chambers. However, the ratio of the Young's moduli between the high alloy steel design and the CPRP has been taken and is multiplied by the thickness of the high alloy steel design to result in the CFRP thickness. This means that the design is over-designed for the buckling the outer tank is designed to resist because buckling is influenced more by the geometry of a design rather than Young's modulus.

The insulation layers for the primary tank are based on existing designs, which therefore do not have to be validated as they are commonly used in liquid hydrogen storage. The secondary tank is insulated with 26 cm thick polyurethane foam for which no reference can be found. However, when the calculation is applied to a situation in which a reference does exist (ST.TANK.1). Then, the calculated thickness becomes 2.0 cm for the polyurethane foam compared to the 2.5 cm thickness for the reference tank, which can be explained by the fact that the situation of the reference tank is of a liquid hydrogen tank designed for space vehicles [38]. This means that a difference in thickness is only logical as the situation of the reference tank is different.

Wingbox and truss program

A number of steps were taken to verify the correct functioning of the Python programs responsible for the calculations and optimisation of the weight of the wingbox and truss configuration. One part of the program runs iterations, and calculates the truss force and truss size for each one. Another part of the program is used to calculate the loads exerted on the wingbox for each iteration and find the criticality.

Both parts calculate the reaction forces and moments at the wing root in different ways. These results were compared (ST.WBTR.1) to verify our forces and moments were consistent throughout the analysis. The difference between the "x", "y" and "z" reaction forces were all within 2% of one another. The reaction moments did however differ significantly. A thorough analysis was performed to locate the issue. In the end, a number of minor bugs related to the signs of loads implemented in stress equations (for the wingbox program) were fixed. This unfortunately did not fix the disparity between the two computing methods. A slight difference is expected as the truss program assumes a constant lift load, but the current disparity is higher than expected; an error 10% to 20% is expected. Further analysis of the cause of this disparity is required.

Furthermore, for both parts of the program, every numerical input is checked for correctness and consistency (UT.WBTR.1, and each equation is checked to see if implemented correctly (UT.WBTR.2). No further issues arose from this test. A follow-up test is performed, in which every input is varied one by one to see if the end result is influenced. Once again, each input passed the test as the end result was consistently changed reasonably (UT.WBTR.3).

Thirdly, manual calculations are performed independently of the program to compare values to the output of a single iteration (UT.WBTR.4). All manual calculations match the outputs of the program, so this test is passed.

The code used in the truss optimisation part of the program can be verified using known in- and outputs from the research that originated the method by Dym and Williams [43] (ST.WBTR.1). The limited inputs used result in comparable sizing and geometry outcomes. Minor fine-tuning is performed to achieve greater alignment.

In addition, the outcome of the program can be compared to existing truss-braced wing specifications as a sanity check (ST.WBTR.3). As most research and development regarding truss-braced wing up to this point consists of conceptual design and theoretical research, the analytical results of a *NASA* research on the aero-structural performance of a composite transonic truss-braced wing by Anderson et al. is used for comparison with the program [46]. It was found that the wingbox and truss sizing for WorldBus are in the same order of magnitude as the results by the *NASA* paper. Moreover, it is also clear that the assumptions leading to an over designed result have their effect, as WorldBus thicknesses exceed those of the *NASA* research.

Lastly, a general sanity check is performed for all calculated forces, loads, output results, and their signs. The reaction forces are in the millions of Newtons, the reaction moments in the tens of millions of Newton-meters, and the loads add up to the required lift forces millions of newtons for reaction forces. Furthermore, the wingbox thickness varies in

[73] https://energies.airliquide.com/resources-planet-hydrogen/how-hydrogen-stored#:~:text=These%20tanks%20are%20a%20genuine,more%20than%201.3%20mm%20thick.

the centimetre range, and the truss cross-sectional area is in the tens of centimetres. All of these values make sense, so ST.WBTR.4 is passed.

Table 13.8: Overview of the unit tests (UT) and system tests (ST) performed on the structural calculations of WorldBus.

ID	Test description	Status
UT.FUS.1	Perform Python unit test (*unittest*)	PASSED
ST.FUS.1	Compare results with manual calculations	PASSED
ST.FUS.2	Manually test stringer number	PASSED
ST.FUS.3	Compare results with existing values	PASSED
UT.TANK.1	Compare results with existing values	PASSED
ST.TANK.1	Compare result with reference	PASSED
UT.WBTR.1	Check if inputs are correct	PASSED
UT.WBTR.2	Check if equations are correct	PASSED
UT.WBTR.3	Perform sensitivity analysis of inputs	PASSED
UT.WBTR.4	Compare results with manual calculations	PASSED
ST.WBTR.1	Compare reaction forces from two different program parts	PASSED
ST.WBTR.2	Run the code with known in- and outputs	PASSED
ST.WBTR.3	Compare results with existing values	PASSED
ST.WBTR.4	Perform general sanity check for signs, sizes, and magnitudes	PASSED

13.4.2. Plan for verification and validation of produced structures

Once the structures are being produced, they also need be subjected to verification and validation analyses. Such analyses confirm whether the parts meet the design expectation and industry standards.

Fuselage structure

Verification of the fuselage structure could be performed using a finite element analysis (FEA). Using FEA, a fast and accurate load representation of the fuselage loads and stress concentration points can be obtained. It is a very effective verification method as no physical structure have t be produced and particular load cases and conditions are able to be simulated. This will generate a more refined result.

The aircraft structure could be validated through pressure testing the fuselage to see whether the skin and structure can withstand the stresses of extreme pressurisation. This is performed by experiencing the aircraft to the differential pressure that surpasses the maximum load case such that the limits of the skin are observed. This ensures that the requirements are met and that the aircraft can be operated in load cases that are greater than the maximum load case.

The WorldBus stringers could be validated using a static load test. With a static load test, it could be validated whether the stringers are able to provide strength against the high loads they experience. It gives an indication whether the design is ready for service or that adjustments need to be made such that catastrophes are averted.

Tank structure

The tank structure design must not underperform at any moment during operation. To validate it, various tests can be performed. First of all, the tank structure can be analysed using a FEM program to identify any unnoticed flaws in the design before a prototype is constructed.

After that, an inner tank prototype should be pressurised up to its failure pressure, to see whether it exceeds the ultimate design pressure difference. Furthermore, an outer tank prototype should be tested with an interior vacuum in a pressure chamber to test its maximum pressure capability.

Secondly, the tanks should be tested for emergency scenarios, such as impact resistance, crush resistance, or penetration by foreign objects. This can be analysed by performing drop tests, press tests, and shooting shards and sharp objects at the tanks.

Lastly, the tank insulation performance should be tested. This can be performed by measuring the boil-off and temperature of a LH_2-filled tank situated in a controlled temperature environment for a prolonged time.

Wingbox and truss structure

To validate the truss-braced wing design, a number of steps should be taken. Firstly, the entire truss-braced wing assembly should be thoroughly analysed in an FEM model. This gives a more reliable result than the simplified numerical approaches used in Section 13.3. Furthermore, it can indicate specific unforeseen failure points before a full-scale prototype needs to be constructed.

Secondly, a full-scale prototype should be tested in a flexing rig up to failure. This will validate whether the wing reaches its designed ultimate load before failure. A similar flexing rig can be used to repetitively exert load on the wing for a prolonged time. This tests for wing fatigue. Inspection should be performed on the wing to locate damage in materials and the ultimate load should be tested after the number of expected loadings too.

Lastly, the truss itself can be tested separately from the wing. It is important to find its maximum load case in tension, which can be found using a large-scale axial tensile stress machine. Furthermore, its buckling needs to be investigated using a large-scale biaxial press where aerodynamic perturbations are also simulated.

13.5. Conclusion and recommendations

The majority of the fuselage structure has been designed, namely the aircraft skin, the stringers, and formers. These provide appropriate representation of the weight of the structural elements. Using the dimensions found previously, a volumetric representation is obtained which gives way to the required volume of the material. Once the material is selected, the structural mass is obtained which can be used to optimise the weight of the aircraft and size other subsystems such as the wing.

Two tanks have been designed, the main tank and a secondary 'buffer' tank. The primary, or main, tank results to be a high alloy steel inner tank to hold the liquid hydrogen. As insulation layer, MLI is placed on the outside of the inner tank along with a vacuum layer. The outer tank is designed to isolated the inner tank from the environment and keep the vacuum layer airtight. Due to weight reasons, the outer tank was designed to be as light as possible and is therefore made out of CFRP. The secondary tank is made from high alloy steel with polyurethane foam as insulation layer. Other components of the fuel system have also been taken into consideration like the venting system, heating system, maintenance, sloshing and fuel dumping.

Further analysis of the structures of WorldBus is recommended of which the focus points are listed below:

- More accurate analysis which includes other structural parts as well.
- Structural optimisation such that more weight is saved and areas requiring more reinforcement strengthened.
- Investigation in the effects of cut-outs for the doors and hatches necessary in the structure.
- More accurate load analysis such that the loads represent reality.
- Further investigation and testing of tank design using CFRP, since assumptions are used that could have a big influence on the design.
- Further investigation into possible materials for the insulation of the fuel tanks.
- Further analysis of the dumping system.

14

Materials & manufacturing

In this chapter, the production of aircraft components and integration of the assemblies and sub-assemblies for the whole aircraft is treated. A materials selection is performed in Section 14.1 for the fuselage and wing. Section 14.2 discusses the production plan that visualises an ordered timeline in which the aircraft is divided into assemblies and sub-assemblies that are manufactured and combined into the final aircraft. Manufacturing methods that could be used for materials and their specific components are described in Section 14.3.

14.1. Suitable materials

As explained in the baseline report [2], there are four main material categories used on aircraft: ceramics, metals, composites and polymers. Ceramics can handle extreme temperatures but lack the flexibility needed to be part of a wingbox structure where deflection of several meters may occur. Polymers are lightweight and flexible but do not provide the strength to carry the loads the wing supports during flight. Metals are flexible, and they can be cheap (aluminium) and/or very strong (titanium). All metals offer homogeneous strength properties, which is beneficial for designing a wingbox as various loads are applied in various directions throughout the flight. Composites on the other hand are very lightweight and extremely strong in the fibre direction.

For the structures, there is a variety of suitable materials. To optimise the selection procedure, reference aircraft have been researched, and the materials used for these will be considered.

14.1.1. Fuselage materials

For the fuselage structure, only a few materials have been considered. These are carbon fibre-reinforced polymer (CFRP), aluminium alloy AL2024-T3, and glass-reinforced laminate (GLARE). These materials have been selected as they are most commonly used in operating aircraft.

The selection process for the most suitable material depends on the following factors: weight, sustainability and cost. After progressing, the weight factor is the most important consideration due to the aircraft being quite heavy. This is followed by sustainability, due to the importance of the requirements established earlier in Section 5.2. Next is cost as the price of the material and accompanying tooling and machining costs influence the budget.

From analysis, CFRP returned as the best material choice for the fuselage and the stiffening elements. Of all the considered materials, it has the lowest density and simultaneously has better performance. Due to the reduced weight, fuel consumption is lowered, reducing the NO_x emissions, as well as improving aerodynamic efficiency. [74] Also, in assembly, it is a suitable material as additional tooling of the stringers and skin panels is reduced significantly, reducing the labour costs and additional material costs for fastening. Furthermore, composites do not experience metal fatigue, which reduces the repair requirements.

The downside is that the process of producing CFRP structures is very energy-intensive due to curing in autoclaves. Also, recycling is hard as tough polymers need to be burned off or chemically dissolved [75]. However, improvements in carbon fibre recycling are made, reducing the amount of CFRP that is sent to landfills at its end-of-life. Finally, identifying internal structural damage is harder as the material breaks less easily.

As weight is the most important factor, CFRP is the best choice. Comparatively, Al2024-T3 and GLARE would return a heavier structure, which would make the design unachievable. Improvements in regard to sustainability, caused by the use of CFRP, are required. One of the sustainability requirements is that 60% of the aircraft must be recyclable. As of now, this is hard to achieve. However, processes are being developed and improved, making the future look bright. CFRP

[74] https://simpleflying.com/aviation-waste-carbon-fibre-fate/
[75] https://simpleflying.com/aviation-waste-carbon-fibre-fate/

is the most expensive material in comparison but still offers investment return over the service period due to the reduced fuel, production, and maintenance costs.

14.1.2. Wing materials

For the wingbox and truss design, two materials were chosen, Al2024-T3 and standard unidirectional CFRP. Both have the material properties to support the applied loads on the wing, however, CFRP came out on top due to its very low density and extremely high performance when handling tension loads. This gives massive benefits in weight reduction (about 7 times lighter), but it is more expensive. Another drawback of CFRP that was considered, is the difficulty to recycle it with today's technology. Still, it is believed that the techniques like pyrolysis for the recyclability of CFRP will have improved by the time WorldBus enters production [76]. More detail on the sustainability of CFRP is discussed in Chapter 15.

14.2. Production plan

The production plan provides a guide for the manufacturing and assembly of WorldBus from its different components. The aircraft consists of various components, which are further divided into sub-components also known as assemblies and sub-assemblies.

Different reasons exist for dividing the manufacturing and assembly process of aircraft into different sections. For example, production efficiency is increased as this accommodates working on multiple smaller parts simultaneously. Besides this, the accessibility of the aircraft is increased. Lastly, producing parts made from different materials separately before joining them together reduces the complexity of manufacturing compared to combining composites and metals in the same part.

The assembly can then be divided into two different divisions, mounting and manufacturing/production divisions. Mounting divisions are where a temporary joint is placed ensuring a part is replaceable. This is advantageous as some parts need to be replaced more often than others and by using this not the whole assembly has to be replaced when a sub-assembly fails. Manufacturing or production divisions are divisions where a permanent connection is made. This is done when parts are not expected to be disassembled. The advantages of permanent joints are that the part will become lighter than with removable joints and that they are simpler and cheaper joints [47].

In Figure 14.1 one can see the production plan visualised as a flow diagram. First, the manufacturing stages can be seen for the different stations in the manufacturing line where the needed materials or parts are ordered and used for the manufacturing of the sub-assemblies. The sub-assemblies are then combined to produce the main assemblies, which are later verified by means of testing. The assemblies are then shipped and, if needed, stored before assembly. The assemblies are then moved to the assembly line and are joined into the final aircraft. The aircraft will then also be tested and verified.

As it is required to produce a total of 300 aircraft over a period of 20 years, 15 aircraft need to be produced each year. In other words, every four months, five WorldBus aircraft need to make their way through the assembly line. The assembly line shows how the aircraft is to be assembled step by step. For example: first, the fuselage sections are joined together while the fuel tanks are integrated into the aircraft, after this, the plumbing and wiring are set. After the fuselage is assembled along with the plumbing and wiring, the wing is attached to the fuselage. The empennage is then attached. Following the assembly line, as described, results in all assemblies being integrated into the final product, while testing of the aircraft is also included in the assembly line. It is estimated that once all parts are produced WorldBus can be assembled in six weeks. This is a conservative estimation as it takes a Boeing 737 about 9 days to finish its assembly line loop. As a result, at least two aircraft need to be worked on in the main assembly line at the same time. However, this is common in aircraft production so it should not provide any issues. Finally, from Figure 14.1 it is clear that the sub-assemblies will be produced in parallel, but it is difficult to find estimates on how long it will take to produce the required sub-assemblies. However, regardless of how long this production takes exactly, a similar approach can be taken for the main assembly line, creating multiple sub-assemblies at the same time. For example, if it takes 2 months to produce the main wing, 4 wings will need to be worked on in parallel at different stages of completion. By doing this, 2 main wings are completed per month.

[76] https://www-asme-org.tudelft.idm.oclc.org/topics-resources/content/unlocking-composite-carbon-fibers-for-recycling

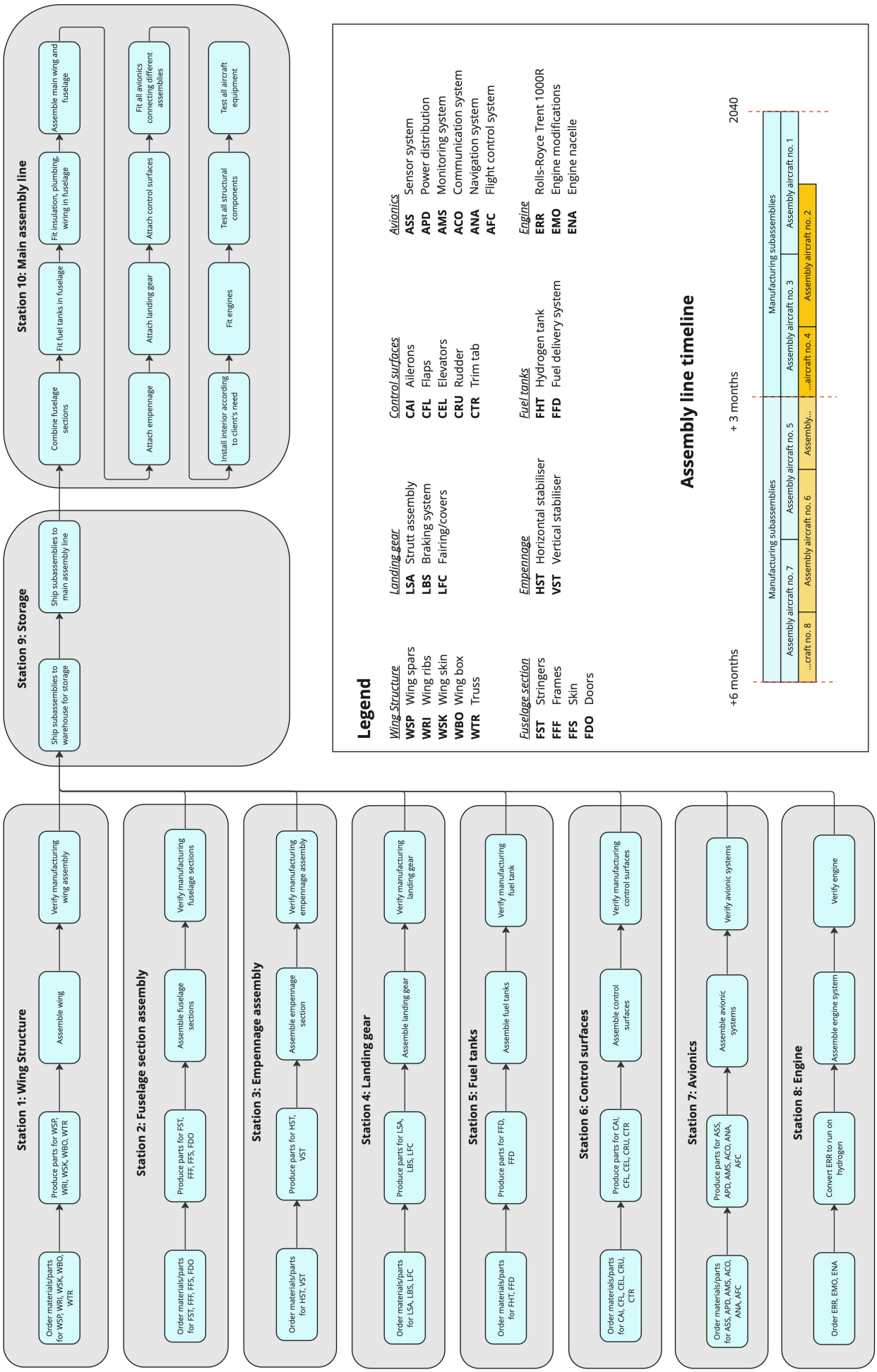

Figure 14.1: Production plan.

14.3. Manufacturing

After making the production plan, the manufacturing methods have to be decided upon. To make clear what different types of methods are conventionally used in the manufacturing of aircraft, the methods are stated and explained after which the most suitable methods can be chosen for the aircraft components.

14.3.1. Manufacturing methods

When considering manufacturing methods for the different components of the aircraft, it is important to account for factors that influence this decision. Some key considerations to ensure reliability, high-quality and cost-effective parts are:

- Design requirements: The manufacturing method should take into account factors such as geometry, tolerances and performance characteristics.
- Volume: The production volume plays its role in the selection of manufacturing method where a high production volume requires processes that keep consistent quality, that are fast and that can be automated.
- Material selection: Some manufacturing methods apply to only a limited type of material. The manufacturing method should then be compatible with the material.
- Cost: Costs for equipment, labour, tooling and materials should be evaluated and kept at a minimum where possible.
- Sustainability: Sustainability should be taken into account to limit the environmental impact of the manufacturing process.

Different manufacturing methods to choose from can be categorised as machining, liquid phase processing, forming, processes for thermoplastics and thermosets and additive manufacturing. The methods are described and discussed according to information obtained from the 'Production of Aerospace Systems' course (AE3211-II), by Jos Sinke [47].

Machining is mainly used for metals as it is the process of removing material to shape the desired part which is harder for other materials as they chip less well. Machining is also an accurate method that can easily be automated with a fast production time. The cost of machining lies in the equipment, which is very costly since the tools wear down over time. The material waste of machining is also very high.

Liquid-phase processing is liquefying a specific material such as metals or polymers, pouring or forcing it into a mould and letting it solidify. Casting can also be automated with large batch sizes. The parts do, however, still need to be treated after the casting. The process of casting is quite complex and, therefore, takes longer to finish. The equipment cost with the use of reusable moulds for casting is also pretty high. The liquid-phase processing of polymers can be performed using injection moulding, the product size is limited and very costly. On the other hand, the method is very accurate and the amount of waste is small.

Forming is essentially asserting force onto a material until it is in the desired shape. This includes metal sheet forming, bending, stretch forming and bulk forming. Sheet forming generally has a long cycle time and the soft tool, when doing rubber forming, wears out over time. The same goes for bending and stretch forming. Rubber forming can be used for large batch sizes, from 100 to 2 500 parts, but then again has a long process time. Deep drawing has larger product series in the range of 10 000-100 000 parts. These methods are, however, cost-effective. On the contrary, bulk-forming has relatively high costs. The series length is in the order of 10 000-50 000 parts and produces high-strength parts.

Processes for thermoplastics and thermosets include different methods to produce fibre-reinforced parts. Some methods considering the forming of fibre reinforces thermosets are lay-up, resin transfer moulding or autoclaving. Material costs for these processes are generally high as fibres are very expensive. Other aspects of costs are generally relatively low to moderate. Methods considering press forming of reinforced thermoplastics are not really suited for fibres. In the case of long fibres, the deformation is based on intra- and inter-ply shear mechanisms. The costs are comparable to metal forming and are significantly lower than that of other composites with thermosets. Processes for thermoplastics and thermosets generally take a long time. Product series are therefore generally short, however, the products are of very good quality and low weight.

Additive manufacturing, also referred to as 3D printing, has a high variety of applications like the conventional way where the material is extruded in a semi-liquid state and layers are printed. Other methods using lasers also exist. The different methods have very different characteristics. Some have weak mechanical properties and low accuracy but are fast and inexpensive, other methods are expensive and slow but are of high quality.

Considering the chosen materials discussed in Section 14.1, the applicable manufacturing methods can be discussed for the aircraft components.

14.3.2. Wing and fuselage

Since the fuselage and wing are made from CFRP the choice of manufacturing methods is pretty limited. The manufacturing method for the wing has been decided to be resin transfer moulding. This is based on the manufacturing method used for wind turbine blades. For which the geometric properties come close to those of an airfoil and have a larger span than the wing itself, so size should not be a problem.[77] For the fuselage, a method of lay-up is used, which is filament winding. Filament winding is where a very long continuous fibre is pulled through a resin and is wound around the fuselage. The fuselage is the rotating element while the other component moves longitudinally with respect to the aircraft. This is done in sections, which are later riveted together. Note that, as earlier mentioned, these methods of manufacturing make use of carbon fibres reinforced thermosets, not thermoplastics.

14.3.3. Truss

The truss in the truss-braced wing configuration carries the loads the wing can not carry itself because of the increased span of the wing in addition to the thinner and lighter wingbox. The truss is then primarily loaded in tension and a bit of compression. The truss has been decided to be a cylinder with an as small as possible cross-section such that the drag created by the truss is minimised. Around the truss, an airfoil is placed to create additional lift and minimise drag. The manufacturing of the truss is therefore not complex. Essentially, the truss is a reinforced conventional airfoil with the use of a cylinder for the reinforcement. Hence, the manufacturing of the truss will not be very different from that of an airfoil, only the internal structure will be slightly different because of the load-carrying cylinder. Therefore, the airfoil iah s made using the same method as the wing. The cylindrical reinforcement is made in sections using filament winding as it is a simple hollow tube with stiffeners that are later attached.

14.3.4. Fuel tanks

The fuel tanks are designed in Section 13.2. The main tank exists of a stainless steel inner tank, MLI, and a carbon fibre outer tank. The secondary fuel tank exists of a stainless steel tank and a polyurethane foam insulation layer. For the main tank, sections of the fuel tank tube can be manufactured using sheets of stainless steel that are formed using sheet forming and welded together. The sections can then again be welded together. The fuel tank heads can also be formed using sheet forming, which again have to be welded to the straight portion of the fuel tank. The secondary tank can also be formed using sheet forming, two half spheres are formed that are later joined using welding. Sheet forming can be performed for the fuel tanks as the thickness of the tanks is $1.5\,\text{mm}$ at most for the main tank and $1\,\text{mm}$ for the secondary tank, which should not pose any problems. The MLI can be joined to the inner tank using tape or velcro. The carbon fibre outer tank is made using the same method as the fuselage. Which means filament winding is used. The set-up for the carbon fibre outer tank and the fuselage is essentially also the same. For the secondary tank, the polyurethane foam can be sprayed on the stainless steel component of the secondary tank.

14.4. Conclusion and recommendations

In this chapter, materials were chosen after careful consideration, for the fuselage and wing structure. These materials resulted to be CFRP for both structures. After the materials were chosen, manufacturing methods were considered and specific manufacturing methods were decided upon that are applicable to the chosen material and structure. These methods resulted to be resin transfer moulding for the wing and the skin of the truss. Filament winding was used for the fuselage, the outer CFRP tank and the reinforcement of the truss. Note that, methods of manufacturing components using CFRP make use of carbon fibres reinforced thermosets, not thermoplastics. The inner tank of the main fuel tank and the secondary tank are both manufactured using metal sheet forming. The production plan is also treated in which a timeline is given where an ordered outline is given of all activities required to construct the aircraft from its individual components.

[77] https://www.ge.com/renewableenergy/stories/lm-castellon-wind-turbine-blade-manufacturing

15

Sustainability analysis

In this chapter, the sustainability of WorldBus will be reviewed using the framework provided in the sustainable development strategy in Chapter 5. Since the driving factor behind the development of WorldBus is the need for a sustainable way of travelling long distances, it is essential to analyse whether these goals have actually been reached. When assessing emissions during flight, a molecule's Global Warming Potential (GWP) is often used. This value showcases the warming effect a molecule has on the environment by relating the warming effect of that molecule to the equivalent amount of CO_2 required for the same warming effect. This considers both the type of molecule and how long the molecule stays in the atmosphere. The chapter is structured by evaluating the sustainability characteristics as established in Chapter 5 and verifying that they meet the corresponding requirement. First, production and manufacturing will be discussed, which will include emissions, waste generation and recyclability. Then, the service life will be considered. This is followed by the emissions corresponding to operations, including the emissions during fuel production. Lastly, an investigation of the aircraft's noise emissions will be performed.

15.1. Production & manufacturing

When considering production and manufacturing, the material used plays a significant role. In most parts of the aircraft, Carbon Fibre Reinforced Polymer (CFRP) is the primary material used as discussed in Chapter 13. This choice for CFRP was made in order to considerably reduce the weight of the aircraft to increase the range in order to meet the range requirement. However, from a sustainability aspect, CFRP has some major disadvantages. In the following sections, these will be discussed with regard to manufacturing and production, repair, recyclability and waste.

15.1.1. Production & manufacturing

Compared to current long-haul aircraft, the WorldBus has two major factors that could increase the emissions during production and manufacturing: the earlier mentioned substantial use of CFRP and the presence of two liquid hydrogen tanks. Both factors will be discussed hereafter.

The production of carbon fibre consumes almost 14 times more energy in its creation than steel. Greenhouse gas (GHG) emissions resulting from conventionally producing carbon fibre are respectively $24.83\,CO_2$eq per kg compared to the $2.75\,CO_2$eq per kg for steel, which is roughly 9 times more. While per kg of aluminium, almost three times the amount of CO_2eq is generated compared to steel, or approximately three times less than CFRP [48].[78] Thus, the significant energy-intensive production of CFRP contributes considerably to the total emissions of the production of the aircraft. It should be noted that on the one hand, for the same thickness, aluminium has a strength of about $500\,kN$ compared to carbon fibre which can have up to $1600\,kN$ of strength, which means CFRP is 3.2 times stronger than aluminium for the same thickness. Note that since the comparison is done with equal thickness, the mass of CFRP would be almost two times lower without compromising strength or rigidity.[79] On the other hand, for CFRP, 30% of the material is wasted in production [49]. Thus, in practice, the use of CFRP would result in approximately 22% more emissions compared to aluminium. Since 22% more emissions compared to aluminium fall below the 43% emissions from the requirement, the requirement is met. However, it is still important to consider methods to minimise the emissions from this environmentally harmful composite.

The most obvious solution would be to use recycled parts of decommissioned aircraft in the manufacturing process. Implementing carbon fibre components from other types of aircraft might not be possible since the design parameters would differ too much, as WorldBus is a unique design. Components from other aircraft interiors such as seats, plastics and lighting can be reused or recycled and integrated into the WorldBus design since essentially all interiors can be recycled

[79] https://smicomposites.com/carbon-fiber-vs-aluminum-why-theyre-used-and-how-they-differ/#:~:text=Aluminum%20has%20a%20strength%20of,to%201600%20kilonewtons%20of%20strength.

nowadays.[80] Furthermore, it is also possible to reuse parts from WorldBus aircraft that are manufactured at an earlier stage and are not operational any longer. This might take some time in the production process as the lifespan is decided to be 20 years. Furthermore, in the production of the parts, recycled CFRP can be used which will reduce emissions as well. This option will be further discussed in Subsection 15.1.3.

Another difference WorldBus has compared to current long-haul aircraft is the presence of two large hydrogen tanks. The primary tank consists of steel, CFRP, and multi-layer insulation of mylar and dacron. The secondary is made up of steel and polyurethane foam. Both tanks were already discussed in Chapter 13. Steel has relatively low production emissions compared to CFRP. The emissions following from the production of polyurethane are approximately $2.86\,CO_2$eq per kg [50]. For mylar, this is approximately $3.64\,CO_2$eq per kg[81] and for dacron this is approximately $2.40\,CO_2$eq per kg [51]. As mylar, dacron, and polyurethane collectively constitute less than 0.05% of the total aircraft weight and exhibit comparable CO2 emissions to steel during production, it is not anticipated that any emission disparities will arise from the tanks in comparison to similar long-haul aircraft.

Lastly, it should be noted that innovative development processes to reduce the carbon footprint of CFRP production are currently under development. An advanced method using fire-resistant fibres already yielded a reduction of 20% in emissions compared to the conventional method [48].

Considering all factors, the production and manufacturing process of WorldBus will result in larger CO2 emissions due to its extensive use of CFRP. However, implementing provided solutions and advancements in the CFPR production processes, a maximum increase of 43% in emissions compared to similar long-haul aircraft is assumed to be achievable at the current design phase. To illustrate this, if by 2040 all waste can be reused and a production method with 20% fewer emissions becomes feasible, the emissions increase could already be reduced to 44% instead of the initially estimated 134%. These assumptions will need to be constantly verified in each future design phase. Additionally, it is important to note that the estimation of a 44% increase in emissions does not yet account for the potential reduction in emissions when reusing parts.

15.1.2. Repair

Currently, the reparation of CFRP parts is limited to secondary structures in the aircraft. Primary structures, which are critical components of the aircraft, need to be designed such that they can endure the entire service life of the aircraft without requiring reparation. To achieve this, primary structures will be over-designed using safety factors to ensure their reliability. A disadvantage of this approach is the increased production costs and added weight to the aircraft. However, an advantage is the cost savings by avoiding costly repairs or replacements during its service life.

The repair of secondary parts can be done in service or on the ground if repair facilities are not readily available. It is important for the repair to be done quickly and effectively since a grounded aircraft significantly cuts down revenues. Several methods already exist for the repair of CFRP, of which the most common method is patching. Patching can be applied in service as a permanent or temporary solution and is a simple and low-cost technique. However, patching is bulky and of limited strength. Another disadvantage is the addition of weight, which is undesirable, especially when done repeatedly. Other methods results in better quality for the repaired CFRP, but are necessary to be performed in good workshop conditions and with trained staff. These methods take longer and are more costly, resulting in the aircraft being inoperable for a longer period of time [52].

15.1.3. End-of-life

To increase the sustainability of an aircraft and ensure it does not end up deteriorating at an aircraft grave, an aircraft should, once its end-of-life is reached, be recycled as much as possible. Especially since the aircraft is designed to be operable for a 20-year lifespan while carbon fibre typically could last for over 50 years.[82]

Airbus states that, as of today, 92% of an aircraft's total weight can be recycled. For the engine, this percentage can go up to 99%. [83] However, this is not always an achievable percentage for composites. Much research is currently being performed in Europe related to the recycling of aircraft composite. The largest project investigating the recycling of aircraft composites is called 'Holistic process for the cost-effective and sustainable management of End of Life of Aircraft Composite Structures' (HELACS). This process uses high water pressure in order to selectively cut composite into suitable dimensions for recycling. [84] Using this process the recycling capacity of composite aircraft components increases by 40%.

As stated in research by F. Meng [53], Airbus aims to distribute 95% of all CFRP material from the aircraft into the recycling

[80] https://www.dwtc.com/en/industry-insights/coming-home-how-aircraft-interiors-are-being-recycled/#:~:text=Our%20studies%20have%20proven%20that,are%20usually%20no%20identifying%20stamps.

[81] https://europe.dupontteijinfilms.com/media/2624/dtf-brochure-photovoltaics.pdf

[82] https://www.fairmat.tech/blog/is-carbon-fiber-recyclable/

[83] https://aircraft.airbus.com/en/newsroom/news/2022-11-end-of-life-reusing-recycling-rethinking

[84] https://www.aitiip.com/helacs.html

industry. A similar target could be set for WorldBus. However, as of today, only 40% of this material is recyclable. This would not meet the to-be-achieved 60% total recyclability as stated in the requirements from Section 5.2. As the global demand for CFRP is expected to grow at 8.7% each year, it is expected that recycling processes will also further improve. Since WorldBus is expected to launch in 2040, the first WorldBus aircraft to undergo recycling would likely be around 2060 or later. This provides an additional 37 years for recycling technologies to advance. Currently, there are new chemical processes under development of which Yu et al. reported a near 100% recyclability of CFRP [54]. Additionally, a two-step thermolysis has yielded 93.47% recovery of carbon fibre [49]. Therefore, it can be safely assumed that by 2060 a target of 60% recyclability of the aircraft mass would be achievable, taking into account the advancements expected in recycling technologies.

15.1.4. Waste

In the production and manufacturing process of an aircraft, it is important to consider waste for two main reasons. First of all, waste in any form like material, energy, or man-hour, adds unnecessary costs to the production process. Secondly, the generated waste will contribute to the amount of emissions during the production and manufacturing process. Both aspects of finance and emissions have already been limited by two requirements. In other words, as long as the generated waste does not lead to too high costs or too high emissions, the generated waste does not provide any further problems besides efficiency considerations. Therefore, a requirement limiting the amount of waste has been deleted from the requirement since it is already indirectly implemented in the cost and emissions requirements.

Although, it is still important to adopt solutions to minimise the generated waste and improve the efficiency of the design process. For this, two solutions will be provided. First of all, by trimming, shaping or possible manufacturing defects, material waste could be generated in the production process. Optimised cutting techniques or improved production processes can limit this amount of waste. Furthermore, the wasted material could also be recycled in order to be used again in the production process. Secondly, in the production process, the concept of lean manufacturing should be adopted. In this concept, waste will continuously be eliminated during the production process. It focuses on eight types of waste: overproduction, waiting time, work in progress, processing waste, transportation, movement, rework, and underutilising people

15.2. Service life

From the market analysis, a service life of 20 years was assumed. In this section, this value will be further assessed.

To begin, it is important to put the required service life of 20 years in perspective with current passenger aircraft. For several of its aircraft, Boeing has a minimum service life design objective of 20 years [85]. Furthermore, Airbus aims to design aircraft that can spend 30 plus years in operational service [86]. Thus, it can be said that current requirement is not different from already existing aircraft and no additional innovations are needed at first sight.

In addition, it is necessary to identify the factors that impact the service life. First of all, material fatigue is crucial for service life. Next to this, maintenance is important to ensure a long lifetime. Lastly, several aspects during the operation of the aircraft also influence the aircraft's service life. These aspects include the number of flights the aircraft performs, the environment in which the aircraft operates and possible accidents. At this point of the design, it can be assumed that the last two factors are comparable to existing aircraft. Moreover, due to the long-range characteristic, WorldBus will have fewer take-offs and landings compared to current aircraft that fly shorter ranges. This will even benefit the service life. Thus, no significant negative deviations in service life could originate from those factors. However, the first factor of material fatigue has different characteristics as will be discussed hereafter.

WorldBus is mostly made of CFRP, which may present challenges in terms of repairability compared to other materials. This limitation of repairability negatively impacts the service life. However, CFRP does offer the advantage of having a high fatigue strength compared to aluminium, which positively impacts the service life. In the design, safety factors are used to ensure safety but this also reduces the chances that repair is needed during the lifetime of WorldBus. Taking that into consideration, it can safely be assumed that the use of CFRP does not negatively impact the service life of WorldBus.

Lastly, it is important to note that it is essential to perform real-world testing in a further design phase. This way it can be ensured that aircraft components can endure the temperature cycles and load cycles over the span of 20 years. Specific attention should be drawn to the testing of the tank and plumbing system, since those technologies for hydrogen fuel have low precedent in existing aircraft.

[85] https://www.boeing.com/commercial/aeromagazine/aero_07/corrosn_sb_table01.html
[86] https://www.airbus.com/en/products-services/commercial-aircraft/the-life-cycle-of-an-aircraft/operating-life

15.3. Operations

In this section, the emissions during operation of WorldBus will be discussed. This includes the emissions during the production of liquid hydrogen, and the combustion of liquid hydrogen during the flight.

15.3.1. Emissions for producing LH_2

Critical to WorldBus being an environmentally friendly aircraft is that the fuel it uses is also produced sustainably. Otherwise, it is the equivalent of running an electric car on power generated by a coal plant. While fewer/no emissions are produced during the operation of the system, the emissions are simply displaced to a different phase in the energy cycle. While green hydrogen is sustainable, as it is made using water and renewable energy, it does pose some challenges regarding availability. Currently, about 69 Mt of hydrogen is produced per year using dedicated processes. However, less than 0.7% of this amount is produced using renewable energy sources or produced using carbon capture and storage. So, every year only about 0.5 Mt of green and blue hydrogen is produced [55]. As stated, this could prove to be a problem for WorldBus. After the production phase is completed, up to 300 aircraft could be in operation. With every aircraft performing 4000 flight hours per year, it is estimated that about 2.8 Mt of liquid hydrogen is required each year. This is more than 5 times higher than what is produced globally by dedicated hydrogen facilities.

But for WorldBus to use grey hydrogen is also not acceptable. The main greenhouse gas that is responsible for the GWP of hydrogen production is CO_2. The annual production of hydrogen emits 830 million tonnes of CO_2, the equivalent of the CO_2 emissions of Indonesia and the United Kingdom combined [55]. Comparing this to the fact that annually 69 Mt of hydrogen is produced worldwide, it can be concluded that for every kg of grey hydrogen production, about 12 kg of CO_2 is produced [55]. Using the fact that WorldBus requires approximately 45 mt of liquid hydrogen per flight, this means that a WorldBus operating on grey hydrogen will emit the equivalent of 568 mt of CO_2 per flight. Or, 144 g of CO_2 per passenger per km, and this does not even take into account the GWP of water after the hydrogen fuel has been combusted in the engine. For comparison, a Boeing 787-9 emits about 3.5 g of CO_2 per passenger per km when only taking the emissions of kerosene production and transportation into account, but not the emissions during operation[56].

So, clearly, grey hydrogen is not a sustainable solution and performs significantly worse when it comes to carbon emissions compared to existing kerosene-powered aircraft from a production standpoint. A crucial difference, however, is that WorldBus in theory can fly on a low-emission fuel. Flying on green hydrogen could result in a twentyfold reduction of greenhouse gas emissions compared to grey hydrogen, with green hydrogen only producing 0.7 kg of CO_2 per kg of hydrogen production [57]. This means that the carbon emissions per passenger per km decrease to just 8.4 g for hydrogen production.

Fortunately, it is expected that the production of green hydrogen will increase to 50 Mt by 2040, and 300 Mt per year, by the year 2070 [58]. Since only 15 aircraft will be produced per year, and the first delivery is not expected until 2040, there should be enough green liquid hydrogen available for WorldBus. But it is important to note that the feasibility of WorldBus is largely dependent on these predictions being true as grey hydrogen is not a viable alternative.

15.3.2. Emissions per passenger km

Assuming that by 2040, the production of green hydrogen will have increased enough for WorldBus, an estimation of the emissions during the flight can be made. The gases that contribute most to the heating of the planet are CO_2, H_2O and NO_X. For hydrogen, the emissions of CO_2 are naturally zero and as a result, the emissions per kg are also zero. Compare this to kerosene, where per kg of burned kerosene approximately 3.146 kg of CO_2 is emitted.[87] Then, the amount of emitted H_2O is higher for liquid hydrogen than for kerosene. This can be seen by looking at the molecular formulas for both molecules. Kerosene is made up of different length hydrocarbons, ranging between $C_{12}H_{26}$ and $C_{15}H_{32}$. For these molecules, two hydrogen atoms will react with oxygen from the air to form H_2O. Using mass ratios, it can be determined that for every kg of kerosene, approximately 1.37 kg of H_2O is formed. Hydrogen is simply H_2 and will react with oxygen to also form H_2O. Using mass ratios again, it is found that for every kg of hydrogen, 9 kg of water is formed. Finally, when it comes to the emissions of NO_X, it is more difficult to find concrete values. The air-to-fuel ratio inside the combustion chamber influences how much nitrous oxides are formed. However, from a study done in 2022, these can be estimated to be about 17.94 g per kg of kerosene, and 3.7 g per kg of hydrogen [59]

This, however, does not show the full picture yet. The metric of interest is the GWP, or, how much heat the molecule will absorb in the atmosphere. Water, for instance, becomes a more potent greenhouse gas when emitted high in the atmosphere. This is also the reason WorldBus will fly at an altitude of 9 km instead of 12 km. Flying at lower altitudes does, however, increase the overall fuel consumption since the aircraft experiences more drag. The benefits from the emissions for flying at 9 km instead of 12 km outweighs this difference in fuel consumption greatly. The effective GWP for flying at 12 km equals 4.04 while the effective GWP for flying at 9 km equals 0.24. Again, this is because of the water absorbed into

[87] https://english.rvo.nl/sites/default/files/2022/05/The%20Netherlands%20list%20of%20fuels%20and%20standard%20CO2%20emission%20factors%20January%202022.pdf

the atmosphere at higher altitudes. For flying at lower altitudes, an increase in the amount of needed fuel of 60 kN is observed. This would result in a decrease in effective GWP of around 150 000 when flying at 9 km compared to 12 km which is a 93% decrease in effective GWP. The GWP for burning hydrogen and kerosene at different altitudes is shown in Figure 15.1.

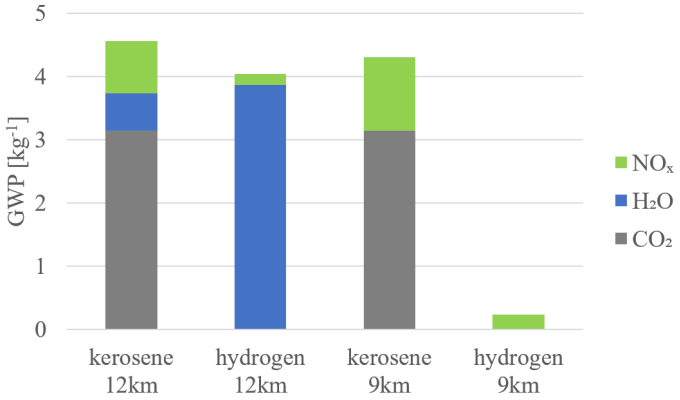

Figure 15.1: GWP of hydrogen and kerosene at different altitudes.

From here, it can easily be deduced that WorldBus emissions during flight have a GWP of 2.86 g per passenger per km. The CO_2 emissions per passenger per km for a Boeing 787-9 are known to be approximately 71.5 g.[88] However, the 787 engine also emits nitrous oxides and water. The carbon emissions are 69% of kerosene's GWP when burning at 12 km. Moreover, as stated earlier, the production of kerosene also emits greenhouse gases. So, a more accurate estimation for the GWP of the 787's emissions is 107 g per passenger per km. Then, for WorldBus, taking into account the greenhouse gases that are emitted during the production of green hydrogen and the GWP of the emissions during operation, a final per passenger per km value of 11.2 g is found for the equivalent carbon emissions. This means WorldBus is able to provide a reduction in emissions of 90% per passenger per km during the flight compared to a Boeing 787-9.

It is important to note that this reduction could be improved even further if the production of green hydrogen becomes more efficient. Currently, only 25% of the per kilometre per passenger emissions for hydrogen are produced during the flight, the remaining 75% is due to the production of hydrogen. If hydrogen were to have a similar footprint as the production of kerosene, WorldBus could attain a 94% reduction. Moreover, if the production of hydrogen and kerosene are not taken into account, WorldBus has a 97% lower impact. Since WorldBus only needs to be operational by 2040, there is still room for hydrogen production to improve and become more efficient and, hence a 90% reduction is considered to be a worst-case scenario. So, a 97% reduction in emissions during operation means that WorldBus meets the sustainability requirement set in Chapter 5 to reduce emissions by 97% compared to a Boeing 787-9. While this is of course dependent on the development of green hydrogen production, it does show that this requirement can be met without changing the design of WorldBus itself.

15.4. Noise emissions

Another of the sustainability requirements of WorldBus is that the noise emissions are reduced compared to current aircrafts. In this section, the regulations around noise emissions for transport aircraft are showcased, and a preliminary analysis is done for the noise emissions of WorldBus. This analysis is split into two parts: a noise analysis of the airframe, and a noise analysis of the engines. It should be noted that due to time constraints and this project's scope, it is impossible to do a complete, accurate analysis of WorldBus' noise production. However, an overview of the regulations and a methodology to analyse the noise emissions will be given. With this, more research and a more elaborate analysis can be performed in the future.

15.4.1. Regulations

As stated, WorldBus aims to not only be more sustainable, but also a quieter aircraft so that people living around airports are disturbed less. One of the requirements that was set by the WorldBus team was to decrease the cumulative noise emissions of WorldBus by 5 dB compared to a Boeing 787-9 This requirement can be made more concrete by looking at how and where noise is measured. First of all, an important metric within noise regulations is the effective-perceived noise levels (EPNdB). This quantifies how annoying a sound is for a human being by looking at the spectral shape of the sound,

[88] https://www.iba.aero/insight/aviation-carbon-emissions-case-study-qatar-airways/

the intensity, tonal content and duration, measured in dB.[89] EPNdB can be calculated with Equation 15.1.[90]

$$\text{EPNdB} = \text{PNL}_{\text{max}} + 10 \log \left(\frac{t_{10}}{20} \right) + F(\text{dB}) \tag{15.1}$$

Where PNL_{max} is the maximum noise level during a flyover, t_{10} the duration of the flyover within 10 dB of the peak loudness, and $F(S)$ a corrective function to take into account that pure tones are perceived as more annoying. Then, there are three certification reference points where aircraft noise is measured: lateral, approach, and flyover. These measurement points are shown in Figure 15.2. Figure 15.3 gives the noise standard for aircraft as a function of the MTOW. Since WorldBus is a jet-driven aircraft it needs to adhere to Chapter 14, meaning that a maximum cumulative EPNdB of 295 dB is permitted.[91]

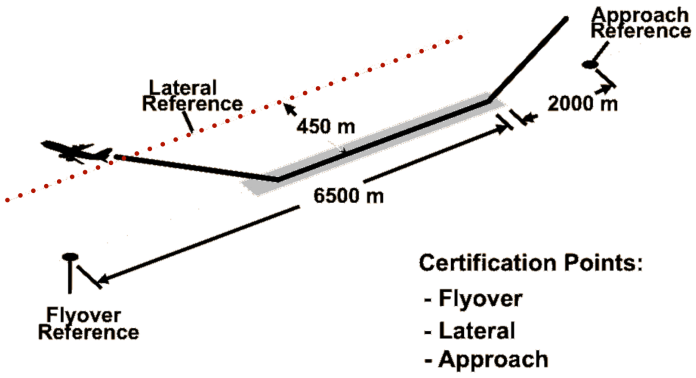

Figure 15.2: Certification reference points for measuring noise levels.[90]

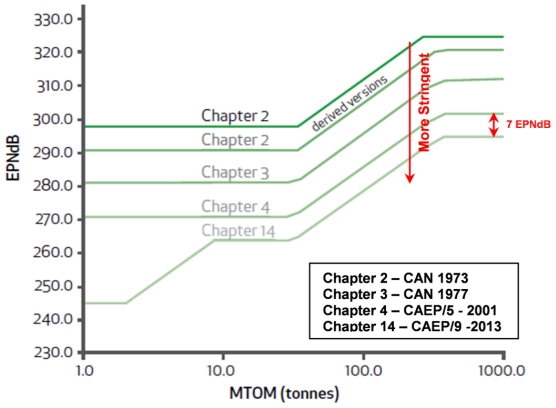

Figure 15.3: ICAO noise standard for aircraft.[91]

Besides needing to meet these regulations, WorldBus is also aiming to be more quiet than comparable aircraft. EASA provides over 20000 noise measurements for a variety of transport aircraft.[92] The average noise levels for four different aircraft are shown in Table 15.1.

Table 15.1: Noise levels of reference aircraft.

Aircraft	Engine	Noise levels [EPNdB]			
		Lateral	Flyover	Approach	Cumulative
Boeing 787-9	Rolls-Royce Trent 1000	91.5	84.9	96.0	272.5
Boeing 777-300ER	General Electric GE90-115B	99.1	90.3	100.5	285.6
Airbus A350-1000	Rolls-Royce Trent XWB-97	94.9	88.2	96.9	290.0
Airbus A380-800	Engine Alliance GP7270	94.6	93.3	97.7	280.0

So, as given in Chapter 5, the team aims to have the cumulative noise levels of WorldBus to be 5.0 dB lower than the Boeing 787-9.

15.4.2. Methodology

One method to model aircraft noise emissions is through the NASA-developed aircraft noise prediction program (ANOPP) method. In this method, the different components of the aircraft that produce noise are modelled separately and can later be combined to give the total noise production [60]. The main contributors to aircraft noise for the engine and the fuselage are shown in Figure 15.4.[93]

[89] https://www.icao.int/Meetings/EnvironmentalWorkshops/Documents/Noise-Certification-Workshop-2006/Depitre_4.pdf
[90] https://www.sfu.ca/sonic-studio-webdav/handbook/Effective_Perceived_Noise_.html
[91] https://www.icao.int/environmental-protection/Pages/Reduction-of-Noise-at-Source.aspx
[92] https://www.easa.europa.eu/en/downloads/16974/en
[93] https://www.aerosociety.com/media/4658/1-progress-in-engine-noise-reductions.pdf

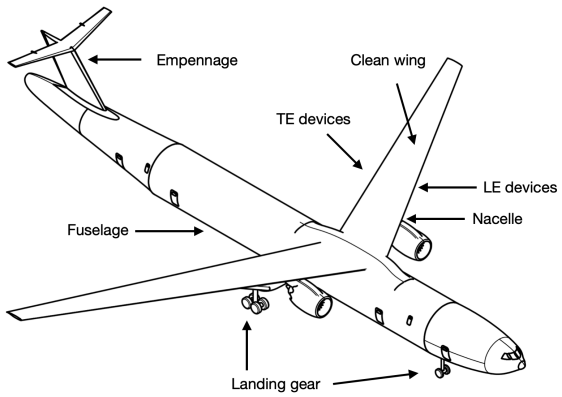

(a) Main airframe components that contribute to noise.

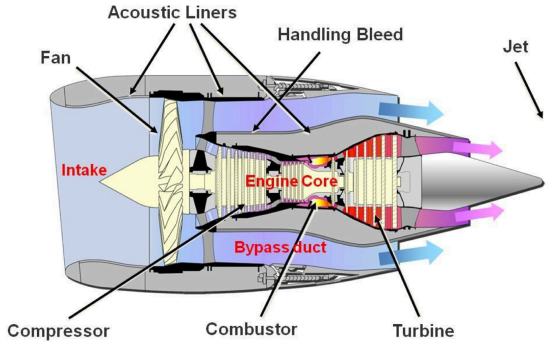

(b) Engine components that contribute to noise.

Figure 15.4

At the core of this analysis lies the sound pressure level (SPL), given in Equation 15.2. This measure indicates how load a sound is in decibels, based on the effective pressure. Each component p_e^2 is then modelled with Equation 15.3. Where p_{e_0} is the reference effective pressure and is equal to $2.5 \cdot 10^{-5}$ N/m^2.

$$\text{SPL} = 10 \log \left(\frac{p_e^2}{p_{e_0}^2} \right) \tag{15.2}$$

$$p_e^2(f, \theta, \phi) = \frac{\rho_\infty c P D(\theta, \phi) F(S)}{4\pi r^2 (1 - M \cos\theta)^4} \tag{15.3}$$

More precisely, p_e is the effective pressure in Pa in different 1/3-octave bands, where f is the centre of each respective 1/3-octave band. Other input variables for the effective pressure are θ and ϕ, which are the polar and azimuthal directivity angles, respectively. These angles are shown in Figure 15.5. Then, ρ_∞ is the density, c the speed of sound in air, P a power function, $D(\theta, \phi)$ a dimensionless directivity function, and $F(S)$ the spectral function. In the denominator, one can recognise $\frac{1}{4\pi r^2}$, or the spherical spreading fact and also the factor $\frac{1}{(M \cos\theta)^4}$. This is to compensate for the forward motion of the aircraft.

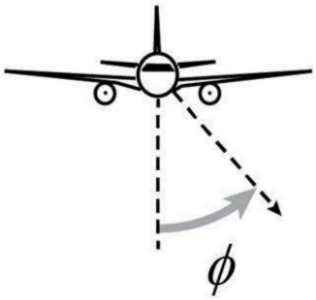

(a) Azimuthal directivity angle ϕ.

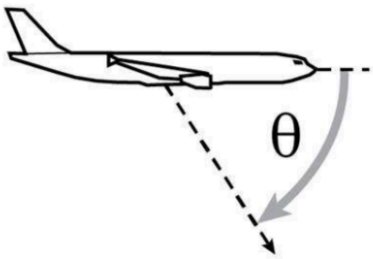

(b) Polar directivity angle θ.

Figure 15.5: Azimuthal and polar directivity angles [60].

Airframe components

For the airframe components, the power P and the Strouhal number S can be calculated through Equation 15.4 and Equation 15.5.

$$P = K M^a G (p_\infty c^3 b_w^2) \tag{15.4}$$

$$S = \frac{f L (1 - M \cos\theta)}{M c} \tag{15.5}$$

Here, K and a are dimensionless constants, G is a dimensionless geometry function and b_w is the total wingspan for Equation 15.4. For Equation 15.5, L is the length scale characteristic for a particular airframe. In Table 15.2, values for G, L, K and a are given for different aircraft components. These can be used as inputs for Equation 15.4.

Table 15.2: Input parameters for airframe power calculation.

Airframe noise source	G	L	K	a
Clean wing	$0.37\frac{Aw}{b_w^2}\left(\frac{\rho_\infty M_\infty c_\infty A_w}{\mu_\infty b_w}\right)^{-0.2}$	$\mathrm{Gb_w}$	$4.464 \cdot 10^{-5}$	5
Leading edge slats	Same as for wing			
Trailing edge flaps	$\frac{A_f}{b_w^2}\sin^2(\delta_f)$	$\frac{A_f}{b_f}$	$2.787 \cdot 10^{-4}$	6
Landing gear	$n\left(\frac{d_{\text{wheel}}}{b_w}\right)^2$	d_{wheel}	$4.349 \cdot 10^{-4}$	6

Then, the spectral and directivity functions for the corresponding noise sources in Table 15.2 are given in Equation 15.6 through Equation 15.13.

Clean wing

$$F(S) = 0.613(10S)^4\left((10S)^{1.5} + 0.5\right)^{-4} \tag{15.6}$$

$$D(\theta, \phi) = 4\cos^2(\phi)\cos^2(\theta/2) \tag{15.7}$$

Slats

$$F(S) = 0.613(10S)^4\left((10S)^{1.5} + 0.5\right)^{-4} + 0.613(2.19S)^4\left((2.19S)^{1.5} + 0.5\right)^{-4} \tag{15.8}$$

$$D(\theta, \phi) = 4\cos^2(\phi)\cos^2(\theta/2) \tag{15.9}$$

Flaps

$$\begin{aligned} F(S) = 0.613(10S)^4\left((10S)^{1.5} + 0.5\right)^{-4} \quad &\text{for } S < 2 \\ F(S) = 0.1406S^{-0.55} \quad &\text{for } 2 \leq S \leq 2 \\ F(S) = 216.49S^{-3} \quad &\text{for} S > 20 \end{aligned} \tag{15.10}$$

$$D(\theta, \phi) = 3(\sin\delta_f \cos(\theta + \cos\delta_f \sin\theta\cos\phi)^2 \tag{15.11}$$

Main landing gear

$$F(S) = 13.59S^2(S^2 + 12.5)^{-2.25} \tag{15.12}$$

$$D(\theta, \phi) = \frac{3}{2}\sin^2\theta \tag{15.13}$$

With this method, an estimation can be made for the noise produced by the airframe of the aircraft. However, it should be noted that this model does not provide estimations for the acoustic effects of the fuselage, empennage, truss, or the podded landing gear.

Engine

As stated in Chapter 10, WorldBus will be using two modified Rolls-Royce Trent 1000R engines for its propulsion system. The Trent 1000R is already one of the quietest engines on the market, having noise levels more than 15 dB lower than the Boeing 777's Trent 700.[94] While it was not possible to find exact figures on how much noise is produced by these engines, it should be possible to verify this information from Rolls-Royce at a later point in the design. However, since the engine is already being modified to run on hydrogen, this also provides the team with an opportunity to make the engine even more quiet. A number of key points where the emitted noise can be reduced include adding a variable area nozzle, optimised inlet geometries and lip liners and optimising the fan speed and jet velocity cycles.[95]

[94] See footnote 93
[95] See footnote 93

15.4.3. Truss-braced vs conventional aircraft

Finally, for the noise analysis some further research has already been done. A team of researchers at NASA's Langley Research Center have compared the noise emissions of a Transonic Truss-Braced Wing (TTBW) and a conventional configuration (CC) [61]. While the aircraft used for the analyses are smaller than WorldBus (e.g., the wingspan is 23.7 m lower), the relative noise performance of the TTBW and the CC can still of interest as it shows what could be expected for WorldBus compared to a similar sized conventional transport aircraft. A big difference between the TTBW and the CC is the geometry and width of the wing. This can be seen in Figure 15.6.

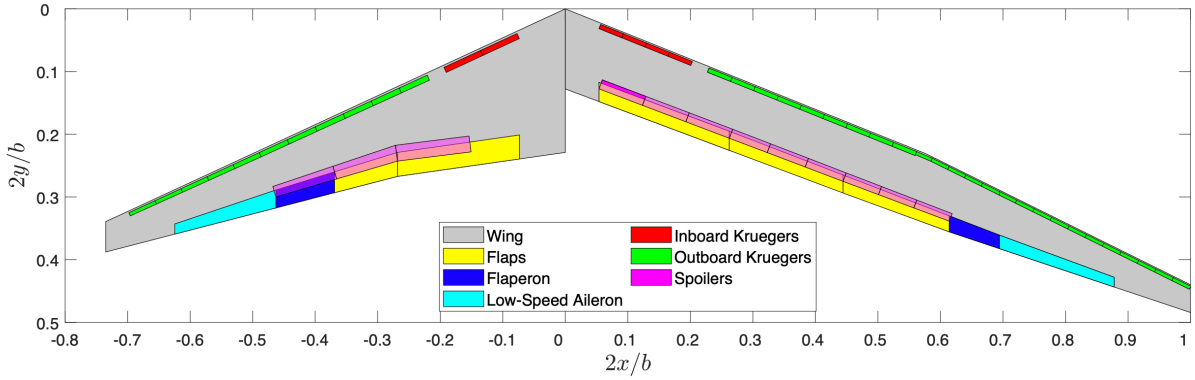

Figure 15.6: Layout for the CC versus the TTBW [61].

Then, using the FLOPS method, the rest of the aircraft is sized, weights are estimated and the thrust of the engines is established. Similar to the method described in Subsection 15.4.2, the researchers use the ANOPP method to determine the noise contributions of all the different aircraft components. Then, the researchers also take into account the so-called propulsion airframe aeroacoustic (PAA) effects. This is the interaction of the noise produced by the engines and the airframe. Depending on how this noise is reflected, PAA effects can be beneficial or detrimental to the noise produced by the aircraft. A positive value for PAA effects indicates that the interaction between the engine noise and the fuselage is advantageous to the noise emitted. In other words, the EPNdB value at the reference points is lower. Conversely, a negative value indicates that the interactions increase the noise measured at the reference points. The results of the noise analysis can be seen in Table 15.3 [61].

Table 15.3: EPNdB levels for TTBW and CC.

Config.	Level with PAA [EPNdB]				Level without PAA [EPNdB]			
	Approach	Flyover	Lateral	Cumulative	Approach	Flyover	Lateral	Cumulative benefit
TTBW	84.0	75.3	92.1	251.4	83.0	73.3	91.1	-4.0
CC	83.8	79.9	92.5	256.2	83.0	78.1	90.5	-4.6

It can be noted that the TTBW performs better with regard to noise pollution compared to the CC. This is thought to be due to the fact that a high-wing aircraft is able to more efficiently use the fuselage as a shield and that as a result, more of the sound is reflected upwards away from the ground. Then, the truss will likely increase this effect by reflecting upwards even more noise produced by the engine. However, additional research and understanding of the relevant physics are needed to draw conclusive results. Finally, compared to the CC, the TTBW has an improved L/D and can achieve a higher rate of climb. This gives the TTBW additional altitude when passing the flyover reference. The results of the ANOPP method can be seen in Figure 15.7. Here, the noise emissions for every aircraft component at the three certification points are given. As can be seen, even though the TTBW performs slightly worse for the approach certification point, it is still the superior choice [61].

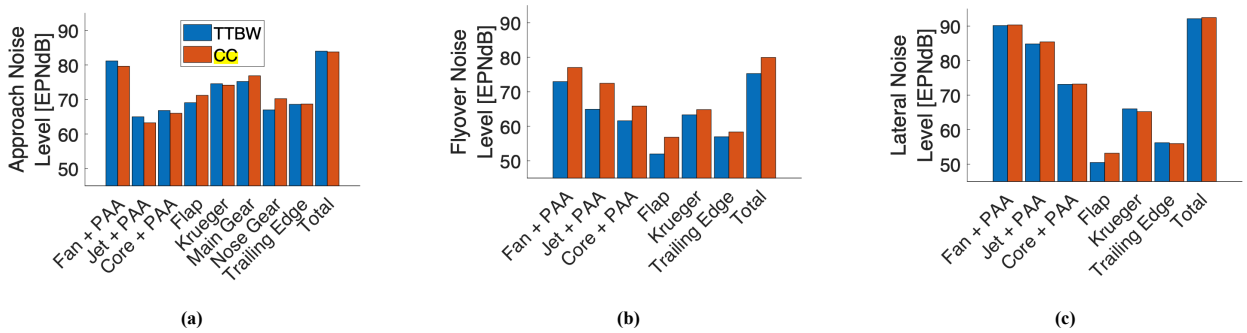

Figure 15.7: Noise performance TTBW versus CC [61].

15.5. Conclusion and recommendations

In conclusion, it is found that WorldBus is able to meet most of its sustainability requirements, however, the production, repair, and recycling qualities of CFRP could prove to be an issue. CFRP requires a lot of energy to produce, is difficult to repair and cannot be recycled easily. It is estimated that only 38% will be recyclable at end-of-life. When it comes to emissions during operation, WorldBus performs quite well, but improvements still need to be made. Flying at 9 km altitude on Green Hydrogen, WorldBus can reduce its emissions to 8.4 g per passenger per km, a 90% reduction compared to the per passenger per km emission of a Boeing 787-9. However, this value can increase to 97% as the production of hydrogen attains a lower carbon footprint. Finally, while the noise analysis does look promising, suggesting that a decrease in airframe noise and engine noise is certainly possible, it is too early to say whether this will also be the case for WorldBus. Listed below are the sustainability requirements from Chapter 5. It is also indicated whether these requirements have been met.

1. **(Compliant)** REQ-SUS-ENRG-1 The aircraft shall reduce total GWP emissions by 97% compared to a Boeing 787-9 during operation.
2. **(Not compliant)** REQ-SUS-ENRG-2 The production of 1 kg of liquid hydrogen will produce emissions with at most a GWP of 0.00 kg.
3. **(Intend to comply)** REQ-SUS-BEF-2 The entire production and manufacturing process of the aircraft shall reduce total GWP emissions by 43% when compared to the production of a Boeing 787-9.
4. **(Intend to comply)** REQ-SUS-NOIS-2 The aircraft shall reduce the cumulative noise by 5 dB compared to a Boeing 787-9.
5. **(Compliant)** REQ-USER-BUD-02 The aircraft shall fly in service for at least 20 years.
6. **(Intend to comply)** REQ-SUS-END-1 A minimum of 60% of the aircraft shall be reusable or recyclable.

Finally, the following recommendations can be made to improve the sustainability of WorldBus:

- It is recommended that alternative, more recyclable materials are still considered if the design allows for it.
- It is recommended to research whether the emissions during hydrogen production can decrease.
- It is recommended that a proper noise analysis is done for the airframe using the ANOPP method.
- It is recommended that Rolls-Royce is contacted for the noise emissions of the Trent 1000R.

16

Operations

During this chapter, multiple aspects of operations related to travel by plane will be discussed. Discussing all operations and their accompanying passing time will yield the available time for the flight. This time allows the average cruise speed to be calculated, ensuring the passenger's journey is completed within 24 hours. Firstly, promising innovations regarding airport and ground operations will be discussed in Section 16.1. Then, the passenger's journey from airport entry until departure is discussed in Section 16.2. The aircraft operations will be investigated in Section 16.3 and after this a complete timeline has been developed in Section 16.4 from which the effective flight time is determined in Section 16.5. After this, the non-flight aircraft operations are discussed in Section 16.6 and operations related to hydrogen storage at the airport are looked into in Section 16.7. Lastly, in Section 16.8 this chapter is concluded and recommendations for further research are made.

16.1. Innovations

As WorldBus aims to be flight-ready in 2040 the most promising innovations regarding airport and ground operations have been analysed to determine viable solutions for the future. Innovations related to sustainability as well as innovations related to the reduction of waiting times at airport have been investigated throughout this section.

16.1.1. Electric green taxiing system

An electric green taxiing system (EGTS) is a simple yet very effective concept [62]. An EGTS is a system which is attached to the landing gear of an aircraft, removing the need for the power supplied by the aircraft engines during taxiing. There are two different types of EGTS, and both will be analysed to determine the most optimal type for WorldBus.

Firstly, onboard EGTSs are evaluated. Implementing an onboard EGTS allows an aircraft to be autonomous during taxiing and even push-back [62]. This will result in shorter taxi times and less traffic on airport grounds because towing trucks will no longer be necessary. Lastly, it allows an aircraft to start its engines just before take-off and shut them down immediately after landing, thus reducing total fuel consumption and noise emissions. As both contribute to a more sustainable aircraft, these are considered to be very positive effects.

However, implementing an onboard EGTS also has disadvantages. First and foremost, adding an onboard EGTS adds extra weight to the aircraft, thus also increasing its fuel consumption during flight. For an internal EGTS of 400 kg a towing capacity of 78 tons is achieved. As WorldBus weighs about 250 tons, assuming a linear relation, an internal EGTS of just under 1300 kg should be used. After performing a weight iteration it was found that 800 kg of extra fuel would be used during the flight to compensate for this weight increase. This results in an increase in fuel weight of 1.5%. As seen in the paper discussing electric taxiing systems [62], for flights of 4000 km a reduction in total consumed fuel is 1%. As the WorldBus aims to fly over 4 times this distance, the reduction in total consumed fuel will be even less. Therefore the decrease in fuel usage due to the onboard EGTS does not compensate for the added fuel usage due to the increased weight of the onboard EGTS. Hence an onboard EGTS will not be considered further.

As it is the aim of the WorldBus to reduce emissions by as much as possible, an external EGTS is also investigated. Starting with the disadvantages, the taxi-in time will be increased after landing as the plane will have to wait until this external EGTS is linked with the landing gear. Furthermore, the autonomy of the pilot is taken away as this EGTS will take over the steering of the aircraft.

External EGTS also add positive value, comparable with onboard EGTS. Less fuel is consumed as the engine is turned off during taxiing, this also results in less noise emissions. These positive effects are achieved without increasing aircraft weight and therefore WorldBus will implement the usage of an external EGTS. The usage of external EGTS will add onto taxi time, however, as this process is expected to be further developed until 2040 it is expected to be negligible.

16.1.2. Biometric identification

Using biometric identification to increase the processing speed at customs and passport control is becoming increasingly common at airports [63]. As concluded in a paper by N. Khan [64], even with increasing passenger numbers, waiting times are significantly improved. During a pilot at Dublin airport, improvements were made as shown in Table 16.1. During the year 2018, no facial recognition was used and in 2019 it had been implemented.

From Table 16.1 it becomes clear that, even with increasing passenger numbers, biometric identification shows great potential in reducing passenger waiting times.

Table 16.1: Improvements in waiting time at Dublin airport due to facial recognition [64]

Year	Number of passengers	Within 30 minutes	Within 45 minutes
2018	110,090	65%	83%
2019	119,419	87%	98%

16.1.3. Self-service check-in

Another innovation that has been spreading throughout major airports worldwide is self-service check-in (SSCI) counters. By making use of this, passenger processing time can be reduced from an average of 7 minutes at a traditional check-in (TCI) counter to 3 min at an SSCI counter, a reduction of over 50% [65].

Next, the reduction in waiting time is to be investigated. Research conducted by S. Tyagi and G. Lodewijks shows that for the foreseeable future, TCI desks will not be completely replaced by SSCI counters [66]. However, SSCI counters will play an increasing role in processing passengers. Waiting times have been analysed at Kingsford Smith Airport in Sydney, whilst varying the ratio between TCI and SSCI desks. Using 40 % TCI desks and 60 % SSCI desks, an average waiting time of 14 minutes was found at both desks.

Concluding, the total time to pass the check-in desks would be reduced to an average of 17 minutes. Accounting for peaks in passenger numbers, a slack of 50% is added, resulting in a maximum processing time of 25 minutes.

16.1.4. 4 doors boarding

Currently, aircraft typically utilise a single door for boarding and deboarding operations. However, the WorldBus aircraft will have four doors on one side of the aircraft. This presents an opportunity to decrease boarding time by employing multiple doors. An average boarding time of 45 minutes is estimated for 200 passengers using a single door, this time decreases to 30 minutes when two doors are utilized. Further improvements can be realized, resulting in a boarding time of 23 minutes for three doors and a mere 20 minutes when all four doors are employed (linear progression assumed for 4 doors) [67]. As not all major airports are expected to be able to provide this infrastructure it has been chosen to take 45 minutes into account for boarding using 2 doors. This also provides for an error margin ensuring it is completed within the expected timeframe.

16.1.5. Ground power unit

When a plane arrives at an airport gate, the auxiliary power unit (APU) is used to provide the plane with energy. This APU is a low-energy system and is used to deliver energy to various operations within an aircraft, such as temperature control and lights, but also activating the engines. These APUs run on aircraft fuel and thus contribute to air pollution around airports. Furthermore, APUs contribute to noise emissions [68]. In order to reduce the noise emissions and fuel consumption of aircraft many airlines and airports have implemented policies restricting APU usage. These policies restrict APU usage so that it is only used the first 5 minutes after landing and before take-off. However, only 6% of the cases comply with this regulation [68].

In order to provide a more direct solution, research has been conducted regarding ground power units (GPU). Analysing the paper by A. Padhra shows that GPUs help in achieving an average reduction in total ground emissions of 47.6% [68]. Since most airports have now started incorporating GPUs, it is assumed that this is available at all major airports in 2040 for WorldBus to use, thus further reducing its emissions.[96]

16.2. Passenger journey

A key requirement for the WorldBus project is that the passenger should be able to travel between any two major airports within 24 hours. This constraint encourages proper research into the different operations that are to be performed by a passenger outside of the flight. Time spent at each operation will be estimated in this section, ultimately resulting in an estimation of the time available for flight.

[96] https://aviationbenefits.org/case-studies/fixed-electrical-ground-power/

16.2.1. Baggage check-in

Once a passenger starts their travel journey, the first step is to check in themselves and their baggage. As of today, major airlines advise checking in 3 hours prior to departure in order to comfortably catch a flight.[97,98] The check-in desk, however, remains open for check-in up until 60 minutes before departure.

As discussed in Subsection 16.1.3, room for improvement exists by making use of SSCI desks. Here, a maximum time of 27 minutes is determined for check-in. Considering the improvement in waiting time due to the combination of SSCI and TCI desks, it is a viable assumption that all major airports make use of this by 2040. Therefore, airlines should advise checking in 2 hours prior to departure and no later than 1 hour prior to departure.

16.2.2. Airport security and passport control

Multiple studies have been performed regarding waiting times at airport security and passport control. Research by N. Khan [64], as discussed in Subsection 16.1.2, shows that biometric identification dramatically reduces waiting times and, thus, should be implemented at airports. A maximum time of 45 minutes will be allocated to pass the airport security and passport control as 98% completes this within 45 minutes as can be seen in Table 16.1.

16.2.3. Travel time to gate

Multiple factors influence one's travel time from security/passport control to the gate. The walking distance contributes, evidently, the most, regarding this travel time. If the 8 longest possible airport walks are disregarded, the maximum walking distance reduces from 3.2 km to 1.1 km.[99] Considering one walks at a usual speed of 4.5 km/hour this would take just under 15 minutes to complete [69]. However, as it is often unclear where one's gate is located extra time should be reserved to ensure all passengers can arrive at the gate during this designated timeslot. 15 minutes of slack is added to account for this resulting in a total of 30 minutes for travel towards the gate.

16.2.4. Time related to boarding aircraft

Major airlines such as KLM and United advise passengers to arrive at the gate 60 minutes, and no later than 30 minutes, prior to departure.[100,101]. However, for the WorldBus, implementing boarding using multiple entrances reduces the time needed for this operation to 20 minutes, as discussed in Subsection 16.1.4. Therefore, for the WorldBus, it should be advised to arrive 45 minutes, and no later than 20 minutes, prior to departure.

16.2.5. Immigration and customs

After the international flight is completed and the passengers arrive at the desired location, people are subjected to pass through immigration and customs. Queue lengths and waiting times related to this procedure are strongly dependent on the airport and the time of the year. Based on data from major airports in the United States of America (USA), the average waiting time can be extracted, yielding 17.88 minutes.[102]

As discussed previously, biometric identification will be used to keep these waiting times as low as possible, as discussed in Subsection 16.1.2. As shown in Table 16.1, only 1% of the passengers waited for at least 45 minutes after implementing biometric identification, even though passenger volume increased by 15.8%. Considering this technique is becoming increasingly common at airports and further improvements in its usage will be made in the coming years [63]. In 2040, a maximum waiting time for immigration and customs of 30 minutes is reserved. This can take place over a span of 45 minutes.

16.2.6. Baggage claim

The time to be reserved for baggage claim is highly dependent on various factors. For example, the arrival airport logistics, the arrival time and the time of the year. When analysing Schiphol Airport, it can be deduced that baggage usually takes somewhere between 25-40 minutes to arrive at the baggage belts for passengers to collect. Baggage handling systems are continuously improved and optimised in order to reduce waiting times and heavy human labour. Taking this into account, a maximum waiting time of 45 minutes in 2040 is allocated to baggage claim.[103]

[97] https://www.klm.com/information/airport/baggage-drop-off

[98] https://www.united.com/ual/en/us/fly/travel/airport/process.html

[99] https://www.theaustralian.com.au/travel/are-we-there-yet-worlds-longest-airport-walks/news-story/54d6a739168d4bc1df6ccac60cc0e03e

[100] https://www.klm.com/information/airport/baggage-drop-off

[101] https://www.united.com/ual/en/us/fly/travel/airport/process.html

[102] https://upgradedpoints.com/travel/airports/average-wait-times-at-immigration-and-customs/#:~:text=Based%5C%20on%5C%20historic%5C%20clearance%5C%20times,International%5C%20Airport)%5C%20will%5C%20take%5C%20longer

[103] https://assets.ctfassets.net/biom0eqyyi6b/1LFrmaEaaI2Kgsw0G8IYgC/48c4c91d2b45712d1bb32b4501ad34a8/Baggage_at_Schiphol.pdf

16.2.7. Disembarking

Aircraft disembarking time has been analysed, resulting in an equation that relates the disembarking time to the number of rows and exits as can be seen in Equation 16.1. In the WorldBus configuration, use can be made of 4 exits to disembark 42 rows.[104] This results in a disembarking time of just over 5 minutes. Seemingly, a very low number, which can be explained by the fact that each exit only has to serve 50 people in total, or 10 people per minute. However, this time is also doubled in order to design for unexpected issues yielding a total disembarking time of 10 minutes.

$$T_{dis}(s) = \frac{\#rows \cdot 30}{\#exits} \tag{16.1}$$

16.3. Aircraft operations time analysis

Now, all major elements specifically related to passenger operations have been determined. However, in order to determine the time available for a flight, two major aspects should still be considered: taxiing time and delay.

16.3.1. Time related to taxiing

The time related to taxiing can be split up into two different components, taxi-in and taxi-out time. The average taxi times at 571 different airports, and their corresponding standard deviation, are published by Eurocontrol.[105] Incorporating the standard deviation twice ensures 95% of all cases fall inside these times. It is then found that a taxi-out time of 17.2 minutes and taxi-in time of 9 minutes should be used. However, as explained in Subsection 16.1.1, using an external EGTS could result in a delayed taxi-in time. For the time to link the external EGTS to the landing gear after touch-down, 3 minutes are reserved. Combining all these times and rounding up results in 30 minutes to be reserved for taxi times.

16.3.2. Delay times

Delays during departure, flight and arrival are important factors to account for when analysing operations related to aircraft. However, as for the WorldBus, passenger time should stay within 24 hours. The only analysed delay will be the arrival delay. Delay times at the largest airports in the USA have been extensively analysed by E. Mueller and G. Chatterji [70]. The average delay time to be accounted for is, after adding two standard deviations to the mean, 37.3 minutes.

16.4. Passenger and aircraft timeline

The complete timeline for operations related to passenger journey and the aircraft has now been analysed in Section 16.2 and Section 16.3. Using these times it can be concluded that 21 hours remain for flight operations. For a clear overview, these activities are portrayed in Figure 16.1. It can be seen that aircraft operations have been added to this figure as well. The starting point for this is an empty, but not clean, aircraft. At first, cleaning, restocking and equipment checks are performed in parallel [71]. After the external checks are completed, the refuelling process starts which lasts for, including purging and chill-down, at least 45 minutes [72].

Table 16.2: Allocated times per passenger and aircraft operational activity

	Activity	Allocated time
Passenger	Luggage check-in	1h
	Security & passport control	45min
	Move to gate	30min
	Boarding	45min
	Disembarking	10min
	Luggage collection	45min
	Customs/passport control	45min
Aircraft	Cleaning and restocking	30min
	Equipment and safety checks	15min
	Refueling	1h
	Luggage loading	1h
	Boarding passengers	45min
	Disembarking passengers	10min
	Luggage unloading	30min

[104] https://www.eldo.co/how-long-does-it-take-to-exit-an-airplane.html#:~:text=While%20it%20appeared%20to%20take,standard%20deviation%20was%205.1%20seconds

[105] https://www.eurocontrol.int/publication/taxi-times-summer-2021

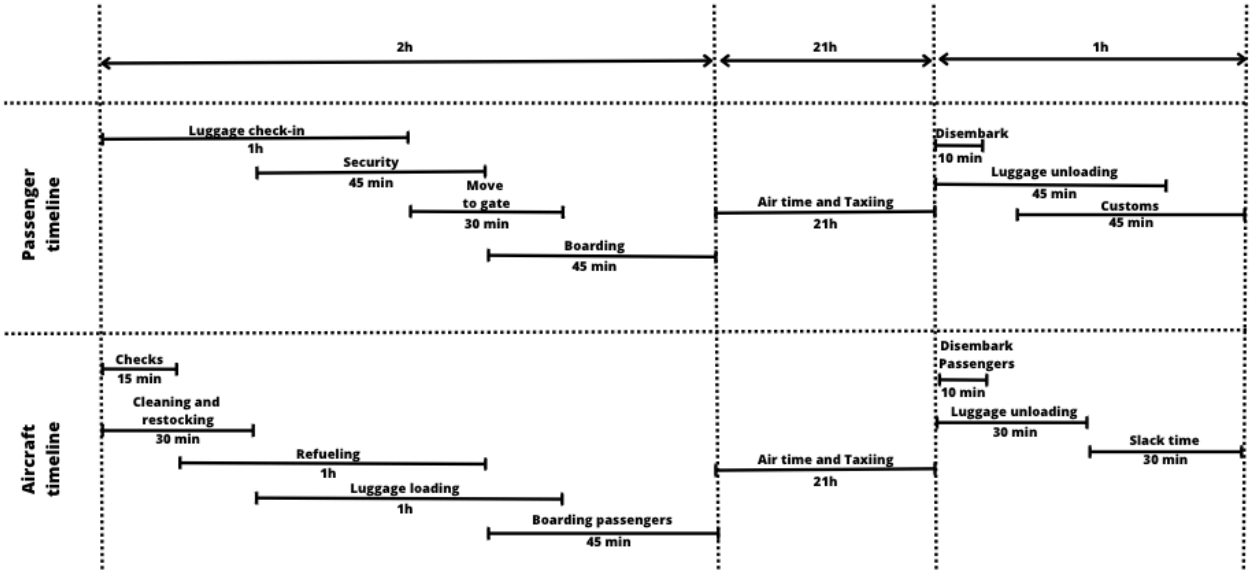

Figure 16.1: Timeline of passengers and aircraft operations

Interpretation of timeline overlaps

As can be seen in Figure 16.1, the operations have many overlapping activities. Some of these operations, especially passenger operations, can not be executed in parallel, thus raising the question about the viability of this timeline. However, it should be noted that this timeline is not to be interpreted as the timeline of one individual, but rather as the complete passenger group. Experienced travellers will pass more quickly through this timeline whereas a more inexperienced/cautious traveller may take longer or cut themselves more slack time.

16.5. Available effective flight time

From a brief look at Figure 16.1 it can be seen that 21 hours are available for air time and taxiing. In order to determine the average speed that WorldBus should fly at, taxiing should still be taken into account. Delay, as determined in Subsection 16.3.2, will be neglected due to certain factors. For the timeline of the operations, as shown in Table 16.2, maximum through-put times have been used, hence it is allowed to assume a best-case travel time scenario without arrival delays. Considering this and the total taxi time, discussed in Subsection 16.3.1, the available effective flight results in a time of 20 hours and 30 minutes.

16.6. Non-flight aircraft operations

Previously, this chapter has investigated operations related to flight. However, multiple operations exist which are to be performed outside of flight. These operations will be analysed in this section.

16.6.1. Maintenance

For commercial aircraft, a periodic maintenance schedule is used. In the USA, a Continuous Airworthiness Maintenance Program (CAMP) is established by each airline, as required by the FAA. An 'ABC check system' is used to perform the periodic maintenance checks. Starting at lighter and more frequent checks (A) up until heavier scarce checks (D) that will be discussed in this subsection.

A-checks

Every 400 to 600 flight hours, an A-check is performed. During this check, filters are changed and critical systems are checked and lubricated. Furthermore, emergency equipment is subjected to detailed inspection. B-checks have been merged into A-checks and are no longer performed separately. B-checks are performed every 6-8 months and consist of checks related to corrosion, fluid leakage or possible torquing of the nose landing gear.[106]

C-checks

C-checks are performed every 18-24 months and keep the aircraft grounded for up to three weeks. Approximately 6000 maintenance hours are spent on tasks such as lubrication of fittings and cables, but also inspection of structures.

[106] https://simpleflying.com/aircraft-maintenance-checks/

D-checks

Finally, D-checks are performed. These are the heaviest maintenance checks due to performed activities, a large number of man-hours and high associated costs. This check is performed every 6-10 years, depending on the aircraft. 30,000 up to 50,000 maintenance hours are needed over a period of 4-6 weeks. During this check, the entire aircraft is stripped down and all equipment is inspected. Often, airlines refurbish and upgrade the aircraft interior during this check as well.[107]

Total pricing

As investigated in the midterm report, the total cost of maintenance is estimated to be between 35-40 million USD during the lifespan of the plane [13].

Table 16.3: Maintenance level with projected cost and time.[106]

Maintenance level	Occurrence	Time out of service	Approximate cost
A	Every 8-10 weeks	up to 24 hours	USD 1-5 thousand
B	Every 6-8 months	up to 72 hours	USD 1-5 thousand
C	Every 18-24 months	4 weeks	USD 2-3 million
D	Every 6-10 years	6-8 weeks	USD 3-6 million

16.6.2. Consumptions

Ensuring that enough consumptions are present is an essential part of accommodating a comfortable flight. For healthy humans, 35 ml of water is needed per kg of body weight per day.[108] For 212 passengers and crew of an average weight of 75 kg, this results in 650l of fluids (incorporating a small safety margin). Assuming 1 kg of food is eaten per day, 250kg of food is necessary to be aboard the plane. Accounting for all packaging, the total weight involved with consumption on a plane will be 1000 kg. The WorldBus shall transport 83 business class passengers and 117 economy class passengers. As the flight will take about 20 hours, 3 meals are served per flight. For an economy meal, this equates to 10.50 USD per flight and for business class 33 USD.[109] This results in 11700 USD cost per flight.

16.6.3. Cabin crew and pilots

For a flight of 200 passengers, the FAA has determined requirements for the number of flight attendants necessary. 1 crew member per 50 passengers. However, as the duration of this flight approaches 20 hours, the crew members should work in shifts. This results in 2 cabin crew members per 50 passengers, or 8 cabin crew members in total.[110] For commercial flights, it is necessary to have two pilots available at all times, therefore, if working in shifts, the WorldBus shall accommodate for 4 pilots.

16.7. Hydrogen usage

As WorldBus will make use of hydrogen, it is important to investigate operations related to the use of hydrogen. How is it produced and transported to the airport and how will the airport store the hydrogen in a safe and sustainable way? These major questions will be answered in this section.

16.7.1. Hydrogen production

Before looking into the production of hydrogen, it should be noted that different types of hydrogen exist. The major types are green, blue and grey hydrogen. Green hydrogen is made from clean electricity such as solar or wind power. This is the preferred way of production as it emits zero-carbon dioxide during this process. Unfortunately, due to the high costs, this is not majorly used today. However, it is expected to become more commonly used in the future [73].

Next, blue hydrogen can be produced. This is done by mixing natural gas with steamed water. This method yields hydrogen, but carbon dioxide as well. Blue hydrogen production does make use of a carbon capture and storage method to trap this greenhouse gas.

Lastly, grey hydrogen is the final type of artificial hydrogen production. As of today, this is the most common form of hydrogen. Grey hydrogen is produced in the same way as blue hydrogen with the only difference being that the carbon

[107] https://www.naa.edu/types-of-aviation-maintenance-checks/

[108] https://www.brita.nl/ervaring-brita/persoonlijke-hydratatie-behoeften#:~:text=Hoeveel%5C%20moet%5C%20ik%5C%20elke%5C%20dag,80%5C%20kilo%5C%202%5C%2C8%5C%20liter.

[109] https://www.news.com.au/travel/travel-advice/flights/what-you-never-knew-about-your-inflight-meal/news-story/8b8c3cc890bda20746c245268ba1eb4d

[110] https://www.faa.gov/about/initiatives/cabin_safety

dioxide is not captured and stored but rather being emitted. Due to it being priced about 1.5 to 6 times lower than green hydrogen, it is so often used [74].

When analysing research conducted by IRENA, it is believed that in the long term, an 80% reduction in costs can be achieved [73]. Another analysis performed by Wood Mackenzie expects a cost reduction of 64% for green hydrogen in 2040 and 82% cost increase for grey hydrogen and 59% for blue hydrogen.[111] Therefore, it is expected for WorldBus to use only green hydrogen, resulting in a major improvement in sustainability which has been analysed in depth in Chapter 15.

As of today, close to no airports have incorporated an infrastructure for hydrogen. However, Airbus and Linde have entered into an agreement to work on the development of hydrogen infrastructure at airports. The aim is to accommodate hydrogen-powered commercial aircraft from 2035 onwards, worldwide. As WorldBus aims to enter the market in 2040, it is expected that there is a hydrogen infrastructure to make use of.

16.7.2. Hydrogen storage

In order to ensure safe hydrogen storage at the airport, multiple solutions exist. As WorldBus will fly on liquid hydrogen, only storage tank that store liquid hydrogen are considered. The safety of these tanks in case of a fire or over-pressure is ensured by a pressure relief valve (PRV), which is used to relieve the pressure safely in the hydrogen tank. Furthermore, even though the liquid hydrogen will be stored at cryogenic temperatures, boil-off is something to account for. Venting is used to ensure this boil-off is safely mitigated [75].

16.8. Conclusion and recommendations

This chapter has investigated multiple innovations increasing the sustainability of aircraft and/or reducing queuing times at airports. Using both an EGTS and a GPU contributes towards lower emissions during total flight operations and would significantly reduce fuel emissions and noise emissions around airports. In Figure 16.1, the timeline is given for passenger operations at airports for the travelling group as a whole. For the WorldBus mission, it is possible to complete these passenger operations quicker than the reserved timeline, thus reducing total travel time as explained in Figure 16.4. In 2040, to account for all types of passengers, it will be advised to arrive 2 hours prior to departure in order to comfortably catch the flight. If people would enjoy performing leisure activities and/or shopping at the airport, they should arrive earlier. This advice only takes the necessary operations into account.

Recommendations can still be made for further investigation into mission-related operations:

- Researching the possibility of pilots keeping steering control after attaching the plane to an external EGTS.
- More research should be performed regarding the optimization of baggage handling at airports to reduce waiting times.
- Further investigating the development of hydrogen infrastructure at major airports worldwide.

[111] https://www.woodmac.com/press-releases/green-hydrogen-costs-to-fall-by-up-to-64-by-2040/

17

Design sensitivity analysis

To find whether the current WorldBus design is a sound culmination of all the user requirements, a sensitivity analysis is performed. If a slight variation of input parameters or requirements results in a radically altered WorldBus design, the design is deemed sensitive, which is not preferable as it suggests the design is not optimised for its specific mission. Preferably, the design changes slightly with a slight input change.

To perform the sensitivity analysis, a number of parameters are varied a step in both the positive and negative reaction direction. For each of these altered parameters, the entire design iteration is reperformed. The MTOW of the aircraft is monitored for change, as all aircraft parameters influence the MTOW, either directly or indirectly. Furthermore, the MTOW directly influences both productional and operational cost. Using this method, the effect the parameters have on all design aspects become immediately apparent, as the MTOW is affected by every single subsystem and design calculation. Furthermore, the wingspan is directly influenced by the MTOW and the planform design, which can additionally indicate an issue if it does not change in line with the MTOW.

17.1. Range

As determined by user requirement REQ-PERF-1, the WorldBus range needs to be 19 000 km. This results in a large amount of required fuel, a large fuel tank, and thus a long fuselage. To find the hypothetical size and MTOW of the aircraft with an altered range, the iterations are repeated for a range of 18 000 km and 20 000 km. The results can be found in Table 17.1

Table 17.1: Results of the passenger number sensitivity analysis. The WorldBus design parameter is indicated in grey. An increase in weight and size is indicated in orange, a decrease in weight and size in green.

Range [km]	Change	MTOW [mt]	Change	Span [m]	Change
18 000	- 5.3%	215.2	- 3.8%	70.5	- 2%
19 000	-	223.8	-	71.9	-
20 000	+ 5.3%	238.4	+ 6.5%	74.2	+ 3.2%

As is shown in Table 17.1, the MTOW and wingspan are exponentially correlated with the range. For an increasing range, the MTOW increases with growing increments. This is in accordance with the effect of the 'snowball effect'. The lowest range of 18 000 km intuitively results in a lower MTOW. However, it does not comply with user requirement REQ-PERF-1. The decrease in MTOW is relatively small and in proportion, indicating that the design is not highly sensitive to changes in range. Therefore, it is deduced that the range requirement is appropriate and does not need to be negotiated about with the user.

17.2. Flight velocity

As determined by user requirement REQ-USER-BUD-01, the airport door-to-door travel time should not exceed 24 hours. Taking into account the operational limitations as defined in Chapter 16, the flight time is limited to approximately 20.5 hours, as defined in Section 16.5. This requires the cruise velocity to be at least 265 m/s. To investigate the effect of the cruise velocity on the WorldBus MTOW, design iterations are performed using cruise velocities of 245 m/s and 285 m/s. A velocity of 245 m/s will not comply with user requirement REQ-USER-BUD-01. The results are displayed in Table 17.2.

Table 17.2: Results of the passenger number sensitivity analysis. The WorldBus design parameter is indicated in grey. An increase in weight and size is indicated in orange, a decrease in weight and size in green.

Flight velocity [m/s]	Change	MTOW [mt]	Change	Span [m]	Change
245	- 7.5%	229.2	+ 2.4%	72.8	+ 1.3%
265	-	223.8	-	71.9	-
285	+ 7.5%	205.1	- 10.5%	68.8	- 4.3%

The differences between the MTOWs included in Table 17.2 are within the expected order of magnitude. No unexpected deviations in the results appear, so the input parameter of flight velocity is deemed to be sound and not overly sensitive. Furthermore, Table 17.2 shows that a decreased flight velocity of 245 m/s is not optimal. This can be justified as the aircraft will need to fly at a lower altitude of 8.4 km to achieve the designated range optimally. This will not comply with REQ-USER-BUD-01. Flying at a higher velocity of 285 m/s solves these issues. The optimal altitude increases to 10.8 km and the weight and size of the aircraft decrease significantly. However, as research in Section 15.3 uncovered, altitudes above 9 km do not comply with REQ-USER-SUS-01 and thus, velocities above 265 m/s, are unfeasible for this mission.

17.3. Flight altitude

As briefly mentioned in Section 17.2, the driving forces behind the decision on flight altitude are the benefits for efficiency of high-altitude flight and user-derived requirements REQ-SUS-ENRG-1 / REQ-SUS-ENRG-2, which dictate that operational flight needs to be at least 90% less GWP emitting than a similar counterpart aircraft. Above altitudes of 9000 m, the GWP of emitted NO_x and H_2O gases greatly increases, which limits the design altitude. Furthermore, high-ground speed flight is most fuel efficient at high altitudes, which is why a lower altitude is not selected for the design altitude. Nevertheless, the aircraft design for altitudes of 8000 m and 10 000 m will be investigated to verify whether its impact on the design in general. The results can be found in Table 17.3.

Table 17.3: Results of the passenger number sensitivity analysis. The WorldBus design parameter is indicated in grey. An increase in weight and size is indicated in orange, a decrease in weight and size in green.

Flight altitude [m]	Change	MTOW [mt]	Change	Span [m]	Change
8 000	- 11.1%	233.5	+ 4.3%	73.5	+ 2.2%
9 000	-	223.8	-	71.9	-
10 000	+ 11.1%	212.0	- 9.2%	70.0	- 2.6%

The differences between the MTOWs included in Table 17.3 are within the expected order of magnitude. Moreover, the found variation is predominantly linear. No unexpected deviation appears in the results, so the input parameter of flight altitude is deemed to be sound and not overly sensitive. A higher altitude allows for a higher ground speed and thus a shorter flight, decreasing the needed fuel and decreasing the MTOW. The worse result for the flight altitude of 8000 m is realistic for the same reasoning. Hence, the outcome of the sensitivity analysis is sensible and trustworthy. Table 17.3 also shows that the current WorldBus design altitude of 9000 m is not the option with the lowest MTOW. A higher altitude allows for a higher ground speed and thus a shorter flight, decreasing the needed fuel and decreasing the MTOW. The worse result for the flight altitude of 8000 m is realistic for the same reasoning. Hence, the outcome of the sensitivity analysis is sensible and trustworthy. However, requirement REQ-SUS-ENRG-1 / REQ-SUS-ENRG-2 would not be complied with at an altitude in excess of 9000 m. Therefore, the WorldBus design altitude is situated at the optimal design point.

17.4. Number of passengers

Another user requirement is that of a minimum passenger count of 200 (REQ-OPS-CMF-1). The current WorldBus design closely adheres to this number. However, the overall payload weight and fuselage length are directly influenced by the passenger count. Therefore, the number of passengers will be investigated by means of a sensitivity analysis, where the required number of 200 pax will be compared to that of 180 pax and 220 pax. It is worth noting that the passenger count not only influences the weight and size of the aircraft, but also either the price of a ticket or the gross revenue of the operator. The results of the sensitivity analyses can be found in Table 17.4.

Table 17.4: Results of the passenger number sensitivity analysis. The WorldBus design parameter is indicated in grey. An increase in weight and size is indicated in orange, a decrease in weight and size in green.

Passenger number [-]	Change	MTOW [mt]	Change	Span [m]	Change
180	- 10.0%	220.7	- 1.4%	71.4	- 0.7%
200	-	223.8	-	71.9	-
220	+ 10.0%	239.1	+ 6.8%	74.3	+ 3.3%

The differences between the MTOWs included in Table 17.4 are within the expected order of magnitude. A peculiar variation in the sensitivity analysis is the difference in MTOW change for the passenger reduction and the passenger increase. This is most likely caused by the increased c.g. shift, resulting from the addition of passengers in the front cabin. Taking this into account, no unexpected deviation appears in the results, so the input parameter of passenger number is deemed to be sufficiently sound and not overly sensitive.

Furthermore, Table 17.4 shows that the aircraft design for fewer passengers than the existing design is lighter, which intuitively makes sense. A lower payload weight and less fuselage space required add up to a significant decrease in MTOW. Hence, a larger MTOW for more passengers makes sense in the same manner. However, as requirement REQ-OPS-CMF-1 requires 200 pax as a minimum, the current WorldBus design is situated at the optimal design point for compliance with the requirement.

17.5. Aspect ratio

The aspect ratio is not constrained by a user requirement. However, one of the main benefits of the truss-braced wing design is its capability to be more slender than a comparable wing. This increases its aspect ratio, which increases the lift over drag and allows for more fuel efficient flight. The aspect ratio directly influences the wingspan, as the wing area is fixed by the required amount of lift. Therefore, the aspect ratio is constrained by the maximum wingspan, which is defined by the maximum available width at airport aprons of 80 m as described in Section 2.2. Therefore, the design point is situated close to this constraint. Nevertheless, a sensitivity analysis is performed for the aspect ratio. As the aspect ratio of the WorldBus design is fixed at 14, the sensitivity analysis will be performed for aspect ratios of 12 and 16. The results are displayed in Table 17.5.

Table 17.5: Results of the passenger number sensitivity analysis. The WorldBus design parameter is indicated in grey. An increase in weight and size is indicated in orange, a decrease in weight and size in green.

Aspect ratio [-]	Change	MTOW [mt]	Change	Span [m]	Change
12	- 14.3%	217.1	- 3.0%	65.6	- 8.8%
14	-	223.8	-	71.9	-
16	+ 14.3%	249.2	+ 11.3%	81.1	+ 12.8%

The differences between the MTOWs included in Table 17.5 are within the expected order of magnitude. Moreover, the found variation is predominantly linear. A lower aspect ratio decreasing the MTOW was, however, not expected. It was expected that the reduction in flight efficiency would be more expensive than the added benefit of a shorter, and thus, lighter wing, but that is not the case. An explanation that is considered is that the effect of assumption AS.WB.GEOM.2 (constant wingbox thickness) is overturning the positive effects of a high aspect ratio. During the design phase, a fixed aspect ratio was selected based on available literature. It is recommended that the aspect ratio is investigated further as a variable parameter in future design stages. Taking this into account, the input parameter of the aspect ratio is deemed to be sound and not overly sensitive.

17.6. Tank placement

The tank placement is another parameter that is not constrained or restricted by any high-level requirements. Instead, its placement strongly influences the centre of gravity variation of the aircraft, and thus dictates the design and placement of aerodynamic surfaces, namely the empennage and the wing. Furthermore, the current design of the two cabins and the tank in between stems from emergency exit requirements and crew requirements. It is not a trivial task to reposition seats from one cabin to the other without losing efficiency in terms of personnel additional emergency exits. Nevertheless, a sensitivity analysis is performed to find the variation in aircraft weight and size for altered tank placements. As the centre of gravity of the main tank is located at 32 m from the aircraft nose, it will be analysed for a centre of gravity at 30 m and 34 m. The results can be found in Table 17.6.

Table 17.6: Results of the passenger number sensitivity analysis. The WorldBus design parameter is indicated in grey. An increase in weight and size is indicated in orange, a decrease in weight and size in green.

Longitudinal dist. from AC nose to tank C.G. [m]	Change	MTOW [mt]	Change	Span [m]	Change
30	- 6.3%	230.3	+ 2.9%	73.0	+ 1.5%
32	-	223.8	-	71.9	-
34	+ 6.3%	229.5	+ 2.5%	72.8	+ 1.3%

The differences between the MTOWs included in Table 17.6 are within the expected order of magnitude. Moreover, the found variation shows very similar behaviour in both the tested tank location directions. It makes sense for the tank location to increase the MTOW if moved in any direction at all. The altered locations result in a repositioning of the aircraft centre of gravity. In turn, this requires a more substantial empennage and increases drag. No unexpected deviation appears in the results, so the input parameter of flight altitude is deemed to be sound and not overly sensitive. Furthermore, Table 17.6 shows that the current design parameter is the most optimal outcome of the sensitivity analysis. This indicates that the tank placement is correctly optimised.

17.7. Wing placement

Lastly, the wing placement is a factor which heavily influences the aircraft centre of gravity, the aircraft scrape and tip-back angles, the empennage sizing and design, and the aircraft flight performance in general. The placement of the wing is based mostly on an appropriate distance between the aerodynamic centre and the aircraft centre of gravity. In this way, it has a significant effect on many flight dynamics properties of the aircraft. A sensitivity analysis is performed for the wing placement. The locations of the subsystems that are part of the wing group will not change with respect to the wing during this analysis. Instead, X_{LEMAC}, the longitudinal distance between the aircraft nose and the leading edge mean aerodynamic chord, will be positioned at 28 m and 32 m, as it is located at 30 m in the WorldBus design. The results can be found in Table 17.7.

Table 17.7: Results of the passenger number sensitivity analysis. The WorldBus design parameter is indicated in grey. An increase in weight and size is indicated in orange, a decrease in weight and size in green.

Longitudinal dist. from AC nose to LEMAC [m]	Change	MTOW [mt]	Change	Span [m]	Change
28	- 7.1%	231.3	+ 3.4%	73.1	+ 1.7%
30	-	223.8	-	71.9	-
32	+ 7.1%	230.8	+ 3.1%	73.0	+ 1.5%

A similar result to Section 17.6 is seen in Table 17.7. The found variation shows very similar behaviour in both wing displacement directions. It makes sense for the wing placement to increase the MTOW if moved in any direction at all. The altered locations result in a repositioning of the aerodynamic centre. In turn, this requires a more substantial empennage and increases drag. Furthermore, moving the wing forward will destabilise the aircraft, as the distance between the aerodynamic centre and the aircraft centre of gravity decreases or 'becomes negative'. The differences between the MTOWs included in Table 17.7 are within the expected order of magnitude. No unexpected deviation appears in the results, so the input parameter of flight altitude is deemed to be sound and not overly sensitive. Lastly, Table 17.7 shows that the current design parameter is the most optimal outcome of the sensitivity analysis. This indicates that the wing placement is correctly optimised.

17.8. Conclusion and recommendations

The sensitivity analyses performed in Section 17.1 up until Section 17.7 provide a variation of results. Section 17.1, Section 17.2, Section 17.3, and Section 17.4 show that the WorldBus design is not necessarily the most efficient design in the broad sense, but that it is optimised well and it is the lightest design within the constraints as posed by the user requirements for a number of parameters. Section 17.6 and Section 17.7 show that the WorldBus design is optimised well for the tank and wing placements, as the current design presents the lightest solution. Lastly, Section 17.5 shows that the WorldBus design may not be designed with an optimal aspect ratio or that assumptions are creating noises in the results. However, the current WorldBus design seems to be somewhat overdesigned as a result of the aspect ratio assumptions, which should not give feasibility problems in later design stages. Furthermore, none of the sensitivity analyses show an unreasonable or out of proportion design reaction to the slight changes in parameters, as can also be seen in the percentage change overview in Table 17.8. This strongly indicates that there are no unnoticed design issues, mistakes, or inaccuracies which may lead to large unexpected changes in later design stages.

To increase the soundness and stability of the WorldBus aircraft design in future stages of the development phase, a single recommendation is made:

- Perform further analysis into the effects of 'decision parameters' (parameters which are determined by a design choice) is performed throughout the early stages of the design process. This would include parameters such as the aforementioned aspect ratio, the taper ratio, the dihedral angle, and the maximum landing weight.

Table 17.8: A tabular overview of all percentage outcomes of the sensitivity tests as performed in Chapter 17.

Parameter	**Parameterchange**	**Max.MTOWchange**	**Max.spanchange**
Range	± 5.3%	+ 6.5%	+ 3.2%
Flight velocity	± 7.5%	- 10.5%	- 4.3%
Flight altitude	± 11.1%	- 9.2%	- 2.6%
Passenger number	± 10.0%	+ 6.8%	+ 3.3%
Aspect ratio	± 14.3%	+ 11.3%	+ 12.8 %
Tank placement	± 6.3 %	+ 2.9 %	+ 1.5%
Wing placement	± 7.1%	+ 3.4%	+ 1.7%

18

RAMS

In this chapter, the reliability, availability, maintainability and safety (RAMS) characteristics are showcased. RAMS characteristics are important to any engineering design and the analysis plays a vital role in making sure that a design has the most optimal and safe performance. For WorldBus, every part of RAMS will be treated separately and each aspect will focus on systems that are novel applications of engineering solutions. So, systems that do not have extensive in-flight track records. For other systems safety regulations still need to be adhered to, but as they are common, proven technologies, they will not be addressed separately in this chapter.

18.1. Reliability

The first part of RAMS characteristics is the reliability of the system. Reliability is defined as the ability of a system to perform a specific function within a certain time period.[112] In other words, the system perform its function without failing.

Fuselage

WorldBus uses CFRP due to weight limitations. Additionally, CFRP is quite a beneficial material due to it being a stronger material than aluminium and GLARE, but also it being corrosion-resistant. Furthermore, it has low degradation due to its high chemical resistance and performance in harsh environments. Due to these characteristics, it requires less regular maintenance. [113]

Hydrogen sensors

WorldBus makes use of novel optical fibre hydrogen sensors, based on tantalum and palladium. These sensors have higher reliability than traditional hydrogen sensors, do not require high temperatures to operate, and can detect hydrogen at very low pressures [76]. By employing multiple sensors for both the main tank and the secondary tank, it is ensured that hydrogen leaks in the fuel tanks can be detected reliably and quickly.

Vents

Venting must be possible when the tank pressure surpasses the upper limit. However, the vent comes with some issues. In this particular case, the vent must only allow a flow of hydrogen from inside the tank towards the outside and prevent backflow of air into the tank. This can be prevented using backflow preventer valves. The conditions matter as well. If hydrogen is released in a moist environment, the valve operating the vent might freeze. Measures to counter this are yet to be developed. Finally, in the case released hydrogen catches fire, the surrounding structure must be prevented from damage. This can be achieved by installing a flare trap such that fire damage towards the surrounding is minimised.

Plumbing

The WorldBus plumbing (feed lines and valves) is also subjected to extremely low temperatures. The hydrogen boil-off will be transported through the lines, with temperatures ranging between $20\,\mathrm{K}$ at the tank exit to $150\,\mathrm{K}$ at the engine entrance. The plumbing will use a similar insulator configuration as the tank insulation such that other lines and wiring do not freeze due to the low temperatures in the fuel lines.

Truss support

The truss support system is responsible for carrying a large part of the loads that act on the wing. Failure of this structure could lead to failure of the entire system as the wing is not designed to carry the loads without the truss. In order to ensure that the truss system is reliable, a safety factor of 1.5 was applied to the ultimate load expected on the truss. Moreover, conservative assumptions were made when designing the truss structure making sure that this structure will be reliable.

[112] https://www.ntnu.no/c/document_library/get_file?uuid=79d5e80e-5cf7-4923-a3d7-0cb8792db310&groupId=10389
[113] https://www.nitprocomposites.com/blog/how-durable-and-reliable-is-cfrp

Taxiing system
The new taxiing system as discussed in Subsection 16.1.1 showcased how EGTS would be employed at airports to facilitate more sustainable taxiing procedures. The reliability of the system itself of course depends on the design of those systems. However, WorldBus still has the capability to taxi using its own propulsion system, so fundamentally it does not affect the system's reliability to taxi to and from the gate.

Rolls-Royce Trent 1000R
The Rolls-Royce Trent 1000R has had some reliability issues in the past. These issues included engine blades that could crack more quickly due to pollutants in the air, high-pressure blades that were not cooled properly, and issues with the resonance frequency of the engine.[114] However, since then, these issues have been mitigated and the Rolls-Royce Trent 1000R now boasts dispatch reliability of 99.9%.[115]

18.2. Availability
The second part of RAMS is availability. This is defined as the ability to keep a functioning system in the current environment.[112] Of course, availability is related to reliability, as a reliable aircraft is available for use. However, it is also important that the support systems that WorldBus require to function are also available. For instance, spare parts that are needed for repair, or the hydrogen fuel itself that is required to power the engines. This section showcases aspects of the WorldBus design that require extra attention in terms of availability.

Carbon fibre
Since a large part of the WorldBus design is made from carbon fibre, and production will not start until late 2030, it is important that enough carbon fibre will be available at a low enough cost. It is expected that the cost of carbon fibre will go down as more efficient production techniques arise and the ability to recycle increases.[116]

Spare parts
The availability of spare parts for the WorldBus aircraft will be significantly lower than that of other conventional aircraft. When an element of the aircraft is specifically designed and manufactured for the use of liquid hydrogen, take specific components of the engine or fuel tank for example, then new parts would have to be manufactured which means that the reparation of the aircraft would have to wait. This could be solved by manufacturing spare parts to be prepared for such occurrences, this has as a downside that these parts would have to be stored somewhere which is undesirable.

Hydrogen
The availability of hydrogen is crucial for the success of WorldBus as it is needed to fuel the aircraft. Currently, hydrogen is relatively expensive and most hydrogen is produced from natural gas and coal, with only 0.1% of the total production coming from water electrolysis. This results in hydrogen production emitting as much CO_2 as the United Kingdom and Indonesia combined. However, it is estimated that as renewable energies become even more popular and widespread, the cost of hydrogen production could fall by 30% by 2030 and green production will increase.[117]

Fuelling system
Complete fuelling systems and fuel storage systems that are applicable for the use of liquid hydrogen would have to be operational and available at airports by 2040. Nowadays, liquid hydrogen is already being used as rocket propulsion. This means that storage and fuelling systems already exist for such applications.[118] Applying this to the aeronautic industry should not be a problem if sufficient storage system are available at airports.

Rolls-Royce Trent 1000R
WorldBus relies on the availability of modified Rolls-Royce Trent 1000R Engines for production. The kerosene-powered Trent 1000s are used to power the Boeing 787. Since this aircraft is still in production, it is safe to assume that Rolls-Royce is still producing these engines and that as such, WorldBus will be able to order engines. After delivery, the engines will be modified to run on liquid hydrogen.[119]

18.3. Maintainability
In this section, the maintainability of WorldBus is discussed. Good maintainability means that the aircraft can easily and timely be expected. This includes the servicing, inspection and repair of WorldBus systems.[112]

[114] https://simpleflying.com/rolls-royce-trent-1000-solved/
[115] https://www.rolls-royce.com/products-and-services/civil-aerospace/widebody/trent-1000.aspx#section-overview
[116] https://www.infosys.com/engineering-services/white-papers/documents/carbon-composites-cost-effective.pdf
[117] https://www.iea.org/reports/the-future-of-hydrogen
[118] https://www.nasa.gov/feature/innovative-liquid-hydrogen-storage-to-support-space-launch-system
[119] https://www.reuters.com/business/aerospace-defense/boeing-has-boosted-787-dreamliner-production-rate-four-month-company-says-2023-05-30/#:~:text=In%20April%2C%20the%20company%20said,of%20these%20jets%20in%202023.&text=Our%20Standards%3A%20The%20Thomson%20Reuters%20Trust%20Principles.

Fuselage
As the exterior of the fuselage is made of CFRP, the maintainability differs from conventional aircraft. As CFRP is stronger compared to its metal counterpart and since it is not fatigue-prone, less maintenance is required. However, damage may not be as visual as in conventional metallic structures, as the damage could be present within the ply. Therefore, different detection methods are possible. Detection of issues within the structures is mainly observed using acoustic devices. Depending on the size and location of the damage, different repair approaches are applicable from surface repairs to repairs within the ply.

Fuel tank
Integral fuel tanks must have facilities for interior inspection and repair (CS 25.963(c)) [18]. To allow for repairs and maintenance, the tank has to be accessible for engineers, which is achieved by using the vents and valves that connect to the tank. In case the tank is beyond repairable, the tank needs to be replaced. This can be achieved by having the aircraft built sectionally, where one of the sections only contains the fuel tank. In case of replacement, two fuselage sections around the tank can be disjoined to allow for this operation.

Truss
The maintainability of the truss should not pose any issues. The truss is a relatively simple structure that can be easily inspected by a maintenance crew.

18.4. Safety
Due to the unconventional approach of the design, safety concerns arise that could be detrimental to the design if not taken into account. The safety risks that differ from conventional aircraft are elaborated and solutions for those risks are given and discussed.

Emergency tank
In case the main tank fails, and the liquid hydrogen has to be jettisoned, a secondary fuel tank is included in the design. The secondary fuel tank is designed such that the aircraft is able to fly for an additional hour in cruise conditions, this gives the pilots enough time to reach either the closest available airport or the safest available place to perform a crash landing.

Ignition of leaked fuel
In each area where flammable fluids or vapours might escape by leakage of a fluid system, there must be means to minimise the probability of ignition of the fluids and vapours, and the resultant hazards if ignition does occur (CS 25.863). No ignition source may be present at each point in the fuel tank or fuel tank system where catastrophic failure could occur due to ignition of fuel or vapours (CS 25.981(a)) [18]. For these reasons, among other things, the fuel tanks are placed in sealed compartments with no other components that could jeopardize the aircraft by igniting the hydrogen.

Jettisoning
In case of detection of hydrogen by the hydrogen sensors when leakage of the tank occurs, leakage in any other component of the fuel system or in case of the loss in vacuum in the layer between the inner and outer tank of the primary fuel tank, the liquid hydrogen in the primary tank is jettisoned into the environment. This is done using heating components in the fuel tank that heats up and vaporises the liquid hydrogen that is then vented out of the fuselage.

Isolation
If leakage would occur, each fuel tank must be isolated from personnel compartments by a fume proof and fuel proof enclosure (CS 25.967(e)) [18]. When leakage of the primary or secondary tank occurs the hydrogen is noticed with the use of hydrogen sensors, the hydrogen is then vented into the environment using a venting system. In case of leakage, the carbon fibre outer tank is designed to be airtight to keep the gaseous hydrogen inside. If leakage would also appear in the outer tank, the bulkheads that isolate the fuel tanks from the passenger compartments are also designed to be airtight to keep the hydrogen from reaching the passengers or crew members.

Fuel sloshing
Fuel sloshing can be problematic in aircraft as it introduces forces on the tank and aircraft and can change the location of the centre of gravity, posing risks for the aircraft structure and stability if not taken into account. To prevent excessive sloshing, baffles have been introduced in the primary and secondary fuel tanks.

One engine inoperative
The regulation for climbing with one engine inoperative states that in climb configuration, the aircraft should be able to perform a specific climb gradient with one engine inoperative as percentages of the climb gradient with all engine operative for different stages in take-off (CS 25.121) [18]. The engines chosen for this design perform well enough to take this into account.

Engine placement w.r.t. the truss
The engine placement on the wing has to be such that when the engine breaks off the wing, the engine should not hit the truss and take the truss with it. Since this would be catastrophic for the aircraft as the wing will most likely fail without a truss. The engine is placed in front of the quarter chord such that when the engine would break off, the engine would fly forward and over the wing to avoid the truss getting hit.

Truss
The truss is of much importance in the structure of the wing. If the truss ended up failing, the wing would most likely follow. Therefore, the truss is a safe-life design as structural failure in flight would be catastrophic.

Lightning
With the use of CFRP as the skin, the weight of the aircraft is significantly reduced. CFRP is however a poorer electrical conductor than aluminium that is conventionally used as fuselage skin material. A protective system is included to minimise the damage the lightning strike would have. A metal meshing is included in the skin to conduct the electricity through the outside of the fuselage. Wire bundle shields are also implemented as additional protection in areas more prone to lightning strikes.

Emergency exits
The entire aircraft, all passengers including crew members, should be able to be evacuated within 90 seconds (CS 25.803(c)) [18]. Since the aircraft includes two cabins, the aircraft should comply with this regulation for both cabins. Each cabin has been decided to have two type I exits on the lower floor and one type III exit on the upper floor, on both sides of the aircraft. This results in six emergency exits for each cabin and 12 emergency exits for the whole aircraft. The type I exits have also been made larger to make them more accessible. This all means that the design is over-redundant for the regulations. This is done in case the configuration is changed for a lower range and more passengers are placed into the cabins, in this instance, the aircraft design already complies with the emergency exit regulations.

Isolated cabin
Because the hydrogen tanks are placed in the middle of the fuselage the rear cabin will be isolated from the front and from the cockpit. This was isolated as a possible safety concern as moving crew and passengers between these sections would not be possible. However, some precedent for isolated passenger cabins was identified. For example, the combi version of the B737-400 has a cargo compartment separating the cockpit and the rest of the cabin, as illustrated in Figure 18.1.[a] With no regulatory restrictions being identified regarding the separation of passenger cabins, and plenty of emergency exits being available in both sections of the aircraft to facilitate timely evacuation. There shouldn't be any complications regarding this design choice.

Figure 18.1: B737-400 combi taking off

[a] https://www.flickr.com/photos/richsnyder/12889744753/in/photostream/

18.5. Conclusion
With the reliability, availability, maintainability and safety characteristics that are showcased, a clear picture is sketched of possible downfalls, regarding these characteristics, one can expect when designing for a truss-braced wing configuration aircraft that flies on liquid hydrogen. These downfalls are discussed and analysed, after which they are disproven to be of any concern.

19

Risk management

In this chapter, both risks of the current design phase and those of future design phases of the project are identified. In Section 19.1, the foundation of the risks is explained and in Section 19.2 the newly identified risks will be mentioned and strategies to mitigate these risks are given.

19.1. General risks

The assessment of the technical risks in the previous section is based on three aspects: cost (R-C), scheduling (R-S), and technical performance (R-P). Previously identified critical risks in the design were R-P-08 (Malfunctioning fuel system) and R-P-09 (Malfunctioning structural system). R-P-08 is a critical system due to the use of hydrogen as fuel. As hydrogen is the smallest molecule and as it is quite flammable, storage can be challenging. For R-P-09, identifying the potential hazards with respect to the material choice is very important. Both metal alloys and composites have advantages and disadvantages.

Mitigation for the original risks have been established in the baseline report [2] and midterm report [13].

As the WorldBus project has a fixed budget, the impact of cost is severe. If the costs exceed the budget, it may be catastrophic for the project. Scheduling is considered as it is important to have a well-established timeline since time influences the design and production quality. For technical performance, risks established in this aspect have an influence could cause the the design to fail, but they also influence cost and scheduling as they also have a dependency on technical performance.

The grading of the risks has been determined according to the following definitions. The definitions for the grades are provided in Table 19.1 and Table 19.2.

Table 19.1: Definitions of likelihood [77]

Likelihood of occurrences			
Grade	**Likelihood**	**Definition**	**Quantitative probability—Average probability per flight hour**
5	Frequent	Happens almost every other flight	Likelihood > 1×10^{-3}
4	Occasional	Happens once or more during each aircraft operational lifetime	1×10^{-5}< likelihood < 1×10^{-3}
3	Remote	Unlikely, but possible to occur	1×10^{-7}< likelihood < 1×10^{-5}
2	Improbably	Very unlikely to occur	1×10^{-9}< likelihood < 1×10^{-7}
1	Extremely improbably	Almost inconceivable to occur	Likelihood <1×10^{-9}

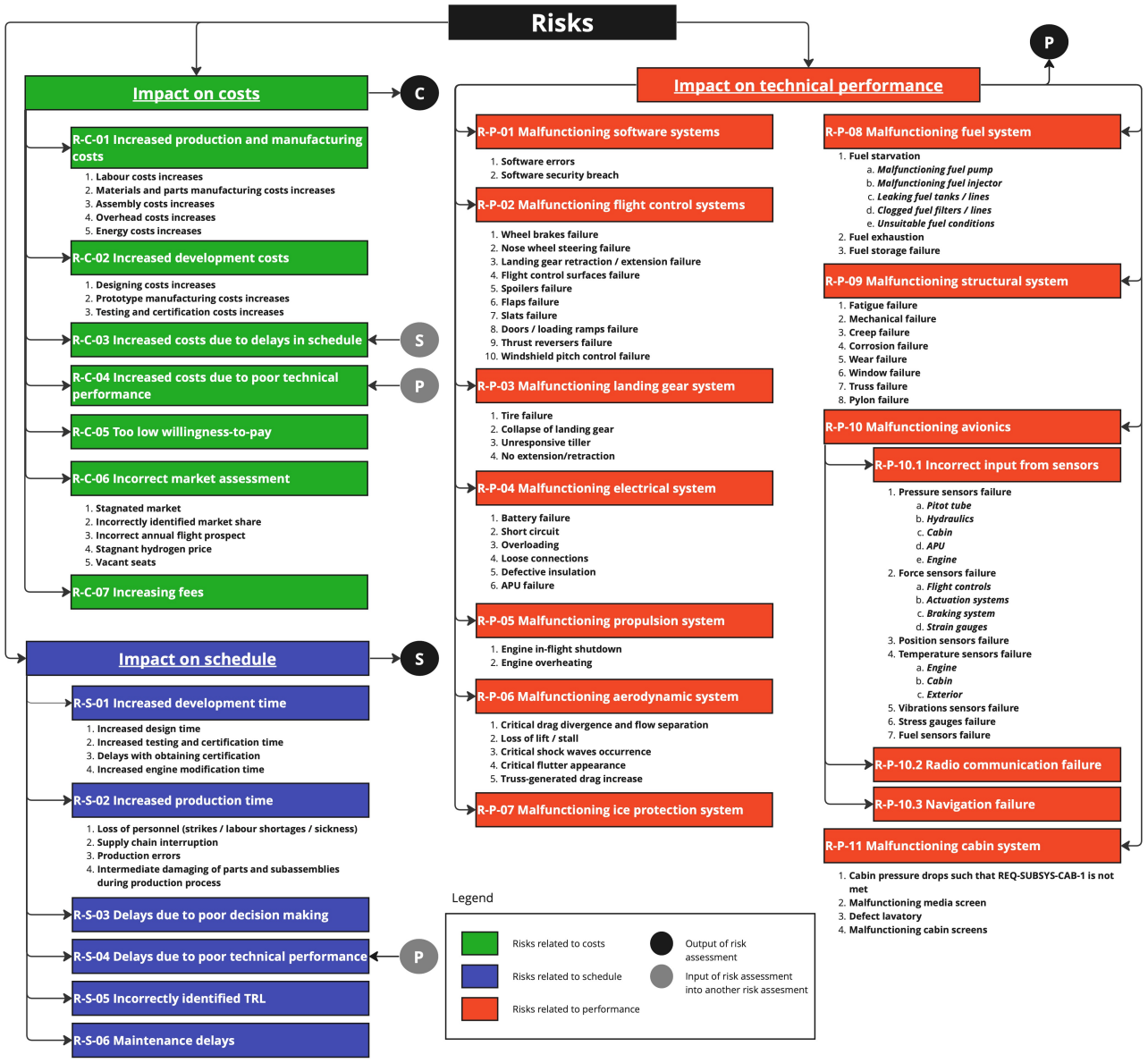

Figure 19.1:
Risk tree after identification of new risks. The coloured bars are the top level risks where the identifiers correspond to the same identifier in Figure 19.2.

Table 19.2: Definitions of impact [77]

Severity of impact			
Grade	**Impact Level**	**Definitions w.r.t technical performance**	**Definitions w.r.t time and costs**
5	Catastrophic	Total aircraft destruction and multiple fatalities or complete failure to achieve the contracted task	Requiring immediate and very significant deviation from project schedule or budget, may result in project failure.
4	Hazardous	Severe impact on safety, potential for multiple deaths and serious equipment damage or high chance aircraft is grounded	Requiring immediate significant deviation from project.
3	Major	Significant impact on safety, potential injury to people, serious incident, or quite a significant delay	Requiring some deviation from project schedule or budget.
2	Minor	Minor incident, operating limitations or inconvenience, or small chance aircraft cannot take off but experiences slight delay	Manageable with meager deviation from project schedule or budget.
1	Negligible	Little consequence	Little consequence.

19.2. New risks

In the original risk identification, particularly the structures system (R-P-09) and the fuel system (R-P-08) are notable systems, due to the novelty of the options used in WorldBus compared to conventional aircraft. In the final design phase, more risks can be identified. Due to the design refinement, limitations in the design are more easily identified which influence cost, compromising the project. The identified risks are evaluated and assigned to a sublevel risk. When a new risk is identified, it will either be assigned to a sublevel or top-level risk. The following risks were newly identified.

- R-C-06: Incorrect market assessment (3 & 5)
- R-C-07: Increasing fares (4 & 2)
- R-S-01-4: Increased engine modification time (3 & 2)
- R-S-06: Maintenance delays (3 & 2)
- R-P-08-1-e: Unsuitable fuel conditions (1 & 4)
- R-P-09-8: Pylon failure (1 & 4)
- R-P-10.1-7: Fuel sensor failure (2 & 3)
- R-P-11-3: Defect lavatories (1 & 3)
- R-P-11-4: Malfunctioning cabin screens (2 & 4)

In these newly identified risks, the scores behind the risk indicate the likelihood and impact, respectively. So for R-C-06 (3 & 5), it means the likelihood is graded of 3 and the impact a score of 5 according to Table 19.1 and Table 19.2. The identified risks cause shifts in the previous risk map and therefore, new mitigation is required for the more critical ones. Only the top-level risks are displayed. The risk map, based on the new risks, is found in Figure 19.2. Furthermore, in Table 19.3 and Table 19.4, the new risks are mitigated and their contingency explained.

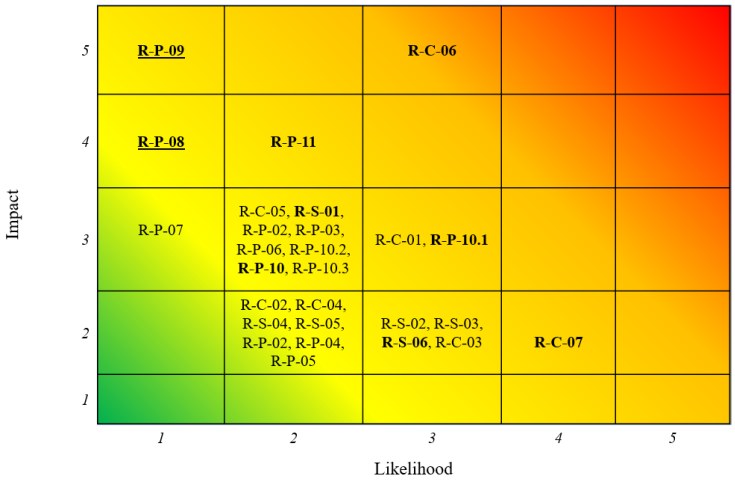

Figure 19.2: WorldBus risk map before mitigation strategies have been applied.

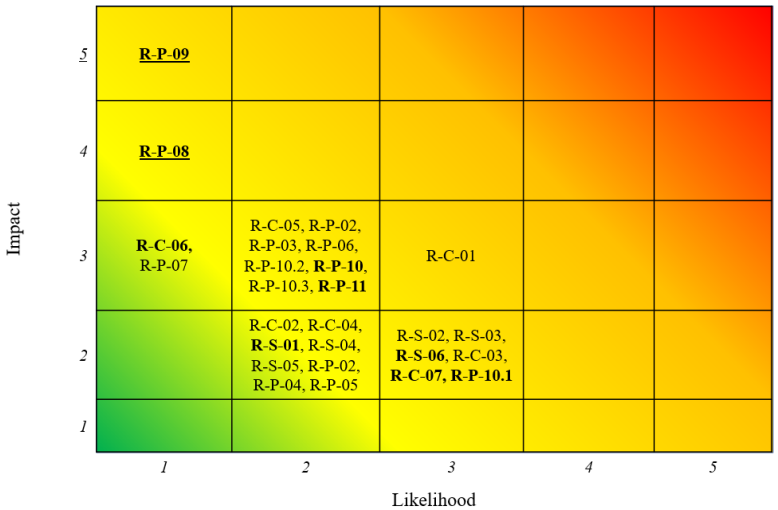

Figure 19.3: WorldBus risk map after mitigation strategies have been applied.

Table 19.3: Risk mitigation for the considered systems after new risk identification, part 1

Identifier	Issue	Likelihood mitigation	Impact mitigation
R-C-06	Incorrect market assessment	In order to mitigate the likelihood of a wrong market analysis, it is useful to analyse multiple scenarios; pessimistic and optimistic, to make sure the project is still profitable for a wide variety of market conditions, like a stagnant market, smaller market than expect, or vacant seats etc.	Allowing the interior of the aircraft to be modular, the configuration can then be adapted to the true market. This would allow the WorldBus project to appeal to a wider market, and be profitable for these various market conditions, mitigating the impact of changes in market.
R-C-07	Increasing fares	Usually, increasing prices are simply the result of a change in the global economy and unfortunately, that cannot be mitigated.	Fuel hedging contracts and multiple crew bases are ways of mitigating the impact of rising fares. internationally
R-S-01-4	Increased engine modification time	The likelihood can be mitigated by building prototypes before production is set to commence. This would allow for obtaining a more efficient engine and better understanding of all subsystems, speeding up the process.	The impact could be mitigated by communicating with the engine manufacturer for a separate production line, such that specific engines are built rather than having to modify each engine continuously.
R-S-06	Additional maintenance due to new design	In order to mitigate the likelihood of additional maintenance, predictive maintenance could be used. From analysis, it has been established at what moment certain systems tend to become weaker and using this type of maintenance this is averted as it is performed prematurely, allowing for safer operations and preventing the aircraft from being out-of-service for a longer period of time	The impact of additional maintenance can be mitigated by having the parts and tools available at every location. Using this, maintenance can commence almost immediately, minimising the delay and allowing the aircraft to return to service as soon as possible.
R-P-08-1-e	Unsuitable fuel conditions	In order to mitigate the likelihood of unsuitable fuel conditions, the pilots need to check the fuel conditions at multiple moments during the flight. This would allow for safer operations and appropriate responses as the crew is aware of the conditions of the fuel.	To mitigate the impact of fuel not having the desired conditions, the fuel would be rerouted through additional heaters and compressors until the desired conditions are obtained, allowing for safe continuous operations and minimising the risk of fuel starvation.
R-P-09-8	Pylon failure	Likelihood mitigation is achieved by inspecting the state of the pylons during maintenance, but also quickly before flight. Visually, substantial issues can be prevented and this allows for safe operations during its lifetime. Furthermore, they could be designed with a safety factor such that the risk of operating close to the limit is reduced.	To mitigate the impact of pylon failure, the pylons need to be designed in such a way that the engines fly over the wing when they disconnect. This minimises the risk of obtaining substantial damage to the structure.

Table 19.4: Risk mitigation for the considered systems after new risk identification, part 2

Identifier	Issue	Likelihood mitigation	Impact mitigation
R-P-10.1-7	Fuel sensor failure	To mitigate the likelihood of the fuel sensors and switches failing, they are required to be inspected during maintenance, due to the extreme conditions they are subjected to. This way the functioning can be verified and this allows for safe operation and minimising the likelihood of faulty responses by the aircraft and the crew.	The impact can be mitigated by having the fuel system not being dependent on a single sensor. Through multiple readings, the actual conditions are charted more accurately and issues by one of the sensors can be limited. This minimises the effect on the aircraft made by the faulty sensor(s) and allows safe service.
R-P-11-3	Defect lavatories	Due to the length of the flight, the toilets will be used more extensively. This may cause clogging of the plumbing. The likelihood can be mitigated by clearing the plumbing at every touchdown and thoroughly cleaning the plumbing at every maintenance round. Furthermore, flight attendants can be trained such that the most basic plumbing issues can be sorted during flight. This allows for a comfortable flight operation and minimises the risk of having to make an emergency stop.	By adhering to CS-25 regulation with respect to the number of lavatories, the impact can be mitigated by having multiple lavatories available per cabin section. Although having less lavatories is less comfortable, the aircraft can continue its service and minimise the chance of having to make an emergency landing.
R-P-11-4	Malfunctioning cabin screens	In order to mitigate the likelihood of malfunctioning cabin screens, it is wise to check the screens while the aircraft is in maintenance. In maintenance the necessary electrical tests can be performed, ensuring the functioning of the screens during continuous service	In the case of emergency situation where the screens go dim, fluorescent paint could be applied that some source of light is still present in the cabin. This allows for passenger to continue having visual orientation.

20

Compliance matrix

At the start of project WorldBus, user requirements have been provided and key requirements have been determined for this mission. In the compliance matrix in Table 20.1, the requirements have been checked to determine if they are met by the current WorldBus design. The table includes the requirement ID, the requirement description, the compliance status, the risk associated with that status, the justification for the status and the risk, and any required action needed to meet the status, if applicable.

Table 20.1: A compliance matrix which includes all user requirements for WorldBus. Colours are included to visually show the requirement statuses.

ID	Requirement	Compliance status	Risk	Justification	Action
REQ-USER-PERF-01	The aircraft shall be able to fly 19 000 km non-stop	Compliant	Medium	Section 12.3 shows the design has a sufficient range. Any unforeseen increases in weight in later design stages can harm the range as there is no contingency.	Focus on lightweight design and develop a weight contingency plan.
REQ-USER-PERF-02	The aircraft shall be able to fly 19 000 km within 21 hours	Compliant	Low	Section 12.2 details the required speed and its achievability. There is some contingency.	-
REQ-USER-PERF-03	The aircraft shall accommodate for 200 passengers + crew members	Compliant	Low	Section 13.1 accounts for 201 passengers and the minimum required number of crew members.	-
REQ-USER-SAF-01	The aircraft shall meet the minimum requirements of the EASA CS-25 Certification Specification for Large Aircraft	Compliant	High	The analysis of the safety regulations as performed in Section 18.4 shows that WorldBus is designed with the currently applicable regulations in mind. All unprecedented design choices are sufficiently designed in accordance to the safety regulations. The regulations can be updated before 2040, however.	Stay up to date with the regulations, stay in close contact with EASA.

REQ-USER-SUS-01	The AC shall produce 90% less environmentally harming emissions over its entire life than comparable aircraft (A380, B787)	Intend to comply	Medium	As Section 14.3, Section 14.3, and Section 15.1, Section 15.3, and Subsection 15.1.3 explore, an operational emissions reduction of 90% is feasible and improvements on end-of-life and production emissions can be made. However, to what these will add up in 2040 remains somewhat unclear. The operational emissions make up the largest part of the total, a high percentage there can compensate somewhat for other parts.	Further research is needed, innovative sustainable production methods and strategies to be devised.
REQ-USER-BUD-01	The aircraft shall be able to fly a minimum of 4000 hours per year	Compliant	Low	Aircraft operations (Chapter 16) allow for 20 hour flights within 24 hours. 4000 flight hours per year then requires approximately 200 days.	-
REQ-USER-BUD-02	The aircraft shall fly in service for at least 10 years (lifetime of 40 000 hours)	Compliant	Low	The material choices and planned production as described in Section 14.1 and Section 14.3 ensure great longevity. Design focus on maintainability ensures that issues can be fixed.	-
REQ-USER-COS-01	Aircraft unit price shall not exceed EUR 484 million	Compliant	Medium	A new price of EUR 484 million was decided on with the customer, as EUR 250 million was unfeasible. As most subsystems are overdesigned, the cost is unlikely to further increase in a later design stage.	-
REQ-USER-COS-02	A total of 300 aircraft shall be manufactured within a time span of 20 years	Compliant	Low	After consulting the user, the initial requirement of 500 aircraft has been changed to 300. This new requirement is met according to Section 14.2. The business case is explained in Section 4.3	-
REQ-USER-OTH-01	The first operational aircraft shall be delivered by 2040	Compliant	Medium	A design outlook is devised in Chapter 21.	-

21

Future design phases

This chapter will discuss the future development strategy of WorldBus. The expected timeline is presented, taking the following into account: research and development (R&D), developing a prototype, testing, and certifying, and, lastly, manufacturing. Afterwards, this chapter is concluded by providing an operations and logistic concept description.

21.1. Project design and development logic

The project design and development logic is used to provide an overview of the to be performed activities after the completion of the design synthesis exercise. A user requirement for WorldBus is to enter service in 2040. This leaves the team 17 years to optimise and deliver the first batch of aircraft. In order to have an indication of the different stages of design and actions necessary to achieve this, Figure 21.1 has been created.

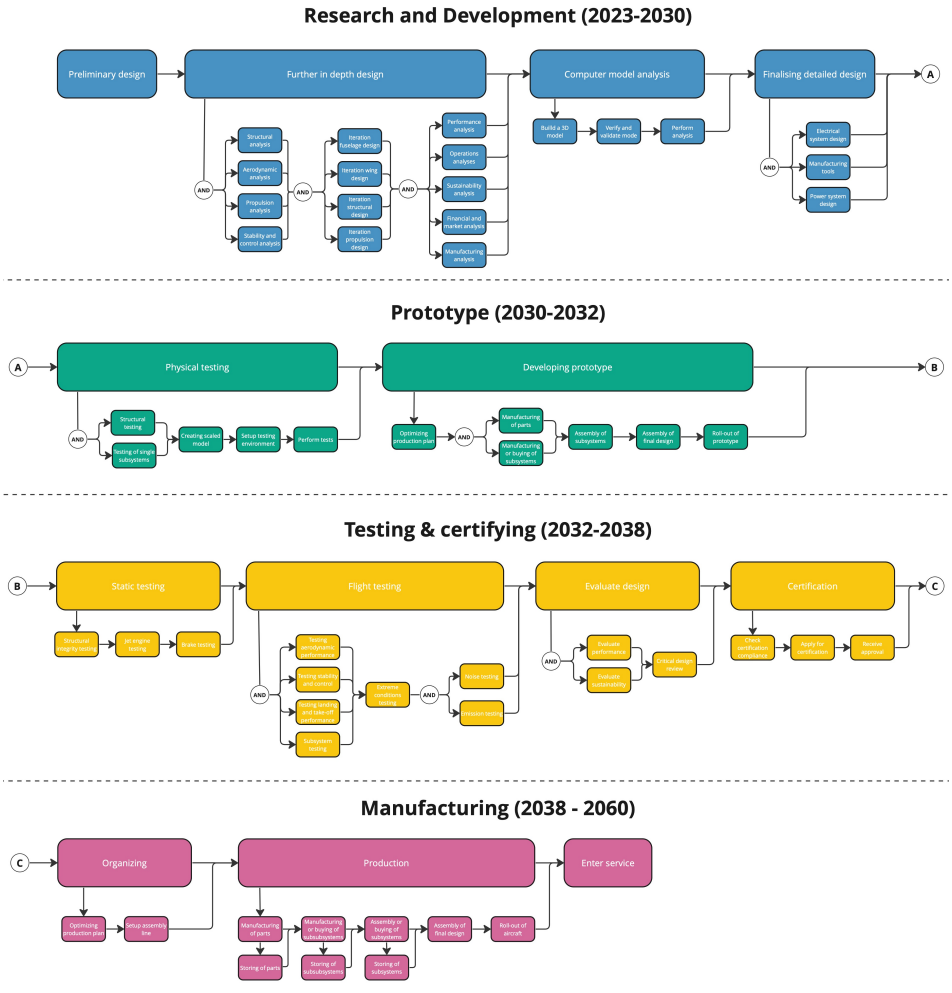

Figure 21.1: Project design and development logic

Figure 21.1 shows the top-level stages of design and the timespan assigned to each. The first phase, the research and design phase, is expected to be finished within six years. In this phase, the preliminary design is further developed and researched into a final design. Next, the prototype phase follows in which physical testing is performed on subsystems after which a first prototype is created. For this phase, two years have been reserved. This prototype is then tested and certified in the next phase over the course of six years, ensuring it is ready for the manufacturing phase of three years. However, for a more detailed overview, each specific action has also been given a timespan in which it should be completed. This is shown in the Gantt chart in Figure 21.2.

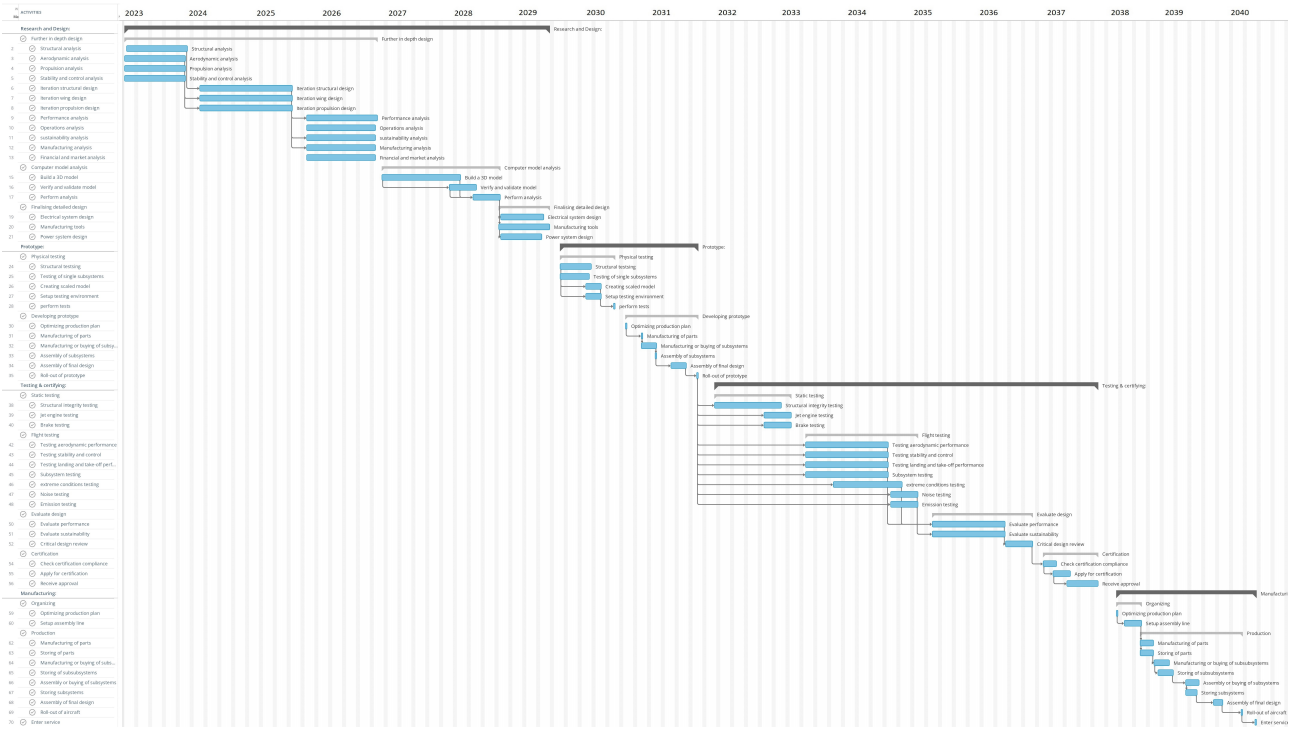

Figure 21.2: Project design and development logic Gantt chart

21.2. Operations and logistic concept definition

The operations and logistic concept definition illustrates, through a block diagram, the support needed to complete the mission. For WorldBus, maintenance and aircraft operations are analysed. Most operations have been discussed in detail in Chapter 16 and are shown in Appendix A. This diagram, therefore, focuses on the main supporting operations as displayed in Figure 21.3.

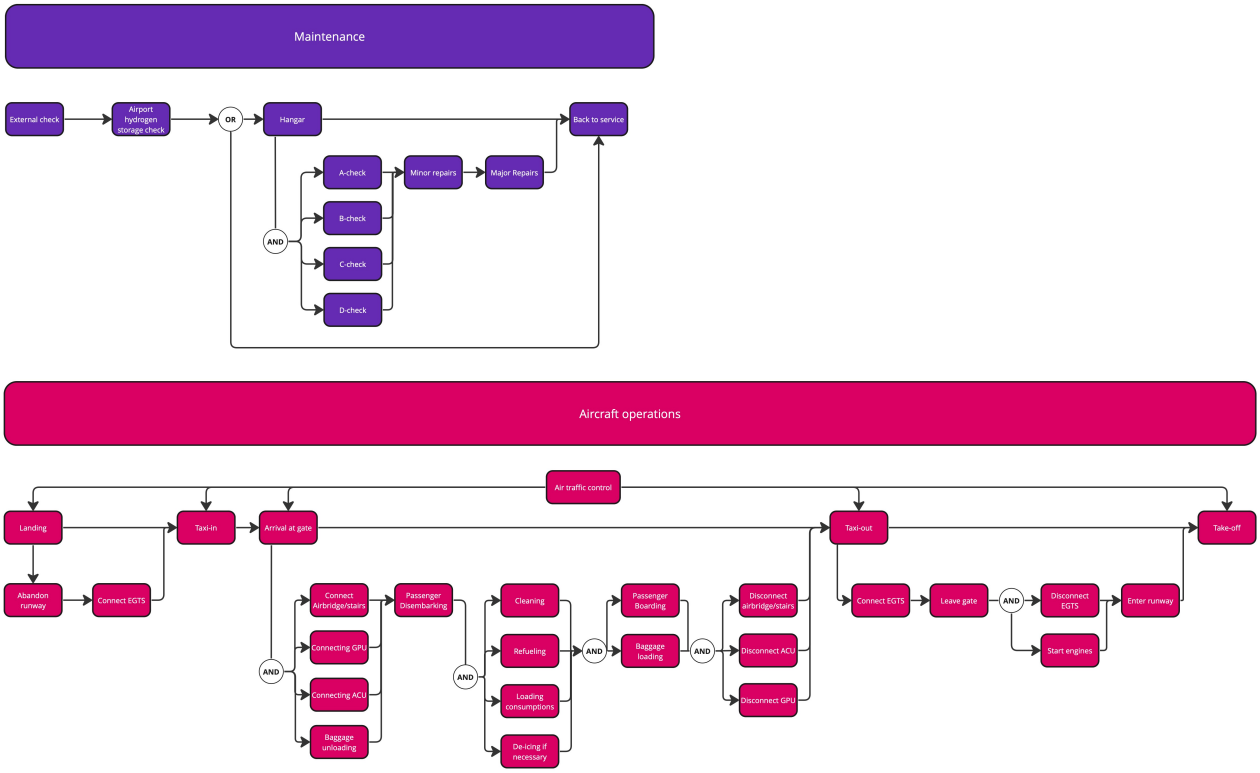

Figure 21.3: Operations and logistics diagram

22

Conclusion and recommendations

So far, Chapters 2 - 7 have examined the mission and project outline, Chapter 8 up until Chapter 14 explored and discussed the detailed subsystem designs, and Chapter 20 up until Chapter 21 have examined the design in its final form. A clear design for WorldBus has been established and a number of conclusions and recommendations have been made for the various subsystems. This chapter aims to make conclusions and recommendations about the preliminary design process and its outcome as a whole. The conclusion is detailed in Section 22.1 and the recommendations are included in Section 22.2. Furthermore, Table 22.1 is a conclusive parameter overview and can be found in Section 22.2 as well.

22.1. Conclusion

A conceptual design for a sustainable, ultra-long-haul aircraft has been created based on the framework created by the 10 initial user requirements. A novel aircraft was asked to fill the need for ultra-long-haul non-stop flight, with a radical reduction in environmental impact of 90%. Furthermore, the flight duration may not exceed 24 hours, including operations and passenger handling. The result is WorldBus, as shown in Figure 22.1

The WorldBus design uses a truss-braced wing configuration, with a wingspan of 71.9 m and a maximum take-off weight of 223.8 mt. It is powered by two Rolls-Royce Trent 1000R engines modified for gaseous hydrogen combustion. The aircraft will contain a 23.9 m tank in between the fore and aft cabins, and the overall fuselage length is 75.3 m. It is designed to fly a distance of 19 000 km non-stop and will fly at a speed of Mach 0.87. An overview with the most important parameters of WorldBus is included in Table 22.1.

Even though truss-braced concepts are increasingly envisioned in the contemporary aviation sector, their novelty and rare usage come with design challenges as opposed to a less innovative design. Firstly, the increased aspect ratio results in a slender wing with a large wingspan. For an aircraft with this range and a heavy LH_2 tank, this results in an excessively large wingspan. To avoid needing to use folding wings, a weight threshold was set to meet the maximum allowable wingspan of 80 m. Furthermore, the need for a high-wing configuration removes the opportunity for efficient integration of the landing gear in the wing. Fortunately, the truss structure is expanded and covered with a cowling near the fuselage to integrate the main landing gear for improved aerodynamic efficiency.

Nevertheless, the innovative and unconventional design of WorldBus allows it to fly with high aerodynamic efficiency due to its high aspect ratio truss-braced wing. In addition, the mid-placement of the fuel tank enables a smaller empennage, reducing its drag contribution. Lastly, the use of slightly modified existing combustion engines avoids additional R&D costs and enables a high flight velocity. The culmination of this results in the possibility to emit 97% less GWP per passenger per kilometer than comparable aircraft during operations.

As presented in Chapter 20, the conceptual design fully complies with seven of the ten initial requirements. Two requirements are complied with since negotiations about the requirements have been had with the user. The design currently 'intends to comply' with one requirement, intending to improve the compliance further in future design stages.

In order to determine the conceptual design's performance regarding the user requirements, thorough research and design was performed into finance, sustainability, and performance, among other disciplines. Major takeaways were that the initial maximum required price of EUR 250 million (REQ-USER-COS-01) was unfeasible. The weight and amount of material of the designed aircraft was too high to meet the low price production-wise. After negotiating with the user, the maximum list price requirement was increased, allowing for the current list price of EUR 484 million. In addition, the total required number of aircraft to be produced of 500 (REQ-USER-COS-02) was deemed too large for the existing market. In agreement with the user, this was changed to 300 aircraft. Even though these initial requirements are not met, the financial analysis (Chapter 4) concludes that an ROI of 20% to 96% is expected.

One other requirement is not yet being complied with; requirement REQ-USER-SUS-01 needs the aircraft to produce 90%

fewer environmentally harming emissions over its entire lifetime. Even though Section 15.3 shows that such improvements can be made for the operational part of the aircraft life, possibly with some margin, improvements in the production and end-of-life processing of the materials that are used in WorldBus are not achievable to that extent with contemporary technologies. Nevertheless, WorldBus is a conceptual design of an aircraft that can fly with near-zero operational emissions and which provides a significant overall reduction in emissions, even if fewer improvements can be made on other segments of the aircraft lifetime. This major innovation will have significant implications for the aviation sector in general.

However, WorldBus does not conclude innovation in the aviation sector. The goal on the horizon will be to design and produce aircraft with an even larger reduction in environmentally harming emissions over their full life cycle. The conceptual design phase of WorldBus has discovered a variety of areas which require further intensive research and innovation over the coming decades. The main focus of this lies in the use of sustainable materials and production methods. In addition, the use of LH_2 has proved to be efficient, but it does require a great increase in green hydrogen production to support the industry moving over to hydrogen. Further top-level recommendations are included in Section 22.2.

With the introduction of WorldBus comes the advent of significantly more sustainable (ultra) long-haul flights. As reasoned in Section 4.1, the market size for long-haul flights is expected to continue showing constant growth. However, clean flight can accelerate the interest in long-haul flights and take away the current major objection to flying. WorldBus passengers will experience less flight shame than conventional fossil fuel-powered aircraft, and low-impact travel is finally becoming a realistic possibility.

Figure 22.1: A render of the final design of WorldBus.

22.2. Recommendations

Over the course of the preliminary design of the WorldBus concept, a number of specific points of improvement were found that would improve a similar design phase for a different concept as well as the further design phases of the WorldBus design. This also includes further study of aspects that were deemed out of the scope of this design phase, although they are relevant for the design. These have been presented as recommendations throughout Chapter 4 until Chapter 17. Aside from these, five top-level and inter-disciplinary recommendations can be made for future design endeavours:

- When focusing on sustainable design, design specifically for deliberately selected sustainable materials, instead of considering their sustainability as an afterthought when the structural designs are established.
- Perform numerical verification throughout the entire design process, instead of after the finalisation of numerical models, to avoid a large number of unexpected changes in the last portion of the design process.
- Start the creation of the computer-aided design (CAD) model of the design early on in the process, as it functions well as an additional verification method for dimensions and integrations that are difficult to visualise without aid.
- Create a numerical model of the aircraft structure in more detail, as the high number of assumptions and superficial buckling analysis lead to an unoptimised design.
- Invest time into the design of innovative productional methods to, possibly, increase the sustainability of the production phase by not being limited to conventional methods.

Table 22.1: An overview of the notable parameters of the WorldBus conceptual design.

Parameter	**Unit**	**Value**	**Parameter**	**Unit**	**Value**
MTOW	[mt]	223.8	No. of business class seats	-	83
OEW	[mt]	158.6	No. of economy+ class seats	-	118
Fuel weight	[mt]	45.2	Range	[km]	19 000
Wingspan	[m]	71.9	Cruise velocity	[m/s]	265
Wing area	[m^2]	369.4	Cruise altitude	[m]	9 000
Leading edge wing sweep	[deg]	32.7	No. of engines	-	2
Wing aspect ratio	-	14	Max. total thrust	[kN]	756.8
Wing dihedral	[deg]	-2.11	CO_2 equivalent GGE per pax per km	[g/pax/km]	2.86
Truss location along half span	[m]	20.8	List price	[million EUR]	484
Fuselage length	[m]	75.3	Max. ROI	-	96%
Fuselage diameter	[m]	6.25	Min. ROI	-	20%

References

[1] Roger Groves. *Project Guide Design Synthesis Exercise WORLDBUS*. TU Delft. Apr. 2023.

[2] J. Bouvy et al. *Worldbus Baseline Report*. Delft University of Technology, 2023.

[3] Eurocontrol. *2022 – The year European aviation bounced back, despite war & Omicron/COVID*. Tech. rep. Eurocontrol, 2022.

[4] J. Wilkerson et al. "Analysis of emission data from global commercial aviation: 2004 and 2006". In: *ATMOSPHERIC CHEMISTRY AND PHYSICS* 2010 (Feb. 2010), pp. 2945–2983. DOI: 10.5194/acpd-10-2945-2010.

[5] Global Viewpoint. *Business class vs. economy (coach) in 2023*. Feb. 2023. URL: https://www.myglobalviewpoint.com/business-class-vs-economy/%5C#:~:text=Busines20class20tickets20can20cost,is20the20way20to20go..

[6] C. Rice et al. "Willingness to pay for sustainable aviation depends on ticket price, greenhouse gas reductions and gender". In: *Technology in Society* 60.101224 (Feb. 2020).

[7] Aviation Specialists Group Inc. *Economic Values for Investment and Regulatory Decisions*. 2018. URL: https://www.faa.gov/regulations_policies/policy_guidance/benefit_cost/media/econ-value-section-4-op-costs.pdf.

[8] Y. Zhang et al. "Exploration and implementation of commonality valuation method in commercial aircraft family design". In: *Chinese Journal of Aeronautics* (May 2019), pp. 1834–1835.

[9] J.Markish. "Valuation Techniques for Commercial Aircraft Program Design". In: *Aeronautics and Astronautics* (June 2002), pp. 1834–1835.

[10] D.D. Hernandez and E. Gençer. "Techno-economic analysis of balancing California's power system on a seasonal basis: Hydrogen vs. lithium-ion batteries". In: *Applied Energy* 300 (2021), p. 117314. ISSN: 0306-2619. DOI: https://doi.org/10.1016/j.apenergy.2021.117314. URL: https://www.sciencedirect.com/science/article/pii/S0306261921007261.

[11] Ministere de l'enseignement superieur et de la recherche. *Advanced materials for hydrogen storage tanks*. Jan. 2013.

[12] R. Daniel. *Aircraft Design: A Conceptual Approach, Sixth Edition*. Sept. 2018. ISBN: 978-1-62410-490-9. DOI: 10.2514/4.104909.

[13] J. Bouvy et al. *Worldbus Midterm Report*. Delft University of Technology, 2023.

[14] The International Organization for Standardization (ISO), the Organisation for Economic Co-operation, and Development (OECD). *ISO 26000 and OECD Guidelines*. 2017.

[15] J. Bouvy et al. *WorldBus Project Plan*. Delft University of Technology, 2023.

[16] M. Kito. "Impact of aircraft lifetime change on lifecycle CO2 emissions and costs in Japan". In: *Ecological Economics* 188 (Oct. 2021), pp. 104–107. DOI: https://doi.org/10.1016/j.ecolecon.2021.107104.

[17] J. Scheelhaase et al. "Economic and Environmental Aspects of Aircraft Recycling". In: *Transportation Research Procedia* 65 (2022), pp. 3–12. DOI: https://doi.org/10.1016/j.trpro.2022.11.002.

[18] European Aviation Safety Agency. *Certification Specifications and Acceptable Means of Compliance for Large Aeroplanes CS-25*. Tech. rep. European Aviation Safety Agency, 2018.

[19] R. Vos and J.A. Melkert. *AE1222-II Aerospace Design and Systems Engineering Elements I*. Delft University of Technology, 2019.

[20] A. Elham et al. *Aerospace Design and Systems Engineering Elements II*. Delft University of Technology, 2020.

[21] S. Gudmundsson. *General Aviation Aircraft Design*. Boston: Butterworth-Heinemann, 2014. Chap. 9 - The Anatomy of the Wing, pp. 299–399. ISBN: 978-0-12-397308-5. DOI: https://doi.org/10.1016/B978-0-12-397308-5.00009-X.

[22] M. H. Sadraey. *Aircraft Design: A Systems Approach*. John Wiley & Sons, Ltd, 2013, pp. 274–352. ISBN: 978-1-119-95340-1.

[23] European Aviation Safety Agency. *Certification Specifications for Large Aeroplanes CS-25*. Tech. rep. European Aviation Safety Agency, 2007.

[24] O. Balli et al. "Thermodynamic comparison of TF33 turbofan engine fueled by hydrogen in benchmark with kerosene". In: 306 (Dec. 2021).

[25] P. Derekhshandeh and A. Ahmadi. "Simulation and technical-economic-environmental optimization of the General Electric GE90 hydrogen turbofan engine". In: 46 (Jan. 2021).

[26] E. Torenbeek. *Synthesis of subsonic airplane design*. Delft University Press, 1976, pp. 303–339. ISBN: 90 298 2505 7.

[27] Dr. F. Oliviero. *Requirement Analysis and Design principles for A/C stability & control (Part 2)*. 2021.

[28] D. Scholz. *Empennage General Design*. HAW Hamburg, 2017.

[29] P. Sforza. *Commercial Airplane Design Principles*. Elsevier Inc., 2014, pp. 213–250. ISBN: 978-0-12-419953-8.

[30] M. Voskuijl. *Flight & Orbital Mechanics*. Delft University of Technology, 2020.

[31] J. D. Anderson. *INTRODUCTION TO FLIGHT*. 3rd ed. McGraw-Hill Book Company.

[32] R. Alderliesten. *Introduction to Aerospace Structures and Materials*. 8th ed. TU Delft Open, 2018. Chap. 7. DOI: 10.5074/t.2018.003.

[33] M.C.Y. Niu. "Airframe Structural Design". In: 2nd ed. Conmilit Press LTD., 1988. Chap. 11, p. 376.

[34] C.S. Chien, A.R. Ingraffea, and P.A. Wawrzynek. "Prediction of Residual Strength and Curvilinear Crack Growth in Aircraft Fuselages". In: *AIAA Journal* 40 (Aug. 2002), pp. 1644–1652. DOI: 10.2514/2.1836.

[35] S. Bagassi, F. Lucchi, and F. Persiani. "Aircraft Preliminary Design: a windowless concept". In: *Challenges in European Aerospace*. Vol. 211. CEAS. CEAS, 2015.

[36] C.S. Chien, A.R. Ingraffea, and P.A. Wawrzynek. "Latency and Cybersickness: Impact, Causes, and Measures. A Review". In: *Frontiers in Virtual Reality* 1 (Nov. 2020). DOI: 10.3389/frvir.2020.582204.

[37] C. Winnefeld et al. "Modelling and Designing Cryogenic Hydrogen Tanks for Future Aircraft Applications". In: *Energies* 11.1 (2018). ISSN: 1996-1073. DOI: 10.3390/en11010105. URL: https://www.mdpi.com/1996-1073/11/1/105.

[38] S. E. Irving. *Low-Density Foam for Insulating Liquid-Hydrogen Tanks*. Technical note ADA308410. National Aeronautics and space administration Cleveland OH Lewis Research Center, 1969.

[39] A. Kogan et al. "Cryogenic Vacuum Insulation for Vessels and Piping". In: 1 (July 2010).

[40] D. R. Moss. *Pressure Vessel Design Manual (Third Edition)*. Third Edition. Burlington: Gulf Professional Publishing, 2004. Chap. 2, pp. 15–107. ISBN: 978-0-7506-7740-0. DOI: https://doi.org/10.1016/B978-075067740-0/50002-0.

[41] M.B. Bertagni et al. "Risk of the hydrogen economy for atmospheric methane". In: *Nature Communications* 13.1 (Dec. 2022). DOI: 10.1038/s41467-022-35419-7. URL: https://doi.org/10.1038/s41467-022-35419-7.

[42] R.C. Hibbeler. *Mechanics of Materials*. 10th ed. Pearson Education Inc., 2018.

[43] C.L. Dym and H.E. Williams. "Feasibility modeling of a truss-braced wing as a beam". In: *International Journal of Mechanical Engineering Education* 43 (2015), pp. 3–14. DOI: 10.1177/0306419015573908.

[44] C. Rans and J.A. Melkert. *AE2135-I Structural Analysis and Design*. Delft University of Technology, 2023.

[45] J. Markish. "Valuation techniques for commercial aircraft program design". In: (Jan. 2002).

[46] E.K. Anderson, A.M. Cardona, and B.H. Mason. "Structural Sizing of a Composite Transonic Truss-Braced Wing". In: *NASA Langley Research Center* (2022). URL: https://ntrs.nasa.gov/citations/20220016677.

[47] J. Sinke. *AE3211-II Production of Aerospace Systems*. Delft University of Technology, 2023.

[48] K. Kawajiri and K. Sakamoto. "Environmental impact of carbon fibers fabricated by an innovative manufacturing process on life cycle greenhouse gas emissions". In: *Sustainable Materials and Technologies* 31 (2022). ISSN: 2214-9937. DOI: https://doi.org/10.1016/j.susmat.2021.e00365. URL: https://www.sciencedirect.com/science/article/pii/S2214993721001202.

[49] A. Isa et al. "A Review on Recycling of Carbon Fibres: Methods to Reinforce and Expected Fibre Composite Degradations". In: *Materials (Basel)* 15 (14 July 2022), pp. 49–91. DOI: https://doi.org/10.3390/ma15144991.

[50] N. von der Assen and A. Bardow. “Life cycle assessment of polyols for polyurethane production using CO2 as feedstock: Insights from an industrial case study”. In: *Green Chemistry* 16 (Apr. 2014), pp. 3272–3280. DOI: https://doi.org/10.1039/C4GC00513A.

[51] G. Bergsma and N. Imholz. “CO2-winst met kunststofrecyclaat”. In: (Nov. 2022). URL: https://cedelft.eu/wp-content/uploads/sites/2/2022/12/CE_Delft_220327_CO2-winst_met_kunststofrecyclaat_DEF.pdf.

[52] S. Halliwell. “Repair of Fibre Reinforces Polymer Structures”. In: (Dec. 2021). URL: https://compositesuk.co.uk/wp-content/uploads/2021/12/repairoffrpstructures.pdf.

[53] F. Meng et al. “From aviation to aviation: Environmental and financial viability of closed-loop recycling of carbon fibre composite”. In: *Composites Part B: Engineering* 200 (2020), p. 108362. ISSN: 1359-8368. DOI: https://doi.org/10.1016/j.compositesb.2020.108362. URL: https://www.sciencedirect.com/science/article/pii/S1359836820334119.

[54] J. Zhang et al. “Current status of carbon fibre and carbon fibre composites recycling”. In: *Composites Part B: Engineering* 193 (2020), pp. 53–108. ISSN: 1359-8368. DOI: https://doi.org/10.1016/j.compositesb.2020.108053. URL: https://www.sciencedirect.com/science/article/pii/S135983681936946X.

[55] IEA. *The Future of Hydrogen*. 2019. URL: https://iea.blob.core.windows.net/assets/9e3a3493-b9a6-4b7d-b499-7ca48e357561/The_Future_of_Hydrogen.pdf.

[56] C. Koroneos et al. “Life Cycle Assessment of Kerosene Used in Aviation”. In: *The International Journal of Life Cycle Assessment* 10 (6 2004). DOI: 10.1065/lca2004.12.191. URL: https://link.springer.com/article/10.1065/lca2004.12.191.

[57] K. Kleijne, H. Coninck R. Zelm M. Huijbregts, and S. Hanssen. “The many greenhouse gas footprints of green hydrogen”. In: *Sustainable Energy & Fuels* 6 (19 2022). DOI: 10.1039/D2SE00444E. URL: https://pubs.rsc.org/en/content/articlehtml/2022/se/d2se00444e?page=search.

[58] IEA. *Energy Technology Perspectives*. 2020. URL: https://iea.blob.core.windows.net/assets/7f8aed40-89af-4348-be19-c8a67df0b9ea/Energy_Technology_Perspectives_2020_PDF.pdf.

[59] A.H. Khan et al. “The Emissions of Water Vapour and NOx from Modelled Hydrogen-Fuelled Aircraft and the Impact of NOx Reduction on Climate Compared with Kerosene-Fuelled Aircraft”. In: *Atmosphere* 13.10 (2022). ISSN: 2073-4433. URL: https://www.mdpi.com/2073-4433/13/10/1660.

[60] D.G. Simons and M. Snellen. *AE4431 Aircraft Noise and Emissions*. Delft University of Technology, 2022.

[61] J. June, R. Thomas, and Y Guo. *System Noise Technology Roadmaps for a Transonic Truss-Braced Wing and Peer Conventional Configuration*. URL: https://ntrs.nasa.gov/api/citations/20220006333/downloads/Jason%5C%20JuneSystem%5C%20Noise%5C%20Technology%5C%20Roadmaps.pdf.

[62] M. Lukic et al. “Review, Challenges, and Future Developments of Electric Taxiing Systems”. In: *IEEE Transactions on Transportation Electrification* 5.4 (2019), pp. 1441–1457. DOI: 10.1109/TTE.2019.2956862.

[63] Open identity exchange. *Biometric Boarding using Identity as a Service: The potential impact on liability in the aviation industry*. Tech. rep. Open identity exchange, 2018.

[64] N. Khan and M. Efthymiou. “The use of biometric technology at airports: The case of customs and border protection (CBP)”. In: *International Journal of Information Management Data Insights* 1.2 (2021), p. 100049. ISSN: 2667-0968. DOI: https://doi.org/10.1016/j.jjimei.2021.100049. URL: https://www.sciencedirect.com/science/article/pii/S2667096821000422.

[65] C.K.M. Lee et al. “Empirical Analysis of a Self-Service Check-In Implementation in Singapore Changi Airport”. In: *International Journal of Engineering Business Management* 6 (2014), p. 6. DOI: 10.5772/56962. URL: https://doi.org/10.5772/56962.

[66] S. Tyagi and G. Lodewijks. “Optimisation of check-in process focused on passenger perception for using self-service technologies at airport in Australia”. In: *Journal of Airline and Airport Management* 12.1 (2022).

[67] M. Schultz, C. Schulz, and H. Fricke. “Efficiency of Aircraft Boarding Procedures”. In: June 2008.

[68] A. Padhra. “Emissions from auxiliary power units and ground power units during intraday aircraft turnarounds at European airports”. In: *Transportation Research Part D: Transport and Environment* 63 (2018), pp. 433–444. ISSN: 1361-9209. DOI: https://doi.org/10.1016/j.trd.2018.06.015. URL: https://www.sciencedirect.com/science/article/pii/S136192091830021X.

[69] E. Murtagh et al. “Outdoor Walking Speeds of Apparently Healthy Adults: A Systematic Review and Meta□analysis”. In: *Sports Medicine* 51 (Jan. 2021), pp. 1–31. DOI: 10.1007/s40279-020-01351-3.

[70] E. Mueller and G. Chatterji. “Analysis of aircraft arrival and departure delay characteristics”. In: *AIAA’s Aircraft Technology, Integration, and Operations (ATIO)* (2002).

[71] D. More and R. Sharma. “The turnaround time of an aircraft: a competitive weapon for an airline company”. In: *DECISION* 41 (Dec. 2014), pp. 489–497. DOI: 10.1007/s40622-014-0062-0.

[72] J. Mangold et al. “Refueling of LH2 Aircraft - Assessment of Turnaround Procedures and Aircraft Design Implication”. In: *Energies* 15.7 (2022). URL: https://www.mdpi.com/1996-1073/15/7/2475.

[73] E. Taibi et al. *Green hydrogen cost reduction: scaling up elektrolisers to meet the 1.5 ° climate goal*. Tech. rep. IRENA, 2020.

[74] A. Ajanovic, M. Sayer, and R. Haas. “The economics and the environmental benignity of different colors of hydrogen”. In: *International Journal of Hydrogen Energy* 47.57 (2022). Hydrogen Society, pp. 24136–24154. ISSN: 0360-3199. DOI: https://doi.org/10.1016/j.ijhydene.2022.02.094. URL: https://www.sciencedirect.com/science/article/pii/S0360319922007066.

[75] J. Schneider. *Multimodel hydrogen airport hub*. Tech. rep. H2-Aero vision, 2023.

[76] L. Bannenberg, H. Schreuders, and B. Dam. “Tantalum-Palladium: Hysteresis-Free Optical Hydrogen Sensor Over 7 Orders of Magnitude in Pressure with Sub-Second Response”. In: *Advanced Functional Materials* 31 (Mar. 2021).

[77] A. Mostafa. *Safety and Risk Assessment of Civil Aircraft during Operation*. IntechOpen, 2020.

A

Functional flow diagram

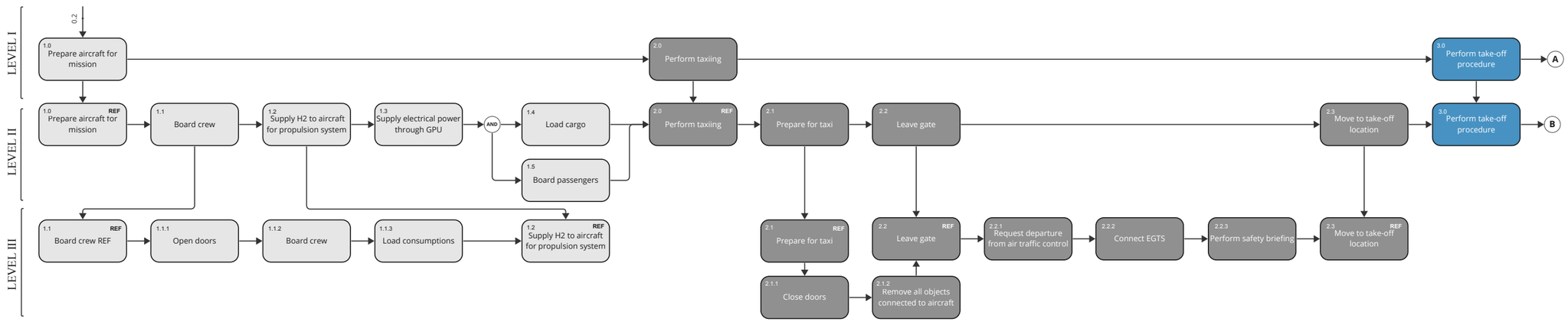

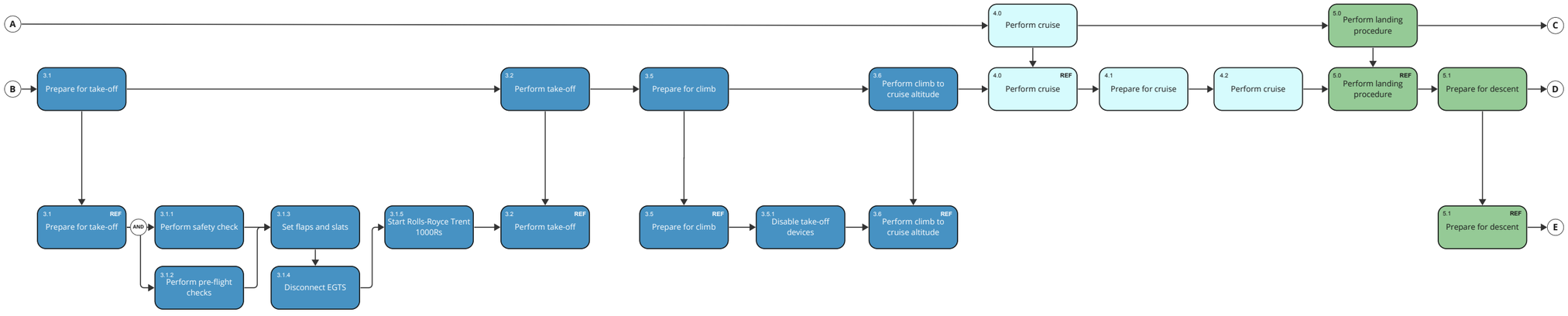

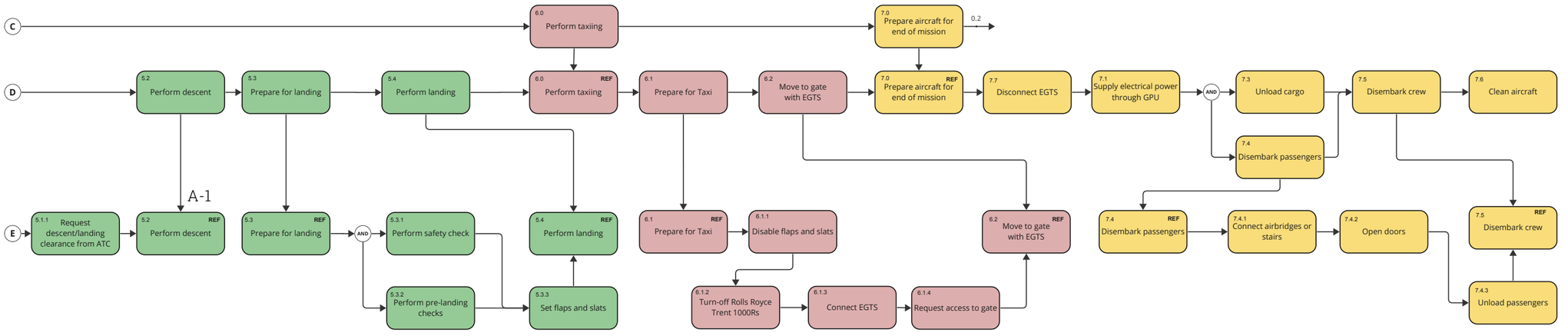

B

Functional breakdown structure

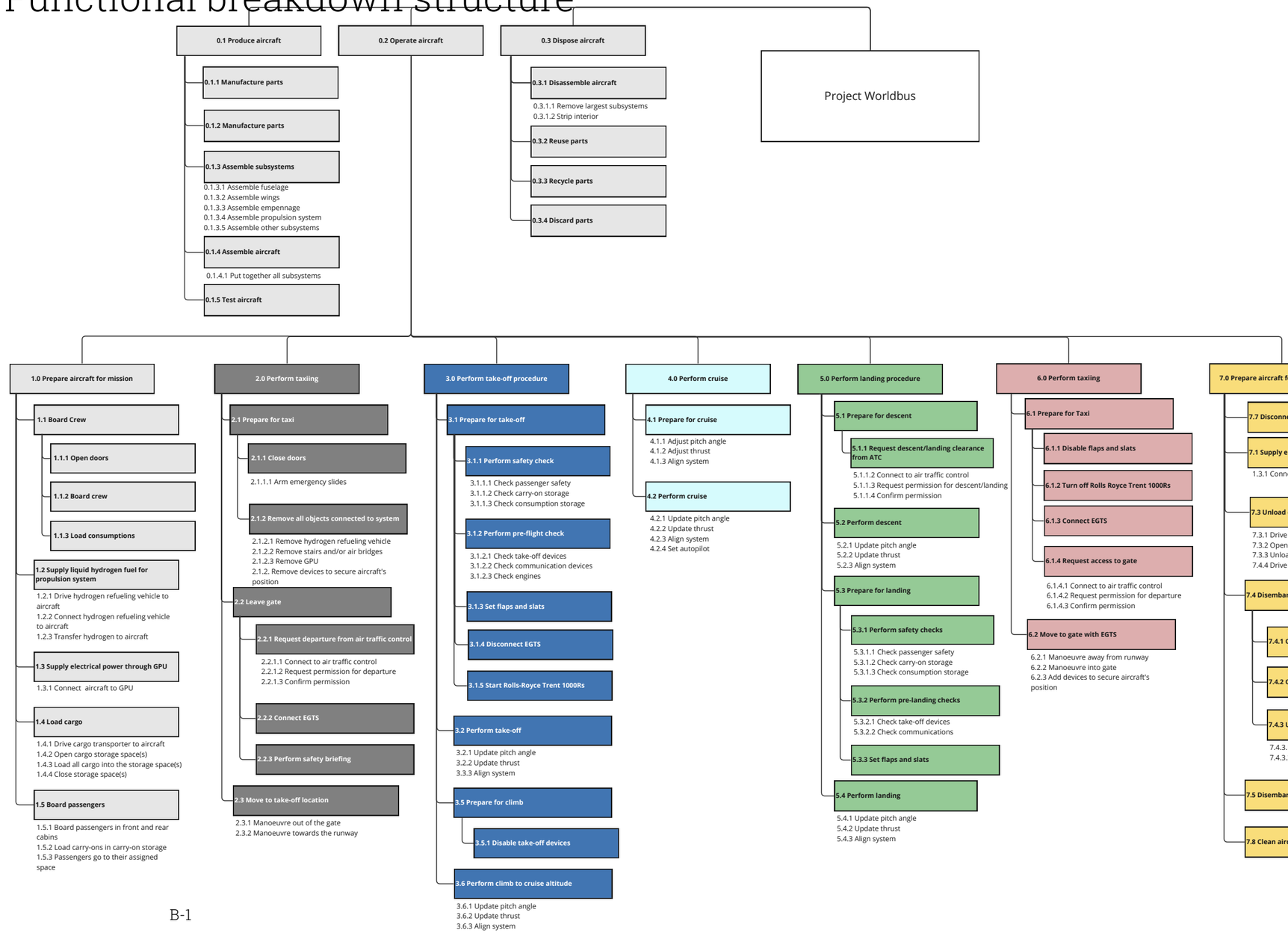

C

Requirements discovery tree

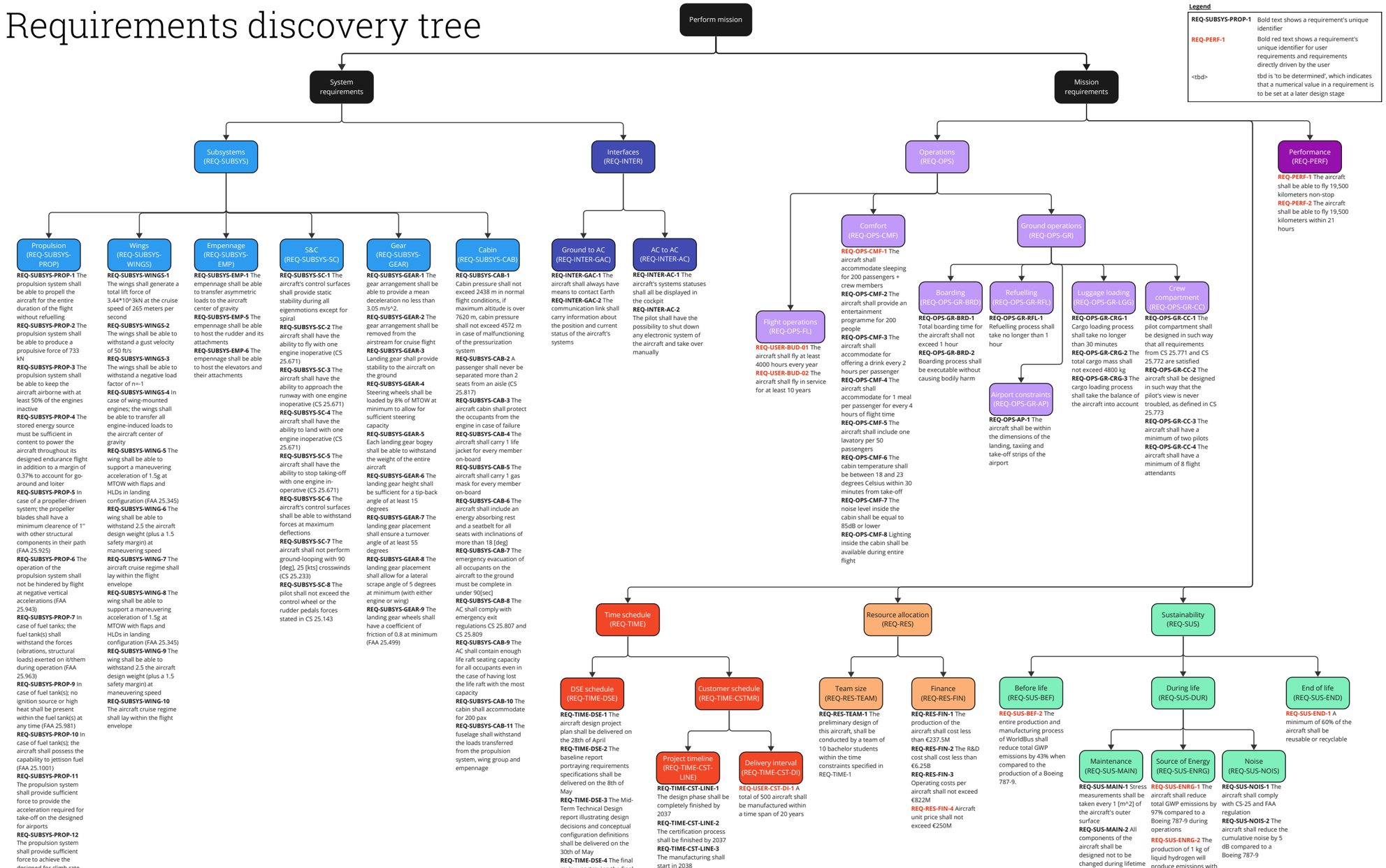

D

Fuselage layout

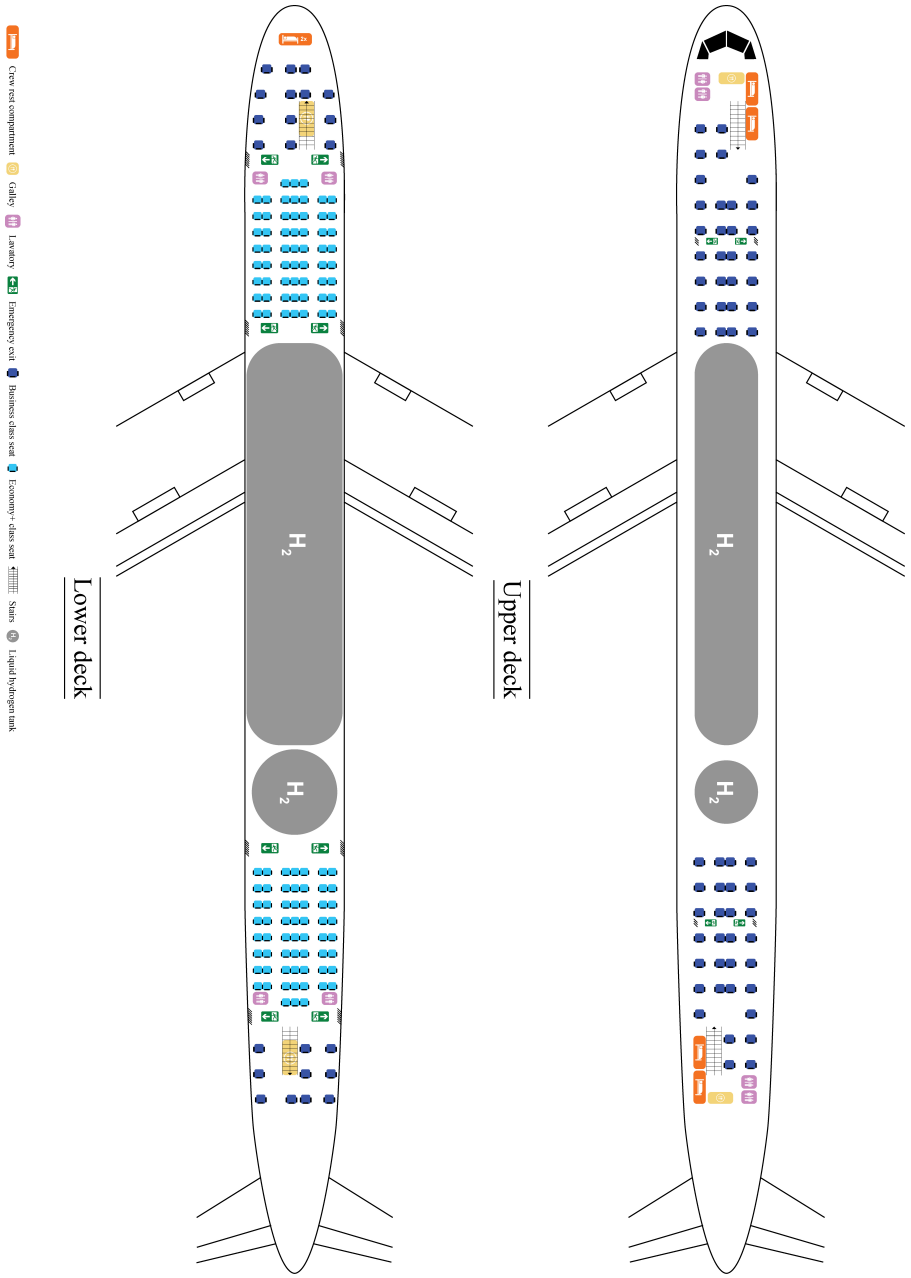

Figure D.1: Fuselage layout, top view

E

Technical Drawing

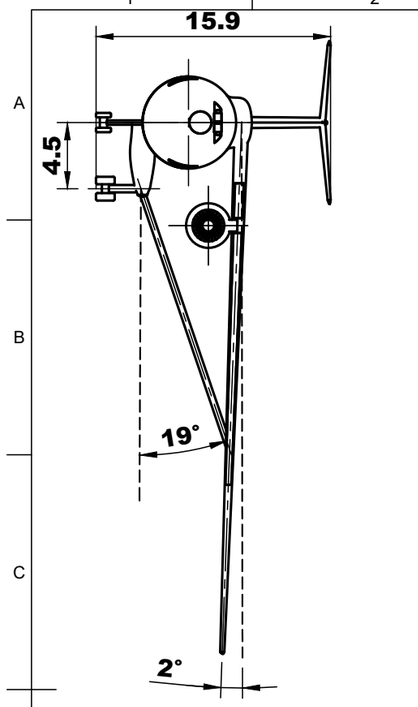

Front view
Scale 1:333

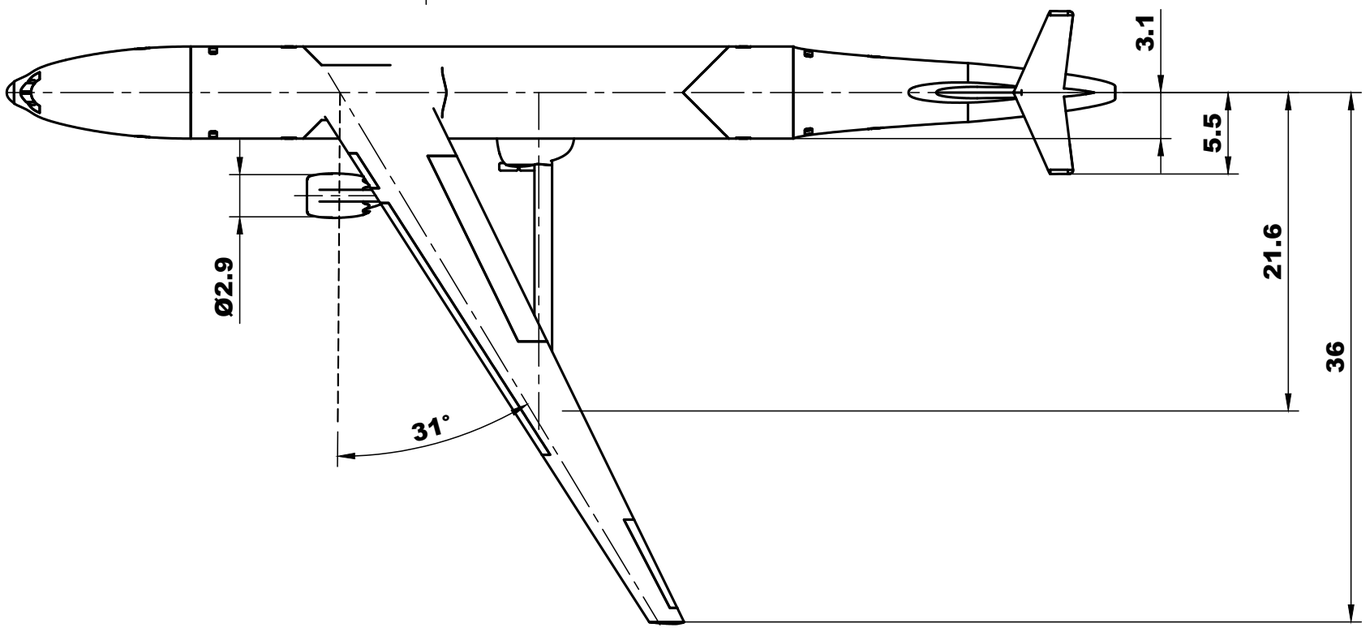

Top view
Scale 1:333

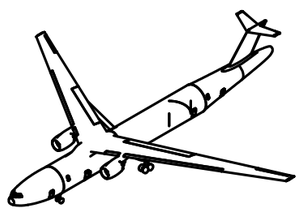

Isometric view
Scale 1:1000

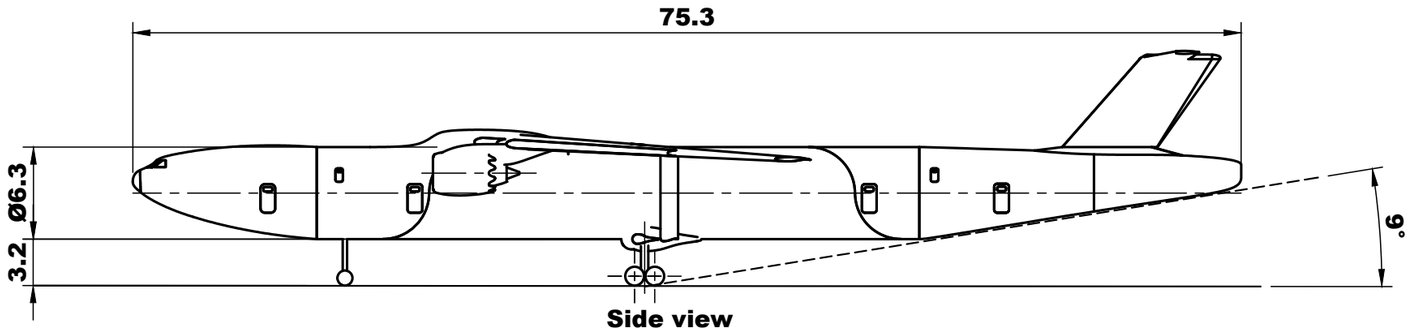

Side view
Scale 1:333

E-1

Dept.	Technical reference	Created by	Approved by
LR	AE-3200	Timo Bruin 20-6-2023	Sylvano Tromp 21-6-2023

Document type	Document status
Tecnical drawing	Draft

Title	DWG No.
WorldBus final assembly	1

Rev.	Date of issue	Sheet
03	21-6-2023	1/1